

Logarithmic corrections in Symanzik's effective theory of lattice QCD

DISSERTATION

zur Erlangung des akademischen Grades

Doctor rerum naturalium
(Dr. rer. nat.)
im Fach Physik
Spezialisierung: Theoretische Physik

eingereicht an der
Mathematisch-Naturwissenschaftlichen Fakultät
der Humboldt-Universität zu Berlin

von
Herrn M. Sc. Nikolai André Husung

Präsidentin der Humboldt-Universität zu Berlin
Prof. Dr.-Ing. Dr. Sabine Kunst

Dekan der Mathematisch-Naturwissenschaftlichen Fakultät
Prof. Dr. Elmar Kulke

Gutachter/innen:

1. *Prof. Dr. Rainer Sommer*
2. *Prof. Dr. Agostino Patella*
3. *Dr. habil. Peter Weisz*

Tag der mündlichen Prüfung: 12.04.2021

Abstract

One of the final steps in simulations of lattice Quantum Chromodynamics (QCD) or lattice pure gauge theory is the continuum extrapolation to extract the actual continuum physics. This extrapolation relies heavily on assumptions regarding the asymptotic dependence on the lattice spacing a , which introduces an inherent systematic uncertainty to the continuum limit. In classical field theories the asymptotic form is a power series in the lattice spacing, where the leading power $a^{n_{\min}}, n_{\min} \in \mathbb{N}$ depends on the chosen lattice discretisation. The quantum nature of lattice QCD and lattice pure gauge theory spoils this behaviour. Instead one finds for asymptotically free theories like QCD the leading asymptotic behaviour $a^{n_{\min}}[\alpha_R(1/a)]^{\hat{\gamma}_i^{(n_{\min})}}$, where $\alpha_R(1/a) \sim -1/\ln(a\Lambda_{\text{QCD}})$ is the renormalised coupling, Λ_{QCD} is the Renormalisation Group Invariant scale and $\hat{\gamma}_i^{(n_{\min})}$ are real numbers. Depending on the values found for $\hat{\gamma}_i^{(n_{\min})}$ the multiplicative powers of the renormalised coupling will then improve or worsen the convergence as $a \searrow 0$, but impact the approach to the continuum limit for $\hat{\gamma}_i^{(n_{\min})} \neq 0$ either way. A particularly worrisome example is the non-linear $O(3)$ model where Balog, Niedermayer and Weisz [1,2] found $\min(\hat{\gamma}_i^{(2)}) = -3$ as the leading power in the coupling, which severely worsens the convergence as $a \searrow 0$. Nonetheless continuum extrapolations in lattice QCD are typically still performed using the naive classical $a^{n_{\min}}$ power law, due to a lack of a theoretical prediction of these corrections and a partial unawareness of the issue.

In this thesis the leading corrections from Wilson and Ginsparg-Wilson (GW) fermion actions as well as pure gauge actions are determined at $O(a)$ and $O(a^2)$ for lattice QCD as well as lattice pure gauge theory. This information suffices for spectral quantities such as hadron masses, while in general each local field involved in a vacuum expectation value will introduce an additional set of powers in the coupling that must be computed separately. Limiting considerations to lattice artifacts originating from the lattice action, each power $\hat{\gamma}_i^{(n_{\min})}$ corresponds to an irrelevant operator of mass-dimension $(n_{\min} + 4)$. These irrelevant operators form a minimal operator basis parametrising all lattice artifacts originating from the lattice action at $O(a^{n_{\min}})$ in terms of a continuum Symanzik Effective theory. The values of $\hat{\gamma}_i^{(n_{\min})}$ are proportional to the 1-loop coefficients of the anomalous dimensions of the minimal operator basis and thus can be obtained through renormalisation of the operator basis to 1-loop order in continuum QCD, here using the $\overline{\text{MS}}$ renormalisation scheme.

The lower bound of the spectrum of leading powers in the coupling is found to be close to zero in the case of lattice QCD with Wilson or GW quarks such that no problems with a worsened convergence to the continuum limit as $a \searrow 0$ are to be expected. However, full lattice QCD at $O(a^2)$ with Wilson or GW fermions has a dense spectrum of leading couplings. This makes finding the operator of the minimal basis giving the dominant contributions to the lattice artifacts difficult. Also complicated cancellations or pile-ups of lattice artifacts may occur. At the same time due to the large number of operators relevant at $O(a^2)$ the spectrum spans a range of roughly $1 \sim 2.5$ powers in the coupling for GW and $O(a)$ improved Wilson quarks respectively.

For lattice pure gauge theory with and without the Gradient flow only three respectively two operators are relevant for the action with leading powers in the coupling of $\hat{\gamma}^{(2)} \in \{0, 7/11, 63/55\}$, where the zero only occurs for the Gradient flow.

Now the leading corrections from lattice actions with Wilson or GW quarks to classical $a^{n_{\min}}$ -scaling are known and should be used when performing the continuum extrapolation both through explicit use in the fit ansatz and as an orientation to estimate the systematic uncertainty inherent to the continuum limit.

Keywords:

Lattice QCD, Symanzik Effective Field Theory, Lattice artifacts, Continuum limit

Zusammenfassung

Einer der finalen Schritte in Simulationen von Gitter Quantenchromodynamik (QCD) oder Gittereichtheorie ist die Kontinuumsextrapolation, um die eigentliche Kontinuumsphysik zu extrahieren. Diese Extrapolation beruht stark auf Annahmen über die asymptotische Abhängigkeit vom Gitterabstand a , was zu systematischen Unsicherheiten des Kontinuumschlimes führt. In klassischen Feldtheorien ist die asymptotische Form schlicht eine Potenzreihe im Gitterabstand, wobei die führende Potenz $a^{n_{\min}}$, $n_{\min} \in \mathbb{N}$ von der gewählten Diskretisierung auf dem Gitter abhängt. Die Quantenkorrekturen in Gitter QCD und Gittereichtheorie brechen dieses Verhalten. Für asymptotisch freie Theorien wie Gitter QCD ergibt sich stattdessen das führende asymptotische Verhalten $a^{n_{\min}} [\alpha_R(1/a)]^{\hat{\gamma}_i^{(n_{\min})}}$ mit renormierter Kopplung $\alpha_R(1/a) \sim -1/\ln(a\Lambda_{\text{QCD}})$, der Renormierungsgruppen Invarianten Skala Λ_{QCD} sowie den reellen Zahlen $\hat{\gamma}_i^{(n_{\min})}$. Abhängig von den Werten von $\hat{\gamma}_i^{(n_{\min})}$ wird die Multiplikation mit den entsprechenden Potenzen der Kopplung die Konvergenz für $a \searrow 0$ beschleunigen oder verlangsamen, in jedem Fall wird für $\hat{\gamma}_i^{(n_{\min})} \neq 0$ die Annäherung an den Kontinuumschlimes modifiziert. Ein besonders beunruhigendes Beispiel ist das nicht-lineare $O(3)$ Modell, für das Balog, Niedermayer und Weisz [1, 2] $\min(\hat{\gamma}_i^{(2)}) = -3$ gefunden haben, wodurch die Konvergenz $a \searrow 0$ stark verlangsamt wird. Dennoch wird in Gitter QCD noch immer die Kontinuumsextrapolation mit Hilfe des naiven klassischen $a^{n_{\min}}$ durchgeführt, was sowohl dem Mangel einer theoretischen Vorhersage für die führenden Korrekturen zuzuschreiben ist als auch der teilweisen Unkenntnis der Problematik geschuldet ist.

Im Rahmen dieser Arbeit werden die führenden Korrekturen der Wilson und Ginsparg-Wilson (GW) Fermion Wirkung sowie verschiedener Gitterwirkungen des Eichfelds auf $O(a)$ und $O(a^2)$ für Gitter QCD und Gittereichtheorie bestimmt. Kenntnis dieser Korrekturen ist ausreichend für spektrale Größen wie beispielsweise Hadronmassen, während im allgemeinen Fall jedes lokale Feld, das Teil des Vakuumerwartungswerts ist, zusätzliche Potenzen nötig macht, welche separat bestimmt werden müssen. Unter Beschränkung auf Gitterartefakte die von der Gitterwirkung herrühren, kann jede Potenz $\hat{\gamma}_i^{(n_{\min})}$ einem irrelevanten Operator mit Massendimension $(n_{\min} + 4)$ zugeordnet werden. Diese irrelevanten Operatoren formen eine minimale Basis und parametrisieren alle Gitterartefakte der Gitterwirkung auf $O(a^{n_{\min}})$ als Teil einer Symanzik Effektiven Theorie. Die Werte der $\hat{\gamma}_i^{(n_{\min})}$ sind proportional zu den 1-Schleifen Koeffizienten der anomalen Dimensionen der minimalen Operatorbasis und können somit aus der 1-Schleifen Renormierung der Operatorbasis in Kontinuums QCD, hier unter Verwendung des $\overline{\text{MS}}$ Renormierungsschemas, bestimmt werden.

Die untere Schranke des Spektrums der führenden Potenzen in der Kopplung liegt nahe null für Gitter QCD mit Wilson oder GW Quarks, weshalb keine Probleme durch eine verschlechterte Konvergenz zum Kontinuumschlimes für $a \searrow 0$ zu erwarten sind. Allerdings ist das Spektrum der führenden Kopplungen für $O(a^2)$ von Wilson und GW Quarks sehr dicht. Dadurch lässt sich der Operator der minimalen Basis mit dominierendem Beitrag zu den Gitterartefakten schlecht bestimmen und ein kompliziertes Zusammenspiel der verschiedenen Gitterartefakte durch Aufsummieren der verschiedenen Beiträge mit gleichem oder umgekehrtem Vorzeichen ist möglich. Gleichzeitig tragen viele verschiedene Operatoren auf $O(a^2)$ bei, sodass das Spektrum einen Bereich von $1 \sim 2.5$ Potenzen in der Kopplung für GW beziehungsweise $O(a)$ verbesserte Wilson Quarks abdeckt.

Für Gittereichtheorie mit und ohne Verwendung des Gradient flows tragen nur drei respektive zwei Operatoren für die Wirkung bei, was zu den führenden Potenzen $\hat{\gamma}^{(2)} \in \{0, 7/11, 63/55\}$ in der Kopplung führt, wobei die Null nur für den Gradient flow auftritt.

Nun, da die führenden Korrekturen der Gitterwirkungen mit Wilson und GW Quarks zur klassischen $a^{n_{\min}}$ -Steigung bekannt sind, sollten diese für die Kontinuumsextrapolation genutzt werden, sowohl für den Ansatz der Extrapolationsfunktion als auch als Orientierungshilfe, um die inhärente systematische Unsicherheit des Kontinuumschlimes abzuschätzen.

Schlagwörter:

Gitter QCD, Symanzik Effektive Feldtheorie, Gitterartefakte, Kontinuumschlimes

List of Publications

Some results of this thesis have already been published in the following articles:

Journal Publications

N. Husung, P. Marquard, R. Sommer, *Asymptotic behavior of cutoff effects in Yang-Mills theory and in Wilson's lattice QCD*, Eur. Phys. J. C **80**, 200 (2020), 1912.08498

Proceedings

N. Husung, P. Marquard, R. Sommer, *Logarithmic corrections to \mathbf{a}^2 scaling in lattice Yang Mills theory*, in *37th International Symposium on Lattice Field Theory (LATTICE2019)* (2019), 1912.02058

N. Husung, A. Nada, R. Sommer, *Yang Mills short distance potential and perturbation theory*, in *37th International Symposium on Lattice Field Theory (LATTICE2019)* (2020)

Contents

1	Introduction	1
2	(Lattice) QCD	5
3	Renormalisation	10
3.1	Asymptotic freedom	11
3.2	Perturbative renormalisation	11
3.2.1	Gauge-fixing	12
3.2.2	Renormalisation of n -point functions and composite operators	14
3.3	Renormalisation Group	16
4	Symanzik Effective Theory	18
4.1	Matching to the lattice theory	19
4.1.1	Perturbative off-shell matching with background fields	22
4.1.2	Lattice artifacts from the renormalisation condition on the lattice	23
4.2	Asymptotic behaviour of lattice artifacts	25
5	Symanzik’s Effective Theory of lattice QCD	27
5.1	Commonly used lattice actions	27
5.1.1	Gauge actions	27
5.1.2	Ginsparg-Wilson fermions	28
5.1.3	Twisted-mass fermions	29
5.1.4	Staggered fermions	31
5.2	Minimal bases for the Symanzik Effective Theory	32
5.2.1	Purely gluonic operators	33
5.2.2	Fermion bilinear operators	34
5.2.3	Four fermion operators	36
5.3	Extension of pure gauge theory to static quarks	37
5.4	Connection of the minimal basis to tmQCD	38
6	Renormalisation of the minimal operator basis	40
6.1	Strategy	40
6.2	Renormalisation of the operator basis in pure gauge theory	42
6.3	Renormalisation of the operator basis in full QCD	43
6.4	Renormalisation of the flavoured 4-fermion operator basis at $N_f = 3$	58
7	Yang-Mills Gradient flow	61
7.1	Operator basis	62
7.2	Strategy	62
7.2.1	Insertion of an $O(4)$ invariant operator	63
7.2.2	Insertion of an $O(4)$ broken operator	66

7.3	NLO matrix elements and the 1-loop mixing matrix	66
8	Consequences and outlook for lattice YM theory and lattice QCD	68
8.1	Lattice YM theory and lattice QCD	68
8.2	Twisted mass QCD with Wilson fermions	72
8.3	Impact of non-zero anomalous dimensions on the continuum extrapolation	73
8.3.1	Symanzik improvement versus improvement of an expectation value	74
8.3.2	Using $\hat{\Gamma}_i$ for an error estimate	81
8.4	Using multiple lattice fermion actions	85
9	Discussion	87
A	Conventions	92
A.1	Abbreviations	92
A.2	Index conventions	92
A.3	$\mathfrak{su}(N)$ algebra	93
A.4	Miscellaneous	94
B	Dimensional regularisation: rules and tools	95
B.1	Useful integrals	95
C	Reduction of the operator basis	97
C.1	Total divergence operators	98
C.2	Equation of motion vanishing operators	99
D	Implementation of the FORM scripts	100
D.1	Obtain Feynman rules from the operator basis	100
D.2	Determine contributing Feynman graphs (QGRAF)	106
D.3	Apply Feynman rules	111
D.4	Use of dimensional regularisation	111
E	Listing of checks and reference values	112
E.1	Reference values	112
E.2	On-shell renormalisation of the minimal basis at non-zero momentum	113
F	Miscellaneous	115
F.1	Expansion of connected graphs yields connected graphs	115
F.2	Conversion between α , g^2 etc.	116
	Bibliography	117

Chapter 1

Introduction

The *Standard Model* (SM) of particle physics has evolved significantly from the 1950s on, where only Quantum Electrodynamics were fully established. Generalisation to non-abelian gauge theories [6] allowed the formulation of more general $SU(N)$ gauge symmetries needed for both the weak and strong interactions. Firstly, the introduction of electroweak unification [7–9] in conjunction with electroweak symmetry breaking through the Higgs mechanism [10, 11] established the electroweak sector. The experimental confirmation of the predicted massive gauge bosons Z [12–14] and W^\pm [14–17] as well as the scalar Higgs boson [18, 19], put the electroweak sector on solid grounds. Secondly, the existence of the Ω^- and Δ^{++} baryon in the ordering scheme called the “eightfold-way” [20, 21] seemingly violated the Pauli principle unless additional quantum numbers were introduced. This led to establish *Quantum Chromodynamics* (QCD) [22] as the theory of strong interactions with $SU(3)$ colour charged quarks [23, 24]. The discovery of asymptotic freedom [25–28], the experimental measurement [29] of partons [30] confirming the quark model and the extension to six different quark flavours as well as experimental evidence of hadronic 3-jets [31] round up today’s understanding of QCD.

Nowadays, the SM contains three of the fundamental interactions, namely the weak, electromagnetic (em) and strong interaction. Due to the lack of a renormalisable formulation of Quantum Gravity, the fourth fundamental interaction is still missing, which restricts the model to special relativity. The SM describes the interaction of fermionic matter, in form of three generations of leptons and quarks each, through the gauge bosons, namely the W^\pm and Z boson and the photon of the electroweak sector and the gluons of the strong sector as well as the scalar Higgs boson. While quarks couple to all the bosons, the leptons do not couple to gluons, i.e., they play no role in QCD. Technically the SM is a renormalisable *Quantum Field Theory* (QFT), which is fully described by the Lagrangian

$$\mathcal{L}_{\text{SM}} = \mathcal{L}_{\text{weak}} + \mathcal{L}_{\text{em}} + \mathcal{L}_{\text{QCD}} + \mathcal{L}_{\text{Higgs}}. \quad (1.1)$$

This thesis focuses on QCD, i.e. only a fraction of the SM is covered here. For an explicit expression of the (other) terms see e.g. [32].

The current SM is in good overall agreement with experimental observations, see e.g. [33, 34]. However, there are also some inadequacies of the SM. A prominent example is dark matter, which has been observed through gravitational effects e.g. in the Coma cluster [35] or in a galaxy cluster merger [36], suggesting that it accounts for up to 85% of the matter in the universe, while not being predicted by the SM. Another difficulty presents the apparent asymmetry of matter and anti-matter in the universe while the SM is inherently symmetric. Furthermore, the SM does not account for massive neutrinos as the electroweak symmetry breaking introduces only mass-terms for the electrically charged leptons and quarks while neutrinos should remain massless. This is contradicted by the observation of neutrino-oscillations [37, 38] suggesting that neutrinos in fact have a mass. The current upper bound of the neutrino masses is $< 1.1 \text{ eV}$ [39].

To further test the SM there are ongoing searches for new physics behind the SM (BSM),

see e.g. [32, p. 889ff.], as well as precision measurements. Two examples of such precision measurements, both with some tension to the SM predictions, are the search for violations of lepton universality, see e.g. [40, 41], and the anomalous magnetic moment of the muon which has a tension of $\sim 3.7\sigma$ with the SM prediction [42]. For the latter QCD gives a small ($\sim 0.006\%$) but important contribution due to the precision at which all the other contributions are known. However, the current most accurate values of the QCD contribution, see e.g. [43–45], are not from first principles but use experimental data as input. To avoid experimental input one needs a first principle prediction, which can be obtained from lattice QCD, see e.g. [46–48], although not yet with competitive uncertainties (and still $\sim 2\sigma$ discrepancies between different groups).

In order to give reliable predictions for the SM all contributions as well as input parameters must be under control. The most difficult contributions are those from QCD as it is in general a non-perturbative theory. In particular the hadron spectra, i.e. strongly coupled bound states such as the pions, kaons or even the neutrons, are entirely non-perturbative quantities. Thus perturbation theory, i.e. an expansion in the coupling, cannot be applied in contrast to the electroweak sector. This changes only in the high energy regime at energies much larger than $\Lambda_{\text{QCD}} \sim 300 \text{ MeV}$ [49], where the coupling of QCD becomes small due to the running of the coupling towards asymptotic freedom. Below and around such energies other approaches are required. The focus lies here on lattice QCD as one possibility.

The general idea of lattice QCD is to discretise the continuum Euclidean QCD onto a 4D hypercubic lattice with lattice spacing a , where the Euclidicity ensures that the QCD Boltzmann weight $\exp(-\int d^4x \mathcal{L}_{\text{QCD}}(x))$ in the path integral is positive and thus offers a viable probability distribution for Monte Carlo simulations. The lattice spacing a introduces a momentum cut-off $|p_\mu| \leq \frac{\pi}{a} \forall \mu \in \{0, 1, 2, 3\}$ suppressing all contributions above this threshold. This introduces a dependence on the cut-off and leads to so called *lattice artifacts* since higher momentum contributions are neglected. Additionally lattice regularisation will inevitably break some symmetries of the theory, such as rotation symmetry, which is then reduced to a symmetry under discrete rotations of 90° around any spacetime axis, while gauge symmetry is kept intact. Breaking symmetries of the continuum theory introduces new physics, i.e. new interactions, at finite lattice spacing which allows for additional lattice artifacts. All lattice artifacts are deviations from the continuum physics of interest and thus need to be eliminated. This can be achieved through the continuum limit, where one extrapolates towards zero lattice spacing using numerical data at small but finite lattice spacings. To get better control over this extrapolation an understanding of the leading lattice artifacts is needed.

In a classical field theory one would expect for the lattice artifacts power corrections of the form a^n with $n \in \mathbb{N}$ and minimal value $n \geq n_{\text{min}}$ depending on the chosen lattice discretisation. The quantum nature of lattice QCD spoils this behaviour by introducing multiplicative corrections to this naive expectation. Due to asymptotic freedom of QCD the renormalised coupling $\alpha_{\text{R}}(1/a) = g_{\text{R}}^2(1/a)/(4\pi) \sim -1/\ln(a\Lambda_{\text{QCD}})$ becomes small for decreasing lattice spacing, i.e. increasing energy scale $1/a$. The leading corrections are then of the form $a^n[\alpha_{\text{R}}(1/a)]^{\hat{\gamma}}$, where the number $\hat{\gamma}$ can be extracted perturbatively from the 1-loop anomalous dimensions of higher dimensional operators parametrising the lattice artifacts in a local effective Lagrangian of the *Symanzik effective theory* (SET) [50–53], see also [54, p. 39ff.]. The canonical mass-dimension of such operators is increased by n compared to the associated continuum quantity, i.e., for small enough lattice spacing the leading contributions are parametrised by a minimal basis of operators with mass-dimension increased by n_{min} . For the Lagrangian this means that the operators of the leading order have canonical mass-dimension $4 + n_{\text{min}}$. Whether the lattice spacing is in fact sufficiently small must be checked empirically and is guided by the relevant scales of QCD such as $a \ll 1/\Lambda_{\text{QCD}}, 1/M_\pi, \dots$, where M_π is the mass of the pion as the lowest lying bound state of QCD.

The corrections due to lattice artifacts can be quite sizeable as shown by Balog, Niedermayer and Weisz [1, 2] for the non-linear $O(3)$ model. Due to values of $\hat{\gamma}$ as low as $\hat{\gamma} = -3$ this model seemed to behave more like a^1 power corrections rather than the naively expected a^2 effects over a large range of lattice spacings. Nonetheless the usually assumed functional dependence in contin-

uum extrapolations of lattice QCD is just the naive power correction, due to a lack of a theoretical prediction of these corrections and a partial unawareness of the issue. This thesis aims at computing the leading corrections originating from the lattice action to the naive classical power law in form of the $\hat{\gamma}$ with use of SET and thus putting continuum extrapolations in lattice QCD on more solid grounds. However, depending on the quantities of interest the lattice action is only one possible source of lattice artifacts. While for spectral quantities such as masses other contributions cancel out this is not in general the case and thus potentially requires additional computations for each quantity of interest. The anomalous dimensions for contributions from the lattice action remain the same.

The minimal basis of higher dimensional operators in the SET depends on the chosen lattice action, i.e. the specifics of the lattice discretisation, as different continuum symmetries get broken. To keep the minimal basis somewhat compact but allow for many different lattice actions a careful choice of the symmetries imposed on the basis is required. Firstly, no assumptions on the masses of the quarks are made, i.e. the basis is valid for general massive QCD, but contains also the cases of massless and mass-degenerate QCD as subsets. Secondly, flavour violating interactions are rejected such that so called *staggered fermions* [55, 56] are excluded as this enlarges the basis significantly. The choice of the action also decides the canonical mass-dimension $4 + n_{\min}$ of the leading order operators contributing to the effective Lagrangian. In case $n_{\min} = 2$ the action is referred to as $O(a)$ -improved, as no contributions of the form $a[\alpha_R(1/a)]^{\hat{\gamma}+l}$ at any order l remain. Whether this is due to symmetry reasons like in typical pure gauge actions [57] or due to non-perturbative improvement, see e.g. for the case of Wilson QCD [58], does not matter. In contrast $(n_I - 1)$ -loop perturbative $O(a)$ -improved lattice actions still yield corrections of the form $a[\alpha_R(1/a)]^{\hat{\gamma}+n_I}$ with typical values $n_I = 2$ and $n_I = 1$ for 1-loop or tree-level (TL) improved actions and $n_I = 0$ for the unimproved case. Improvement can of course also be performed at $O(a^2)$ as e.g. in the case of perturbative improvement of pure gauge theory [57, 59–62].

Instead of systematically reducing all lattice artifacts through use of SET and introducing proper counterterms into the lattice action (and local fields) one may also individually improve observables, see e.g. [63–68]. This approach is typically employed for short-distance observables such as the coupling $\alpha_{qq}(1/r)$ defined through the force between two static quarks separated by distance r . In contrast to SET this keeps the leading logarithms unchanged and thus lacks Renormalisation Group Improvement. Knowing the leading anomalous dimensions $\hat{\gamma}$ these leading logarithms can be eliminated as well ensuring that expectation values, which are TL-improved and Renormalisation Group improved, have lattice artifacts of the form $a^{n_{\min}}[\alpha_R(1/a)]^{\hat{\gamma}+1}$ rather than $a^{n_{\min}}[\alpha_R(1/a)]^{\hat{\gamma}+1} \ln(a)$ as the name tree-level improvement suggests. For perturbative improvement with $n_I > 0$ and Renormalisation Group Improvement one also needs the subleading coefficients of the anomalous dimensions, which are beyond the scope of this thesis.

In chapter 2 the basic concepts of lattice QCD are highlighted in terms of Wilson’s lattice QCD and the connection to continuum QCD are pointed out. General aspects of renormalisation and the concept of the background field method for perturbative operator renormalisation with its pros and cons are explained in chapter 3, where also the continuum limit and its connection to asymptotic freedom are elaborated. The background field method is central to our approach on the 1-loop renormalisation of the minimal operator basis, which then allows to obtain the 1-loop anomalous dimensions $\hat{\gamma}$. In chapter 4 the Symanzik Effective theory is introduced with focus on lattice QCD again using Wilson’s lattice QCD as an example to explain the general idea of Symanzik Effective theory. Also some ideas for matching the effective theory to the lattice theory perturbatively are highlighted. Eventually the minimal operator basis at mass-dimensions 5 and 6 is derived in chapter 5. The minimal basis is compatible to all the symmetries of Wilson’s lattice QCD, thus including Ginsparg-Wilson fermions with lattice chiral symmetry as a subset. Also the connection of this minimal basis to twisted mass QCD with Wilson fermions and to static quarks in the case of pure gauge theory is discussed. The actual renormalisation of the minimal operator basis takes place in chapter 6 including diagonalisation of the mixing matrix to obtain the 1-loop anomalous dimension for each element of the diagonalised minimal basis. Before discussing the

implications of the results for the anomalous dimensions for pure gauge theory and full QCD we take a short detour in chapter 7 to the Yang-Mills Gradient flow and compute the only additionally missing anomalous dimension relevant at zero flow-time for the Gradient flow in pure gauge theory. In chapter 8 the overall spectrum of anomalous dimensions is discussed in detail taking into account the tree-level coefficients and highlighting some more elaborate applications in pure gauge theory with and without the Gradient flow, some ideas on how to use these spectra for full QCD and an outlook on how to treat the case of different lattice actions for separate flavours. Finally all results are summarised again in chapter 9, what they imply and what remains to be done or seen.

Chapter 2

(Lattice) QCD

Euclidean QCD as a theory separated from the SM is fully described by the continuum Lagrangian

$$\mathcal{L}_{\text{QCD}}(x) = -\frac{1}{2g_0^2} \text{tr} (F_{\mu\nu}(x)F_{\mu\nu}(x)) + \bar{\Psi}(x)[\gamma_\mu D_\mu + M]\Psi(x), \quad (2.1)$$

where $\Psi = (\psi^1, \dots, \psi^{N_f})$ are the quarks with N_f different flavours and the corresponding anti-quarks $\bar{\Psi} = (\bar{\psi}^1, \dots, \bar{\psi}^{N_f})$. Their masses are given by $M = \text{diag}(m^1, \dots, m^{N_f})$. Every (anti-)quark is an anticommuting spinor with 4 Dirac components, each being a colour vector of size N . The 4×4 hermitian γ -matrices of the Euclidean Clifford algebra

$$\{\gamma_\mu, \gamma_\nu\} = 2\delta_{\mu\nu} \mathbb{1}_{4 \times 4}, \quad (2.2)$$

act on the spinor space while the covariant derivative $D_\mu = \partial_\mu + A_\mu$ couples the N colour components of the quarks to the algebra valued gluons $A_\mu = A_\mu^a T^a \in \mathfrak{su}(N)$. Here T^a are the $N^2 - 1$ anti-hermitian generators of the $\mathfrak{su}(N)$ algebra fulfilling

$$[T^a, T^b] = f^{abc} T^c, \quad \text{tr}(T^a T^b) = -T_F \delta^{ab}, \quad (2.3)$$

where f^{abc} is the fully antisymmetric structure constant and $T_F = 1/2$ is the chosen normalisation. For more details on the $\mathfrak{su}(N)$ algebra see also appendix A.3. Gluodynamics, i.e. the propagation and self-interaction of the gluons, are described by the term containing the field strength tensor $F_{\mu\nu} = [D_\mu, D_\nu]$. In the absence of quarks, i.e. $N_f = 0$, this is usually referred to as *pure gauge* theory or *Yang-Mills* (YM) theory.

The whole theory is invariant under **local** gauge transformations $\Omega(x) = \exp(\omega^a(x)T^a) \in \text{SU}(N)$ with $\omega^a \in \mathbb{R}$

$$\bar{\Psi}(x) \rightarrow \bar{\Psi}(x)\Omega^\dagger(x), \quad \Psi(x) \rightarrow \Omega(x)\Psi(x), \quad D_\mu \rightarrow \Omega(x)D_\mu\Omega^\dagger(x), \quad (2.4)$$

where $\Omega^\dagger(x)$ is the hermitian conjugate of $\Omega(x)$. This gauge symmetry is the defining property of gauge theories.

With help of the action

$$S_{\text{QCD}} = \int d^4x \mathcal{L}_{\text{QCD}}(x) \quad (2.5)$$

one can define n -point functions of local fields Φ_i , which may be fundamental fields of the theory or composite ones,

$$\langle \Phi_1(x_1) \dots \Phi_n(x_n) \rangle = \frac{1}{\mathcal{Z}} \int \mathcal{D}A \mathcal{D}\bar{\Psi} \mathcal{D}\Psi \Phi_1(x_1) \dots \Phi_n(x_n) \exp(-S_{\text{QCD}}[A, \bar{\Psi}, \Psi]), \quad (2.6)$$

$x_i \neq x_j \forall i \neq j$

with the *partition function*

$$\mathcal{Z} = \int \mathcal{D}A \mathcal{D}\bar{\Psi} \mathcal{D}\Psi \exp(-S_{\text{QCD}}[A, \bar{\Psi}, \Psi]) \quad (2.7)$$

acting as normalisation and the measure of the path integral $\mathcal{D}A = \prod_{x,\mu} dA_\mu(x)$, $\mathcal{D}\Psi = \prod_x d\Psi(x)$ and $\mathcal{D}\bar{\Psi} = \prod_x d\bar{\Psi}(x)$. Such n -point functions are the central quantities both in perturbation theory to compute scattering amplitudes of fundamental fields and lattice QCD to extract physical matrix elements or the spectrum of hadrons from n -point functions of composite fields with appropriate quantum numbers.

In general the partition function and the related n -point functions are mathematically not well-defined without the introduction of a regulator. In lattice QCD the lattice spacing a plays this role and serves as a UV-regulator since it limits the momenta $a|p_\mu| \leq \pi$ in all four spacetime directions $\mu \in \{0, 1, 2, 3\}$. Historically, the first formulation of QCD on a lattice was Wilson's lattice QCD [69, 70]

$$S^{\text{W}} = S_{\text{G}}^{\text{W}} + S_{\text{F}}^{\text{W}}, \quad S_{\text{G}}^{\text{W}} = \frac{1}{g_0^2} \sum_{\substack{x \\ \mu \neq \nu}} \text{Re tr}(\mathbb{1} - U_{\mu\nu}(x)), \quad S_{\text{F}}^{\text{W}} = a^4 \sum_x \bar{\Psi}(x) [\hat{D}^{\text{W}} + M] \Psi(x), \quad (2.8)$$

where the sum of x runs over all lattice sites. The Wilson Dirac operator \hat{D}^{W} is defined as [70]

$$\begin{aligned} \hat{D}^{\text{W}} &= \frac{1}{2} \{ \gamma_\mu (\nabla_\mu^* + \nabla_\mu) - ar \nabla_\mu^* \nabla_\mu \}, \quad r \in [0, 1], \\ \nabla_\mu^* \Psi(x) &= \frac{\Psi(x) - U_\mu^\dagger(x - a\hat{\mu}) \Psi(x - a\hat{\mu})}{a}, \quad \nabla_\mu \Psi(x) = \frac{U_\mu(x) \Psi(x + a\hat{\mu}) - \Psi(x)}{a}. \end{aligned} \quad (2.9)$$

In the original paper [69] the term with $\nabla_\mu^* \nabla_\mu$ was absent, which is today known as *naive fermions*, and has only later [70] been added in a similar form to the one given here. The necessity of this term can be seen by considering the free ($U_\mu = \mathbb{1}$) propagator of massless Wilson fermions [71, p. 111ff.] in momentum space, for the definition of the lattice Fourier transform see appendix A.4,

$$[\tilde{D}_{\text{free}}^{\text{W}}(p)]^{-1} = a \left[\sum_\mu \{ i\gamma_\mu \sin(ap_\mu) - r \cos(ap_\mu) \} + 4r \right]^{-1} \quad (2.10)$$

$$= a \frac{4r - \sum_\mu [r \cos(ap_\mu) + i\gamma_\mu \sin(ap_\mu)]}{[4r - r \sum_\mu \cos(ap_\mu)]^2 + \sum_\mu \sin^2(ap_\mu)}. \quad (2.11)$$

One finds already in the first line that $[\tilde{D}_{\text{free}}^{\text{W}}(p)]^{-1}$ has a pole at $p = (0, 0, 0, 0)$. Since $ap_\mu \in]-\pi, \pi]$ there are additional poles if $r = 0$

$$ap \in \{(\pi, 0, 0, 0), (\pi, \pi, 0, 0), (\pi, \pi, \pi, 0), (\pi, \pi, \pi, \pi), \text{and permutations}\}. \quad (2.12)$$

These additional poles are unphysical and lead to so called *doublers* which manifest as additional degenerate flavours, i.e. instead of a single flavour one would simulate 16 degenerate ones. Setting $r = 1$, which is our default choice, decouples the doublers in the continuum limit as their masses scale like $1/a$.

The *plaquette* variable is defined as

$$U_{\mu\nu}(x) = U_\mu(x) U_\nu(x + a\hat{\mu}) U_\mu^\dagger(x + a\hat{\nu}) U_\nu^\dagger(x), \quad (2.13)$$

with *gauge links* $U_\mu(x) \in \text{SU}(N)$ located on the link connecting the lattice points x and $x + a\hat{\mu}$. In contrast to the continuum gauge field these gauge links are elements of the gauge group rather than the algebra. This ensures invariance of the action under the lattice gauge transformation $\Omega(x) \in \text{SU}(N)$

$$\bar{\Psi}(x) \rightarrow \bar{\Psi}(x) \Omega^\dagger(x), \quad \Psi(x) \rightarrow \Omega(x) \Psi(x), \quad U_\mu(x) \rightarrow \Omega(x) U_\mu(x) \Omega^\dagger(x + a\hat{\mu}), \quad (2.14)$$

i.e. the gauge links transform like the continuum Wilson line, see e.g. [72, p. 491],

$$W(x, y) = \text{Pexp} \left(- \int_y^x dz_\nu A_\nu(z) \right) \quad (2.15)$$

with the path-ordered exponential Pexp increasing from the right to the left and the special choice $y = x + a\hat{\mu}$.

To give an example on how to extract e.g. the pion mass from the lattice consider the connected pseudoscalar 2-point function in infinite volume

$$C_{\pi^0\pi^0}(x; a) = \langle P^0(x) P^{0\dagger}(0) \rangle_{\text{lattice}}^{\text{con}} = \langle P^0(x) P^{0\dagger}(0) \rangle_{\text{lattice}} - \langle P^0(x) \rangle_{\text{lattice}} \langle P^{0\dagger}(0) \rangle_{\text{lattice}}, \quad |x| > 0, \\ P^0(x) = \frac{1}{\sqrt{2}} [\bar{u}\gamma_5 u - \bar{d}\gamma_5 d](x) \quad (2.16)$$

where u and d denote up and down quark flavours. Eq. (2.16) can be rewritten in operator notation using the Transfer matrix $\hat{\mathbb{T}} = e^{-a\hat{H}(a)}$ [73], where $\hat{H}(a)$ is the Hamiltonian of the lattice theory,

$$C_{\pi^0\pi^0}(x; a) = \lim_{T \rightarrow \infty} \frac{\text{tr} \left(\hat{\mathbb{T}}^{T/a-x_0/a} P^0(x_0, \mathbf{x}) \hat{\mathbb{T}}^{x_0/a} P^{0\dagger}(0, \mathbf{0}) \right)}{\text{tr} \hat{\mathbb{T}}^{T/a}}. \quad (2.17)$$

Summing over all spatial points \mathbf{x} projects all states annihilated at time slice x_0 to $\mathbf{p} = \mathbf{0}$, such that the Hamiltonian yields the bound states with appropriate quantum numbers at rest

$$a^3 \sum_{\mathbf{x}} C_{\pi^0\pi^0}(x_0, \mathbf{x}; a) = \lim_{T \rightarrow \infty} \frac{1}{\text{tr} \hat{\mathbb{T}}^{T/a}} \sum_{m,n} |\langle m | \tilde{P}^0(x_0, \mathbf{0}) | n \rangle|^2 e^{-E_n(a)x_0} e^{-E_m(a)[T-x_0]} \quad (2.18)$$

$$= \sum_n |\langle 0 | \tilde{P}^0(x_0, \mathbf{0}) | n \rangle|^2 e^{-E_n(a)x_0} \quad (2.19)$$

$$= |A|^2(a) e^{-M_\pi(a)x_0} \left\{ 1 + \mathcal{O}(e^{-\Delta E(a)x_0}) \right\}, \quad (2.20)$$

where M_π is the mass of the lowest lying bound state, here the pion, ΔE the energy gap to the next eigenstate, $|0\rangle$ the vacuum and $|A|^2$ the amplitude of the contribution of the pion. The pion mass at finite lattice spacing can now be extracted through

$$aM_\pi(a) = \lim_{x_0 \rightarrow \infty} \ln \frac{\sum_{\mathbf{x}} C^0(x_0, \mathbf{x}; a)}{\sum_{\mathbf{x}} C^0(x_0 + a, \mathbf{x}; a)}, \quad (2.21)$$

where the $x_0 \rightarrow \infty$ limit ensures that no heavier bound states contribute.

The example of the pion mass assumed an infinite volume. However, to compute e.g. the 2-point function in eq. (2.16) through Monte Carlo simulations of lattice QCD a finite number of integrals is required. While discretising spacetime reduces the measure in eq. (2.7) to a countable number of differentials, the volume must be limited as well. This is achieved by introducing a finite box of size $T \times L^3$ with temporal extent T and spatial extent L respectively and some boundary conditions. The simplest choice are periodic boundaries, which keep translation invariance intact. There exist also alternative boundary conditions. An important class are non-periodic boundary conditions in time direction while spatial boundaries remain periodic, see e.g. the Schrödinger functional [74, 75] or open boundary conditions [76]. This leads to three distinct systematic errors contributing to lattice quantities like the pion mass:

1. *Lattice artifacts* are due to the non-zero lattice spacing, which corresponds to a momentum cut-off $|p_\mu| \leq \frac{\pi}{a} \forall \mu \in \{0, 1, 2, 3\}$ affecting all high-momentum contributions of the theory. Additionally the discretisation breaks symmetries of the continuum theory such as $\mathcal{O}(4)$

invariance, i.e. the analogue of Minkowskian Lorentz symmetry in Euclidean spacetime. This introduces additional unphysical interactions at finite lattice spacing which are allowed due to the less restrictive symmetries. Which symmetries apart from $O(4)$ invariance are broken depends on the chosen lattice formulation of QCD.

2. *Finite size effects* occur for spatially periodic boundary conditions (assuming for the moment $T \gg L$) due to the self-interaction between different periods [77, 78]. For QCD and sufficiently large volumina the leading corrections are suppressed like $e^{-M_\pi L}$ with M_π being again the pion mass as the lowest bound state of the theory [71, p. 152].
3. *Boundary effects* originate from the interaction of excited states on the boundary with quantities on the bulk of the lattice and therefore are exponentially suppressed by the distance towards the boundary analogously to the finite size effects. They depend on the chosen boundary condition, see e.g. [79–82], and are absent for (anti-)periodic boundaries. The resulting effects amount to both lattice artifacts from the lattice implementation of the boundary and continuum physics as in the continuum theory the boundary persists.

While the focus of this thesis is on the lattice artifacts and therefore all computations are performed in infinite volume the results carry over to finite volume as well as manifolds with boundaries. In the presence of boundaries another set of operators contributes to the local effective Lagrangian directly at the boundary. For more details we refer the reader to the discussion on the Schrödinger functional in [3].

To better understand where additional lattice artifacts come from, we go back to the Wilson action eq. (2.8) and its breaking of $O(4)$ invariance. Due to the reduction of continuous rotation symmetry to discrete rotations of 90° around any spacetime axis only hypercubic symmetry H_4 persists. While, e.g., a 2-point function depends in the continuum theory only on the distance, it has lattice artifacts that will depend on whether the distance is realised along any spacetime axis, a 2-, 3- or 4-dimensional diagonal and so on as rotational symmetry is no longer realised. Other examples of symmetries which tend to get broken apart from spacetime symmetries are global flavour symmetries. A prominent example is the $SU(N_f)_L \times SU(N_f)_R \times U(1)_V$ flavour symmetry of massless continuum QCD, which corresponds to the invariance under a global phase transformation as well as the flavour rotations

$$\begin{aligned} \bar{\Psi}_{L,R} &\rightarrow \bar{\Psi}_{L,R} \exp(-\vartheta_{L,R}^a T_{L,R}^a), & \Psi_{L,R} &\rightarrow \exp(\vartheta_{L,R}^a T_{L,R}^a) \Psi_{L,R}, \\ \Psi_{L,R} &= \frac{1 \pm \gamma_5}{2} \Psi, & \vartheta_{L,R}^a &\in \mathbb{R}, \quad \gamma_5 = \gamma_0 \gamma_1 \gamma_2 \gamma_3, \end{aligned} \quad (2.22)$$

where $\Psi_{L,R}$ denotes left and right-handed spinors and $T_{L,R}^a \in \mathfrak{su}(N_f)_{L,R}$ acts in flavour space on left and right-handed spinors respectively. Each left-handed spinor transforms as a singlet under the right-handed $SU(N_f)_R$ transformations and vice versa. For Wilson's QCD in eq. (2.8) the term carrying $\nabla_\mu^* \nabla_\mu$ breaks this symmetry explicitly and reduces it to $SU(N_f)_V \times U(1)_V$ symmetry, i.e. invariance under a phase transformation as well as the transformation

$$\bar{\Psi} \rightarrow \bar{\Psi} \exp(-\vartheta^a T^a), \quad \Psi \rightarrow \exp(\vartheta^a T^a) \Psi, \quad \vartheta^a \in \mathbb{R}, \quad T^a \in \mathfrak{su}(N_f), \quad (2.23)$$

which is the same symmetry one finds for mass-degenerate QCD with Wilson quarks (and in the continuum theory for mass-degenerate quarks).

To extract continuum physics from lattice QCD the continuum limit $a \searrow 0$ is needed to eliminate all lattice artifacts contributing at finite lattice spacing. For simplicity we consider for now only hadron masses like the previously discussed pion mass, which do not require renormalisation such that we can postpone the discussion of renormalisation to chapter 3. Since the continuum limit is not directly accessible in numerical lattice QCD it is substituted by an extrapolation $a \searrow 0$ of the data measured at different small lattice spacings $a > 0$. The different lattice spacings are chosen by varying the bare coupling g_0 in eq. (2.8), which is the only free parameter of lattice QCD apart from the quark masses.

To extract for example in mass-degenerate 2-flavour lattice QCD a hadron mass M_{had} one needs to determine three distinct scales, where one is the mass $aM_{\text{had}}(a)$ of interest in lattice units, which can be extracted analogously to the pion mass eq. (2.21) by choosing local fields with the appropriate quantum numbers in the 2-point function. The other two scales, here chosen as the pion mass $aM_{\pi}(a)$ and neutron mass $aM_{\text{N}}(a)$, are needed twofold. Firstly to fix the degenerate renormalised quark mass am_{R} in lattice units for different lattice spacings (up to lattice artifacts) one keeps $\frac{aM_{\text{N}}(a)}{aM_{\pi}(a)} = \text{fixed}$. Secondly to translate the lattice units into physical units one expresses the lattice spacing in terms of e.g. the pion mass $a^{\text{scale}} = \frac{aM_{\pi}(a)}{M_{\pi}^{\text{scale}}}$ whose value is taken as input parameter, which is known as *scale setting*. Varying now g_0 allows to extract the ratio $\frac{aM_{\text{had}}(a)}{aM_{\pi}(a)}$ at different small lattice spacings. Since this ratio is a dimensionless quantity it is a constant up to lattice artifacts, which allows to perform the continuum extrapolation

$$\frac{aM_{\text{had}}(a)}{aM_{\pi}(a)} = \frac{M_{\text{had}}}{M_{\pi}^{\text{scale}}} + \mathcal{O}(a^{n_{\text{min}}}), \quad (2.24)$$

where the $\mathcal{O}(a^{n_{\text{min}}})$ is a sloppy notation for the leading terms of the form $a^{n_{\text{min}}}[-\ln(a\Lambda_{\text{QCD}})]^{\hat{\gamma}}$, $\hat{\gamma} \in \mathbb{R}$. Eventually one has M_{had} in terms of the pion mass whose value is known in physical units. Due to finite volume the dimensionless quantity $M_{\pi}L$ (or $M_{\pi}T$) either must remain fixed, if one is interested in finite volume physics, or the limit $M_{\pi}L \rightarrow \infty$ must be taken **before** doing the continuum extrapolation.

Chapter 3

Renormalisation

So far the discussion of the lattice regulator has been primarily focused on its use in lattice simulations at finite lattice spacings. However, the effect of being an ultraviolet (UV) cutoff in momentum space of the form $|p_\mu| \leq \frac{\pi}{a}$ has a more important quantum field theoretical implication as it regulates high momentum contributions which would otherwise amount to so called *UV divergences* or *poles*. In an analytical computation like in lattice perturbation theory (LPT), see e.g. [83], these UV poles will manifest in terms of the form $\frac{1}{a}$ and $\ln^n(a)$ with $n \in \mathbb{N}$. In order to extract the physical and hence finite information these poles must be removed ensuring the existence of the continuum limit.

The mapping [84, 85] of the *bare* expressions carrying poles to the *renormalised* ones having a well defined continuum limit is referred to as *renormalisation*. In case such a mapping exists for all n -point functions, the theory is *renormalisable*, see e.g. [86, p. 116ff.]. This property has been proven to all orders in perturbation theory for asymptotically free theories like QCD [87] and in particular for Wilson’s lattice QCD [88] as well as for massless Ginsparg-Wilson fermions on the lattice [89]. The specific choice of the mapping is referred to as *renormalisation scheme*. To give an example of a renormalisation scheme consider the renormalisation condition for the connected 2-point function of the composite operator $\mathcal{O} = \bar{\Psi}\Psi$

$$\langle \mathcal{O}_{\text{RI}}(x_{\text{RI}}) \mathcal{O}_{\text{RI}}(0) \rangle = \langle \mathcal{O}(x_{\text{RI}}) \mathcal{O}(0) \rangle_{\text{free}} = \text{finite} \quad (3.1)$$

$$= \lim_{a \searrow 0} \left(Z^{\mathcal{O}}(\alpha_{\text{RI}}; a) \right)^2 \langle \mathcal{O}(x_{\text{RI}}) \mathcal{O}(0) \rangle_{\text{lattice}}, \quad (3.2)$$

where the subscript “free” denotes the leading order contribution, e.g. by setting the gauge links to unity on the lattice, and the subscript “lattice” denotes the result obtained nonperturbatively on a lattice with spacing a or through LPT. Eq. (3.1) defines a regulator independent (RI) scheme [90] at renormalisation scale $\mu = |x_{\text{RI}}|^{-1}$ as the equality in the second line can be given for any regulator. Here $\mathcal{O}_{\text{RI}}(y) = Z^{\mathcal{O}}(\alpha_{\text{RI}}; a) \mathcal{O}(y)$ is the renormalised field with renormalisation factor $Z^{\mathcal{O}}(\alpha_{\text{RI}}; a)$ assuming no mixing with other fields under renormalisation as is the case for our example $\mathcal{O} = \bar{\Psi}\Psi$. To obtain the renormalised 2-point function at another separation $y \neq x_{\text{RI}}$ one can then use the prescription

$$\langle \mathcal{O}_{\text{RI}}(y) \mathcal{O}_{\text{RI}}(0) \rangle = \lim_{a \searrow 0} \langle \mathcal{O}(x_{\text{RI}}) \mathcal{O}(0) \rangle_{\text{free}} \frac{\langle \mathcal{O}(y) \mathcal{O}(0) \rangle_{\text{lattice}}}{\langle \mathcal{O}(x_{\text{RI}}) \mathcal{O}(0) \rangle_{\text{lattice}}}. \quad (3.3)$$

The physics described by renormalised n -point functions is independent of the chosen regularisation and can always be translated into other schemes, see e.g. [86, p. 200ff.].

As the renormalisation scale $\mu = |x_{\text{RI}}|^{-1}$ is chosen arbitrarily a change is always possible and

governed by the so called *Renormalisation Group Equation* (RGE) [91, 92]

$$\begin{aligned} \mu^2 \frac{d \langle \mathcal{O}_{\text{RI}}(y) \mathcal{O}_{\text{RI}}(0) \rangle}{d\mu^2} \Big|_{\mu=\frac{1}{|x_{\text{RI}}|}} &= - \lim_{a \searrow 0} |x_{\text{RI}}|^2 \frac{d}{d|x_{\text{RI}}|^2} \left(\frac{\langle \mathcal{O}(x_{\text{RI}}) \mathcal{O}(0) \rangle_{\text{free}}}{\langle \mathcal{O}(x_{\text{RI}}) \mathcal{O}(0) \rangle_{\text{lattice}}} \right) \langle \mathcal{O}(y) \mathcal{O}(0) \rangle_{\text{lattice}} \\ &= 2 \lim_{a \searrow 0} \gamma_{\text{RI}}^{\mathcal{O}}(\alpha_{\text{RI}}; a) \langle \mathcal{O}_{\text{RI}}(y) \mathcal{O}_{\text{RI}}(0) \rangle \Big|_{\mu=\frac{1}{|x_{\text{RI}}|}}, \end{aligned} \quad (3.4)$$

where $\gamma_{\text{RI}}^{\mathcal{O}}$ is the *anomalous dimension* of the operator \mathcal{O} in the RI scheme

$$\gamma_{\text{RI}}^{\mathcal{O}}(\alpha_{\text{RI}}; 0) = \lim_{a \searrow 0} \mu^2 \frac{d \ln Z^{\mathcal{O}}(\alpha_{\text{RI}}; a)}{d\mu^2}. \quad (3.5)$$

3.1 Asymptotic freedom

Asymptotically free theories like QCD have a coupling vanishing as [25–28]

$$\lim_{\mu \rightarrow \infty} \alpha_{\mathcal{S}}(\mu) = 0, \quad (3.6)$$

where \mathcal{S} denotes an arbitrary renormalisation scheme. Thus the coupling is small provided that the renormalisation scale is sufficiently large, which then allows the use of perturbation theory. The renormalisation scale dependence of the coupling is again given by its RGE, the so called *β -function*, for which we give the perturbative series in the small coupling region of a Yang-Mills theory optionally coupling to matter fields,

$$\mu^2 \frac{d\alpha_{\mathcal{S}}}{d\mu^2} = \beta_{\mathcal{S}}(\alpha_{\mathcal{S}}) = -\alpha_{\mathcal{S}}^2 (\beta_0 + \beta_1 \alpha_{\mathcal{S}} + \beta_{2;\mathcal{S}} \alpha_{\mathcal{S}}^2 + \mathcal{O}(\alpha_{\mathcal{S}}^3)). \quad (3.7)$$

Both coefficients β_0 and β_1 are renormalisation scheme independent and $4\pi\beta_0 = \frac{11}{3}C_A - \frac{4}{3}N_f T_F$ for QCD [26]. In general vanishing of the β -function at any coupling $\beta(\alpha_{\mathcal{S}}^*) = 0$ implies that the theory has a fixed point in the renormalisation group evolution. The special case $\alpha_{\mathcal{S}}^* = 0$ can be trivially identified as such a fixed point. A positive sign of β_0 ensures that the theory has a UV stable fixed point at $\alpha_{\mathcal{S}}(\mu) \rightarrow 0$ as $\mu \rightarrow \infty$ [25], because in the vicinity of the fixed point $\alpha_{\mathcal{S}} \simeq \alpha_{\mathcal{S}}^*$ one finds $\beta(\alpha_{\mathcal{S}}) < 0$. The opposite sign for β_0 would yield an infrared (IR) stable fixed point at $\alpha_{\mathcal{S}}(\mu) \rightarrow 0$ as $\mu \rightarrow 0$, breaking asymptotic freedom. As a consequence QCD is asymptotically free if $2N_f < 11C_A$.

The UV fixed point at $\mu \rightarrow \infty$ is the same fixed point one is trying to reach in the continuum limit $a \searrow 0$ of the lattice theory. Thus $\mu = 1/a$ is the relevant scale for lattice artifacts and perturbation theory is applicable to describe the asymptotic lattice spacing dependence if the lattice spacing is sufficiently small.

3.2 Perturbative renormalisation

To describe the leading lattice spacing dependence we will work in a continuum Symanzik Effective Theory (SET) as will be explained in chapter 4 and make use of perturbation theory. This allows us to choose another regulator. We choose dimensional regularisation [93, 94], which is commonly used in continuum perturbation theory. There one defines the integrals in $D = 4 - 2\epsilon$ dimensions, which regulates both UV and IR divergences. In contrast to other regulators dimensional regularisation preserves gauge and $O(4)$ symmetries (generalised to D dimensions). This regulator usually combined with the *modified minimal subtraction* ($\overline{\text{MS}}$) renormalisation scheme [93–95], where the occurring $1/\epsilon^k$ poles are subtracted. In particular the renormalised coupling is defined as

$$\alpha_{\overline{\text{MS}}}(\mu) = \bar{\mu}^{-2\epsilon} Z^{\alpha}(\alpha_{\overline{\text{MS}}}; \epsilon) \alpha, \quad Z^{\alpha}(\alpha_{\overline{\text{MS}}}; \epsilon) = 1 + \left\{ \frac{11}{3}C_A - \frac{4}{3}N_f T_F \right\} \frac{\alpha_{\overline{\text{MS}}}}{4\pi\epsilon} + \mathcal{O}(\alpha_{\overline{\text{MS}}}^2), \quad (3.8)$$

where $4\pi\bar{\mu}^2 = e^{\gamma_E}\mu^2$ with the Euler-Mascheroni constant γ_E and Z^α is given for QCD [95]. The factor $\bar{\mu}^{-2\epsilon}$ is introduced in the $\overline{\text{MS}}$ scheme [95] to obtain renormalised quantities with the correct mass dimension for $\epsilon > 0$, while $(4\pi e^{-\gamma_E})^{-2\epsilon}$ subtracts an overall recurring constant.

For later reference we also introduce the *lattice minimal subtraction* (MS lat) scheme [96], that is typically employed with LPT. In analogy to the $\overline{\text{MS}}$ scheme, one subtracts only the poles arising in LPT of the form $\ln(a\mu)$, e.g. for the renormalised coupling in the MS lat scheme one finds

$$\alpha_{\text{lat}}(\mu) = Z^\alpha(\alpha; a\mu)\alpha, \quad Z^\alpha(\alpha; a\mu) = 1 - \left\{ \frac{11}{3}C_A - \frac{4}{3}N_f T_F \right\} \ln[(a\mu)^2] \frac{\alpha}{4\pi} + \mathcal{O}(\alpha^2, a^2 \ln(a\mu)\alpha). \quad (3.9)$$

The coupling in the MS lat scheme gives an interesting insight into the continuum limit as setting the scale $\mu = 1/a$ implies

$$\alpha_{\text{lat}}(1/a) = \alpha \quad (3.10)$$

and with use of the 1-loop running of the coupling this leads to

$$\alpha_{\text{lat}}(1/a) = \alpha = \frac{\alpha_{\text{lat}}(\mu)}{1 - 2\beta_0 \ln(a\mu) \alpha_{\text{lat}}(\mu)} \xrightarrow[\mu \text{ fixed}]{a \searrow 0} 0. \quad (3.11)$$

This shows how the bare coupling must be changed to approach the continuum limit on the lattice as we stated earlier.

3.2.1 Gauge-fixing

Perturbation theory describes small perturbations in terms of the coupling from the free theory, i.e. zero coupling, and amounts to a saddle point expansion. For gauge theories this saddle point is severely degenerate as gauge transformations shift the saddle point without changing the action, see e.g. [97, p. 32ff.]. To eliminate this degeneracy *gauge fixing* is needed which we will perform in the continuum theory using the Faddeev-Popov method [98]. For differences in the use of the Faddeev-Popov method for LPT see e.g. [83, 99].

Before getting started we substitute $A_\mu \rightarrow B_\mu + g_0 \mathcal{A}_\mu$ [99, 100] in the partition function eq. (2.7), where \mathcal{A} is the “quantum field” fluctuating around the classical background field B , and drop overall powers of g_0 originating from substituting the measure $\mathcal{D}A$

$$\mathcal{Z} = \int \mathcal{D}\mathcal{A} \mathcal{D}\bar{\Psi} \mathcal{D}\Psi e^{-S_{\text{QCD}}[B+g_0\mathcal{A}, \bar{\Psi}, \Psi]}. \quad (3.12)$$

Having an additional factor of g_0 in front of \mathcal{A} is identical to the conventional substitution when switching to perturbation theory. This substituted partition function is still invariant under the original local gauge transformation

$$(B + g_0 \mathcal{A})_\mu(x) \rightarrow \Omega(x) D_\mu[B + g_0 \mathcal{A}] \Omega^\dagger(x), \quad \bar{\Psi}(x) \rightarrow \bar{\Psi}(x) \Omega^\dagger(x), \quad \Psi(x) \rightarrow \Omega(x) \Psi(x). \quad (3.13)$$

At the level of both fields B and \mathcal{A} this can be realised two-fold, firstly the gauge transformation of B

$$\begin{aligned} B_\mu(x) &\rightarrow \Omega(x) D_\mu[B] \Omega^\dagger(x), & \mathcal{A}_\mu(x) &\rightarrow \Omega(x) \mathcal{A}_\mu(x) \Omega^\dagger(x), \\ \bar{\Psi}(x) &\rightarrow \bar{\Psi}(x) \Omega^\dagger(x), & \Psi(x) &\rightarrow \Omega(x) \Psi(x) \end{aligned} \quad (3.14)$$

and secondly the gauge transformation of the quantum field \mathcal{A}

$$\begin{aligned} B_\mu(x) &\rightarrow \Omega(x) B_\mu(x) \Omega^\dagger(x), & \mathcal{A}_\mu(x) &\rightarrow \frac{1}{g_0} \Omega(x) D_\mu[g_0 \mathcal{A}] \Omega^\dagger(x), \\ \bar{\Psi}(x) &\rightarrow \bar{\Psi}(x) \Omega^\dagger(x), & \Psi(x) &\rightarrow \Omega(x) \Psi(x). \end{aligned} \quad (3.15)$$

Turning now to the Faddeev-Popov method one uses the fact that

$$1 = \int \mathcal{D}\zeta \delta(G[A^\zeta, B] - w) \det\left(\frac{\delta G[A^\zeta, B]}{\delta \zeta}\right), \quad (3.16)$$

where ζ is an infinitesimal gauge transformation, $w = w(x)$ is the gauge condition, A_μ^ζ the gauge field infinitesimally transformed under eq. (3.13)

$$A_\mu^\zeta(x) = A_\mu(x) + D_\mu[A]\zeta(x), \quad A = B + g_0\mathcal{A}, \quad (3.17)$$

and $G[A, B]$ is the unconventional BGF gauge-fixing term [99–102]

$$G[A, B] = D_\mu[B]A_\mu - \partial_\mu B_\mu. \quad (3.18)$$

Keep in mind that the gauge fields as well as their gauge condition are algebra valued. Inserting this particular expression into the partition function yields

$$\mathcal{Z}[B] = \int \mathcal{D}A \mathcal{D}\bar{\Psi} \mathcal{D}\Psi \mathcal{D}\zeta \delta(G[A^\zeta, B] - w) \det\left(\frac{\delta G[A^\zeta, B]}{\delta \zeta}\right) e^{-S_{\text{QCD}}[B+g_0\mathcal{A}, \bar{\Psi}, \Psi]}. \quad (3.19)$$

With use of the gauge invariance of \mathcal{L} the partition function takes the form

$$\mathcal{Z}[B] = \int \mathcal{D}\zeta \int \mathcal{D}A \mathcal{D}\bar{\Psi} \mathcal{D}\Psi \delta(G[B + g_0\mathcal{A}, B] - w) \det(D_\mu[B]D_\mu[B + g_0\mathcal{A}]) e^{-S_{\text{QCD}}[B+g_0\mathcal{A}, \bar{\Psi}, \Psi]}. \quad (3.20)$$

Instead of a specific choice for the gauge condition $w(x)$ a Gaussian average can be used

$$\begin{aligned} \mathcal{Z}[B] = \mathcal{N}(\lambda) \int \mathcal{D}\zeta \int \mathcal{D}A \mathcal{D}\bar{\Psi} \mathcal{D}\Psi \mathcal{D}w \delta(G[B + g_0\mathcal{A}, B] - w) \det(D_\mu[B]D_\mu[B + g_0\mathcal{A}]) \\ \times \exp\left(-S_{\text{QCD}}[B + g_0\mathcal{A}, \bar{\Psi}, \Psi] + \int d^Dx \frac{\lambda}{g_0^2} \text{tr}(w^2(x))\right), \end{aligned} \quad (3.21)$$

where $\mathcal{N}^{-1}(\lambda) = \int \mathcal{D}w \exp\left(\int d^Dx \frac{\lambda}{g_0^2} \text{tr}(w^2(x))\right)$ and λ is the bare gauge parameter. Note that physical gauge-invariant quantities are by construction independent of λ . The prefactor $(\mathcal{N}(\lambda) \int \mathcal{D}\zeta)$ will always cancel out of n -point functions due to the division with the partition function as normalisation. Hence we drop this factor and use instead

$$\begin{aligned} \mathcal{Z}_{\text{gf}}[B] = \int \mathcal{D}A \mathcal{D}\bar{\Psi} \mathcal{D}\Psi \det(D_\mu[B]D_\mu[B + g_0\mathcal{A}]) \\ \times \exp\left(-S_{\text{QCD}}[B + g_0\mathcal{A}, \bar{\Psi}, \Psi] - \int d^Dx \mathcal{L}_{\text{gf}}[\mathcal{A}, B]\right) \end{aligned} \quad (3.22)$$

with gauge-fixing Lagrangian

$$\mathcal{L}_{\text{gf}}[\mathcal{A}, B] = -\lambda \text{tr}(\{D_\mu[B]\mathcal{A}_\mu(x)\}^2). \quad (3.23)$$

To eliminate the occurring determinant additional anti-commuting fields in the adjoint representation, so called *ghosts*, can be introduced

$$\begin{aligned} \mathcal{Z}_{\text{gf}}[B] = \int \mathcal{D}A \mathcal{D}\bar{\Psi} \mathcal{D}\Psi \mathcal{D}\bar{c} \mathcal{D}c \\ \times \exp\left(-S_{\text{QCD}}[B + g_0\mathcal{A}, \bar{\Psi}, \Psi] - \int d^Dx \left\{\mathcal{L}_{\text{gf}}[\mathcal{A}, B] + \mathcal{L}_{\text{gh}}[\mathcal{A}, B, \bar{c}, c]\right\}\right), \end{aligned} \quad (3.24)$$

where

$$\mathcal{L}_{\text{gh}}[\mathcal{A}, B, \bar{c}, c] = 2 \text{tr}(\bar{c}D_\mu[B]D_\mu[B + g_0\mathcal{A}]c). \quad (3.25)$$

This concludes the Faddeev-Popov method as we have a gauge-fixed local Lagrangian. Revisiting the two original gauge symmetry transformations eqs. (3.14) and (3.15) we notice that eq. (3.24) is still invariant under the first transformation if the ghost fields transform as [99]

$$\bar{c}(x) \rightarrow \Omega(x)\bar{c}(x)\Omega^\dagger(x), \quad c(x) \rightarrow \Omega(x)c(x)\Omega^\dagger(x). \quad (3.26)$$

Thus the background field gauge transformation is still a symmetry transformation of the gauge-fixed theory. Only the second symmetry transformation has to be replaced by the BRST symmetry [103, 104] transformation

$$\begin{aligned} B_\mu(x) &\rightarrow B_\mu(x), & \mathcal{A}_\mu(x) &\rightarrow D_\mu[B + g_0\mathcal{A}]c(x)\xi, \\ \bar{\Psi}(x) &\rightarrow \bar{\Psi}(x)\{1 - g_0c(x)\xi\}, & \Psi(x) &\rightarrow \{1 + g_0c(x)\xi\}\Psi(x), \\ \bar{c}(x) &\rightarrow \bar{c}(x) - \lambda D_\mu[B]\mathcal{A}_\mu(x)\xi, & c(x) &\rightarrow c(x) + g_0c^2(x)\xi, \end{aligned} \quad (3.27)$$

with anticommuting parameter ξ such that $\{\bar{c}, \xi\} = \{c, \xi\} = 0$. The parameter ξ mediates between commuting and anticommuting fields which get mixed during the transformation. For an alternative approach without the use of ξ see [99]. This new transformation arises as the quantum field \mathcal{A} has been gauge-fixed.

3.2.2 Renormalisation of n -point functions and composite operators

Having the gauge-fixed partition function we can turn to perturbative renormalisation at the level of n -point functions of gluons and (anti-)quarks as well as composite operators thereof. We will start the discussion in terms of the generating functional of connected n -point functions

$$W[j, \eta, \bar{\eta}, \hat{j}; B] = \ln \left(\int \mathcal{D}\mathcal{A} \mathcal{D}\bar{\Psi} \mathcal{D}\Psi \mathcal{D}\bar{c} \mathcal{D}c e^{-S[\mathcal{A}, B, \bar{\Psi}, \Psi, \bar{c}, c] + j \cdot \mathcal{A} + \bar{\eta} \cdot \Psi - \bar{\Psi} \cdot \eta + \hat{j}_i \cdot \Phi_i[B + g_0\mathcal{A}, \bar{\Psi}, \Psi]} \right), \quad (3.28)$$

where $S = S_{\text{QCD}} + S_{\text{gf}} + S_{\text{gh}}$ is the full action of the gauge fixed theory and $j, \eta, \bar{\eta}$ are the classical sources for gluons and (anti-)quarks respectively with shorthand

$$j \cdot \mathcal{A} = \int d^D x j_\mu^a(x) \mathcal{A}_\mu^a(x) \quad (3.29)$$

and analogously for the other sources. There is also another source \hat{j}_i added for composite operators Φ_i that we will discuss later on. To obtain the connected $(l + m + n)$ -point function one takes the functional derivative, see e.g. [105, p. 27f.],

$$\begin{aligned} \mathcal{G}^{(l, m, n)}(x_1, \dots, x_{l+m+n}; \alpha; \epsilon) &= \langle \mathcal{A}(x_1) \dots \mathcal{A}(x_l) \Psi(x_{l+1}) \dots \Psi(x_{l+m}) \bar{\Psi}(x_{l+m+1}) \dots \bar{\Psi}(x_{l+m+n}) \rangle_{\text{con}} \\ &= \frac{\delta^{l+m+n} W[j, \eta, \bar{\eta}, \hat{j}; B]}{\delta j(x_1) \dots \delta j(x_l) \delta \eta(x_{l+1}) \dots \delta \eta(x_{l+m}) \delta \bar{\eta}(x_{l+m+1}) \dots \delta \bar{\eta}(x_{l+m+n})} \Big|_{j=\eta=\bar{\eta}=\hat{j}=0}, \\ &x_i \neq x_j \forall i \neq j, \end{aligned} \quad (3.30)$$

where flavour, spacetime and colour indices were omitted for readability. The renormalisation of this connected $(l + m + n)$ -point function takes the form

$$\mathcal{G}_{\overline{\text{MS}}}^{(l, m, n)}(\dots; \alpha_{\overline{\text{MS}}}; \epsilon) = Z_{\mathcal{A}}^l(\alpha_{\overline{\text{MS}}}; \epsilon) Z_{\Psi}^{m+n}(\alpha_{\overline{\text{MS}}}; \epsilon) \mathcal{G}^{(l, m, n)}(\dots; \alpha; \epsilon) \quad (3.31)$$

with wavefunction renormalisations $Z_{\mathcal{A}}$ and Z_{Ψ} of the gluons and (anti-)quarks respectively.

In case one is only interested in the different renormalisation factors the procedure can be simplified by switching to the vertex functional

$$\Gamma[\hat{\mathcal{A}}, \hat{\Psi}, \hat{\bar{\Psi}}; B] = W[j, \eta, \bar{\eta}; B] - j \cdot \hat{\mathcal{A}} - \hat{\bar{\Psi}} \cdot \eta - \bar{\eta} \cdot \hat{\Psi} \quad (3.32)$$

with vacuum expectation values

$$\hat{\mathcal{A}}_\mu^a(x) = \frac{\delta W}{\delta j_\mu^a(x)}, \quad \hat{\Psi}_A^f(x) = \frac{\delta W}{\delta \bar{\eta}_A^f}, \quad \hat{\bar{\Psi}}_A^f(x) = \frac{\delta W}{\delta \eta_A^f}. \quad (3.33)$$

Functional derivatives with respect to $\hat{\mathcal{A}}$, $\hat{\Psi}$ and $\hat{\bar{\Psi}}$ then yield so called vertex functions (or *one-particle irreducible* (1PI) graphs)

$$\begin{aligned} \Gamma^{(l,m,n)}(x_1, \dots, x_{l+m+n}; \alpha; \epsilon) &= \langle \mathcal{A}(x_1) \dots \mathcal{A}(x_l) \Psi(x_{l+1}) \dots \Psi(x_{l+m}) \bar{\Psi}(x_{l+m+1}) \dots \bar{\Psi}(x_{l+m+n}) \rangle_{\text{1PI}} \\ &= \frac{\delta^{l+m+n} \Gamma[\hat{\mathcal{A}}, \hat{\Psi}, \hat{\bar{\Psi}}, \hat{j}; B]}{\delta \hat{\mathcal{A}}(x_1) \dots \delta \hat{\mathcal{A}}(x_l) \delta \hat{\Psi}(x_{l+1}) \dots \delta \hat{\Psi}(x_{l+m}) \delta \hat{\bar{\Psi}}(x_{l+m+1}) \dots \delta \hat{\bar{\Psi}}(x_{l+m+n})} \Big|_{\hat{\mathcal{A}}=\hat{\Psi}=\hat{\bar{\Psi}}=\hat{j}=0}, \\ &\quad x_i \neq x_j \forall i \neq j, \end{aligned} \quad (3.34)$$

which renormalise as

$$\Gamma_{\overline{\text{MS}}}^{(l,m,n)}(\dots; \alpha_{\overline{\text{MS}}}; \epsilon) = Z_{\mathcal{A}}^{-l}(\alpha_{\overline{\text{MS}}}; \epsilon) Z_{\Psi}^{-m-n}(\alpha_{\overline{\text{MS}}}; \epsilon) \Gamma^{(l,m,n)}(\dots; \alpha; \epsilon). \quad (3.35)$$

Taking the functional derivative with respect to \hat{j}_i before setting $\hat{j}_i = 0$ inserts a composite operator Φ_i into both the connected and 1PI n -point functions. This complicates the renormalisation due to so called mixing of operators with identical symmetries and thus identical quantum numbers under renormalisation. Moreover gauge-fixing breaks gauge symmetry and allows non-gauge-invariant operators to mix as well. Eventually renormalising gauge-invariant operators requires the contributions of three different classes of operators, which are closed under renormalisation [106–108]:

1. Gauge-invariant operators (\mathcal{O}) that do not vanish according to the equations of motion (EOM) and have the correct symmetries and mass-dimension.
2. BRST-exact operators (\mathfrak{B}), which can be obtained from the BRST-variation [86, p. 317f.], see also [107],

$$\mathfrak{B}\xi = \delta_{\text{BRST}}(Q_\mu \partial_\mu c), \quad (3.36)$$

where δ_{BRST} denotes the change under a BRST-variation as given in eq. (3.27). The resulting operator is then BRST-invariant up to terms vanishing by the gauge-fixed EOMs. The possible choices for Q_μ are only restricted by the mass dimension and symmetries (apart from gauge symmetry) of the operator \mathcal{O} .

3. EOM-vanishing operators (\mathcal{E}) with the correct mass-dimension and symmetries (apart from gauge symmetry).

The renormalisation of such operators then takes the form [86, p. 317f.]

$$\begin{pmatrix} \mathcal{O} \\ \mathfrak{B} \\ \mathcal{E} \end{pmatrix}_{\overline{\text{MS}}} = \begin{pmatrix} Z^{\mathcal{O}} & Z^{\mathcal{O}\mathfrak{B}} & Z^{\mathcal{O}\mathcal{E}} \\ 0 & Z^{\mathfrak{B}} & Z^{\mathfrak{B}\mathcal{E}} \\ 0 & 0 & Z^{\mathcal{E}} \end{pmatrix} \begin{pmatrix} \mathcal{O} \\ \mathfrak{B} \\ \mathcal{E} \end{pmatrix}, \quad (3.37)$$

where we dropped the additional indices distinguishing different operators in each operator class for readability. Of course contributions of the operator classes \mathfrak{B} and \mathcal{E} vanish for physical on-shell matrix elements, hence the triangular structure of the mixing matrix.

Due to the reduced constraints on the classes \mathfrak{B} and \mathcal{E} there exists an impractically large number of operator candidates for higher mass dimensions. To circumvent this difficulty we will make use of the background field (BGF) method [99–102] and consider external background fields B rather than gluons \mathcal{A} , i.e. in the presence of an operator insertion Φ_i ,

$$\begin{aligned} \hat{\Gamma}_i^{(l,m,n)}(x_1, \dots, x_{l+m+n}; y; \alpha; \epsilon) &= \\ &= \frac{\delta^{l+m+n+1} \Gamma[0, \hat{\Psi}, \hat{\bar{\Psi}}, \hat{j}; B]}{\delta B(x_1) \dots \delta B(x_l) \delta \hat{\Psi}(x_{l+1}) \dots \delta \hat{\Psi}(x_{l+m}) \delta \hat{\bar{\Psi}}(x_{l+m+1}) \dots \delta \hat{\bar{\Psi}}(x_{l+m+n}) \delta \hat{j}_i(y)} \Big|_{B=\hat{\Psi}=\hat{\bar{\Psi}}=\hat{j}=0}, \end{aligned} \quad (3.38)$$

where $x_i \neq x_j \forall i \neq j$ and $y \neq x_i \forall i$. Since these vertex functions are manifestly invariant under gauge transformations of the background field eq. (3.14) any contributions from non gauge-invariant operators vanish thus leaving only contributions from the class \mathcal{O} and from the gauge-invariant ones of class \mathcal{E} . At the level of vertex functions this implies for the renormalisation

$$\begin{pmatrix} \hat{\Gamma}_{\mathcal{O}}^{(l,m,n)} \\ \hat{\Gamma}_{\mathcal{E}}^{(l,m,n)} \end{pmatrix}_{\overline{\text{MS}}}(\dots; y; \alpha_{\overline{\text{MS}}}; \epsilon) = Z_{\Psi}^{-m-n}(\alpha_{\overline{\text{MS}}}; \epsilon) \begin{pmatrix} Z^{\mathcal{O}} & Z^{\mathcal{O}\mathcal{E}} \\ 0 & Z^{\mathcal{E}} \end{pmatrix} \begin{pmatrix} \hat{\Gamma}_{\mathcal{O}}^{(l,m,n)} \\ \hat{\Gamma}_{\mathcal{E}}^{(l,m,n)} \end{pmatrix}(\dots; y; \alpha; \epsilon) \quad (3.39)$$

as the background fields do not require any renormalisation (notice the relative power of g_0 in the initial substitution $A_{\mu} \rightarrow B_{\mu} + g_0 \mathcal{A}_{\mu}$, unlike the original BGF method cf. [100, 102]) and from the class \mathcal{E} only the subset of gauge-invariant EOM vanishing operators must be considered. We again dropped operator indices and substituted them by their operator class to highlight the general mixing structure.

This concludes the renormalisation of n -point functions with operator insertions and allows us to extract the mixing matrix $Z^{\mathcal{O}}$ from such n -point functions by including only the redundant operators \mathcal{E}_i . The operators \mathcal{E}_i are redundant in the sense that they vanish for physical (“on-shell”) matrix elements [57, 109].

3.3 Renormalisation Group

The generalisation of the anomalous dimension from eq. (3.5) to operators mixing under renormalisation is straight forward and leads to (we revert to a general multiplicative renormalisation scheme)

$$(\gamma_{\mathcal{S}}^{\mathcal{O}})_{ik} = \mu^2 \frac{dZ_{ij}^{\mathcal{O}}(\alpha_{\mathcal{S}})}{d\mu^2} [Z^{\mathcal{O}}(\alpha_{\mathcal{S}})]_{jk}^{-1}. \quad (3.40)$$

For asymptotically free theories the anomalous dimension can be written as a perturbative series

$$(\gamma_{\mathcal{S}}^{\mathcal{O}})_{ij}(\alpha_{\mathcal{S}}) = -\alpha_{\mathcal{S}} \{(\gamma_0^{\mathcal{O}})_{ij} + (\gamma_{1;\mathcal{S}}^{\mathcal{O}})_{ij} \alpha_{\mathcal{S}} + \mathcal{O}(\alpha_{\mathcal{S}}^2)\}. \quad (3.41)$$

As indicated in eq. (3.41) the leading order coefficient $\gamma_0^{\mathcal{O}}$ is independent of the renormalisation scheme while in general all higher order coefficients are scheme dependent [86, p. 202]. Before we continue we make a change of basis such that the new basis \mathcal{B} has a diagonal 1-loop anomalous dimension matrix, i.e. no 1-loop mixing of the basis,

$$(\gamma_{\mathcal{S}}^{\mathcal{B}})_{ij}(\alpha_{\mathcal{S}}) = -\alpha_{\mathcal{S}} \{(\gamma_0^{\mathcal{B}})_{ij} + (\gamma_{1;\mathcal{S}}^{\mathcal{B}})_{ij} \alpha_{\mathcal{S}} + \mathcal{O}(\alpha_{\mathcal{S}}^2)\}, \quad \gamma_0^{\mathcal{B}} = \text{diag}\{(\gamma_0^{\mathcal{B}})_1, \dots, (\gamma_0^{\mathcal{B}})_n\}, \quad (3.42)$$

where $(\gamma_0^{\mathcal{B}})_i$ is the i -th diagonal entry corresponding to the 1-loop anomalous dimension of the i -th operator \mathcal{B}_i . Using this anomalous dimension one can trade the scale dependent operator $\mathcal{B}_{i;\mathcal{S}}(\mu)$ for the *Renormalisation Group Invariant* (RGI) operator $\mathcal{B}_{i;\text{RGI}}$, see e.g. [110, 111] and [54, p. 21f.],

$$\mathcal{B}_{i;\mathcal{S}}(\mu) = \left\{ W_{\mathcal{S}}^{-1}(\mu) [2\beta_0 \alpha_{\mathcal{S}}(\mu)]^{\hat{\gamma}^{\mathcal{B}}} \right\}_{ij} \mathcal{B}_{j;\text{RGI}}, \quad (3.43)$$

$$\mu^2 \frac{W_{\mathcal{S}}(\mu)}{\partial \mu^2} = [\gamma_{\mathcal{S}}^{\mathcal{B}}(\alpha_{\mathcal{S}}), W_{\mathcal{S}}(\mu)] - \beta_{\mathcal{S}}(\alpha_{\mathcal{S}}) \left\{ \frac{\gamma_{\mathcal{S}}^{\mathcal{B}}(\alpha_{\mathcal{S}})}{\beta_{\mathcal{S}}(\alpha_{\mathcal{S}})} - \hat{\gamma}^{\mathcal{B}} \right\} W_{\mathcal{S}}(\mu), \quad (3.44)$$

$$\mathcal{B}_{i;\text{RGI}} = \lim_{\mu \rightarrow \infty} [2\beta_0 \alpha_{\mathcal{S}}(\mu)]^{-\hat{\gamma}_i^{\mathcal{B}}} \mathcal{B}_{i;\mathcal{S}}(\mu), \quad \hat{\gamma}^{\mathcal{B}} = \frac{\gamma_0^{\mathcal{B}}}{\beta_0}, \quad (3.45)$$

where the $2\beta_0$ in front of $\alpha_{\mathcal{S}}$ are the conventional normalisation. The implicitly defined $W_{\mathcal{S}}$ takes care of the fact that in general $[\gamma_0^{\mathcal{B}}, \gamma_{\mathcal{S}}^{\mathcal{B}}(\alpha_{\mathcal{S}})] = \mathcal{O}(\alpha_{\mathcal{S}}^2)$ for an operator basis mixing under renormalisation. $\mathcal{B}_{i;\text{RGI}}$ is by construction independent of the scheme and renormalisation scale, i.e. all scale and scheme dependence is absorbed into the prefactor. Expanding eq. (3.43) and using $W_{\mathcal{S}}(\mu) = 1 + \mathcal{O}(\alpha_{\mathcal{S}}(\mu))$ then yields

$$\mathcal{B}_{i;\mathcal{S}}(\mu) = [2\beta_0 \alpha_{\mathcal{S}}(\mu)]^{\hat{\gamma}_i^{\mathcal{B}}} \mathcal{B}_{i;\text{RGI}} \times [1 + \mathcal{O}(\alpha_{\mathcal{S}}(\mu))] \quad (3.46)$$

as the leading asymptotic scale dependence, which for $\mu = 1/a$ is precisely what this thesis is aiming at in terms of a continuum Symanzik Effective Theory as will be explained in chapter 4.

Chapter 4

Symanzik Effective Theory

When doing lattice field theory numerically one extracts dimensionless quantities Q at finite lattice spacing a whereas one eventually requires the information at zero lattice spacing, i.e., the *continuum limit*

$$Q_R = \lim_{a \searrow 0} Q_{\text{lattice};R}(a), \quad (4.1)$$

which is the usual limit for removing the regulator **after** the renormalisation has been performed as discussed in the previous chapter. This limit can be approximated by measuring the same quantity at different lattice spacings and then performing a continuum extrapolation, which can only be attempted if the dependence on the lattice spacing is under control. Therefore we need to understand the leading lattice artifacts at small but non-zero lattice spacing.

This can be done in terms of a continuum Symanzik effective theory (SET) [50–53], see also [54, p. 39ff.]. Each local field as well as the lattice action involved in the computation of the quantity Q can contribute lattice artifacts both classically and through quantum corrections in the lattice regularised theory (LRT). Furthermore the renormalisation condition chosen on the lattice for the local composite fields may introduce additional lattice artifacts. We will ignore such contributions for the moment by choosing the $\overline{\text{MS}}$ lat scheme in the lattice theory, which does not have this property, and postpone the discussion of such contributions to section 4.1.2. The leading contributions at classical order $a^{n_{\min}}$ can be parametrised in the effective theory by contributions of operators with higher mass dimension to the continuum Lagrangian \mathcal{L}_{QCD}

$$\mathcal{L}_{\text{eff}} = \mathcal{L}_{\text{QCD}} + a^{n_{\min}} \delta \mathcal{L} + \mathcal{O}(a^{n_{\min}+1}), \quad \delta \mathcal{L} = b_i^{\mathcal{O}}(a\mu, \alpha_{\overline{\text{MS}}}) Z_{ij}^{\mathcal{O}}(\alpha_{\overline{\text{MS}}}; \epsilon) \mathcal{O}_j, \quad (4.2)$$

as well as to any renormalised local field $\Phi_{\overline{\text{MS}}}$

$$\Phi_{\text{eff};\overline{\text{MS}}} = \Phi_{\overline{\text{MS}}} + a^{n_{\min}} \delta \Phi + \mathcal{O}(a^{n_{\min}+1}), \quad \delta \Phi = c_i^{\Upsilon}(a\mu, \alpha_{\overline{\text{MS}}}) Z_{ij}^{\Upsilon}(\alpha_{\overline{\text{MS}}}; \epsilon) \Upsilon_j, \quad (4.3)$$

where \mathcal{O}_i and Υ_i are local fields with mass dimensions $[\mathcal{O}_i] = n_{\min} + [\mathcal{L}]$ and $[\Upsilon_i] = n_{\min} + [\Phi]$. In the perturbative description of the SET we will stick to the $\overline{\text{MS}}$ renormalisation scheme throughout this thesis. The coefficients $b_i^{\mathcal{O}}$ and c_i^{Υ} can still depend logarithmically on the lattice spacing. Only fields complying with the symmetries of their lattice counterparts are allowed to contribute, i.e., have coefficients $b_i^{\mathcal{O}} \neq 0$ or $c_i^{\Upsilon} \neq 0$. Note that we introduced the coefficients already accompanied with some mixing matrices $Z^{\mathcal{O}}$ and Z^{Υ} in the $\overline{\text{MS}}$ scheme satisfying

$$\mathcal{O}_{i;\overline{\text{MS}}} = Z_{ij}^{\mathcal{O}}(\alpha_{\overline{\text{MS}}}; \epsilon) \mathcal{O}_j, \quad \Upsilon_{i;\overline{\text{MS}}} = Z_{ij}^{\Upsilon}(\alpha_{\overline{\text{MS}}}; \epsilon) \Upsilon_j, \quad \Phi_{\overline{\text{MS}}} = Z^{\Phi}(\alpha_{\overline{\text{MS}}}; \epsilon) \Phi, \quad (4.4)$$

where we assume for simplicity no mixing of Φ under renormalisation without loss of generality. In order to describe all deviations from the continuum theory up to $\mathcal{O}(a^{n_{\min}+1})$ we then need complete (but minimal) bases of such operators for each quantity.

Taking again Wilson's lattice QCD from eq. (2.8) as an example we find for the mass-degenerate case the symmetry constraints:

- Local $SU(N)$ gauge symmetry,
 - Parity (\mathcal{P}),
 - Euclidean time reflection (\mathcal{T}),
 - Charge conjugation (\mathcal{C}),
 - Hypercubic symmetry H_4 ,
 - $SU(N_f)_V \times U(1)_V$ flavour symmetry.
- } See appendix C for the behaviour of gauge and fermion fields under these transformations.

At mass dimension 5 operators of the form $\bar{\Psi}\Gamma\Psi$, $\bar{\Psi}\Gamma_\mu D_\mu[A]\Psi$ and $\bar{\Psi}\Gamma_{\mu\nu}D_\mu[A]D_\nu[A]\Psi$ involving two fermions are to be expected, where $\Gamma_{\{\dots\}}$ is Dirac algebra valued. Notice that this makes use of *integration by parts* (IBP) to discard covariant derivatives acting on the anti-quark, e.g.

$$\bar{\Psi}\Gamma_\mu(\overleftarrow{D}_\mu[A] - D_\mu[A])\Psi \stackrel{\text{IBP}}{=} \partial_\mu(\bar{\Psi}\Gamma_\mu\Psi) - 2\bar{\Psi}\Gamma_\mu D_\mu[A]\Psi, \quad (4.5)$$

where the total divergence can be dropped in the action. Due to parity, see also table 5.2 and the accompanying discussion in section 5.2.2, one finds [112]

$$\Gamma = \mathbb{1}, \quad \Gamma_\mu = \gamma_\mu, \quad \Gamma_{\mu\nu} \in \{\delta_{\mu\nu}, i\sigma_{\mu\nu}\}, \quad (4.6)$$

where $\sigma_{\mu\nu} = \frac{i}{2}[\gamma_\mu, \gamma_\nu]$. The left over operator candidates are (adding the only purely gluonic massive operator allowed at $O(a)$)

$$\begin{aligned} \mathcal{O}_1^{(1)} &= m^2 \bar{\Psi}\Psi, & \mathcal{O}_2^{(1)} &= m \bar{\Psi}\gamma_\mu D_\mu \Psi, & \mathcal{O}_3^{(1)} &= \bar{\Psi}D^2\Psi, \\ \mathcal{O}_4^{(1)} &= i\bar{\Psi}\sigma_{\mu\nu}F_{\mu\nu}\Psi, & \mathcal{O}_5^{(1)} &= \frac{m}{g_0^2} \text{tr}(F_{\mu\nu}F_{\mu\nu}), \end{aligned} \quad (4.7)$$

with bare degenerate mass m . Being only interested in physical matrix-elements allows us to make use of the continuum equations of motions [57, 109]

$$(D_\nu[A]F_{\nu\mu})^a = g_0^2 \bar{\Psi}\gamma_\mu T^a \Psi, \quad (4.8)$$

$$\gamma_\mu D_\mu[A]\Psi = -M\Psi, \quad (4.9)$$

$$\bar{\Psi}\overleftarrow{D}_\mu[A]\gamma_\mu = \bar{\Psi}M, \quad (4.10)$$

where $M = m\mathbb{1}_{N_f \times N_f}$ in the mass-degenerate case. This reduces the operator basis further

$$\mathcal{O}_2^{(1)} \stackrel{\text{EOM}}{=} -\mathcal{O}_1^{(1)}, \quad (4.11)$$

$$\mathcal{O}_3^{(1)} \stackrel{\text{EOM}}{=} \frac{1}{2}\mathcal{O}_4^{(1)} + \mathcal{O}_5^{(1)}, \quad (4.12)$$

to a set of 3 linearly independent operators, here chosen as $\mathcal{O}_1^{(1)}$, $\mathcal{O}_4^{(1)}$ and $\mathcal{O}_5^{(1)}$ forming the on-shell basis at mass-dimension 5.

4.1 Matching to the lattice theory

Until now the coefficients $b_i^\mathcal{O}$ and $c_j^\mathcal{F}$ in eqs. (4.2) and (4.3) were kept free. Consequently the SET defined in this way is still applicable to different choices of the lattice action complying with the symmetries chosen for the minimal basis. In order to describe a specific choice for the LRT the coefficients $b_i^\mathcal{O}$ and $c_j^\mathcal{F}$ must be adjusted accordingly, which is referred to as *matching*.

To use the SET as an effective description of the renormalised lattice observables at small lattice spacing $a > 0$, i.e. without removing the regulator, we require equivalent results from both

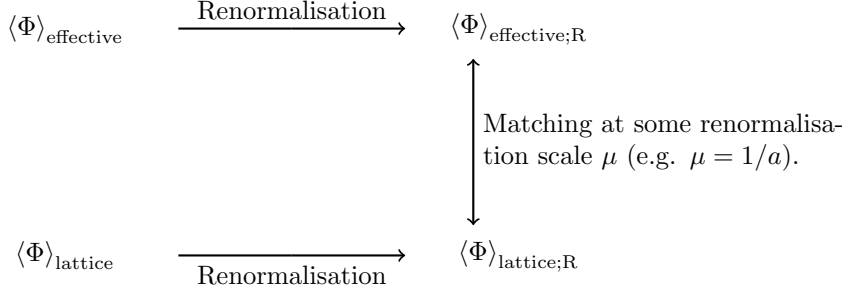


Figure 4.1: Schematic of the full matching procedure between lattice theory and the Symanzik effective theory.

the renormalised lattice and renormalised effective theory. Of course this equivalence holds only up to a given order in the lattice spacing and coupling at which the (perturbative) matching has been carried out.

To fix all coefficients a sufficient number of independent matching conditions is needed. Traditionally so called on-shell matching is performed, where the same physical matrix elements or spectral quantities are computed in both the lattice and effective theory before being renormalised and then matched as depicted in figure 4.1. Two such examples are the perturbative on-shell improvement at $O(a^2)$ of a general pure gauge action [57, 59–62] and non-perturbative $O(a)$ -improvement of Wilson’s lattice QCD [58]. To explain the general idea consider the connected 2-point function of a composite field Φ (the generalisation to an n -point function with different fields is straight forward) in the effective theory

$$\begin{aligned} \left\langle \Phi_{\text{eff};\overline{\text{MS}}}(x) \Phi_{\text{eff};\overline{\text{MS}}}(y) \right\rangle_{\text{eff}}^{\text{con}} = \\ \frac{1}{Z_{\text{eff}}} \int \mathcal{D}A \mathcal{D}\bar{\Psi} \mathcal{D}\Psi \Phi_{\text{eff};\overline{\text{MS}}}[A, \bar{\Psi}, \Psi](x) \Phi_{\text{eff};\overline{\text{MS}}}[A, \bar{\Psi}, \Psi](y) e^{-S_{\text{eff}}[A, \bar{\Psi}, \Psi]}, \end{aligned} \quad (4.13)$$

where

$$Z_{\text{eff}} = \int \mathcal{D}A \mathcal{D}\bar{\Psi} \mathcal{D}\Psi e^{-S_{\text{eff}}[A, \bar{\Psi}, \Psi]}, \quad S_{\text{eff}}[A, \bar{\Psi}, \Psi] = \int d^D y \mathcal{L}_{\text{eff}}[A, \bar{\Psi}, \Psi](y). \quad (4.14)$$

The expression in eq. (4.13) is typically not renormalisable and first must be formally expanded in the lattice spacing, which is treated like a classical free parameter in the effective theory. Following the formal derivation in appendix F.1, connected n -point functions in the effective theory can be expressed in terms of the continuum theory

$$\begin{aligned} \left\langle \Phi_{\text{eff};\overline{\text{MS}}}(x) \Phi_{\text{eff};\overline{\text{MS}}}(y) \right\rangle_{\text{eff}}^{\text{con}} = \\ \left\langle \left(\Phi_{\overline{\text{MS}}}(x) \Phi_{\overline{\text{MS}}}(y) + a^{n_{\text{min}}} [\delta\Phi(x) \Phi_{\overline{\text{MS}}}(y) + \Phi_{\overline{\text{MS}}}(x) \delta\Phi(y)] + O(a^{n_{\text{min}}+1}) \right) e^{-\delta S} \right\rangle_{\text{con}}, \end{aligned} \quad (4.15)$$

with the small perturbation from the continuum action

$$\delta S = \int d^D x \left(a^{n_{\text{min}}} \delta\mathcal{L}(x) + O(a^{n_{\text{min}}+1}) \right). \quad (4.16)$$

Expanding eq. (4.15) further in the lattice spacing yields

$$\begin{aligned}
 \left\langle \Phi_{\text{eff};\overline{\text{MS}}}(x) \Phi_{\text{eff};\overline{\text{MS}}}(y) \right\rangle_{\text{eff}}^{\text{con}} &= \left\langle \Phi_{\overline{\text{MS}}}(x) \Phi_{\overline{\text{MS}}}(y) \right\rangle_{\text{con}} \\
 &+ a^{n_{\min}} c_j^{\Upsilon}(a\mu, \alpha_{\overline{\text{MS}}}) \left\langle \Upsilon_{j;\overline{\text{MS}}}(x) \Phi_{\overline{\text{MS}}}(y) + \Phi_{\overline{\text{MS}}}(x) \Upsilon_{j;\overline{\text{MS}}}(y) \right\rangle_{\text{con}} \\
 &- a^{n_{\min}} b_i^{\mathcal{O}}(a\mu, \alpha_{\overline{\text{MS}}}) \int d^D z \left\langle \Phi_{\overline{\text{MS}}}(x) \Phi_{\overline{\text{MS}}}(y) \mathcal{O}_{i;\overline{\text{MS}}}(z) \right\rangle_{\text{con}} \\
 &+ \mathcal{O}(a^{n_{\min}+1}), \tag{4.17}
 \end{aligned}$$

where only renormalised connected n -point functions in the original continuum theory remain, i.e. all remaining terms are now renormalisable. The corresponding renormalised connected 2-point function in the LRT, can be computed via lattice perturbation theory to (perturbatively) match both results at renormalisation scale $\hat{\mu}$ [50]

$$\left\langle \Phi_{\text{lat}}(x) \Phi_{\text{lat}}(y) \right\rangle_{\text{lattice}}^{\text{con}} \Big|_{\hat{\mu}} \stackrel{!}{=} [\varrho^{\Phi}(\alpha_{\text{lat}}(\hat{\mu}), \alpha_{\overline{\text{MS}}}(\hat{\mu}))]^2 \left\langle \Phi_{\text{eff};\overline{\text{MS}}}(x) \Phi_{\text{eff};\overline{\text{MS}}}(y) \right\rangle_{\text{eff}}^{\text{con}} \Big|_{\hat{\mu}}, \tag{4.18}$$

where $x \neq y$, $\langle \dots \rangle_{\text{lattice}}^{\text{con}}$ denotes a connected n -point function at finite lattice spacing $a > 0$ and

$$\varrho^{\Phi}(\alpha_{\text{lat}}, \alpha_{\overline{\text{MS}}}) = \exp \left(\int^{\alpha_{\text{lat}}} dx \frac{\gamma_{\text{lat}}^{\Phi}(x)}{\beta_{\text{lat}}(x)} - \int^{\alpha_{\overline{\text{MS}}}} dx \frac{\gamma_{\overline{\text{MS}}}^{\Phi}(x)}{\beta_{\overline{\text{MS}}}(x)} \right) \tag{4.19}$$

relates both the MS lat scheme and $\overline{\text{MS}}$ renormalisation scheme with anomalous dimension γ^{Φ} of the field Φ . In case Φ is a RGI quantity, e.g. a vector current, no renormalisation of Φ is needed as $Z^{\Phi} \equiv 1$ leading to $\varrho^{\Phi}(\alpha_{\text{lat}}, \alpha_{\overline{\text{MS}}}) \equiv 1$.

Since the matching can be performed at an arbitrary scale $\hat{\mu}$ [113, p. 545ff.], we choose $\hat{\mu} = 1/a$ as the lattice cutoff is the relevant scale for lattice artifacts. Renormalised couplings and quark masses on both sides of eq. (4.18) are then related via [86, p. 200ff.]

$$\alpha_{\text{lat}}(1/a) = \alpha_{\overline{\text{MS}}}(1/a) + \mathcal{O}(\alpha_{\overline{\text{MS}}}^2), \tag{4.20}$$

$$m_{\text{lat}}(1/a) = m_{\overline{\text{MS}}}(1/a)[1 + \mathcal{O}(\alpha_{\overline{\text{MS}}})]. \tag{4.21}$$

In principle the matching of the coefficients $b_i^{\mathcal{O}}$ and c_j^{Υ} can now be performed order by order in the coupling using perturbation theory. Notice, that the tree-level coefficients $b_i^{\mathcal{O}}$ and c_j^{Υ} are independent of one another and can be extracted from the naive $\mathcal{O}(a)$ expansion [50]. For our example of the mass-degenerate Wilson fermion action we thus find in the naive expansion in the lattice spacing

$$S_{\text{F}}^{\text{W}} = \int d^4x \bar{\Psi}(x) \left[\gamma_{\mu} D_{\mu} + m - \frac{a}{2} D^2 + \frac{a^2}{6} \sum_{\mu} \gamma_{\mu} D_{\mu}^3 + \mathcal{O}(a^3) \right] \Psi(x), \tag{4.22}$$

which leads to

$$b_1^{\mathcal{O}} = -\frac{1}{2} + \mathcal{O}(\alpha_{\overline{\text{MS}}}), \quad b_4^{\mathcal{O}} = -\frac{1}{4} + \mathcal{O}(\alpha_{\overline{\text{MS}}}), \quad b_5^{\mathcal{O}} = \mathcal{O}(\alpha_{\overline{\text{MS}}}). \tag{4.23}$$

The plaquette action only yields terms at $\mathcal{O}(a^2)$ in the naive expansion in the lattice spacing which ensure that $b_5^{\mathcal{O}}$ vanishes at tree-level, see also section 5.1.1 for the naive expansion of lattice pure gauge actions to $\mathcal{O}(a^2)$ in the lattice spacing.

4.1.1 Perturbative off-shell matching with background fields

Instead of perturbative on-shell matching we want to highlight here a different strategy namely perturbative off-shell matching at the level of 1PI graphs with external background fields rather than gluons. For details on how to implement the background field gauge on the lattice see [99]. This alternative approach is motivated by the work of Parisi [114] pointing out that matching at the level of connected n -point functions of fundamental fields rather than composite ones amounts to the matching condition (both functionals are gauge-fixed)

$$W_{\text{lattice}}[j, \eta, \bar{\eta}, 0; B; a] \stackrel{!}{=} \lim_{\epsilon \searrow 0} W_{\text{eff}}[j, \eta, \bar{\eta}, \hat{j}; B; \epsilon] \Big|_{\hat{j}_k = -a^{n_{\min}} b_i^{\mathcal{O}}(1, \alpha_{\overline{\text{MS}}}) Z_{ik}(\alpha_{\overline{\text{MS}}}; \epsilon)} + \mathcal{O}(a^{n_{\min}+1}) \quad (4.24)$$

$$= \lim_{\epsilon \searrow 0} \left\{ W[j, \eta, \bar{\eta}, 0; B; \epsilon] - a^{n_{\min}} b_i(1, \alpha_{\overline{\text{MS}}}) Z_{ik}(\alpha_{\overline{\text{MS}}}; \epsilon) \int d^D x \frac{\delta W[j, \eta, \bar{\eta}, \hat{j}; B; \epsilon]}{\delta \hat{j}_k(x)} \Big|_{\hat{j}=0} \right\} + \mathcal{O}(a^{n_{\min}+1}) \quad (4.25)$$

and thus relates the generating functional of connected graphs as defined in eq. (3.28) from the effective theory to the lattice theory. Due to the independence of both W_{lattice} and W_{eff} from the BGF [99] we are free to choose the BGFs B identically in both theories. This matching condition holds up to additional lattice artifacts arising from the renormalisation condition, which we still neglect by using the MS lat scheme in the lattice theory. Notice that due to gauge-fixing the operator basis corresponding to \hat{j}_i is enlarged as discussed in section 3.2.2 and thus includes BRST-exact and EOM-vanishing operators.

To get back to the naive matching conditions one takes the functional derivative with respect to the renormalised sources, e.g. $j_{\text{lat}} = j/Z^{\mathcal{A}}(\alpha_{\text{lat}}; a)$

$$\begin{aligned} \frac{\delta W_{\text{lattice}}[j, \eta, \bar{\eta}, 0; B; a]}{\delta j_{\text{lat}}(x)} &\equiv Z^{\mathcal{A}}(\alpha_{\text{lat}}; a) \frac{\delta W_{\text{lattice}}[j, \eta, \bar{\eta}, 0; B; a]}{\delta j(x)} \\ &\stackrel{!}{=} \int d^D y \frac{\delta j_{\overline{\text{MS}}}(y)}{\delta j_{\text{lat}}(x)} \lim_{\epsilon \searrow 0} \left\{ \frac{\delta W[j, \eta, \bar{\eta}, 0; B; \epsilon]}{\delta j_{\overline{\text{MS}}}(y)} \right. \\ &\quad \left. - a^{n_{\min}} b_i(1, \alpha_{\overline{\text{MS}}}) Z_{ik}(\alpha_{\overline{\text{MS}}}; \epsilon) \int d^D z \frac{\delta^2 W[j, \eta, \bar{\eta}, \hat{j}; B; \epsilon]}{\delta j_{\overline{\text{MS}}}(y) \delta \hat{j}_k(z)} \Big|_{\hat{j}=0} \right\} + \mathcal{O}(a^{n_{\min}+1}) \\ &\equiv \varrho^{\mathcal{A}}(\alpha_{\text{lat}}, \alpha_{\overline{\text{MS}}}) \lim_{\epsilon \searrow 0} Z^{\mathcal{A}}(\alpha_{\overline{\text{MS}}}; \epsilon) \left\{ \frac{\delta W[j, \eta, \bar{\eta}, 0; B; \epsilon]}{\delta j(x)} \right. \\ &\quad \left. - a^{n_{\min}} b_i(1, \alpha_{\overline{\text{MS}}}) Z_{ik}(\alpha_{\overline{\text{MS}}}; \epsilon) \int d^D z \frac{\delta^2 W[j, \eta, \bar{\eta}, \hat{j}; B; \epsilon]}{\delta j(x) \delta \hat{j}_k(z)} \Big|_{\hat{j}=0} \right\} + \mathcal{O}(a^{n_{\min}+1}) \quad (4.26) \end{aligned}$$

and so on. Finally all sources are set to zero.

A typical application of effective field theories is to “integrate out” heavy fields such that the effective theory describes the low energy physics. In such a case the matching condition can be stated in terms of the *one-light-particle-irreducible* (1LPI) graphs, i.e., the analogue of 1PI graphs only for the light particles remaining in the effective theory [115, p. 229f.]. Since we do not integrate out any fields the 1LPI and 1PI graphs coincide allowing us to perform the matching at the level of vertex functions with the generating functionals

$$\begin{aligned} \Gamma_{\text{lattice}}[\hat{\mathcal{A}}_{\text{lattice}}, \hat{\Psi}_{\text{lattice}}, \hat{\bar{\Psi}}_{\text{lattice}}, 0; B; a] &= \lim_{\epsilon \searrow 0} \left\{ \Gamma[\hat{\mathcal{A}}, \hat{\Psi}, \hat{\bar{\Psi}}, 0; B; \epsilon] \right. \\ &\quad \left. - a^{n_{\min}} b_i(1, \alpha_{\overline{\text{MS}}}) Z_{ik}(\alpha_{\overline{\text{MS}}}; \epsilon) \int d^D z \frac{\delta \Gamma[\hat{\mathcal{A}}, \hat{\Psi}, \hat{\bar{\Psi}}, \hat{j}; B; \epsilon]}{\delta \hat{j}_k(z)} \Big|_{\hat{j}=0} \right\} + \mathcal{O}(a^{n_{\min}+1}), \quad (4.27) \end{aligned}$$

where the vacuum expectation values are related as

$$\begin{aligned}\hat{\mathcal{A}}_{\text{lattice}}(x; a) &= \mathcal{A}_{\text{eff}}(x) + \mathcal{O}(a^{n_{\text{min}}+1}) \\ &= \left\{ 1 - a^{n_{\text{min}}} b_i(1, \alpha_{\overline{\text{MS}}}) Z_{ik}(\alpha_{\overline{\text{MS}}}; \epsilon) \int d^D z \frac{\delta}{\delta \hat{j}_k(z)} \Big|_{\hat{j}=0} + \mathcal{O}(a^{n_{\text{min}}+1}) \right\} \hat{\mathcal{A}}(x) \quad (4.28)\end{aligned}$$

$$\Rightarrow \frac{\delta \hat{\mathcal{A}}_{\text{lattice}}(x; a)}{\delta \hat{\mathcal{A}}(y)} = \delta(x - y) + \mathcal{O}(a^{n_{\text{min}}+1}) \quad (4.29)$$

and analogously for $\hat{\Psi}$ and $\hat{\bar{\Psi}}$ as follows from eq. (4.25). Both generating functionals are by construction invariant under gauge transformations of the background field B allowing us to perform the matching with help of the BGF method from section 3.2.2

$$\begin{aligned}\tilde{\Gamma}_{\text{lat}}^{(l,m,n)}(\dots; \alpha_{\text{lat}}; a) &\stackrel{!}{=} [\varrho^{\Psi}(\alpha_{\text{lat}}, \alpha_{\overline{\text{MS}}})]^{-m-n} \\ &\times \lim_{\epsilon \searrow 0} \left\{ \tilde{\Gamma}_{\overline{\text{MS}}}^{(l,m,n)}(\dots; \alpha_{\overline{\text{MS}}}; \epsilon) - a^{n_{\text{min}}} b_i(1, \alpha_{\overline{\text{MS}}}) \int d^D z \tilde{\Gamma}_{i;\overline{\text{MS}}}^{(l,m,n)}(\dots; z; \alpha_{\overline{\text{MS}}}; \epsilon) \right\} \\ &+ \mathcal{O}(a^{n_{\text{min}}+1}) \quad (4.30)\end{aligned}$$

such that we can safely ignore all non-gauge-invariant operators during the matching by using external background fields B rather than quantum fields \mathcal{A} . The extension to gauge-invariant local fields should be straight forward and still only involve 1PI graphs but we are content with matching of the effective action.

Notice that gauge-invariant EOM-vanishing operators still contribute and thus enlarge the minimal basis e.g. for mass-degenerate Wilson QCD

$$\mathcal{E}_1^{(1)} = m \bar{\Psi}[\gamma_{\mu} D_{\mu} + m] \Psi, \quad \mathcal{E}_2^{(1)} = \bar{\Psi}[\gamma_{\mu} D_{\mu} + m]^2 \Psi, \quad (4.31)$$

without changing the on-shell physics. This leads to the enlarged set of TL coefficients

$$\begin{aligned}b_1^{\mathcal{O}} &= -\frac{1}{2} + \mathcal{O}(\alpha_{\overline{\text{MS}}}), & b_4^{\mathcal{O}} &= -\frac{1}{4} + \mathcal{O}(\alpha_{\overline{\text{MS}}}), & b_5^{\mathcal{O}} &= \mathcal{O}(\alpha_{\overline{\text{MS}}}), \\ b_1^{\mathcal{E}} &= \frac{1}{2} + \mathcal{O}(\alpha_{\overline{\text{MS}}}), & b_2^{\mathcal{E}} &= -\frac{1}{2} + \mathcal{O}(\alpha_{\overline{\text{MS}}}),\end{aligned} \quad (4.32)$$

where the coefficients $b^{\mathcal{O}}$ remain unchanged as they describe contributions relevant to on-shell physics.

The next step would be to perform the 1-loop matching by computing a set of 1PI n -point functions on the lattice in LPT and do the same in continuum perturbation theory with insertion of each higher dimensional operator \mathcal{O}_i (and \mathcal{E}_j) separately. After renormalisation both results are required to be identical to 1-loop order and leading order in the lattice spacing thus fixing the coefficients for each operator of the minimal basis to 1-loop order. Performing the full matching to 1-loop order lies beyond the scope of this thesis as we are content with the tree-level coefficients. Nonetheless the method presented here is viable for systematic 1-loop matching without the need for connected on-shell graphs in LPT.

4.1.2 Lattice artifacts from the renormalisation condition on the lattice

So far we restricted ourselves to the perturbative description using the MS lat scheme on the lattice although this is an oversimplification because the renormalisation itself will in general yield lattice artifacts as well. To give an example on how to account for these additional contributions we switch back to the RI scheme from chapter 3.

Using eq. (3.1) we can relate the RI scheme with the MS lat scheme

$$Z^{\Phi}(\alpha_{\text{RI}}; a) = \varrho^{\Phi}(\alpha_{\text{RI}}, \alpha_{\text{lat}}; a) Z^{\Phi}(\alpha_{\text{lat}}; a) \quad (4.33)$$

and find for the intermediate factor between both schemes

$$[\varrho^\Phi(\alpha_{\text{RI}}, \alpha_{\text{lat}}; a)]^2 = \frac{\langle \Phi(x_{\text{RI}})\Phi(0) \rangle|_{\text{free}}}{\langle \Phi_{\text{lat}}(x_{\text{RI}})\Phi_{\text{lat}}(0) \rangle_{\text{lattice}}}. \quad (4.34)$$

This intermediate factor is now treated similarly to an observable. In case Φ mixes with other fields under renormalisation this step becomes more complicated and involves solving the system of equations. We will restrict considerations to the non-mixing case. Now, taking the lattice artifacts from the renormalisation into account amounts to a change in the renormalisation scheme as described by eq. (4.34). This yields for the full lattice artifacts of the 2-point function in eq. (4.18)

$$\langle \Phi_{\text{RI}}(y)\Phi_{\text{RI}}(0) \rangle_{\text{lattice}} = [\varrho^\Phi(\alpha_{\text{RI}}, \alpha_{\text{lat}}; a)]^2 \langle \Phi_{\text{lat}}(y)\Phi_{\text{lat}}(0) \rangle_{\text{lattice}} \quad (4.35)$$

$$= \langle \Phi_{\text{RI}}(y)\Phi_{\text{RI}}(0) \rangle_{\text{cont}} \left[1 + a^{n_{\text{min}}} c_j^\Upsilon(1, \alpha_{\overline{\text{MS}}}) \left\{ \delta_{j;\overline{\text{MS}}}^\Upsilon(y, 0; 1/a; 0) - \delta_{j;\overline{\text{MS}}}^\Upsilon(x_{\text{RI}}, 0; 1/a; 0) \right\} \right. \\ \left. - a^{n_{\text{min}}} b_i^\mathcal{O}(1, \alpha_{\overline{\text{MS}}}) \left\{ \delta_{i;\overline{\text{MS}}}^\mathcal{O}(y, 0; 1/a; 0) - \delta_{i;\overline{\text{MS}}}^\mathcal{O}(x_{\text{RI}}, 0; 1/a; 0) \right\} + \mathcal{O}(a^{n_{\text{min}}+1}) \right], \quad (4.36)$$

where $\langle \dots \rangle_{\text{cont}} = \lim_{a \searrow 0} \langle \dots \rangle_{\text{lattice}}$ is the true continuum limit and we introduced the shorthands

$$\delta_{i;\overline{\text{MS}}}^\mathcal{O}(x, y; \mu; \epsilon) \stackrel{\text{def}}{=} \int d^D z \frac{\langle \Phi_{\overline{\text{MS}}}(x)\Phi_{\overline{\text{MS}}}(y)\mathcal{O}_{i;\overline{\text{MS}}}(z) \rangle}{\langle \Phi_{\overline{\text{MS}}}(x)\Phi_{\overline{\text{MS}}}(y) \rangle}, \quad (4.37)$$

$$\delta_{j;\overline{\text{MS}}}^\Upsilon(x, y; \mu; \epsilon) \stackrel{\text{def}}{=} \frac{\langle \Phi_{\overline{\text{MS}}}(x)\Upsilon_{j;\overline{\text{MS}}}(y) + \Upsilon_{j;\overline{\text{MS}}}(x)\Phi_{\overline{\text{MS}}}(y) \rangle}{\langle \Phi_{\overline{\text{MS}}}(x)\Phi_{\overline{\text{MS}}}(y) \rangle} \quad (4.38)$$

for the different relative contributions of lattice artifacts. Notice that the lattice artifacts depend on the specific choice for x_{RI} , i.e., even for different orientations of x_{RI} like on axis, face diagonal etc. we expect different lattice artifacts.

Here the generalisation to different or more fields Φ, Φ' etc. is neither straight forward nor free of ambiguities. This can be seen by going back to eq. (3.1) to define appropriate renormalisation factors for the additional fields. Already at the level of the 2-point function of two different fields Φ and Φ' there are different strategies to extract both ϱ^Φ and $\varrho^{\Phi'}$ as we may choose to extract it from either

$$\langle \Phi_{\text{RI}}(x_{\text{RI}})\Phi'_{\text{RI}}(0) \rangle_{\text{lattice}} \quad \text{or} \quad \begin{cases} \langle \Phi_{\text{RI}}(x_{\text{RI}})\Phi_{\text{RI}}(0) \rangle_{\text{lattice}} \\ \langle \Phi'_{\text{RI}}(x_{\text{RI}})\Phi'_{\text{RI}}(0) \rangle_{\text{lattice}} \end{cases}, \quad (4.39)$$

where both strategies introduce different additional lattice artifacts. Of course this ambiguity resembles the freedom one has on the lattice and the overall procedure remains the same.

Remark: Let us stress again that the computation of the full contributions to the leading lattice artifacts can be done perturbatively in a 2-step procedure:

1. Perturbative matching of the coefficients $b_i^\mathcal{O}$ and c_j^Υ for the operator bases from favorable chosen matching conditions.
2. Use the perturbative result to determine lattice artifacts for the renormalisation condition chosen during the lattice computation and combine both contributions leading to equation (4.36).

The matrix elements in step 2 do not need to be the same as the ones for the perturbative matching in step 1 and thus can be computed entirely in the continuum effective theory.

Actually, a continuum extrapolation requires scaleless quantities, which is achieved by multiplying the quantity of interest with a properly chosen power of the reference scale used for scale setting. Consequently this reference scale will introduce additional lattice artifacts that need to be taken into account as well.

4.2 Asymptotic behaviour of lattice artifacts

Instead of matching all the coefficients we are more interested in the lattice artifacts which may occur and their asymptotic behaviour as $a \searrow 0$. To extract this we first switch to the bases \mathcal{B} and \mathcal{Y} with diagonal mixing matrices at 1-loop

$$\begin{aligned} \frac{\langle \Phi_{\text{RI}}(y) \Phi_{\text{RI}}(0) \rangle_{\text{lattice}}}{\langle \Phi_{\text{RI}}(y) \Phi_{\text{RI}}(0) \rangle_{\text{cont}}} &= 1 + a^{n_{\min}} c_j^{\mathcal{Y}}(1, \alpha_{\overline{\text{MS}}}) \left\{ \delta_{j;\overline{\text{MS}}}^{\mathcal{Y}}(y, 0; 1/a) - \delta_{j;\overline{\text{MS}}}^{\mathcal{Y}}(x_{\text{RI}}, 0; 1/a) \right\} \\ &\quad - a^{n_{\min}} b_i^{\mathcal{B}}(1, \alpha_{\overline{\text{MS}}}) \left\{ \delta_{i;\overline{\text{MS}}}^{\mathcal{B}}(y, 0; 1/a) - \delta_{i;\overline{\text{MS}}}^{\mathcal{B}}(x_{\text{RI}}, 0; 1/a) \right\} \\ &\quad + \mathcal{O}(a^{n_{\min}+1}), \end{aligned} \quad (4.40)$$

where $c^{\mathcal{Y}}, b^{\mathcal{B}}$ are the coefficients matching the diagonal bases. Introducing now RGI quantities as defined in eq. (3.43)

$$\delta_{i;\overline{\text{MS}}}^{\chi}(\dots; \mu; 0) = [2\beta_0 \alpha_{\overline{\text{MS}}}(\mu)]^{\hat{\gamma}_i^{\chi}} \delta_{i;\text{RGI}}^{\chi}(\dots) \times [1 + \mathcal{O}(\alpha_{\overline{\text{MS}}})], \quad \chi = \mathcal{B}, \mathcal{Y}, \quad (4.41)$$

we obtain for the leading lattice artifacts

$$\begin{aligned} \frac{\langle \Phi_{\text{RI}}(y) \Phi_{\text{RI}}(0) \rangle_{\text{lattice}}}{\langle \Phi_{\text{RI}}(y) \Phi_{\text{RI}}(0) \rangle_{\text{cont}}} &= 1 + \left[2a^{n_{\min}} \sum_i c_i^{\mathcal{Y}}(1, 0) [2\beta_0 \alpha_{\overline{\text{MS}}}(1/a)]^{\hat{\gamma}_i^{\mathcal{Y}} - \hat{\gamma}^{\Phi}} \left\{ \delta_{i;\text{RGI}}^{\mathcal{Y}}(y, 0) - \delta_{i;\text{RGI}}^{\mathcal{Y}}(x_{\text{RI}}, 0) \right\} \right. \\ &\quad \left. - a^{n_{\min}} \sum_i b_i^{\mathcal{B}}(1, 0) [2\beta_0 \alpha_{\overline{\text{MS}}}(1/a)]^{\hat{\gamma}_i^{\mathcal{B}}} \left\{ \delta_{i;\text{RGI}}^{\mathcal{B}}(y, 0) - \delta_{i;\text{RGI}}^{\mathcal{B}}(x_{\text{RI}}, 0) \right\} \right] \\ &\quad \times [1 + \mathcal{O}(\alpha_{\overline{\text{MS}}})] + \mathcal{O}(a^{n_{\min}+1}), \end{aligned} \quad (4.42)$$

where $c^{\mathcal{Y}}(1, 0), b^{\mathcal{B}}(1, 0)$ are the tree-level coefficients.

One important feature of this equation is that the right hand side consists only of constants w.r.t. the lattice spacing a except for the occurring powers of a and $2\beta_0 \alpha_{\overline{\text{MS}}}(1/a) \approx -1/\ln(a\Lambda_{\overline{\text{MS}}})$. Thus we can distinguish the different contributions and their behaviour as $a \searrow 0$.

In order to determine the complete asymptotic dependence on the lattice spacing one needs to compute the leading order anomalous dimension of each quantity Φ one is interested in and their higher dimensional corrections Υ_i . We will restrict ourselves to the contributions from the action that one will face independent of the chosen quantity. As found in equation (4.42), these contributions and their leading logarithms are independent of the anomalous dimensions of the Φ .

This analysis is sufficient for spectral quantities, such as energies, masses etc., which do not depend on the details of the composite field, i.e., the coefficients $c_j^{\mathcal{Y}}$. As an example let us consider the pion mass from eq. (2.21), i.e., $\Phi = P^0$

$$\begin{aligned} dM_{\pi}(a) &= - \lim_{x_0 \rightarrow \infty} \left[\ln \frac{\int d^3 \mathbf{x} C^0(x_0, \mathbf{x}; 0)}{\int d^3 \mathbf{x} C^0(x_0 + d, \mathbf{x}; 0)} \right. \\ &\quad \left. + \ln \left\{ 1 - a^{n_{\min}} b_i^{\mathcal{B}}(1, 0) \int d^3 \mathbf{x} \left\{ \delta_{i;\overline{\text{MS}}}^{\mathcal{B}}(x, 0; 1/a; 0) - \delta_{i;\overline{\text{MS}}}^{\mathcal{B}}(x + d\hat{0}, 0; 1/a; 0) \right\} + \mathcal{O}(a^{n_{\min}+1}) \right\} \right] \\ &= dM_{\pi}(0) - \frac{a^{n_{\min}}}{2} d \sum_i b_i^{\mathcal{B}}(1, 0) [2\beta_0 \alpha_{\overline{\text{MS}}}(1/a)]^{\hat{\gamma}_i^{\mathcal{B}}} \langle \pi_0 | \mathcal{B}_{i;\text{RGI}}(0) | \pi_0 \rangle \times [1 + \mathcal{O}(\alpha_{\overline{\text{MS}}}(1/a))] \\ &\quad + \mathcal{O}(a^{n_{\min}+1}), \end{aligned} \quad (4.43)$$

where we dropped the $\delta^{\mathcal{Y}}$ terms already in the first line as they cancel in the $x_0 \rightarrow \infty$ limit and introduced the ground state $|\pi_0\rangle$ with correct symmetries and normalisation $\langle \pi_0 | \pi_0 \rangle = 2L^3$ in case of a finite box. The leading factor $d = \text{fixed}$ is a small integer multiple of the lattice spacing for on-axis distance d and should remind the reader that one would actually extract dM_{π} from the lattice before setting the scale. Only then the continuum extrapolation of $r_0 M_{\pi}(a)$ can be

performed with additional lattice artifacts from r_0 or any other scale. For non-spectral quantities additional observable-dependent anomalous dimensions are required as input.

Notice that in case of $c_i^{\mathcal{T}}(1, 0) = 0$ or $b_i^{\mathcal{B}}(1, 0) = 0$ there are no tree-level contributions of the corresponding term. Without further knowledge of higher order terms we will then assume the 1-loop contributions as the leading terms. These are suppressed by the previously stated factor $\alpha_{\overline{\text{MS}}}(1/a) \approx 1/[-2\beta_0 \ln(a\Lambda_{\overline{\text{MS}}})]$.

Chapter 5

Symanzik's Effective Theory of lattice QCD

Today's simulations of lattice QCD typically do not use unimproved Wilson fermions from eq. (2.8) but employ non-perturbatively $O(a)$ improved fermions. Those fermions are either Wilson fermions with a non-perturbatively chosen coefficient of the Sheikholeslami-Wohlert term as well as adjusted mass and coupling renormalisation [58, 112] or completely different lattice fermion actions that automatically satisfy $O(a)$ improvement due to symmetry constraints.

5.1 Commonly used lattice actions

In the following we will give a short overview of the more commonly used lattice actions and what symmetry constraints they impose on their Symanzik Effective Theory description and thus the minimal operator basis at mass-dimension 5 and 6. In anticipation of tree-level matching we will also perform the naive expansion in the lattice spacing of the lattice action, from which one can read off the tree-level matching coefficients once the minimal (on-shell) basis has been worked out.

5.1.1 Gauge actions

A general class of lattice Yang-Mills actions is [57, 59, 60]

$$S_G^{\text{latt}} = \frac{2}{g_0^2} \sum_x \sum_{i \in \{0,1,2,3\}} e_i(g_0^2) \sum_{\mathcal{U} \in \mathcal{C}_i} \text{Re tr} \left(\mathbb{1} - \mathcal{U}(x) \right) \quad (5.1)$$

with the convention¹ $e_0(g_0^2) + 8e_1(g_0^2) + 8e_2(g_0^2) + 16e_3(g_0^2) = 1$. The occurring contours build of link variables are

$$\begin{aligned} \mathcal{C}_0(x) &= \{U_\mu(x)U_\nu(x+a\hat{\mu})U_\mu^\dagger(x+a\hat{\nu})U_\nu^\dagger(x) \mid \mu < \nu\} \\ \mathcal{C}_1(x) &= \{U_\mu(x)U_\mu(x+a\hat{\mu})U_\nu(x+a\hat{\mu})U_\mu^\dagger(x+a\hat{\mu}+a\hat{\nu})U_\mu^\dagger(x+a\hat{\nu})U_\nu^\dagger(x) \mid \mu \neq \nu\} \\ \mathcal{C}_2(x) &= \{U_\mu(x)U_\nu(x+a\hat{\mu})U_\rho(x+a\hat{\mu}+a\hat{\nu})U_\mu^\dagger(x+a\hat{\nu}+a\hat{\rho})U_\nu^\dagger(x+a\hat{\rho})U_\rho^\dagger(x) \mid \mu < \nu < \rho\} \cup \\ &\quad \{U_\mu(x)U_\nu(x+a\hat{\mu})U_\rho^\dagger(x+a\hat{\mu}+a\hat{\nu}-a\hat{\rho})U_\mu^\dagger(x+a\hat{\nu}-a\hat{\rho})U_\nu^\dagger(x-a\hat{\rho})U_\rho(x-a\hat{\rho}) \mid \mu < \nu < \rho\} \cup \\ &\quad \{U_\mu(x)U_\nu^\dagger(x+a\hat{\mu}-a\hat{\nu})U_\rho(x+a\hat{\mu}-a\hat{\nu})U_\mu^\dagger(x-a\hat{\nu}+a\hat{\rho})U_\nu(x-a\hat{\nu}+a\hat{\rho})U_\rho^\dagger(x) \mid \mu < \nu < \rho\} \cup \\ &\quad \{U_\mu(x)U_\nu^\dagger(x+a\hat{\mu}-a\hat{\nu})U_\rho^\dagger(x+a\hat{\mu}-a\hat{\nu}-a\hat{\rho})U_\mu^\dagger(x-a\hat{\nu}-a\hat{\rho})U_\nu(x-a\hat{\nu}-a\hat{\rho})U_\rho(x-a\hat{\rho}) \mid \\ &\quad \mu < \nu < \rho\} \end{aligned}$$

¹We renamed the coefficients $c_i \rightarrow e_i$, cf. [57], to avoid confusion with the matching coefficients of the SET.

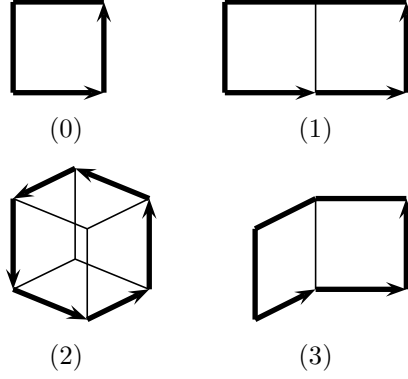


Figure 5.1: Graphical representations [54, p. 45] of the terms $\mathcal{C}_i(x)$ with $i \in \{0, 1, 2, 3\}$ contributing to the lattice gauge action in eq. (5.1). We will refer to these shapes as plaquette, rectangle, twisted chair and chair from (0) to (3).

$$\begin{aligned} \mathcal{C}_3(x) = & \{U_\mu(x)U_\nu(x+a\hat{\mu})U_\mu^\dagger(x+a\hat{\nu})U_\rho(x)U_\nu^\dagger(x+a\hat{\rho})U_\rho^\dagger(x+a\hat{\nu}) \mid \mu \neq \nu \wedge \mu \neq \rho \wedge \nu \neq \rho\} \cup \\ & \{U_\mu(x)U_\nu(x+a\hat{\mu})U_\mu^\dagger(x+a\hat{\nu})U_\rho^\dagger(x)U_\nu^\dagger(x-a\hat{\rho})U_\rho(x+a\hat{\nu}) \mid \mu \neq \nu \wedge \mu \neq \rho \wedge \nu \neq \rho\}, \end{aligned}$$

where $\mu, \nu, \rho \in \{0, 1, 2, 3\}$ and \mathcal{C}_0 is the set of all (oriented) Wilson plaquettes, see also figure 5.1 for the graphical representation of all Wilson loops in the different sets \mathcal{C}_i . To make a connection to the continuum gauge field A_μ remember the definition of the Wilson line eq. (2.15), which has the same behaviour under gauge transformations

$$U_\mu(x) = \text{Pexp} \left(- \int_{x+a\hat{\mu}}^x dz_\mu A_\mu(z) \right). \quad (5.2)$$

This assumes that a lattice with lattice spacing a is embedded into the continuous space-time [60]. The naive expansion in the lattice spacing then yields [57]

$$\begin{aligned} S_G^{\text{latt}} = & -\frac{1}{2g_0^2} \int d^4x \left\{ \text{tr} (F_{\mu\nu} F_{\mu\nu}) - \frac{2}{3} a^2 e_2(g_0^2) \text{tr} (D_\mu F_{\nu\rho} D_\mu F_{\nu\rho}) \right. \\ & - a^2 \left(2e_1(g_0^2) - 2e_3(g_0^2) + \frac{1}{6} \right) \sum_\mu \text{tr} (D_\mu F_{\mu\rho} D_\mu F_{\mu\rho}) \\ & \left. - a^2 \left(\frac{2}{3} e_2(g_0^2) + 2e_3(g_0^2) \right) \text{tr} (D_\mu F_{\mu\rho} D_\nu F_{\nu\rho}) + \mathcal{O}(a^4) \right\}. \end{aligned} \quad (5.3)$$

This covers most of the common choices for the lattice gauge actions which typically have $n_{\min} = 2$.

As was the case for the Wilson plaquette action, this more general ansatz for lattice gauge actions is invariant under parity, time reversal and charge conjugation, with the transformations listed in appendix C, but again breaks $O(4)$ invariance down to hyper-cubic H_4 symmetry.

5.1.2 Ginsparg-Wilson fermions

The Wilson term of Wilson fermions eq. (2.8) breaks chiral symmetry of massless quarks explicitly, i.e. the Wilson action is not invariant under independent $SU(N_f)_L \times SU(N_f)_R \times U(1)_V \times U(1)_A$ rotations of left- and right-handed quarks. One way out are Ginsparg-Wilson fermions [116] with lattice Dirac operator \hat{D}^{GW} complying with the *Ginsparg-Wilson equation*

$$\hat{D}^{\text{GW}} \gamma_5 + \gamma_5 \hat{D}^{\text{GW}} = a \hat{D}^{\text{GW}} \gamma_5 \hat{D}^{\text{GW}}, \quad (5.4)$$

see also [71, p. 163ff.]. Then Ginsparg-Wilson fermions transforming as

$$\bar{\psi}^f \rightarrow \bar{\psi}^f \exp \left[i\gamma_5 \vartheta (1 - a\hat{D}^{\text{GW}}/2) \right], \quad \psi^f \rightarrow \exp \left[i\gamma_5 \vartheta (1 - a\hat{D}^{\text{GW}}/2) \right] \psi^f, \quad \vartheta \in \mathbb{R}, \quad (5.5)$$

keep the lattice action invariant, which is the exact lattice chiral symmetry [117] of Ginsparg-Wilson fermion actions. As $a \searrow 0$ these transformations formally reduce to the continuum chiral rotations

$$\bar{\psi}^f \rightarrow \bar{\psi}^f \exp (i\gamma_5 \vartheta), \quad \psi^f \rightarrow \exp (i\gamma_5 \vartheta) \psi^f, \quad \vartheta \in \mathbb{R}. \quad (5.6)$$

Adding a mass term, which then breaks lattice chiral symmetry explicitly, gives the general action for (massive) Ginsparg-Wilson fermions [118]

$$S_{\text{F}}^{\text{GW}} = a^4 \sum_x \bar{\Psi}(x) \left\{ \hat{D}^{\text{GW}} + M \left(1 - \frac{a}{2} \hat{D}^{\text{GW}} \right) \right\} \Psi(x). \quad (5.7)$$

A possible solution to \hat{D}^{GW} in eq. (5.4) are e.g. Overlap fermions [119, 120] with lattice Dirac operator (we choose here the conventions from [121])

$$\hat{D}^{\text{OV}} = \frac{1}{a} \left\{ 1 - A (A^\dagger A)^{-1/2} \right\}, \quad A = 1 - a\hat{D}^{\text{W}}. \quad (5.8)$$

For a discussion on the locality of the overlap operator see [121]. The naive expansion in the lattice spacing then yields

$$\begin{aligned} S_{\text{F}}^{\text{GW}} &= \int d^4x \bar{\Psi}(x) \left[\gamma_\mu D_\mu + M - \frac{a}{2} \gamma_\mu D_\mu (M + \gamma_\nu D_\nu) \right. \\ &\quad \left. + \frac{a^2}{6} \sum_\mu \gamma_\mu D_\mu^3 + \frac{a^2}{2} (\gamma_\mu D_\mu)^3 - \frac{a^2}{4} \{ \gamma_\mu D_\mu, D^2 \} + \frac{a^2}{4} M (\gamma_\mu D_\mu)^2 \right] \Psi(x) + \mathcal{O}(a^3) \\ &\stackrel{\text{EOM}}{=} \int d^4x \bar{\Psi}(x) \left\{ \gamma_\mu D_\mu + M + \frac{a^2}{6} \sum_\mu \gamma_\mu D_\mu^3 - \frac{a^2}{4} M^3 + \frac{a^2}{2} M D^2 \right\} \Psi(x) + \mathcal{O}(a^3). \end{aligned} \quad (5.9)$$

Domain-Wall fermions [122, 123] comply with eq. (5.4) in the limit of infinite extent of the auxiliary 5th dimension [124], while for finite extent chiral symmetry violations are only exponentially suppressed as the extent of the 5th dimension increases.

For Ginsparg-Wilson fermions local $\text{SU}(N)$ gauge symmetry, \mathcal{C} -, \mathcal{P} - and \mathcal{T} -invariance as well as hypercubic H_4 symmetry remain the same as for Wilson fermions. Due to invariance under eq. (5.5) of massless Ginsparg-Wilson fermions no operators are allowed in the SET that break $\text{SU}(N_{\text{f}})_{\text{L}} \times \text{SU}(N_{\text{f}})_{\text{R}}$ flavour symmetry unless they are explicitly mass-dependent and thus vanish as $M \rightarrow 0$. In particular no operators without explicit mass-dependence are allowed at mass-dimension 5 thus excluding the Sheikholeslami-Wohlert term and setting $n_{\text{min}} \geq 2$.

5.1.3 Twisted-mass fermions

Twisted-mass fermions [125, 126] were originally introduced as an infrared regulator for two mass-degenerate flavours, ensuring that the fermion determinant is strictly positive, which excludes exceptional configurations having a zero eigenvalue for the lattice Dirac operator. Nowadays, there are extensions to non mass-degenerate flavours [127] and/or higher number of flavours [128].

We will stick here to two mass-degenerate flavours in combination with the Wilson Dirac operator eq. (2.8) (in principle one could also use another lattice Dirac operator, see e.g. [126]). The corresponding lattice action is

$$\begin{aligned} S_{\text{F}}^{\text{tm}} &= a^4 \sum_x \bar{\chi}(x) \left(\hat{D}^{\text{W}} + m_{\text{q}} + i\mu_{\text{q}} \gamma_5 \tau^3 \right) \chi(x) \\ &= a^4 \sum_x \bar{\chi}(x) \left(\hat{D}^{\text{W}} + m e^{i\omega \gamma_5 \tau^3} \right) \chi(x), \end{aligned} \quad (5.10)$$

where m is the mass of the mass-degenerate quarks, χ is a 2-flavour vector in the twisted basis and τ^j with $j \in \{1, 2, 3\}$ are the Pauli matrices

$$\tau^1 = \begin{pmatrix} 0 & 1 \\ 1 & 0 \end{pmatrix}, \quad \tau^2 = \begin{pmatrix} 0 & -i \\ i & 0 \end{pmatrix}, \quad \tau^3 = \begin{pmatrix} 1 & 0 \\ 0 & -1 \end{pmatrix} \quad (5.11)$$

here acting in flavour space. From the first to the second line one identifies

$$m_q = m \cos(\omega), \quad \mu_q = m \sin(\omega) \quad (5.12)$$

with twist angle ω . This angle ω describes a chiral rotation

$$\bar{\Psi} \rightarrow \bar{\chi} e^{i\omega\gamma_5\tau^3/2}, \quad \Psi \rightarrow e^{i\omega\gamma_5\tau^3/2} \chi, \quad (5.13)$$

which transforms non-twisted continuum QCD into twisted mass QCD (tmQCD). For lattice Wilson QCD the Wilson term removing the doublers spoils this connection. The explicit breaking of chiral symmetry due to the Wilson term [70] is closely related to this issue such that lattice Dirac operators preserving the lattice chiral symmetry of the action [126] can be related with their twisted mass counterparts through eq. (5.13).

Introducing the twisted mass term breaks parity and time reversal invariance. Instead tmQCD is invariant under the modified symmetry transformations

1. Modified parity:

$$\begin{aligned} \mathcal{P}_j^{\text{tm}} : \quad & \bar{\chi}(x_0, \mathbf{x}) \rightarrow -i\bar{\chi}(x_0, -\mathbf{x})\gamma_0\tau^j, \quad \chi(x_0, \mathbf{x}) \rightarrow i\gamma_0\tau^j\chi(x_0, -\mathbf{x}), \quad j \in \{1, 2\}, \\ \mathcal{P}_{\mu_q}^{\text{tm}} : \quad & \bar{\chi}(x_0, \mathbf{x}) \rightarrow \bar{\chi}(x_0, -\mathbf{x})\gamma_0, \quad \chi(x_0, \mathbf{x}) \rightarrow \gamma_0\chi(x_0, -\mathbf{x}), \quad \mu_q \rightarrow -\mu_q, \end{aligned} \quad (5.14)$$

2. Modified time reversal:

$$\begin{aligned} \mathcal{T}_j^{\text{tm}} : \quad & \bar{\chi}(x_0, \mathbf{x}) \rightarrow -i\bar{\chi}(-x_0, \mathbf{x})\gamma_5\gamma_0\tau^j, \quad \chi(x_0, \mathbf{x}) \rightarrow i\gamma_0\gamma_5\tau^j\chi(-x_0, \mathbf{x}), \quad j \in \{1, 2\}, \\ \mathcal{T}_{\mu_q}^{\text{tm}} : \quad & \bar{\chi}(x_0, \mathbf{x}) \rightarrow \bar{\chi}(-x_0, \mathbf{x})\gamma_5\gamma_0, \quad \chi(x_0, \mathbf{x}) \rightarrow \gamma_0\gamma_5\chi(-x_0, \mathbf{x}), \quad \mu_q \rightarrow -\mu_q, \end{aligned} \quad (5.15)$$

where the gauge field transforms as usual and both $\mathcal{P}_{\mu_q}^{\text{tm}}$ and $\mathcal{T}_{\mu_q}^{\text{tm}}$ are spurionic symmetry transformations. Invariance under charge conjugation from eq. (C.1) remains intact. In the massive continuum theory the $\text{SU}(2)_V$ symmetry is replaced by its twisted version [129, p. 171] with corresponding symmetry transformation

$$\text{SU}(2)_{\text{tw}} : \quad \bar{\chi} \rightarrow \bar{\chi} e^{i\omega\gamma_5\tau^3/2} \Omega^\dagger e^{-i\omega\gamma_5\tau^3/2}, \quad \chi \rightarrow e^{-i\omega\gamma_5\tau^3/2} \Omega e^{i\omega\gamma_5\tau^3/2} \chi, \quad \Omega \in \text{SU}(2), \quad (5.16)$$

where Ω and τ^3 act in flavour space. Again tmQCD with Wilson fermions explicitly breaks this flavour symmetry due to the Wilson term. Only invariance under the transformation

$$\bar{\chi} \rightarrow \bar{\chi} e^{-i\varphi\tau^3/2}, \quad \chi \rightarrow e^{i\varphi\tau^3/2} \chi, \quad \varphi \in \mathbb{R} \quad (5.17)$$

remains as a remnant of the full symmetry.

Due to modified parity and time reversal symmetries there exist additional operators necessary for the SET of lattice tmQCD. By construction these new operators are explicitly μ_q dependent operators as all others are contained within the original parity and time reversal invariant operators, e.g. at mass-dimension 6

$$O = i\mu_q \bar{\chi} \gamma_5 \tau^3 D^2 \chi. \quad (5.18)$$

The spurionic $\mathcal{P}_{\mu_q}^{\text{tm}}$ and $\mathcal{T}_{\mu_q}^{\text{tm}}$ symmetries ensure that only operators with odd powers of μ_q are truly new operators while even powers of μ_q only occur multiplying the already known operators of lower mass-dimension invariant under the unmodified \mathcal{P} and \mathcal{T} transformations.

Moreover in the continuum effective theory the operator O and any other truly new operator can be obtained from the chiral rotation of a \mathcal{P} and \mathcal{T} even operator, e.g.

$$\mathcal{O} = m\bar{\Psi}D^2\Psi \xrightarrow{(5.13)} \mathcal{O}^{\text{tw}} = m_{\text{q}}\bar{\chi}D^2\chi + i\mu_{\text{q}}\bar{\chi}\gamma_5\tau^3D^2\chi, \quad (5.19)$$

where $m_{\text{q}}\bar{\chi}D^2\chi$ remains as a remnant of the \mathcal{P} and \mathcal{T} even operator. This enables us to infer the anomalous dimension of such operators from the non-twisted operators due to [130, p. 204]

$$\langle \mathcal{O}_{i;\mathcal{S}} O_{\text{ext}} \rangle_{\text{QCD}} = Z_{ij}^{\mathcal{O}} \langle \mathcal{O}_j O_{\text{ext}} \rangle_{\text{QCD}} \equiv Z_{ij}^{\mathcal{O}} \langle \mathcal{O}_j^{\text{tw}} O_{\text{ext}} \rangle_{\text{tmQCD}}, \quad (5.20)$$

where the subscripts QCD and tmQCD denote the choice of the mass term in the action and O_{ext} is assumed to be invariant under chiral rotations. This equivalence holds in case a mass independent multiplicative renormalisation scheme \mathcal{S} is used and the regularisation is invariant under chiral rotations. Then the chiral rotation eq. (5.13) amounts only to a substitution in the path integral. One possible regularisation having this property is Ginsparg-Wilson fermions. For our previous example this ensures identical anomalous dimensions of $m\bar{\Psi}D^2\Psi$, $m_{\text{q}}\bar{\chi}D^2\chi$ and $i\mu_{\text{q}}\bar{\chi}\gamma_5\tau^3D^2\chi$ as mass-independence of the renormalisation scheme ensures independence of $Z_{ij}^{\mathcal{O}}$ from ω . Consequently all anomalous dimensions needed for tmQCD can be inferred from \mathcal{P} and \mathcal{T} even lower dimensional operators in non-twisted continuum QCD and thus do not require any additional computation. Being only interested in 1-loop anomalous dimensions, which are scheme independent, further allows to stick to the $\overline{\text{MS}}$ renormalisation scheme in continuum perturbation theory.

In anticipation of the discussion on the leading asymptotic behaviour of lattice artifacts we mention another important feature of tmQCD, the so called “automatic” $\mathcal{O}(a)$ improvement at maximal twist, i.e. $\omega = \pi/2$. This is due to an additional discrete symmetry of the continuum theory (or lattice theory with a chiral symmetry preserving Dirac operator) at this angle [129, 131]

$$T_1 : \quad \bar{\chi} \rightarrow i\bar{\chi}\tau^1\gamma_5, \quad \chi \rightarrow i\gamma_5\tau^1\chi. \quad (5.21)$$

Again this symmetry is broken by the Wilson term. Since this is only a symmetry of the continuum theory understanding this effect is a bit more involved than having an explicit symmetry on the lattice. Following the lines of [131] any operator can be split into a T_1 -even and T_1 -odd part, i.e., parts having eigenvalues ± 1 under the transformation eq. (5.21) respectively. This carries over to n -point functions of operators which can then be split into a T_1 -even and T_1 -odd part as well, where the T_1 -odd part vanishes by construction.

As we will see later on, all operators of mass-dimension 5 parametrising $\mathcal{O}(a)$ lattice artifacts are T_1 -odd ensuring that an insertion of such operators into a T_1 -even n -point function vanishes such that no $\mathcal{O}(a)$ corrections can occur. This does not imply that the $\mathcal{O}(a)$ corrections can be ignored as they become relevant at $\mathcal{O}(a^2)$ due to double insertions of mass-dimension 5 operators when expanding eq. (4.17) further. Furthermore, T_1 -odd n -point functions have $\mathcal{O}(a)$ corrections, but are known to vanish trivially in the continuum limit. This difficulty is a consequence from being only a symmetry of the continuum theory.

5.1.4 Staggered fermions

Wilson QCD without the Wilson term has 15 doublers for each simulated quark flavour thus leading to 16 degenerate quarks. We restrict considerations here to a single flavour. Instead of removing the doublers systematically staggered fermions [55] make use of a spacetime dependent variable transformation, see e.g. [71, p. 243ff.],

$$\bar{\psi}(x) = \bar{\psi}'(x)\gamma_3^{x_3/a}\gamma_2^{x_2/a}\gamma_1^{x_1/a}\gamma_0^{x_0/a}, \quad \psi(x) = \gamma_0^{x_0/a}\gamma_1^{x_1/a}\gamma_2^{x_2/a}\gamma_3^{x_3/a}\psi'(x). \quad (5.22)$$

Applying this transformation to eq. (2.8) leads to

$$S_F^W|_{r=0} = a^4 \sum_{x,\mu} \bar{\psi}'(x) \left\{ \frac{\eta_\mu(x)}{2a} (U_\mu(x) \psi'(x + a\hat{\mu}) - U_\mu^\dagger(x - a\hat{\mu}) \psi'(x - a\hat{\mu})) + m \psi'(x) \right\}, \quad (5.23)$$

$$\eta_0(x) = 1, \quad \eta_1(x) = (-1)^{x_0/a}, \quad \eta_2(x) = (-1)^{x_0/a + x_1/a}, \quad \eta_3(x) = (-1)^{x_0/a + x_1/a + x_2/a}.$$

Since each of the four spinor components now appears in the identical way in the action one may limit considerations to one specific component $\chi = \psi'_\alpha$ (α is the Dirac index) thus reducing the degeneracy from 16 to 4 degenerate quarks

$$S_F^{\text{stag}} = a^4 \sum_{x,\mu} \bar{\chi}(x) \left\{ \frac{\eta_\mu(x)}{2a} (U_\mu(x) \chi(x + a\hat{\mu}) - U_\mu^\dagger(x - a\hat{\mu}) \chi(x - a\hat{\mu})) + m \chi(x) \right\}. \quad (5.24)$$

In the massless case this action is invariant under the $U(1)_{\bar{A}}$ transformation

$$\bar{\chi}(x) \rightarrow \bar{\chi}(x) e^{i\vartheta \eta_5(x)}, \quad \chi(x) \rightarrow e^{i\vartheta \eta_5(x)} \chi(x), \quad \vartheta \in \mathbb{R}, \quad \eta_5(x) = (-1)^{x_0/a + x_1/a + x_2/a + x_3/a}, \quad (5.25)$$

which is a remnant of the global chiral symmetry transformation for the case of staggered quarks. Gauge invariance and space-time symmetries remain the same as for Wilson quarks, see e.g. [132]. Apart from the trivial global $U(1)_B$ symmetry all flavour symmetries one would typically expect for massless or mass-degenerate quarks are broken due to so called *taste breaking*, i.e. the existence of “flavour” changing interactions at finite lattice spacing. For more details see e.g. [71, p. 245ff.].

5.2 Minimal bases for the Symanzik Effective Theory

From the above discussion we infer the symmetry constraints for the SET of different lattice discretisations regarding both spacetime and flavour symmetries. For a summary of the latter see table 5.1. To keep the operator basis as small as possible, we exclude staggered quarks as they allow for taste breaking, which increases the minimal basis significantly. The full set of symmetry constraints we impose on our SET bases then reads:

- Local $SU(N)$ gauge symmetry,
- \mathcal{C} -, \mathcal{P} -, \mathcal{T} -invariance,
- Hypercubic H_4 symmetry,
- $SU(N_f)_L \times SU(N_f)_R \times U(1)_V$ for chiral symmetry preserving lattice fermion actions, i.e. no Wilson quarks,
- $SU(N_f)_V$ flavour symmetry for massless Wilson quarks.

Generalisation to massive quarks is straight forward and only requires inclusion of explicitly mass-dependent operators such that vanishing renormalised quark masses $m_{\overline{\text{MS}}}^q \rightarrow 0$ restore the symmetries of the massless lattice action. The relevant operators with explicit mass-dependence and their anomalous dimensions can be inferred from operators of lower mass dimensions. Consequently we will discard operators with explicit mass-dependence for now from the minimal basis as we are only interested in determining the anomalous dimension matrix for a minimal massless basis from which the full anomalous dimension matrix can be reconstructed.

As argued in section 5.1.3 we may infer the anomalous dimension of mass-dimension 5 and 6 operators of tmQCD from non-twisted continuum QCD. Thus we can limit ourselves to \mathcal{P} and \mathcal{T} symmetric operators for the minimal basis to obtain all relevant 1-loop anomalous dimensions and postpone the discussion of the tmQCD operator basis to section 5.4.

Table 5.1: Flavour symmetries of lattice fermion actions.

fermion action	massless	mass-degenerate	massive	n_{\min}
Continuum				—
Ginsparg-Wilson	$SU(N_f)_L \times SU(N_f)_R \times U(1)_V$	$SU(N_f)_V \times U(1)_V$	$\bigtimes_{f=1}^{N_f} U(1)_f$	2
Domain wall				2
Wilson	$SU(N_f)_V \times U(1)_V$	$SU(N_f)_V \times U(1)_V$	$\bigtimes_{f=1}^{N_f} U(1)_f$	1
staggered	$U(1)_B \times U(1)_{\bar{A}}$	$U(1)_B$	$U(1)_B$	2

5.2.1 Purely gluonic operators

Starting with the operators of lowest mass dimension 4 only the trivial one occurs

$$\mathcal{O}_1^{(0)} = \frac{1}{g_0^2} \text{tr} (F_{\mu\nu} F_{\mu\nu}). \quad (5.26)$$

We introduce this operator only for convenience as it reoccurs multiplied by powers of quark masses when going to higher mass-dimension. For example, due to parity there is no pure gauge operator of mass-dimension 5 [57]. However, multiplying the operator $\mathcal{O}_1^{(0)}$ by a quark mass is allowed, such that

$$\frac{1}{g_0^2} \text{tr} (M) \text{tr} (F_{\mu\nu} F_{\mu\nu}) = \text{tr} (M) \mathcal{O}_1^{(0)} \quad (5.27)$$

is a valid operator compatible with the symmetry constraints as found before in chapter 4. Due to the explicit mass-dependence this operator is only relevant if $m_{\text{MS}}^q \neq 0$ for any quark flavour q . However, multiplying an operator of lower mass-dimension by masses only affects the diagonal entries of the mixing matrix and is otherwise fully covered by the renormalisation of the lower dimensional operator. As mentioned earlier we thus drop explicitly mass-dependent operators from the minimal basis to keep it small.

For mass-dimension 6 we need a systematic approach to obtain all candidates for our basis complying with \mathcal{C} , \mathcal{P} and \mathcal{T} symmetry. We start with the general form

$$\frac{1}{g_0^2} \text{tr} (F_{\mu\nu} \overleftrightarrow{\Gamma}_{\mu\nu\rho\sigma} F_{\rho\sigma}),$$

without specifying for the moment on which field strength tensor potential derivatives in $\overleftrightarrow{\Gamma}$ act. Taking now the behaviour of the field strength tensor under parity transformation (C.5) into account yields

$$\overleftrightarrow{\Gamma}_{0jkl} \xrightarrow{\mathcal{P}} -\overleftrightarrow{\Gamma}_{0jkl}, \quad \overleftrightarrow{\Gamma}_{ijkl} \xrightarrow{\mathcal{P}} \overleftrightarrow{\Gamma}_{ijkl}, \quad \overleftrightarrow{\Gamma}_{0j0l} \xrightarrow{\mathcal{P}} \overleftrightarrow{\Gamma}_{0j0l}, \quad (5.28)$$

for all permutations of the indices. Additionally we know $[\overleftrightarrow{\Gamma}] = 2$, which rules out most monomials of masses, field strength tensors and derivatives. The only non-zero candidates left are

$$\overleftrightarrow{\Gamma}_{\mu\nu\rho\sigma} \in \left\{ m^e m^f \delta_{\mu\rho} \delta_{\nu\sigma}, F_{\sigma\mu} \delta_{\nu\rho}, \overleftrightarrow{D}_\mu \overleftrightarrow{D}_\rho \delta_{\nu\sigma}, \overleftrightarrow{D}_\kappa \overleftrightarrow{D}_\kappa \delta_{\mu\rho} \delta_{\nu\sigma}, \overleftrightarrow{D}_\kappa \overleftrightarrow{D}_\lambda \delta_{\kappa\lambda} \delta_{\mu\rho} \delta_{\nu\sigma} \right\},$$

where already the cyclicity of the trace as well as the antisymmetry of the field strength tensor have been used. Finally, using equations (C.9) and (C.10) leaves us with

$$\begin{aligned} \mathcal{O}_1^{(2)} &= \frac{1}{g_0^2} \text{tr} (F_{\mu\nu} F_{\nu\rho} F_{\rho\mu}), & \mathcal{O}_2^{(2)} &= \frac{1}{g_0^2} \text{tr} (D_\mu F_{\rho\nu} D_\mu F_{\rho\nu}), \\ \mathcal{O}_3^{(2)} &= \frac{1}{g_0^2} \text{tr} (D_\mu F_{\mu\nu} D_\rho F_{\rho\nu}), & \mathcal{O}_4^{(2)} &= \frac{1}{g_0^2} \sum_\mu \text{tr} (D_\mu F_{\mu\nu} D_\mu F_{\mu\nu}). \end{aligned} \quad (5.29)$$

Again, the explicitly mass-dependent operators $m^e m^f \mathcal{O}_1^{(0)}$ have been dropped from the minimal basis. The operators are related via

$$\begin{aligned} \mathcal{O}_2^{(2)} &\stackrel{\text{IBP}}{=} \frac{1}{g_0^2} \partial_\mu \text{tr} (F_{\rho\nu} D_\mu F_{\rho\nu}) - \frac{1}{g_0^2} \text{tr} (F_{\mu\nu} D^2 F_{\mu\nu}) \\ &\stackrel{\text{BI}}{=} \mathcal{O}_5^{(2)} + 2 \left(\mathcal{O}_3^{(2)} - \mathcal{O}_1^{(2)} - \frac{1}{g_0^2} \partial_\nu \text{tr} (F_{\nu\rho} D_\mu F_{\mu\rho}) \right), \end{aligned} \quad (5.30)$$

$$\mathcal{O}_3^{(2)} \stackrel{\text{EOM}}{=} -\frac{g_0^2}{2} \sum_a (\bar{\Psi} \gamma_\mu T^a \Psi)^2 = -\frac{1}{2} \mathcal{O}_{18}^{(2)}, \quad (5.31)$$

where \mathcal{O} denotes total divergence operators, which are listed in appendix C.1 and are irrelevant operators for the action of our SET as will become clear in the introduction of chapter 6. Here $\stackrel{\text{BI}}{=}$ denotes use of the Bianchi identity

$$D_\mu F_{\nu\rho} + D_\rho F_{\mu\nu} + D_\nu F_{\rho\mu} = 0 \quad \text{or equivalently} \quad \varepsilon_{\mu\nu\rho\sigma} D_\mu F_{\nu\rho} = 0, \quad (5.32)$$

where $\varepsilon_{\mu\nu\rho\sigma}$ is the 4-dimensional fully antisymmetric Levi-Civita tensor. The purely gluonic operators without mass-dependence found for our basis are $\mathcal{O}_2^{(2)}$ and $\mathcal{O}_4^{(2)}$ identical to the ones found in [57] and equivalent to the ones in [133].

5.2.2 Fermion bilinear operators

Since the analysis for operators involving two fermions is equivalent for mass dimension 3 to 6, we perform it altogether here. First one needs to write down all possible contributions to our set of operator candidates

$$\bar{\Psi} \Gamma \Psi, \bar{\Psi} \Gamma_\mu D_\mu \Psi, \bar{\Psi} \Gamma_{\mu\nu} D_\mu D_\nu \Psi, \bar{\Psi} \Gamma_{\mu\nu\rho} D_\mu D_\nu D_\rho \Psi,$$

where the possible insertions of Γ are dictated by the Clifford algebra, see also [112],

$$\begin{aligned} \Gamma &\in \{\mathbb{1}, \gamma_5\}, \\ \Gamma_\mu &\in \{\gamma_\mu, i\gamma_\mu \gamma_5\}, \\ \Gamma_{\mu\nu} &\in \{\delta_{\mu\nu}, \delta_{\mu\nu\rho} \gamma_\rho, \delta_{\mu\nu} \gamma_5, \delta_{\mu\nu\rho} \gamma_\rho \gamma_5, i\sigma_{\mu\nu}, i\varepsilon_{\mu\nu\rho\sigma} \sigma_{\rho\sigma}\}, \\ \Gamma_{\mu\nu\rho} &\in \{\delta_{\mu\nu} \gamma_\rho, i\delta_{\mu\nu} \gamma_\rho \gamma_5, \delta_{\mu\nu\rho}, \delta_{\mu\nu\rho} \gamma_5, \delta_{\mu\nu\rho\sigma} \gamma_\sigma, i\delta_{\mu\nu\rho\sigma} \gamma_\sigma \gamma_5, \\ &\quad \text{all index permutations}\} \end{aligned} \quad (5.33)$$

with $\sigma_{\mu\nu} = \frac{i}{2} [\gamma_\mu, \gamma_\nu]$ and generalisation of the Kronecker delta as defined in eq. (A.18). Taking now \mathcal{P} , \mathcal{T} and \mathcal{C} symmetry into account yields the constraints in table 5.2, which exclude all Γ written in blue font due to parity (\mathcal{P}) violation. For the transformation rules see also appendix C. As already stated in [112], parity suffices to exclude all symmetry violating Γ . This leaves us for the operators involving two fermions with

$$\begin{aligned} \Gamma &= \mathbb{1}, & \Gamma_\mu &= \gamma_\mu, \\ \Gamma_{\mu\nu} &\in \{\delta_{\mu\nu}, i\sigma_{\mu\nu}\}, & \Gamma_{\mu\nu\rho} &\in \{\delta_{\mu\nu} \gamma_\rho, i\sigma_{\mu\nu} \gamma_\rho, \delta_{\mu\nu\rho\sigma} \gamma_\sigma, \text{all index permutations}\}. \end{aligned}$$

Starting with the trivial operators of mass-dimension 3 and 4 we have

$$\mathcal{O}_1^{(-1)} = \bar{\Psi} \Psi, \quad \mathcal{O}_2^{(0)} = \bar{\Psi} \gamma_\mu D_\mu \Psi. \quad (5.34)$$

Using the fermionic EOM (4.9) yields

$$\mathcal{O}_2^{(0)} \stackrel{\text{EOM}}{=} -\bar{\Psi} M \Psi. \quad (5.35)$$

Table 5.2: Constraints on the Γ insertions for two fermion bilinears from equation (5.33), where $\bar{\Psi}^C \Gamma \Psi^C = \bar{\Psi} \Gamma^C \Psi$, $\bar{\Psi}^P \Gamma \Psi^P = \bar{\Psi} \Gamma^P \Psi$ and $\bar{\Psi}^T \Gamma \Psi^T = \bar{\Psi} \Gamma^T \Psi$ define Γ^C , Γ^P and Γ^T respectively, with transformations from eqs. (C.1), (C.2) and (C.3).

Γ	Γ^C	Γ^P	Γ^T
Γ	$(C \Gamma C^{-1})^T$	$\gamma_0 \Gamma \gamma_0$	$\gamma_5 \gamma_0 \Gamma \gamma_0 \gamma_5$
Γ_μ	$-(C \Gamma_\mu C^{-1})^T$	$-(-1)^{\delta_{\mu 0}} \gamma_0 \Gamma_\mu \gamma_0$	$(-1)^{\delta_{\mu 0}} \gamma_5 \gamma_0 \Gamma_\mu \gamma_0 \gamma_5$
$\Gamma_{\mu\nu}$	$(C \Gamma_{\nu\mu} C^{-1})^T$	$(-1)^{\delta_{\mu 0} + \delta_{\nu 0}} \gamma_0 \Gamma_{\mu\nu} \gamma_0$	$(-1)^{\delta_{\mu 0} + \delta_{\nu 0}} \gamma_5 \gamma_0 \Gamma_{\mu\nu} \gamma_0 \gamma_5$
$\Gamma_{\mu\nu\rho}$	$-(C \Gamma_{\rho\nu\mu} C^{-1})^T$	$-(-1)^{\delta_{\mu 0} + \delta_{\nu 0} + \delta_{\rho 0}} \gamma_0 \Gamma_{\mu\nu\rho} \gamma_0$	$(-1)^{\delta_{\mu 0} + \delta_{\nu 0} + \delta_{\rho 0}} \gamma_5 \gamma_0 \Gamma_{\mu\nu\rho} \gamma_0 \gamma_5$

For mass-dimension 5 we find two distinct 2-fermion operators that are allowed by eq. (5.33) and not explicitly mass-dependent, see also [112],

$$\mathcal{O}_3^{(1)} = \bar{\Psi} D^2 \Psi, \quad \mathcal{O}_4^{(1)} = i \bar{\Psi} \sigma_{\mu\nu} F_{\mu\nu} \Psi. \quad (5.36)$$

Both operators break chiral symmetry and thus are only allowed for Wilson quarks unless they carry an additional factor of quark masses. This set of operators can be reduced right away by applying the fermionic EOM (4.9)

$$\mathcal{O}_3^{(1)} \stackrel{\text{EOM}}{=} \frac{1}{2} \mathcal{O}_4^{(1)} + \bar{\Psi} M^2 \Psi, \quad (5.37)$$

leaving only one operator linearly independent and without explicit mass-dependence. Hence we keep $\mathcal{O}_4^{(1)}$ in our basis and drop $\mathcal{O}_3^{(1)}$.

For mass dimension 6 the entire set of dimension 5 operators resurfaces multiplied by a quark mass, but is then of course explicitly mass-dependent. These operators are accompanied by some new operators

$$\begin{aligned} \mathcal{O}_5^{(2)} &= \bar{\Psi} \gamma_\mu D^2 D_\mu \Psi, & \mathcal{O}_6^{(2)} &= \bar{\Psi} \gamma_\mu D_\mu D^2 \Psi, & \mathcal{O}_7^{(2)} &= \bar{\Psi} \gamma_\mu D_\nu D_\mu D_\nu \Psi, \\ \mathcal{O}_8^{(2)} &= \bar{\Psi} \gamma_\nu D_\mu F_{\mu\nu} \Psi, & \mathcal{O}_9^{(2)} &= \bar{\Psi} \gamma_\mu F_{\mu\nu} D_\nu \Psi, & \mathcal{O}_{10}^{(2)} &= \sum_\mu \bar{\Psi} \gamma_\mu D_\mu^3 \Psi. \end{aligned} \quad (5.38)$$

All these new operators comply with chiral symmetry and are thus also applicable to lattice fermion actions keeping chiral symmetry intact. Again applying the fermionic EOMs (4.9) and (4.10) as well as some algebra we find

$$\mathcal{O}_5^{(2)} \stackrel{\text{EOM}}{=} -\bar{\Psi} M D^2 \Psi, \quad (5.39)$$

$$\begin{aligned} \mathcal{O}_6^{(2)} &\stackrel{\text{IBP}}{=} \partial_\mu (\bar{\Psi} \gamma_\mu D^2 \Psi) - \bar{\Psi} \overleftarrow{D}_\mu \gamma_\mu D^2 \Psi \\ &\stackrel{\text{EOM}}{=} \mathcal{O}_2^{(2)} - \bar{\Psi} M D^2 \Psi, \end{aligned} \quad (5.40)$$

$$\mathcal{O}_9^{(2)} = \mathcal{O}_6^{(2)} - \mathcal{O}_7^{(2)}, \quad (5.41)$$

$$\mathcal{O}_7^{(2)} = \mathcal{O}_5^{(2)} - \mathcal{O}_8^{(2)} + \mathcal{O}_9^{(2)}, \quad (5.42)$$

$$\mathcal{O}_8^{(2)} \stackrel{\text{EOM}}{=} \frac{g_0^2}{2} \sum_a (\bar{\Psi} \gamma_\mu T^a \Psi)^2 = \frac{1}{2} \mathcal{O}_{18}^{(2)}. \quad (5.43)$$

Hence the operators $\mathcal{O}_5^{(2)}$, $\mathcal{O}_6^{(2)}$, $\mathcal{O}_7^{(2)}$, $\mathcal{O}_8^{(2)}$ and $\mathcal{O}_9^{(2)}$ can be dropped from the basis as well. This leaves $\mathcal{O}_{10}^{(2)}$ as the only linearly independent operator involving two fermions in the mass-dimension 6 basis neglecting total divergence operators and operators with explicit mass-dependence.

5.2.3 Four fermion operators

At mass-dimension 6 also 4-fermion operators become relevant, which take the form

$$(\bar{\Psi}\Gamma_{\{\mu\}}\Psi)^2, \quad (\bar{\Psi}\Gamma_{\{\mu\}}T^a\Psi)^2 \quad (5.44)$$

with $\Gamma_{\{\mu\}} \in \{1, \gamma_5, \gamma_\mu, \gamma_\mu\gamma_5, \sigma_{\mu\nu}\}$ dictated by the Clifford algebra and the requirement of having scalar operators. There exist 10 linearly independent operators compatible with $SU(N_f)_V$ flavour symmetry relevant for our on-shell basis

$$\begin{aligned} \mathcal{O}_{11}^{(2)} &= g_0^2 (\bar{\Psi}\Psi)^2, & \mathcal{O}_{12}^{(2)} &= g_0^2 (\bar{\Psi}\gamma_5\Psi)^2, & \mathcal{O}_{13}^{(2)} &= g_0^2 (\bar{\Psi}\gamma_\mu\Psi)^2, \\ \mathcal{O}_{14}^{(2)} &= g_0^2 (\bar{\Psi}\gamma_\mu\gamma_5\Psi)^2, & \mathcal{O}_{15}^{(2)} &= g_0^2 (\bar{\Psi}\sigma_{\mu\nu}\Psi)^2, & & \\ \mathcal{O}_{16}^{(2)} &= g_0^2 (\bar{\Psi}T^a\Psi)^2, & \mathcal{O}_{17}^{(2)} &= g_0^2 (\bar{\Psi}\gamma_5T^a\Psi)^2, & \mathcal{O}_{18}^{(2)} &= g_0^2 (\bar{\Psi}\gamma_\mu T^a\Psi)^2, \\ \mathcal{O}_{19}^{(2)} &= g_0^2 (\bar{\Psi}\gamma_\mu\gamma_5T^a\Psi)^2, & \mathcal{O}_{20}^{(2)} &= g_0^2 (\bar{\Psi}\sigma_{\mu\nu}T^a\Psi)^2, & & \end{aligned} \quad (5.45)$$

where the sum over the occurring algebra index a as well as spacetime indices μ and ν is implicit. The operators $\mathcal{O}_{11}^{(2)}, \mathcal{O}_{12}^{(2)}, \mathcal{O}_{15}^{(2)}, \mathcal{O}_{16}^{(2)}, \mathcal{O}_{17}^{(2)}$ and $\mathcal{O}_{20}^{(2)}$ break chiral symmetry. Additionally there are also 5 linearly independent operators that are only compatible with flavour permutation symmetry and $\times_{f=1}^{N_f} U(1)_f$ flavour symmetry

$$\begin{aligned} \mathcal{O}_{21}^{(2)} &= g_0^2 \sum_q (\bar{q}\Gamma_i q)^2, & \mathcal{O}_{22}^{(2)} &= g_0^2 \sum_q (\bar{q}\gamma_5 q)^2, & \mathcal{O}_{23}^{(2)} &= g_0^2 \sum_q (\bar{q}\gamma_\mu q)^2, \\ \mathcal{O}_{24}^{(2)} &= g_0^2 \sum_q (\bar{q}\gamma_\mu\gamma_5 q)^2, & \mathcal{O}_{25}^{(2)} &= g_0^2 \sum_q (\bar{q}\sigma_{\mu\nu} q)^2. & & \end{aligned} \quad (5.46)$$

Although the operators $\mathcal{O}_{21-25}^{(2)}$ are compatible with the symmetry constraints of general massive quarks they do neither vanish in the limit of mass-degenerate quarks nor for vanishing quark masses $m_{\overline{\text{MS}}}^q \rightarrow 0$. Therefore they must be excluded from the minimal basis and would only become relevant at higher mass-dimension carrying an additional explicit mass-dependence.

Note that we choose to prepend an additional factor of g_0^2 to each 4-fermion operator motivated by the gluonic EOM (4.8) as well as the vanishing of lower order contributions in the effective action. The latter happens due to the absence of terms with more than one quark-anti-quark pair in the classical expansion of the action in the lattice spacing a as discussed in [112], i.e. the tree-level coefficients of 4-fermion operators without the factor g_0^2 would vanish anyway.

In principle one could also expect more complicated colour, flavour and spinor structures, but due to Fierz identities

$$\begin{pmatrix} \bar{\psi}_1\psi_2\bar{\psi}_3\psi_4 \\ \bar{\psi}_1\gamma_\mu\psi_2\bar{\psi}_3\gamma_\mu\psi_4 \\ \bar{\psi}_1\sigma_{\mu\nu}\psi_2\bar{\psi}_3\sigma_{\mu\nu}\psi_4 \\ -\bar{\psi}_1\gamma_\mu\gamma_5\psi_2\bar{\psi}_3\gamma_\mu\gamma_5\psi_4 \\ \bar{\psi}_1\gamma_5\psi_2\bar{\psi}_3\gamma_5\psi_4 \end{pmatrix} = \frac{1}{8} \begin{pmatrix} -2 & -2 & -1 & -2 & -2 \\ -8 & 4 & 0 & -4 & 8 \\ -24 & 0 & 4 & 0 & -24 \\ -8 & -4 & 0 & 4 & 8 \\ -2 & 2 & -1 & 2 & -2 \end{pmatrix} \begin{pmatrix} \bar{\psi}_1\psi_4\bar{\psi}_3\psi_2 \\ \bar{\psi}_1\gamma_\mu\psi_4\bar{\psi}_3\gamma_\mu\psi_2 \\ \bar{\psi}_1\sigma_{\mu\nu}\psi_4\bar{\psi}_3\sigma_{\mu\nu}\psi_2 \\ -\bar{\psi}_1\gamma_\mu\gamma_5\psi_4\bar{\psi}_3\gamma_\mu\gamma_5\psi_2 \\ \bar{\psi}_1\gamma_5\psi_4\bar{\psi}_3\gamma_5\psi_2 \end{pmatrix}, \quad (5.47)$$

as well as eq. (A.9)

$$\bar{\psi}_A\Gamma_{\{\mu\}}T_{AB}^a\psi_B\bar{\eta}_C\Gamma_{\{\mu\}}T_{CD}^a\eta_D = -T_F \left(\bar{\psi}_A\Gamma_{\{\mu\}}\psi_B\bar{\eta}_B\Gamma_{\{\mu\}}\eta_A - \frac{1}{N}\bar{\psi}_A\Gamma_{\{\mu\}}\psi_A\bar{\eta}_B\Gamma_{\{\mu\}}\eta_B \right), \quad (5.48)$$

$$\bar{\psi}_A\Gamma_{\{\mu\}}T_{AB}^a\eta_B\bar{\eta}_C\Gamma_{\{\mu\}}T_{CD}^a\psi_D = -T_F \left(\bar{\psi}_A\Gamma_{\{\mu\}}\eta_B\bar{\eta}_B\Gamma_{\{\mu\}}\psi_A - \frac{1}{N}\bar{\psi}_A\Gamma_{\{\mu\}}\eta_A\bar{\eta}_B\Gamma_{\{\mu\}}\psi_B \right) \quad (5.49)$$

these more complicated operators can be written in terms of our minimal basis in eq. (5.45). **Here** ψ and η indicate different flavours and the subscripts A, B, C, D are colour indices. The choice of our basis in eq. (5.45) is identical to the one in [134] and, as argued there, equivalent to the basis chosen in [112].

5.3 Extension of pure gauge theory to static quarks

From Wilson loops $\mathcal{W}(\mathbf{r}, t)$ with extent $|\mathbf{r}| \times T$ one can extract the static quark potential V_{qq}

$$rV_{\text{qq}}(\mathbf{r}; a) = \frac{r}{a} \lim_{T \rightarrow \infty} \ln \frac{\mathcal{W}(\mathbf{r}, T; a)}{\mathcal{W}(\mathbf{r}, T - a; a)} = rV_{\text{qq}}(r; 0) + \mathcal{O}(a^2), \quad r = |\mathbf{r}|, \quad (5.50)$$

where we keep explicitly the dependence on the lattice spacing and direction of \mathbf{r} for later reference.

The connection to static quarks becomes clear in the framework of *Heavy Quark Effective Theory* (HQET) [135–139], where one expands around infinite quark masses, i.e. in powers of $1/m^q$. In quenched HQET the static quark potential corresponds to the leading order of the potential between heavy quarks.

From this connection to quenched HQET arise some subtleties as the full action involves not only gauge fields but also static quarks, which may introduce additional lattice artifacts. These lattice artifacts could in principle contribute already to $\mathcal{O}(a)$, whose absence has been worked out in [64] such that the leading contribution in eq. (5.50) is indeed $\mathcal{O}(a^2)$ as in usual pure gauge theory. The corresponding lattice action for (naive) static quarks reads

$$S_{\text{F}}^{\text{static}} = a^4 \sum_x \left[\bar{\psi}_{\text{h}}(x) \hat{D}_0^{\text{static}} \psi_{\text{h}}(x) - \bar{\psi}_{\text{h}}(x) (\hat{D}_0^{\text{static}})^* \psi_{\text{h}}(x) \right], \quad (5.51)$$

where $\psi_{\text{h}} = \frac{1+\gamma_0}{2} \psi$ and $\psi_{\text{h}} = \frac{1-\gamma_0}{2} \psi$ are static quarks propagating forward and backward in time respectively. The covariant derivative in time direction is defined as

$$a \hat{D}_0^{\text{static}} [U] \psi_{\text{h}}(x) = V_0[U](x) \psi_{\text{h}}(x + a\hat{0}) - \psi_{\text{h}}(x), \quad (5.52)$$

$$a (\hat{D}_0^{\text{static}})^* [U] \psi_{\text{h}}(x) = \psi_{\text{h}}(x) - V_0^\dagger[U](x - a\hat{0}) \psi_{\text{h}}(x - a\hat{0}), \quad (5.53)$$

where the use of both forward and backward derivative ensures exact invariance under time reversal and charge conjugation on the lattice. It does not matter whether $V_0(x)$ is chosen to be the gauge link $U_0(x)$ pointing in time direction or some smeared version² of it with the same transformation properties and as such we keep it general at this point.

The symmetries associated with the static quark action are then relevant for the SET of static quarks [144]

- Local $\text{SU}(N)$ gauge symmetry.
- \mathcal{C} -, \mathcal{P} -, \mathcal{T} -symmetry.
- Spatially local flavour number conservation, i.e., invariance under

$$\bar{\psi}_{\text{h}, \bar{\mathbf{h}}} \rightarrow e^{-i\eta_{\text{h}, \bar{\mathbf{h}}}(\mathbf{x})} \bar{\psi}_{\text{h}, \bar{\mathbf{h}}}, \quad \psi_{\text{h}, \bar{\mathbf{h}}} \rightarrow e^{i\eta_{\text{h}, \bar{\mathbf{h}}}(\mathbf{x})} \psi_{\text{h}, \bar{\mathbf{h}}}, \quad \eta_{\text{h}, \bar{\mathbf{h}}}(\mathbf{x}) \in \mathbb{R}. \quad (5.54)$$

- Heavy quarks spin symmetry for

$$\bar{\psi}_{\text{h}, \bar{\mathbf{h}}} \rightarrow \bar{\psi}_{\text{h}, \bar{\mathbf{h}}} e^{-i\varphi_i \epsilon_{ijk} \sigma_{jk}}, \quad \psi_{\text{h}, \bar{\mathbf{h}}} \rightarrow e^{i\varphi_i \epsilon_{ijk} \sigma_{jk}} \psi_{\text{h}, \bar{\mathbf{h}}}, \quad \varphi_i \in \mathbb{R}. \quad (5.55)$$

- Spatial rotations by 90° as well as rotations by 90° around the time axis.

Before deriving the minimal basis we first have another look at the quenched approximation to understand what kind of corrections are actually to be expected. The generating functional for static quarks on the lattice (and analogously in the continuum) reads

$$Z[j_{\text{h}}, \bar{j}_{\text{h}}, j_{\bar{\mathbf{h}}}, \bar{j}_{\bar{\mathbf{h}}}] = - \int \mathcal{D}U \mathcal{D}\bar{\psi}_{\text{h}} \mathcal{D}\psi_{\text{h}} \mathcal{D}\bar{\psi}_{\bar{\mathbf{h}}} \mathcal{D}\psi_{\bar{\mathbf{h}}} \frac{\exp(-S_{\text{F}}^{\text{static}}[U, \bar{\psi}_{\text{h}}, \psi_{\text{h}}, \bar{\psi}_{\bar{\mathbf{h}}}, \psi_{\bar{\mathbf{h}}}] - S_{\text{G}}^{\text{latt}}[U])}{\det(D_0^{\text{static}}[U])^2} \times \exp \left(a^4 \sum_x \{ \bar{\psi}_{\text{h}}(x) j_{\text{h}}(x) + \bar{j}_{\text{h}}(x) \psi_{\text{h}}(x) + \bar{\psi}_{\bar{\mathbf{h}}}(x) j_{\bar{\mathbf{h}}}(x) + \bar{j}_{\bar{\mathbf{h}}}(x) \psi_{\bar{\mathbf{h}}}(x) \} \right). \quad (5.56)$$

²We allow here smearing techniques which keep the transformation properties of the smeared link intact and are to some extent local. This can be for example HYP [140, 141], APE [142] or Stout smearing [143].

For vanishing static quark sources this generating functional reduces to the partition function of lattice gauge theory, which is precisely what one expects in the quenched approximation. The additional lattice artifacts due to static quarks may thus only affect the static propagator as well as the coupling of static quarks to gauge fields. Consequently no new pure gauge operators will be encountered nor does the gluonic EOM change.

The continuum Eichten-Hill Lagrangian of static quarks takes the form [136]

$$\mathcal{L}_{\text{EH}} = \bar{\psi}\gamma_0 D_0 \psi = \bar{\psi}_h D_0 \psi_h - \bar{\psi}_{\bar{h}} D_0 \psi_{\bar{h}} \quad (5.57)$$

resulting in the continuum EOMs of static quarks

$$D_0 \psi_{h,\bar{h}} = 0 = \bar{\psi}_{h,\bar{h}} \overleftarrow{D}_0. \quad (5.58)$$

All additional higher dimensional operators contributing to the SET of static quarks are then static quark bilinears of the form

$$\bar{\psi}_h(x) \Gamma_{\{\mu\}} X_{\{\mu\}}(x) \psi_h(x) \pm \bar{\psi}_{\bar{h}}(x) \Gamma_{\{\mu\}} X_{\{\mu\}}(x) \psi_{\bar{h}}(x), \quad (5.59)$$

where $\Gamma_{\{\mu\}}$ is a constant element of the Dirac algebra while $X_{\{\mu\}}$ is unity in spinor space. From eq. (5.54) and the EOMs we learn that $X_{\{\mu\}}$ carries no covariant derivatives acting on the static quarks. Heavy quarks spin symmetry in eq. (5.55) furthermore excludes $\Gamma_{\{\mu\}} \sim \gamma_j, \gamma_5 \gamma_j, \sigma_{ij}, \sigma_{0j}$ where $i, j = 1, 2, 3$, while the presence of γ_5 or $\gamma_5 \gamma_0$ vanishes because

$$\frac{1 \pm \gamma_0}{2} \gamma_5 \frac{1 \pm \gamma_0}{2} = 0. \quad (5.60)$$

The only candidates left are $\Gamma_{\{\mu\}} \sim \mathbb{1}, \gamma_0$, where γ_0 can always be absorbed into the projectors $\frac{1 \pm \gamma_0}{2}$. The only two operator candidates remaining at this point are

$$\bar{\psi}_h(x) X_0(x) \psi_h(x) \pm \bar{\psi}_{\bar{h}}(x) X_0(x) \psi_{\bar{h}}(x). \quad (5.61)$$

The variant with a relative minus sign has to transform \mathcal{C} -even and \mathcal{P} -even but \mathcal{T} -odd, i.e. like a time component of a vector, limiting it to even mass-dimensions. The variant with a relative plus sign has to transform \mathcal{C} -even, \mathcal{P} -even and \mathcal{T} -even, i.e. like a scalar, thus limiting it to odd mass-dimensions. We could have started from any fermion action before taking the infinite mass-limit, also naive Wilson fermions would be a valid choice, such that terms with a relative plus sign must be mass-dependent and thus can be dropped. This excludes all operators with odd mass-dimension and not only $\mathcal{O}(a)$ effects, cf. [64]. At mass-dimension 6 we only find additional operators vanishing due to EOMs such as

$$\bar{\psi}_h D_0^3 \psi_h - \bar{\psi}_{\bar{h}} D_0^3 \psi_{\bar{h}} \stackrel{\text{EOM}}{=} 0. \quad (5.62)$$

An example of a non-vanishing operator can be found at mass-dimension 8

$$\mathcal{O}^{(8)} = \bar{\psi}_h D_0 (F_{\mu\nu} F_{\mu\nu}) \psi_h - \bar{\psi}_{\bar{h}} D_0 (F_{\mu\nu} F_{\mu\nu}) \psi_{\bar{h}}. \quad (5.63)$$

This implies that no new operators contribute to $\mathcal{O}(a^2)$ or any odd power $\mathcal{O}(a^{2n+1})$ such that the first new contributions are of $\mathcal{O}(a^4)$. The reasoning holds true for use of smeared links in eq. (5.52) as long as these smeared links have the correct transformation behaviour.

5.4 Connection of the minimal basis to tmQCD

To highlight the connection between tmQCD and non-twisted QCD once more we will first discuss the academic possibility of using twisted Ginsparg-Wilson fermions and then emphasize the complications which arise when using twisted Wilson fermions instead. Due to lattice chiral symmetry of the Ginsparg-Wilson Dirac operator the one-to-one correspondence between non-twisted

mass-degenerate QCD and lattice QCD is apparent in form of the transformation in eq. (5.13). As a consequence the SET is invariant under $SU(2)_{\text{tw}}$ flavour symmetry transformations and all mass-independent operators allowed for the minimal basis must comply with chiral symmetry when rotated back to non-twisted QCD, such that in the limit of zero renormalised mass chiral symmetry is realised in the effective action. Since operators compatible with chiral symmetry transform trivially under the rotation in eq. (5.13), e.g.

$$\mathcal{O}_{10}^{(2)} = \sum_{\mu} \bar{\Psi} \gamma_{\mu} D_{\mu}^3 \Psi \xrightarrow{(5.13)} \sum_{\mu} \bar{\chi} \gamma_{\mu} D_{\mu}^3 \chi, \quad (5.64)$$

the operator basis is just the one from usual Ginsparg-Wilson fermions in the twisted basis plus additional mass-dependent operators with now two different masses m_q and μ_q . The mass-dependent operators are further restricted by $SU(2)_{\text{tw}}$ flavour symmetry and the spurionic symmetries $\mathcal{P}_{\mu_q}^{\text{tm}}$ and $\mathcal{T}_{\mu_q}^{\text{tm}}$.

Turning now to twisted Wilson fermions the $SU(2)_{\text{tw}}$ flavour symmetry gets broken and with it the simple connection to non-twisted QCD in eq. (5.13). In the corresponding SET we thus expect to find not only the rotated versions of the chiral symmetry violating operators

$$\begin{aligned} \mathcal{O}_1^{(-1)} &= \bar{\Psi} \Psi \rightarrow \cos(\omega) \bar{\chi} \chi + i \sin(\omega) \bar{\chi} \gamma_5 \tau^3 \chi, \\ \mathcal{O}_4^{(1)} &= i \bar{\Psi} \sigma_{\mu\nu} F_{\mu\nu} \Psi \rightarrow \cos(\omega) \bar{\chi} \sigma_{\mu\nu} F_{\mu\nu} \chi + \sin(\omega) \bar{\chi} \sigma_{\mu\nu} \tilde{F}_{\mu\nu} \tau^3 \chi, \\ (\bar{\Psi} \Gamma \Psi)^2 &\rightarrow (\cos(\omega) \bar{\chi} \Gamma \chi + i \sin(\omega) \bar{\chi} \gamma_5 \tau^3 \Gamma \chi)^2, \quad \Gamma \in \{\mathbb{1}, \gamma_5, \sigma_{\mu\nu}\}, \\ (\bar{\Psi} \Gamma T^a \Psi)^2 &\rightarrow (\cos(\omega) \bar{\chi} \Gamma T^a \chi + i \sin(\omega) \bar{\chi} \gamma_5 \tau^3 \Gamma T^a \chi)^2, \quad \Gamma \in \{\mathbb{1}, \gamma_5, \sigma_{\mu\nu}\}, \end{aligned} \quad (5.65)$$

with dual field strength tensor $\tilde{F}_{\mu\nu} = \frac{1}{2} \varepsilon_{\mu\nu\rho\sigma} F_{\rho\sigma}$, but also the “unpaired” operators

$$\begin{aligned} \mathcal{O}_2^{(-1)} &= \bar{\chi} \chi, & \mathcal{O}_6^{(1)} &= i \bar{\chi} \sigma_{\mu\nu} F_{\mu\nu} \chi, \\ \mathcal{O}_{26}^{(2)} &= (\bar{\chi} \chi)^2, & \mathcal{O}_{27}^{(2)} &= (\bar{\chi} \gamma_5 \chi)^2, & \mathcal{O}_{28}^{(2)} &= (\bar{\chi} \sigma_{\mu\nu} \chi)^2, \\ \mathcal{O}_{29}^{(2)} &= (\bar{\chi} T^a \chi)^2, & \mathcal{O}_{30}^{(2)} &= (\bar{\chi} \gamma_5 T^a \chi)^2, & \mathcal{O}_{31}^{(2)} &= (\bar{\chi} \sigma_{\mu\nu} T^a \chi)^2. \end{aligned} \quad (5.66)$$

These “unpaired” operators are compatible with $SU(2)_V$ flavour symmetry of Wilson fermions in the massless limit while the operators from eq. (5.65) or to be precise the second part with insertion of τ^3 violate this symmetry and hence may only occur with explicit mass-dependence. One may also be tempted to include 4-fermion operators of the kind

$$(\bar{\chi} \Gamma \tau^3 \chi)^2 \text{ or } i(\bar{\chi} \Gamma \chi)(\bar{\chi} \gamma_5 \tau^3 \Gamma \chi), \quad \Gamma \in \{\mathbb{1}, \gamma_5, \gamma_{\mu}, \gamma_{\mu} \gamma_5, \sigma_{\mu\nu}, T^a, \gamma_5 T^a, \gamma_{\mu} T^a, \gamma_{\mu} \gamma_5 T^a, \sigma_{\mu\nu} T^a\}, \quad (5.67)$$

but these again break $SU(2)_V$ flavour symmetry in the limit of vanishing masses. This ensures that up to mass-dimension 6 for the mass-independent operators only the chirally symmetric operators from non-twisted Wilson QCD and the operators from eq. (5.66) are relevant. Both operators $\mathcal{O}_2^{(-1)}$ and $\mathcal{O}_6^{(1)}$ are T_1 -odd such that no T_1 -even operators exist in our basis below mass-dimension 6.

When using a regulator respecting chiral symmetry, $SU(2)_{\text{tw}}$ is a flavour symmetry of continuum tmQCD. Thus we may use all the relations in eqs. (5.64) and (5.65) obtained through the twisted rotation from eq. (5.13) to infer the anomalous dimensions of operators in the twisted basis from those of non-twisted Wilson QCD in our SET, see also eq. (5.20). Notice that the masses m , m_q and the twisted mass μ_q have the same anomalous dimension as they renormalise identically if the regularisation does not break chiral symmetry.

Chapter 6

Renormalisation of the minimal operator basis

In order to renormalise the chosen operator basis we will perform all computations in dimensional regularisation. This means that we work in $D = 4 - 2\epsilon$ dimensional **momentum space** and eventually use the $\overline{\text{MS}}$ renormalisation scheme. We then require our set of operators in momentum space representation. The operators to be considered are composite operators and each contributing term with n fundamental fields can be translated into a Feynman rule of a vertex with n legs, see appendix D.1. Such a term with n fields has the form

$$\mathcal{O}(x) = \varphi_1(x) \dots \varphi_n(x), \quad (6.1)$$

where φ_i is any fundamental field in $\{A, \bar{\psi}, \psi\}$ or their higher order derivatives and for the moment colour, space-time or flavour indices are omitted. Switching to momentum space yields

$$\begin{aligned} \tilde{\mathcal{O}}(q) &= \int d^D x \mathcal{O}(x) e^{-iqx} = \int d^D x \int_{\{k\}} \tilde{\varphi}_1(k_1) \dots \tilde{\varphi}_n(k_n) \exp\left(i \sum_j k_j x - i q x\right) \\ &= (2\pi)^{D/2} \int_{\{k\}} \tilde{\varphi}_1(k_1) \dots \tilde{\varphi}_n(k_n) \delta^{(D)}\left(\sum_j k_j - q\right), \end{aligned} \quad (6.2)$$

with the integral conventions from eq. (A.16) and conventions for the Fourier transform eq. (A.19). For a more complete explanation on how the Feynman rules were derived see appendix D.1.

The choice for the momentum q of the operator depends on whether the considered operator basis is intended to parametrise lattice artifacts for a local composite field, in which case $q \neq 0$ is obligatory, or the action, where $q = 0$ would be sufficient. For $q \neq 0$ one has to take total divergence operators into account, which otherwise do not contribute. This can be easily seen by taking as an example the derivative $\Phi_\mu(x) = \partial_\mu \mathcal{O}(x)$ instead of just $\mathcal{O}(x)$ in equation (6.2), which yields

$$\tilde{\Phi}_\mu(q) = \int d^D x e^{-iqx} \partial_\mu \mathcal{O}(x) = i q_\mu \tilde{\mathcal{O}}(q). \quad (6.3)$$

Obviously it does not matter for our reasoning, whether the index μ is free or in fact contracted with any of the omitted space-time indices of the fields φ_i as setting $q_\mu = 0 \forall \mu$ ensures vanishing of $\tilde{\Phi}_\mu(0)$ trivially.

6.1 Strategy

Starting from the minimal bases found in section 5.2, we want to obtain the corresponding mixing matrices $Z^{\mathcal{O}}$ required for renormalisation. With use of the background field method we consider

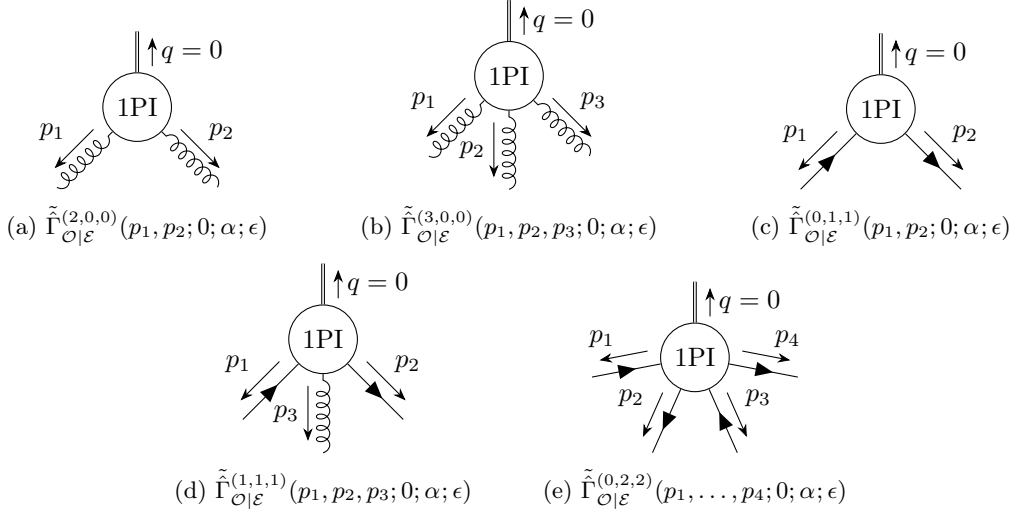


Figure 6.1: Graphical representation of all 1PI n -point functions of fundamental quark fields or background fields with insertion of an operator \mathcal{O} or \mathcal{E} considered for the renormalisation of the basis. Here the double line indicates the momentum contribution of the inserted operator, which may also be seen as an additional leg and is set to zero momentum. The wiggly lines are external background fields and the straight lines carrying arrows are quarks. The graphs (a) and (b) are the only ones required for pure gauge, while graph (e) is only needed at mass-dimension 6 to include 4-fermion operators.

n -point functions of fundamental quark and background fields with insertion of an operator of the minimal basis at momentum $q = 0$. In contrast to eq. (3.39) we work here in momentum space

$$\left(\begin{array}{c} \tilde{\Gamma}_{\mathcal{O}}^{(l,m,n)} \\ \tilde{\Gamma}_{\mathcal{E}}^{(l,m,n)} \end{array} \right)_{\overline{\text{MS}}} (p_1, \dots, p_{l+m+n}; q; \alpha_{\overline{\text{MS}}}; \epsilon) = Z_{\Psi}^{-m-n}(\alpha_{\overline{\text{MS}}}; \epsilon) \begin{pmatrix} Z^{\mathcal{O}} & Z^{\mathcal{O}\mathcal{E}} \\ 0 & Z^{\mathcal{E}} \end{pmatrix} \left(\begin{array}{c} \tilde{\Gamma}_{\mathcal{O}}^{(l,m,n)} \\ \tilde{\Gamma}_{\mathcal{E}}^{(l,m,n)} \end{array} \right) (p_1, \dots, p_{l+m+n}; q; \alpha; \epsilon), \quad q = 0. \quad (6.4)$$

This does not affect the previously discussed background field approach. To extract $Z^{\mathcal{O}}$ we then need a minimal basis of EOM vanishing operators \mathcal{E} as listed in appendix C.2. Keep in mind that these EOM vanishing operators are irrelevant for our on-shell basis and are only used to perform an off-shell renormalisation.

Extracting $Z^{\mathcal{O}}$ unambiguously forces us to consider 2- and 3-point functions of background fields as well as fermionic 2- and 4-point functions and a 3-point function with two fermions and one background field. All of these n -point functions are 1PI graphs with insertion of an operator \mathcal{O} or \mathcal{E} . The insertions are considered at momentum $q = 0$ to eliminate redundant total divergence operators. The momenta of the external fundamental fields are only constrained by energy momentum conservation, i.e., $\sum_i p_i = 0$. For a graphical representation see figure 6.1. All relevant 1PI graphs contributing to a specific n -point function were obtained using QGRAF [145, 146] in version 3.4 with the model files in appendix D.2.

Using a mass-independent renormalisation scheme like $\overline{\text{MS}}$ allows to simplify the computation of anomalous dimensions, as e.g. done in [147], because anomalous dimensions are simply related to counterterms renormalising ultraviolet divergences. Thus, being only interested in the 1-loop anomalous dimensions, we can restrict attention to the 1-loop UV-divergences. Making use of so called *infrared rearrangement*, see e.g. in [147, 148], enables us to separate the UV-divergent part of a 1-loop momentum integral from UV-finite but potentially IR divergent parts through the exact

relation [147, 148]

$$\frac{1}{(k+p)^2 + M^2} = \frac{1}{k^2 + \Omega} - \frac{2kp + p^2 + M^2 - \Omega}{[k^2 + \Omega][(k+p)^2 + M^2]}. \quad (6.5)$$

Here k is the loop momentum, p is an external momentum, M is a mass and we choose $\Omega > 0$ as an arbitrary real number. It can be noticed through naive power counting, see e.g. [149, p. 315ff.], that the second term in eq. (6.5) is one power less UV-divergent. Hence we can iterate this step n times

$$\begin{aligned} \frac{1}{(k+p)^2 + M^2} &= \frac{1}{k^2 + \Omega} \left\{ \sum_{j=0}^n \left(-\frac{2kp + p^2 + M^2 - \Omega}{k^2 + \Omega} \right)^j \right. \\ &\quad \left. + \frac{(-1)^{n+1}}{(k+p)^2 + M^2} \left(\frac{2kp + p^2 + M^2 - \Omega}{k^2 + \Omega} \right)^n \right\}, \end{aligned} \quad (6.6)$$

until the $(n+1)$ th term is UV-finite. Being only interested in the UV-divergent part then allows to drop the $(n+1)$ th term, because it does not contribute to the UV-pole structure and thus is irrelevant for determining $Z^{\mathcal{O}}$. The generalisation to multiple denominators is straight forward. The UV-divergent remainder are integrals of the form $\int d^D k f(k)/[k^2 + \Omega]^l$, where $l \in \mathbb{N}$ and $f(k)$ is a monomial of components of k . This is the most basic integral one can encounter in dimensional regularisation and can be easily integrated using eqs. (B.1) and (B.2). As a by-product we get a test condition, because the UV-divergences must of course be independent of Ω [147], since it originates only from a computational trick.

As a check of our renormalisation condition we also performed an on-shell renormalisation of the massless operator basis inserted with non-zero momentum q . The details can be found in appendix E.2.

6.2 Renormalisation of the operator basis in pure gauge theory

In pure gauge theory only two operators are present in our minimal basis plus one redundant EOM vanishing operator that is necessary due to our renormalisation strategy

$$\mathcal{O}_2^{(2)} = \frac{1}{g_0^2} \text{tr}(D_\mu F_{\nu\rho} D_\mu F_{\nu\rho}), \quad \mathcal{O}_4^{(2)} = \frac{1}{g_0^2} \sum_\mu \text{tr}(D_\mu F_{\mu\nu} D_\mu F_{\mu\nu}), \quad \mathcal{E}_2^{(2)} = \frac{1}{g_0^2} \text{tr}(D_\mu F_{\mu\rho} D_\nu F_{\nu\rho}).$$

Performing the steps described in the preceding part of this chapter we find the 1-loop anomalous dimension matrix from the 1PI 2- and 3-point function in figures 6.1a and 6.1b

$$4\pi\gamma_0^{\mathcal{O}} = \left(\begin{array}{cc|c} \frac{7N}{3} & 0 & \left(\frac{23N}{6} - \frac{3N}{2\lambda_{\overline{\text{MS}}}} \right) \\ -\frac{7N}{15} & \frac{21N}{5} & \left(\frac{7N}{15} - \frac{1N}{2\lambda_{\overline{\text{MS}}}} \right) \end{array} \right), \quad (6.7)$$

where the vertical line separates the redundant part belonging to the EOM vanishing operator and the basis is chosen in the order $\{\mathcal{O}_2^{(2)}, \mathcal{O}_4^{(2)}\}$. The triangular structure of $\gamma_0^{\mathcal{O}}$ is due to the O(4) breaking of $\mathcal{O}_4^{(2)}$ excluding any mixing contributions to O(4) invariant operators.

From eq. (6.7) we infer a change in the basis such that the non-redundant part is diagonal under renormalisation at 1-loop order

$$\mathcal{B}_1^{(2)} = \mathcal{O}_2^{(2)}, \quad \mathcal{B}_2^{(2)} = \mathcal{O}_4^{(2)} - \frac{1}{4}\mathcal{O}_2^{(2)}, \quad (6.8)$$

with 1-loop anomalous dimensions normalised by β_0

$$\hat{\gamma}_1^{\mathcal{B}} = \frac{7}{11} \approx 0.636, \quad \hat{\gamma}_2^{\mathcal{B}} = \frac{63}{55} \approx 1.145. \quad (6.9)$$

Both $\hat{\gamma}_i^{\mathcal{B}}$ are independent of the number of colours N . The anomalous dimension for the O(4) invariant operator $\hat{\gamma}_1^{\mathcal{B}}$ agrees with results in the literature [133, 150, 151].

6.3 Renormalisation of the operator basis in full QCD

Considering full QCD introduces the issue of flavour symmetries which depend on the choices for the quark masses and of course the lattice fermion action. The different symmetry constraints resurface in the mixing of the operators. To account for this we will order the operator bases according to the symmetry constraints they obey and expect for operators of mass-dimension d a triangular mixing matrix of the form

$$[\gamma_0^{\mathcal{O}}]^{(d-4)} = \left(\begin{array}{ccc|c} \gamma_0^{\text{massive}} & 0 & 0 & \gamma_0^{\text{massive},\mathcal{E}} \\ \gamma_0^{\text{SU}(N_f)_{\text{L|R}},\text{massive}} & \gamma_0^{\text{SU}(N_f)_{\text{L|R}}} & 0 & \gamma_0^{\text{SU}(N_f)_{\text{L|R}},\mathcal{E}} \\ \gamma_0^{\text{SU}(N_f)_{\text{V}},\text{massive}} & \gamma_0^{\text{SU}(N_f)_{\text{V}},\text{SU}(N_f)_{\text{L|R}}} & \gamma_0^{\text{SU}(N_f)_{\text{V}}} & \gamma_0^{\text{SU}(N_f)_{\text{V}},\mathcal{E}} \end{array} \right)^{(d-4)}, \quad (6.10)$$

where the vertical line again separates the mixing contributions from the redundant EOM vanishing operators. The overall superscript $(d-4)$ indicates the mass-dimension d of the operator basis, where $(d-4)$ is the accompanying power of the lattice spacing in the SET. The other superscripts denote sets of operators which comply with the following flavour symmetries (see also chapter 5):

- $\text{SU}(N_f)_{\text{L|R}}$:
Includes operators which are invariant under $\text{SU}(N_f)_{\text{L}} \times \text{SU}(N_f)_{\text{R}}$ flavour rotations, i.e. separate rotations for left- and right-handed quarks.
- $\text{SU}(N_f)_{\text{V}}$:
Operators which are only invariant under $\text{SU}(N_f)_{\text{V}}$ flavour rotations. These operators are in general needed for massless Wilson quarks.
- massive:
These operators are lower-dimensional operators with explicit powers of masses added.

Using different lattice fermion actions for different flavours breaks flavour permutation symmetry and is discussed in some detail in section 8.4.

Apart from the operators included in our minimal basis in section 5.2 we also need the explicitly mass-dependent operators that we discarded earlier. In the mass-degenerate case it suffices to multiply lower dimensional operators of our minimal basis by $\text{tr}(M^n)$ with appropriate power $n > 0$ to obtain the correct mass-dimension. Allowing for arbitrary quark masses then reduces symmetries to the flavour permutation symmetry (and $\prod_{f=1}^{N_f} \text{U}(1)_f$), which introduces additional massive operators.

To keep the mixing matrix applicable to the different choices possible for the masses we will split the massive operators into those relevant for mass-degenerate quarks, i.e., operators that only depend on $\text{tr}(M)$ and powers thereof, and those only relevant for the general massive case by introducing a term of the form

$$\Delta M^n \stackrel{\text{def}}{=} M^n - \mathbb{1} \frac{\text{tr}(M^n)}{N_f}, \quad (6.11)$$

such that the latter vanishes in the mass-degenerate case. Since the bases from mass-dimension 3, 4 and later on also 5 get reused for the massive operators at mass-dimensions 5 and 6 it pays out to immediately diagonalise these bases at each mass-dimension. Then the anomalous dimension matrix $\gamma_0^{\text{massive}}$ is diagonal where the diagonal entries can be inferred from

$$[\gamma_0^{\text{massive}}]_{\#m=n}^{(d-4)} \sim [\gamma_0^{\mathcal{B}}]^{(d-n-4)} + \mathbb{1} n \gamma_0^m. \quad (6.12)$$

Here $\#m$ selects the minimal power of quark masses present in the operator and \sim accounts for different versions of the same fermion bilinears at higher mass-dimension due to the insertion of

either $\text{tr}(M)^n$ or ΔM^n and so on. We introduced the 1-loop coefficient of the anomalous mass dimension, see e.g. [72, p. 523],

$$4\pi\gamma_0^m = 3\frac{N^2 - 1}{2N}. \quad (6.13)$$

The entries $\gamma_0^{\text{massive}, \mathcal{E}}$ are known from lower mass-dimensions and remain unchanged (up to a proper mass prefactor for the EOM vanishing operators).

In the initial listing of massive operators only those are included which are necessary to renormalise the mass-independent ones at a given mass-dimension. This keeps the overall mixing matrix small by excluding unnecessary zeros. Only when listing the full diagonalised basis we include all massive operators and write them in a form such that they vanish in the mass-degenerate or massless case.

Mass-dimensions 3 and 4 As a preparation of the massive operators required at mass-dimensions 5 and 6 we give here the only operators relevant for the on-shell basis at mass-dimension 3 and 4. Starting with mass-dimension 3 there is only one operator

$$\text{SU}(N_f)_V : \quad \mathcal{O}_1^{(-1)} = \bar{\Psi}\Psi,$$

with 1-loop anomalous dimension

$$4\pi [\gamma_0^{\mathcal{O}}]_1^{(-1)} = -3\frac{N^2 - 1}{2N}. \quad (6.14)$$

At mass-dimension 4 there is again only one new massless operator

$$\begin{aligned} \text{SU}(N_f)_{L|R} : \quad \mathcal{O}_1^{(0)} &= \frac{1}{g_0^2} \text{tr}(F_{\mu\nu}F_{\mu\nu}), \\ \text{massive} : \quad \bar{\Psi}M\Psi, \\ \mathcal{E} : \quad \mathcal{E}_1^{(0)} &= \bar{\Psi}(\gamma_\mu D_\mu + M)\Psi. \end{aligned}$$

The corresponding 1-loop anomalous dimension submatrices read

$$\begin{aligned} 4\pi [\gamma_0^{\text{SU}(N_f)_{L|R}}]^{(0)} &= -\frac{11}{3}N + \frac{2}{3}N_f, & 4\pi [\gamma_0^{\text{SU}(N_f)_{L|R}, \text{massive}}]^{(0)} &= 3\frac{N^2 - 1}{N}, \\ 4\pi [\gamma_0^{\text{SU}(N_f)_{L|R}, \mathcal{E}}]^{(0)} &= 0. \end{aligned} \quad (6.15)$$

Then the diagonal basis at mass-dimension 4 with full massive operator basis is

$$\mathcal{B}_1^{(0)} = \mathcal{O}_1^{(0)} - \frac{3(N^2 - 1)}{N\hat{\beta}_0} (\mathcal{B}_3^{(0)} + \mathcal{B}_2^{(0)}), \quad \mathcal{B}_2^{(0)} = \frac{\text{tr}(M)}{N_f} \bar{\Psi}\Psi, \quad \mathcal{B}_3^{(0)} = \bar{\Psi}\Delta M^1\Psi, \quad (6.16)$$

where $\hat{\beta}_0 = 4\pi\beta_0$. The corresponding 1-loop coefficients of the anomalous dimensions are

$$[\hat{\gamma}_0^{\mathcal{B}}]_1^{(0)} = -1, \quad [\hat{\gamma}_0^{\mathcal{B}}]_2^{(0)} = [\hat{\gamma}_0^{\mathcal{B}}]_3^{(0)} = 0. \quad (6.17)$$

Mass-dimension 5 To renormalise the minimal basis of mass-dimension 5 operators we must consider all graphs in figure 6.1 except figure 6.1e. The only relevant operator for massless quarks is the Sheikholeslami-Wohlert term accompanied by an EOM vanishing operator

$$\mathcal{O}_4^{(1)} = i\bar{\Psi}\sigma_{\mu\nu}F_{\mu\nu}\Psi, \quad \mathcal{E}_2^{(1)} = \bar{\Psi}(\gamma_\mu D_\mu + M)^2\Psi.$$

For mass-degenerate quarks the lower dimensional operators reoccur multiplied by appropriate powers of quark masses and are allowed to mix during renormalisation. Extension to arbitrary quark masses only introduces more mass-dependent operators.

The resulting anomalous dimension submatrices take the form

$$\begin{aligned} 4\pi \left[\gamma_0^{\text{SU}(N_f)_V} \right]^{(1)} &= \frac{N^2 - 5}{2N}, \quad 4\pi \left[\gamma_0^{\text{SU}(N_f)_V, \text{massive}} \right]^{(1)} = \begin{pmatrix} -4 & -6\frac{N^2-1}{N} \end{pmatrix}, \\ 4\pi \left[\gamma_0^{\text{SU}(N_f)_V, \mathcal{E}} \right]^{(1)} &= \begin{pmatrix} 3N - \frac{3}{N} & 0 & \frac{3}{N} - 3N \end{pmatrix}, \end{aligned} \quad (6.18)$$

where the on-shell basis, ordered by symmetry constraints and accompanied by the set of EOM vanishing operators, is chosen as

$$\begin{aligned} \text{SU}(N_f)_V : & \quad \left\{ \mathcal{O}_4^{(1)} \right\}, \\ \text{massive} : & \quad \left\{ \text{tr}(M) \mathcal{O}_1^{(0)}, \bar{\Psi} M^2 \Psi \right\}, \\ \mathcal{E} : & \quad \left\{ \mathcal{E}_2^{(1)}, \text{tr}(M) \mathcal{E}_1^{(0)}, \bar{\Psi} M (\gamma_\mu D_\mu + M) \Psi \right\}. \end{aligned}$$

Accordingly the diagonal basis at mass-dimension 5 with the full set of massive operators is

$$\begin{aligned} \mathcal{B}_1^{(1)} &= \mathcal{O}_4^{(1)} + \frac{4NN_f}{1 - \hat{\beta}_0 N + N^2} \mathcal{B}_2^{(1)} + \frac{6(N^2 - 1)}{1 + N^2} \left\{ \mathcal{B}_6^{(1)} + \mathcal{B}_4^{(1)} + \mathcal{B}_3^{(1)} + \frac{2N_f}{\hat{\beta}_0} \mathcal{B}_5^{(1)} + \frac{2N_f}{\hat{\beta}_0} \mathcal{B}_3^{(1)} \right\}, \\ \mathcal{B}_2^{(1)} &= \frac{\text{tr}(M)}{N_f} \mathcal{B}_1^{(0)}, \quad \mathcal{B}_3^{(1)} = \frac{\text{tr}(M)^2}{N_f^2} \bar{\Psi} \Psi, \\ \mathcal{B}_4^{(1)} &= \frac{\text{tr}(M \Delta M^1)}{N_f} \bar{\Psi} \Psi, \quad \mathcal{B}_5^{(1)} = \frac{\text{tr}(M)}{N_f} \bar{\Psi} \Delta M^1 \Psi, \quad \mathcal{B}_6^{(1)} = \bar{\Psi} \Delta M^2 \Psi, \end{aligned} \quad (6.19)$$

with 1-loop coefficients of the anomalous dimension matrix

$$\left[\hat{\gamma}_0^{\mathcal{B}} \right]_1^{(1)} = \frac{N^2 - 5}{2N\hat{\beta}_0}, \quad \left[\hat{\gamma}_0^{\mathcal{B}} \right]_2^{(1)} = 3 \frac{N^2 - 1}{2N\hat{\beta}_0} - 1, \quad \left[\hat{\gamma}_0^{\mathcal{B}} \right]_{3-6}^{(1)} = 3 \frac{N^2 - 1}{2N\hat{\beta}_0}. \quad (6.20)$$

The coefficient $\left[\hat{\gamma}_0^{\mathcal{B}} \right]_1^{(1)}$ agrees with results found in the literature [150].

Mass-dimension 6 Due to the much larger number of operators the case of full QCD at mass-dimension 6 is more involved. We start by considering the sector of 4-fermion operators and (for now) set the quark masses to zero. These 4-fermion operators are the most difficult operators to renormalise that we encountered in this thesis. We thus discuss them more extensively. Following the literature [152, 153] we first consider single flavoured operator and 2-flavour operators, i.e. no flavour singlets. From these we can both infer the mixing of the basis in eqs. (5.45) and (5.46) through a change of basis and eventually check in section 6.4 the validity of our results having multiple reference values at hand.

Single flavour operators $O^q = g_0^2 (\bar{q} \Gamma q)^2$ with flavour $q = u, d, s, \dots$ and $\Gamma \in \{1, \gamma_5, \gamma_\mu, \gamma_5 \gamma_\mu, \sigma_{\mu\nu}\}$ are the only 4-fermion operators that require some care due to the combinatorics when having multiple identically flavoured (anti-)quarks. This is realised through the introduction of an additional

scalar field acting as a mediator (here denoted by the dotted line)

$$\begin{array}{c} B, j \\ \swarrow p_2 \\ \otimes \\ \swarrow p_1 \quad \searrow p_4 \\ A, i \quad \searrow p_3 \quad C, k \end{array} = \begin{array}{c} B, j \\ \swarrow p_2 \\ \bullet \cdots \bullet \\ \swarrow p_1 \quad \searrow p_4 \\ A, i \quad \searrow p_3 \quad C, k \end{array} - \begin{array}{c} B, j \\ \swarrow p_2 \\ \bullet \cdots \bullet \\ \swarrow p_1 \quad \searrow p_4 \\ A, i \quad \searrow p_3 \quad C, k \end{array} \quad (6.21)$$

$$= 2(\delta_{AB}\delta_{CD}\Gamma_{ij}\Gamma_{kl} - \delta_{AD}\delta_{CB}\Gamma_{il}\Gamma_{kj}) \quad (6.22)$$

$$\begin{array}{c} B, j \\ \swarrow p_2 \\ \bullet \cdots \\ \swarrow p_1 \\ A, i \end{array} = \sqrt{2}g_0\Gamma_{ij}\delta_{AB} \quad (6.23)$$

such that each of the fermion lines belonging to this operator (\otimes) is always represented through the above 3-vertex, see also appendix D.2. The mediator ensures that relative minuses due anti-commutativity of fermions are taken care of and that any spacetime indices encapsulated in Γ are equal at the second vertex of this kind completing the 4-fermion operator. In the same fashion one can also define $(\bar{u}\Gamma T^a u)^2$, which are redundant due to Fierz identities eqs. (5.47) – (5.49)

$$\begin{pmatrix} (\bar{q}T^a q)^2 \\ (\bar{q}\gamma_5 T^a q)^2 \\ (\bar{q}\gamma_\mu T^a q)^2 \\ (\bar{q}\gamma_\mu \gamma_5 T^a q)^2 \\ (\bar{q}\sigma_{\mu\nu} T^a q)^2 \end{pmatrix} = \frac{1}{8} \underbrace{\begin{pmatrix} \frac{4}{N} + 1 & 1 & 1 & -1 & \frac{1}{2} \\ 1 & \frac{4}{N} + 1 & -1 & 1 & \frac{1}{2} \\ 4 & -4 & \frac{4}{N} - 2 & -2 & 0 \\ -4 & 4 & -2 & \frac{4}{N} - 2 & 0 \\ 12 & 12 & 0 & 0 & \frac{4}{N} - 2 \end{pmatrix}}_{=\hat{F}} \begin{pmatrix} (\bar{q}q)^2 \\ (\bar{q}\gamma_5 q)^2 \\ (\bar{q}\gamma_\mu q)^2 \\ (\bar{q}\gamma_\mu \gamma_5 q)^2 \\ (\bar{q}\sigma_{\mu\nu} q)^2 \end{pmatrix} \quad (6.24)$$

but simplify the overall renormalisation. In dimensional regularisation these Fierz identities only hold to 1-loop order and beyond 1-loop additional terms occur leading among other things to the presence of so called *evanescent operators* [154]. The simplification of the overall renormalisation can already be seen when staying at $N_f = 1$ and renormalising $(\bar{u}\Gamma u)^2$ with the overcomplete set and only then making use of the Fierz identities

$$O_{i;\overline{\text{MS}}}^u = X_{ij}O_j^u + Y_{ij}(\bar{u}\Gamma_j T^a u)^2 + W_{i1}\check{\mathcal{E}}_1 + W_{i2}\check{\mathcal{E}}_2^u = \underbrace{(X_{ik} + Y_{ij}\hat{F}_{jk})}_{=Z_{ik}^O} O_k^u + W_{i1}\check{\mathcal{E}}_1 + W_{i2}\check{\mathcal{E}}_2^u, \quad (6.25)$$

where $\check{\mathcal{E}}_1 = \frac{1}{g_0^2} \text{tr}(D_\mu F_{\mu\nu} D_\rho F_{\rho\nu})$ and $\check{\mathcal{E}}_2^u = \bar{u}\gamma_\mu D_\nu F_{\nu\mu} u$ are a basis for the EOM vanishing operators. Keep in mind that $\check{\mathcal{E}}_1^u$ and $\check{\mathcal{E}}_2^u$ are not yet EOM vanishing and require a change of basis as will be done later on in eq. (6.29c).

From the 1PI graphs in figure 6.1 one infers the mixing of the single flavour 4-fermion operator basis and the $\check{\mathcal{E}}_1$, $\check{\mathcal{E}}_2^q$. As it turns out at 1-loop $\check{\mathcal{E}}_1$ does not contribute to either single flavour or 2-flavour 4-fermion operators, i.e. $W_{i1} = 0$ in eq. (6.25), and we drop it for the 4-fermion operators.

In the case of the single flavour operators O we then find

$$4\pi(\gamma_0^O - \mathbb{1}\beta_0) = \left(\begin{array}{ccccc|c} \frac{3}{2} - 3N + \frac{3}{N} & \frac{3}{2} & 0 & 0 & \frac{1}{2N} - \frac{1}{4} & \frac{2}{3} \\ \frac{3}{2} & \frac{3}{2} - 3N + \frac{3}{N} & 0 & 0 & \frac{1}{2N} - \frac{1}{4} & -\frac{2}{3} \\ 3 & -3 & \frac{3}{2} & \frac{3}{2} - \frac{3}{N} & 0 & -\frac{4}{3} \\ -3 & 3 & \frac{3}{2} - \frac{3}{N} & \frac{3}{2} & 0 & -\frac{4}{3} \\ \frac{12}{N} + 6 & \frac{12}{N} + 6 & 0 & 0 & N - \frac{1}{N} + 3 & 0 \end{array} \right), \quad (6.26)$$

where the part separated by the vertical line separates the contributions of $\check{\mathcal{E}}_2^u$.

Moving on to $N_f = 2$ introduces the 2-flavour 4-fermion operators

$$Q = g_0^2(\bar{u}\Gamma u)(\bar{d}\Gamma d), \quad \mathcal{Q} = g_0^2(\bar{u}\Gamma T^a u)(\bar{d}\Gamma T^a d), \quad u \neq d, \quad (6.27)$$

and of course a copy of $O^{u \rightarrow d}$ as well as another element of the basis $\check{\mathcal{E}}_2^d = \bar{d}\gamma_\mu D_\nu F_{\nu\mu} d$ needed to construct the EOM vanishing part. The new anomalous dimension matrix for the 2-flavour 4-fermion operators does not involve mixing with the single flavour 4-fermion operators (unless the basis $\check{\mathcal{E}}$ is changed to the EOM vanishing operators). It takes the form

$$4\pi(\gamma_0^{Q \cup \mathcal{Q}} - \mathbb{1}\beta_0) = \left(\begin{array}{cccccccccc|cc} \frac{3}{N} - 3N & 0 & 0 & 0 & 0 & 0 & 0 & 0 & 0 & 0 & 1 & 0 & 0 \\ 0 & \frac{3}{N} - 3N & 0 & 0 & 0 & 0 & 0 & 0 & 0 & 0 & 1 & 0 & 0 \\ 0 & 0 & 0 & 0 & 0 & 0 & 0 & 0 & 0 & -6 & 0 & 0 & 0 \\ 0 & 0 & 0 & 0 & 0 & 0 & 0 & -6 & 0 & 0 & 0 & 0 & 0 \\ 0 & 0 & 0 & 0 & N - \frac{1}{N} & 24 & 24 & 0 & 0 & 0 & 0 & 0 & 0 \\ 0 & 0 & 0 & 0 & \frac{1}{4} - \frac{1}{4N^2} & \frac{3}{N} & 0 & 0 & 0 & \frac{1}{N} - \frac{N}{4} & 0 & 0 & 0 \\ 0 & 0 & 0 & 0 & \frac{1}{4} - \frac{1}{4N^2} & 0 & \frac{3}{N} & 0 & 0 & \frac{1}{N} - \frac{N}{4} & 0 & 0 & 0 \\ 0 & 0 & 0 & \frac{3}{2N^2} - \frac{3}{2} & 0 & 0 & 0 & -\frac{3N}{2} & \frac{3N}{2} - \frac{6}{N} & 0 & \frac{2}{3} & \frac{2}{3} & 0 \\ 0 & 0 & \frac{3}{2N^2} - \frac{3}{2} & 0 & 0 & 0 & 0 & \frac{3N}{2} - \frac{6}{N} & -\frac{3N}{2} & 0 & 0 & 0 & 0 \\ 6 - \frac{6}{N^2} & 6 - \frac{6}{N^2} & 0 & 0 & 0 & \frac{24}{N} - 6N & \frac{24}{N} - 6N & 0 & 0 & -2N - \frac{1}{N} & 0 & 0 & 0 \end{array} \right) \quad (6.28)$$

where the part separated by the vertical line separates the contributions of $\check{\mathcal{E}}_2^u$ and $\check{\mathcal{E}}_2^d$. The extension towards $N_f > 2$ does not yield anything new as all mixing between different flavours is contained inside $\check{\mathcal{E}}_2^u$, $\check{\mathcal{E}}_2^d$ and their counterparts for each new flavour. Generalisation to arbitrary number of flavours is thus straight forward.

To switch back to our original 4-fermion operator basis in eqs. (5.45) and (5.46) we use (fixed $i \in \{1, \dots, 5\}$)

$$\begin{aligned} \mathcal{O}_{10+i}^{(2)} &= g_0^2(\bar{\Psi}\Gamma_i\Psi)^2 \\ &= g_0^2 \sum_q (\bar{q}\Gamma_i q)^2 + 2g_0^2 \sum_{q < q'} (\bar{q}\Gamma_i q)(\bar{q}'\Gamma_i q'), \end{aligned} \quad (6.29a)$$

$$\begin{aligned} \mathcal{O}_{15+i}^{(2)} &= g_0^2(\bar{\Psi}\Gamma_i T^a \Psi)(\bar{\Psi}\Gamma_i T^a \Psi) \\ &= g_0^2 \sum_q (\bar{q}\Gamma_i T^a q)(\bar{q}\Gamma_i T^a q) + 2g_0^2 \sum_{q < q'} (\bar{q}\Gamma_i T^a q)(\bar{q}'\Gamma_i T^a q') \\ &= g_0^2 \sum_{q,j} \hat{F}_{ij}(\bar{q}\Gamma_j q)^2 + 2g_0^2 \sum_{q < q'} (\bar{q}\Gamma_i T^a q)(\bar{q}'\Gamma_i T^a q'), \end{aligned} \quad (6.29b)$$

for a proper change of basis. The 30 left over flavoured operators are not relevant here, while some of those are needed when using different lattice fermion actions for some flavours which breaks flavour permutation symmetry. The full set is only used in section 6.4 as a check against the literature while we are content here with all flavour singlets. We also need to switch to the EOM vanishing operators, i.e. switching to

$$\mathcal{E}_4^{(2)} = \sum_q \left\{ \tilde{\mathcal{E}}_2^q - g_0^2 \bar{q} \gamma_\mu T^a q \sum_{q'} \bar{q}' \gamma_\mu T^a q' \right\}, \quad (6.29c)$$

which finally gives the full on-shell mixing and a separate contribution from EOM vanishing operators due to the chosen off-shell renormalisation.

Now reordering the operators according to their particular flavour symmetries and adding the remaining mass-dimension 6 operators

$$\mathcal{O}_2^{(2)} = \frac{1}{g_0^2} \text{tr} (D_\mu F_{\rho\sigma} D_\mu F_{\rho\sigma}), \quad \mathcal{O}_4^{(2)} = \frac{1}{g_0^2} \sum_\mu \text{tr} (D_\mu F_{\mu\nu} D_\mu F_{\mu\nu}), \quad \mathcal{O}_{10}^{(2)} = \sum_\mu \bar{\Psi} \gamma_\mu D_\mu^3 \Psi$$

finally yields the anomalous dimension submatrices ($\hat{\beta}_0 = 4\pi\beta_0$)

$$4\pi \left[\gamma_0^{\text{SU}(N_f)_{\text{L|R}}} \right]^{(2)} = \begin{pmatrix} \frac{7N}{3} + \frac{2N_f}{3} & 0 & 0 & 0 & \frac{3}{2} - \frac{3}{2N^2} & \frac{N}{6} + \frac{2}{3N} & \frac{6}{N} - \frac{3N}{2} \\ -\frac{7N}{15} & \frac{21N}{5} + \frac{2N_f}{3} & -\frac{11}{60} \frac{N^2-1}{N} & 0 & \frac{1}{2} - \frac{1}{2N^2} & \frac{47N}{240} + \frac{19}{80N} & \frac{2}{N} - \frac{N}{2} \\ \frac{11}{60} N_f & -\frac{11}{15} N_f & \frac{157N}{60} - \frac{157}{60N} & 0 & \frac{1}{8} - \frac{1}{8N^2} & \frac{3N}{80} - \frac{13}{80N} - \frac{7}{60} N_f & \frac{1}{2N} - \frac{N}{8} \\ 0 & 0 & 0 & \hat{\beta}_0 & 0 & -\frac{4}{3} & -6 \\ 0 & 0 & 0 & 0 & \hat{\beta}_0 & -\frac{22}{3} & 0 \\ 0 & 0 & 0 & 0 & \frac{3}{2N^2} - \frac{3}{2} & \hat{\beta}_0 - \frac{3N}{2} - \frac{2}{3N} + \frac{4}{3} N_f & \frac{3N}{2} - \frac{6}{N} \\ 0 & 0 & 0 & \frac{3}{2N^2} - \frac{3}{2} & 0 & \frac{3N}{2} - \frac{20}{3N} & \hat{\beta}_0 - \frac{3N}{2} \end{pmatrix},$$

$$4\pi \left[\gamma_0^{\text{SU}(N_f)_V} \right]^{(2)} = \begin{pmatrix} \hat{\beta}_0 + \frac{3}{N} - 3N & 0 & 0 & 0 & 0 & 1 \\ 0 & \hat{\beta}_0 + \frac{3}{N} - 3N & 0 & 0 & 0 & 1 \\ 0 & 0 & \hat{\beta}_0 + N - \frac{1}{N} & 24 & 24 & 0 \\ 0 & 0 & \frac{1}{4} - \frac{1}{4N^2} & \hat{\beta}_0 + \frac{3}{N} & 0 & \frac{1}{N} - \frac{N}{4} \\ 0 & 0 & \frac{1}{4} - \frac{1}{4N^2} & 0 & \hat{\beta}_0 + \frac{3}{N} & \frac{1}{N} - \frac{N}{4} \\ 6 - \frac{6}{N^2} & 6 - \frac{6}{N^2} & 0 & \frac{24}{N} - 6N & \frac{24}{N} - 6N & \hat{\beta}_0 - 2N - \frac{1}{N} \end{pmatrix},$$

$$4\pi \left[\gamma_0^{\text{SU}(N_f)_V, \text{SU}(N_f)_{\text{L|R}}} \right]^{(2)} = \begin{pmatrix} 0 & 0 & 0 & 0 & 0 & \frac{2}{3} & 0 \\ 0 & 0 & 0 & 0 & 0 & -\frac{2}{3} & 0 \\ 0 & 0 & 0 & 0 & 0 & 0 & 0 \\ 0 & 0 & 0 & 0 & 0 & \frac{1}{3N} & 0 \\ 0 & 0 & 0 & 0 & 0 & -\frac{1}{3N} & 0 \\ 0 & 0 & 0 & 0 & 0 & 0 & 0 \end{pmatrix},$$

6.3. Renormalisation of the operator basis in full QCD

$$\begin{aligned}
4\pi \left[\gamma_0^{\text{SU}(N_f)_{\text{L|R}}, \text{massive}} \right]^{(2)} &= \begin{pmatrix} 0 & \frac{3N}{2} & 0 & 0 & 4N - \frac{4}{N} \\ 0 & \frac{79N}{240} + \frac{11}{240N} & 0 & 0 & \frac{149N}{120} - \frac{149}{120N} \\ 0 & \frac{37N}{240} + \frac{83}{240N} & 1 & 0 & \frac{197N}{120} - \frac{197}{120N} \\ 0 & 0 & 0 & 0 & 8 \\ 0 & 0 & 0 & 0 & -8 \\ 0 & 0 & 0 & 0 & \frac{4}{N} - 4N \\ 0 & 0 & 0 & 0 & 4N - \frac{4}{N} \end{pmatrix}, \\
4\pi \left[\gamma_0^{\text{SU}(N_f)_{\text{V}}, \text{massive}} \right]^{(2)} &= \begin{pmatrix} 0 & 1 & 0 & -8 & 10 - 8N \\ 0 & 1 & 0 & 0 & 2 \\ 0 & -4 & 0 & 0 & 24 \\ 0 & \frac{1}{2N} & 0 & 0 & \frac{1}{N} - N \\ 0 & \frac{1}{2N} & 0 & 0 & \frac{1}{N} - N \\ 4 & -\frac{2}{N} & 0 & 0 & \frac{12}{N} - 12N \end{pmatrix}, \quad 4\pi \left[\gamma_0^{\text{SU}(N_f)_{\text{V}}, \mathcal{E}} \right]^{(2)} = \begin{pmatrix} \frac{2}{3} & 0 & 0 & 0 & 0 & 0 \\ -\frac{2}{3} & 0 & 0 & 0 & 0 & 0 \\ 0 & 0 & 0 & 0 & 0 & 0 \\ \frac{1}{3N} & 0 & 0 & 0 & 0 & 0 \\ -\frac{1}{3N} & 0 & 0 & 0 & 0 & 0 \\ 0 & 0 & 0 & 0 & 0 & 0 \end{pmatrix}, \\
4\pi \left[\gamma_0^{\text{SU}(N_f)_{\text{L|R}}, \mathcal{E}} \right]^{(2)} &= \begin{pmatrix} \frac{2}{3N} - \frac{3N}{4\lambda_{\overline{\text{MS}}}} - \frac{7N}{12} & \frac{23N}{6} - \frac{3N}{2\lambda_{\overline{\text{MS}}}} & 0 & \frac{N}{2} - \frac{1}{2N} & \frac{3}{2N} - \frac{3N}{2} & 0 \\ \frac{19}{80N} - \frac{N}{4\lambda_{\overline{\text{MS}}}} - \frac{13N}{240} & \frac{7N}{15} - \frac{N}{2\lambda_{\overline{\text{MS}}}} & \frac{11N_c}{240} - \frac{11}{240N_c} & \frac{N^2-1}{6N} & -\frac{71(N^2-1)}{120N} & \frac{11(N^2-1)}{60N} \\ \frac{3N}{80} - \frac{13}{80N} - \frac{7}{20} & \frac{7}{10} & \frac{97}{240N_c} - \frac{97N_c}{240} & \frac{(\lambda_{\overline{\text{MS}}}+3)(1-N^2)}{12\lambda_{\overline{\text{MS}}}N} & \frac{(53\lambda_{\overline{\text{MS}}}-90)(1-N^2)}{120\lambda_{\overline{\text{MS}}}N} & \frac{83(N^2-1)}{60N} \\ -\frac{4}{3} & 0 & 0 & 0 & 0 & 0 \\ -\frac{4}{3} & 0 & 0 & 0 & 0 & 0 \\ 4 - \frac{2}{3N} & 0 & 0 & 0 & 0 & 0 \\ -\frac{2}{3N} & 0 & 0 & 0 & 0 & 0 \end{pmatrix}. \tag{6.30}
\end{aligned}$$

The basis is ordered as

$$\begin{aligned}
\text{SU}(N_f)_{\text{L|R}} : & \left\{ \mathcal{O}_{\textcolor{red}{2}}^{(2)}, \mathcal{O}_{\textcolor{red}{4}}^{(2)}, \mathcal{O}_{\textcolor{red}{10}}^{(2)}, \mathcal{O}_{\textcolor{red}{13}}^{(2)}, \mathcal{O}_{\textcolor{red}{14}}^{(2)}, \mathcal{O}_{\textcolor{red}{18}}^{(2)}, \mathcal{O}_{\textcolor{red}{19}}^{(2)} \right\}, \\
\text{SU}(N_f)_{\text{V}} : & \left\{ \mathcal{O}_{\textcolor{red}{11}}^{(2)}, \mathcal{O}_{\textcolor{red}{12}}^{(2)}, \mathcal{O}_{\textcolor{red}{15}}^{(2)}, \mathcal{O}_{\textcolor{red}{16}}^{(2)}, \mathcal{O}_{\textcolor{red}{17}}^{(2)}, \mathcal{O}_{\textcolor{red}{20}}^{(2)} \right\}, \\
\text{massive} : & \left\{ \text{tr}(M) i \bar{\Psi} \sigma_{\mu\nu} F_{\mu\nu} \Psi, i \bar{\Psi} M \sigma_{\mu\nu} F_{\mu\nu} \Psi, \text{tr}(M^2) \text{tr}(F_{\mu\nu} F_{\mu\nu}), \text{tr}(M^3) \bar{\Psi} \Psi, \bar{\Psi} M^3 \Psi \right\}, \\
\mathcal{E} : & \left\{ \mathcal{E}_{\textcolor{red}{4}}^{(2)}, \mathcal{E}_{\textcolor{red}{2}}^{(2)}, \mathcal{E}_{\textcolor{red}{3}}^{(2)}, \mathcal{E}_{\textcolor{red}{1}}^{(2)}, \bar{\Psi} M (\gamma_\mu D_\mu + M)^2 \Psi, \bar{\Psi} M^2 (\gamma_\mu D_\mu + M) \Psi \right\}.
\end{aligned}$$

The full diagonalised on-shell basis at mass-dimension 6 is more complicated due to a severely increased number of operators leading to complicated radicals in the analytical expressions.

Due to symmetry constraints the mass-independent operators breaking chiral symmetry do not mix into to the ones compatible with chiral symmetry. The diagonalised basis reflects this feature and we can give the 1-loop anomalous dimensions for both symmetry constraints separately. We

find for the 1-loop anomalous dimensions of the chirally symmetric basis

$$\begin{aligned}
 4\pi [\gamma_0^{\mathcal{B}}]_{\mathbf{1}}^{(2)} &= \frac{7N}{3} + \frac{2N_f}{3}, \\
 4\pi [\gamma_0^{\mathcal{B}}]_{\mathbf{2,3}}^{(2)} &= \pm \frac{\sqrt{1600N_f^2N^2 + 9536N_fN^3 + 10624N_fN + 9025N^4 + 29830N^2 + 24649}}{120N} \\
 &\quad + \frac{409N}{120} - \frac{157}{120N} + \frac{N_f}{3}, \\
 4\pi [\gamma_0^{\mathcal{B}}]_{\mathbf{4-7}}^{(2)} &= \mp \frac{1}{12N^2} \sqrt{\frac{Y(N, N_f)}{X(N, N_f)}} \\
 &\quad + \frac{1}{12N^2} \left[35N^3 - 4N_fN^2 - 2N \mp Y(N, N_f) \right], \tag{6.31}
 \end{aligned}$$

where we introduced a generalisation of \pm , that must be read row-wise, and the shorthands

$$\begin{aligned}
 X(N, N_f) &\stackrel{\text{def}}{=} 36N^2 \sqrt[3]{\frac{-8N_f^3(N^4 + 18N^2 - 18)N^5 + 240N_f^2(3N^2 - 4)(N^4 + 6N^2 - 6)N^2}{-3N_fN(297N^8 + 4467N^6 - 11784N^4 + 7676N^2 + 144)} \\
 &\quad + 90(297N^6 - 693N^4 + 1196N^2 - 1600)N^2 + 64000} \\
 &\quad + 3\sqrt{-3N(N^2 - 1)} \\
 &\quad \times \sqrt[3]{\frac{256N_f^6N^5(N^4 + 16N^2 - 16) - 5120N_f^5N^6(3N^2 - 4) + 32N_f^4N^3(101N^8 + 1604N^6 - 12956N^4 + 38544N^2 - 25600)}{-1280N_f^3N^2(3N^2 - 4)(51N^6 - 397N^4 + 755N^2 + 36)} \\
 &\quad + N_f^2N\{9801N^{12} + 319176N^{10} - 4186520N^8 + 19610432N^6 - 52327856N^4 + 81169280N^2 - 40966912\} \\
 &\quad - 20N_f(3N^2 - 4)(9801N^{10} - 154836N^8 + 938980N^6 - 2536144N^4 + 2515200N^2 + 25600)} \\
 &\quad + N^3(99N^2 + 1)(99N^4 - 800N^2 + 1600)^2} \tag{6.32}
 \end{aligned}$$

$$Y(N, N_f) \stackrel{\text{def}}{=} \frac{1}{\sqrt{3X(N, N_f)}} \sqrt{\frac{5184N_f^2N^{10} + 62208N_f^2N^8 - 62208N_f^2N^6 - 311040N_fN^9}{+414720N_fN^7 + 384912N^{10} + 1170288N^8 - 3110400N^6 + 2073600N^4} \\
 + \{1452N^2 - 48N_fN^3 + 108N^4 + 48N_f^2N^4 - 72N_fN^5 + 243N^6\}X(N, N_f)} \\
 + X^2(N, N_f) \tag{6.33}$$

Both anomalous dimensions $[\gamma_0^{\mathcal{B}}]_{\mathbf{1}}^{(2)}$ and $[\gamma_0^{\mathcal{B}}]_{\mathbf{2}}^{(2)}$ yield the known results from pure gauge theory in eq. (6.9) in the limit $N_f = 0$. Since the symbolic expressions of the diagonal basis are very complicated we discard the additional massive mixing contributions, i.e., the following mass-dimension 6 basis is only applicable to massless QCD¹. The diagonal basis in the sector of chiral symmetry preserving operators is

$$\begin{aligned}
 \mathcal{B}_1^{(2)} &= \mathcal{O}_2^{(2)} + \mathcal{O}_{18}^{(2)}, \\
 \mathcal{B}_2^{(2)} &= \mathcal{O}_4^{(2)} - \frac{1}{4}\mathcal{O}_2^{(2)} \\
 &\quad - \frac{2N(N_f(681N^2 - 121) + 7(4\pi[\gamma_0^{\mathcal{B}}]_{\mathbf{3}}^{(2)} - 4\pi[\gamma_0^{\mathcal{B}}]_{\mathbf{2}}^{(2)} + 190N^3 + 314N))}{44\pi N_f[\gamma_0^{\mathcal{B}}]_{\mathbf{2}}^{(2)}} \mathcal{O}_{10}^{(2)} \\
 &\quad + \frac{N_f(44\pi[\gamma_0^{\mathcal{B}}]_{\mathbf{2}}^{(2)} - 1362N^3 + 242N) - 14N(4\pi[\gamma_0^{\mathcal{B}}]_{\mathbf{3}}^{(2)} - 4\pi[\gamma_0^{\mathcal{B}}]_{\mathbf{2}}^{(2)} + 190N^3 + 314N)}{528\pi N_f[\gamma_0^{\mathcal{B}}]_{\mathbf{2}}^{(2)}} \mathcal{O}_{18}^{(2)}, \tag{6.34}
 \end{aligned}$$

¹For a specific choice of N and N_f the proper diagonal basis can be obtained using the *Mathematica* notebook holding the non-diagonalised mixing matrix. It can be found at https://zppt.desy.de/download/husung_thesis_results.

$$\begin{aligned}
 \mathcal{B}_3^{(2)} = & \mathcal{O}_{10}^{(2)} + \frac{44\pi N_f [\gamma_0^{\mathcal{B}}]_3^{(2)}}{8N \left(N_f (681N^2 - 121) + 7 \left(4\pi [\gamma_0^{\mathcal{B}}]_2^{(2)} - 4\pi [\gamma_0^{\mathcal{B}}]_3^{(2)} + 190N^3 + 314N \right) \right)} \mathcal{O}_2^{(2)} \\
 & - \frac{44\pi N_f [\gamma_0^{\mathcal{B}}]_3^{(2)}}{2N \left(N_f (681N^2 - 121) + 7 \left(4\pi [\gamma_0^{\mathcal{B}}]_2^{(2)} - 4\pi [\gamma_0^{\mathcal{B}}]_3^{(2)} + 190N^3 + 314N \right) \right)} \mathcal{O}_4^{(2)} \\
 & - \frac{N_f \left(44\pi [\gamma_0^{\mathcal{B}}]_3^{(2)} - 1362N^3 + 242N \right) + 14N \left(4\pi [\gamma_0^{\mathcal{B}}]_2^{(2)} - 4\pi [\gamma_0^{\mathcal{B}}]_3^{(2)} + 190N^3 + 314N \right)}{24N \left(N_f (681N^2 - 121) + 7 \left(4\pi [\gamma_0^{\mathcal{B}}]_2^{(2)} - 4\pi [\gamma_0^{\mathcal{B}}]_3^{(2)} + 190N^3 + 314N \right) \right)} \mathcal{O}_{18}^{(2)},
 \end{aligned} \tag{6.36}$$

$$\begin{aligned}
 \mathcal{B}_{4,5}^{(2)} = & \mathcal{O}_{19}^{(2)} \\
 & + \frac{(A(N, N_f) - 40N(-4N_f N + 9N^2 + 2))^2 - B_-^2(N, N_f)}{7299072000N^4(N^2 - 1)} \\
 & \times \{A(N, N_f) + 40N(-4N_f N + 9N^2 + 2) \mp B_+(N, N_f)\} \mathcal{O}_{13}^{(2)} \\
 & + \frac{\mathcal{O}_{14}^{(2)}}{80289792000N^4(N^4 - 5N^2 + 4)} \left\{ A^3(N, N_f)(8N_f N - 11N^2 + 4) \right. \\
 & + 40A^2(N, N_f)N(N^2((4N_f - 9N)(8N_f - 11N) + 778) - 800) \\
 & + A(N, N_f)[B_-^2(N, N_f)(-8N_f N + 11N^2 - 4) \\
 & - 1600N^2(4N_f N - 9N^2 - 2)(N^2((4N_f - 9N)(8N_f - 11N) + 1570) - 1592)] \\
 & + 40N[B_-^2(N, N_f)(N^2((4N_f - 9N)(8N_f - 11N) + 778) - 800) \\
 & - 1600N^2(N\{512N_f^4 N^3 - 64N_f^3 N^2(65N^2 + 8) + 48N_f^2 N(261N^4 + 850N^2 - 792) \\
 & - 4N_f(9N^2 + 2)(459N^4 + 4782N^2 - 4768) \\
 & + 27N^3(297N^4 + 7218N^2 + 42476) - 2585432N\} + 1244992)] \\
 & \pm B_+(N, N_f)[A^2(N, N_f)(-8N_f N + 11N^2 - 4) \\
 & - 80A(N, N_f)N(N^2((4N_f - 9N)(8N_f - 11N) + 778) - 800) \\
 & + B_-^2(N, N_f)(8N_f N - 11N^2 + 4) \\
 & \left. - 1600N^2(4N_f N - 9N^2 - 2)(N^2((4N_f - 9N)(8N_f - 11N) + 1570) - 1592)] \right\} \\
 & + \frac{\mathcal{O}_{18}^{(2)}}{1824768000N^3(N^4 - 5N^2 + 4)} \left\{ A^3(N, N_f) - 40A^2(N, N_f)N(-4N_f N + 9N^2 + 2) \right. \\
 & - A(N, N_f)B_-^2(N, N_f) - 40B_-^2(N, N_f)N(-4N_f N + 9N^2 + 2) \\
 & - 1600A(N, N_f)N^2(N(16N_f^2 N - 8N_f(9N^2 + 2) + 81N^3 + 1620N) - 1580) \\
 & + 64000N^3[54(8N_f^2 + 273)N^4 + 16N_f(369 - 4N_f^2)N^3 \\
 & + 12(8N_f^2 - 1443)N^2 - 972N_f N^5 - 6384N_f N + 729N^6 + 3176] \\
 & \pm B_+(N, N_f)[-A^2(N, N_f) + 80A(N, N_f)N(-4N_f N + 9N^2 + 2) + B_-^2(N, N_f) \\
 & \left. - 1600N^2(N(16N_f^2 N - 8N_f(9N^2 + 2) + 81N^3 + 1620N) - 1580)] \right\},
 \end{aligned} \tag{6.37}$$

$$\begin{aligned}
 \mathcal{B}_{6,7}^{(2)} = & \mathcal{O}_{19}^{(2)} \\
 & - \frac{(A(N, N_f) + 40N(-4N_f N + 9N^2 + 2))^2 - B_+^2(N, N_f)}{7299072000N^4(N^2 - 1)}
 \end{aligned}$$

$$\begin{aligned}
 & \times \left\{ A(N, N_f) - 40N(-4N_f N + 9N^2 + 2) \pm B_-(N, N_f) \right\} \mathcal{O}_{13}^{(2)} \\
 & + \frac{\mathcal{O}_{14}^{(2)}}{80289792000N^4(N^4 - 5N^2 + 4)} \left\{ A^3(N, N_f)(-8N_f N + 11N^2 - 4) \right. \\
 & \quad + 40A^2(N, N_f)N(N^2((4N_f - 9N)(8N_f - 11N) + 778) - 800) \\
 & \quad + A(N, N_f) \left[B_+^2(N, N_f)(8N_f N - 11N^2 + 4) \right. \\
 & \quad + 1600N^2(N^2((4N_f - 9N)(8N_f - 11N) + 1570) - 1592)(4N_f N - 9N^2 - 2) \left. \right] \\
 & \quad + 40N \left[B_+^2(N, N_f)(N^2((4N_f - 9N)(8N_f - 11N) + 778) - 800) \right. \\
 & \quad - 1600N^2 \left(N \left\{ 512N_f^4 N^3 - 64N_f^3 N^2(65N^2 + 8) + 48N_f^2 N(261N^4 + 850N^2 - 792) \right. \right. \\
 & \quad - 4N_f(9N^2 + 2)(459N^4 + 4782N^2 - 4768) \\
 & \quad \left. \left. + 27N^3(297N^4 + 7218N^2 + 42476) - 2585432N \right\} + 1244992 \right) \left. \right] \\
 & \quad \pm B_-(N, N_f) \left[A^2(N, N_f)(-8N_f N + 11N^2 - 4) \right. \\
 & \quad + 80A(N, N_f)N(N^2((4N_f - 9N)(8N_f - 11N) + 778) - 800) \\
 & \quad + B_+^2(N, N_f)(8N_f N - 11N^2 + 4) \\
 & \quad \left. \left. - 1600N^2(4N_f N - 9N^2 - 2)(N^2((4N_f - 9N)(8N_f - 11N) + 1570) - 1592) \right] \right\} \\
 & - \frac{\mathcal{O}_{18}^{(2)}}{1824768000N^3(N^4 - 5N^2 + 4)} \left\{ A^3(N, N_f) + 40A^2(N, N_f)N(9N^2 - 4N_f N + 2) \right. \\
 & \quad - A(N, N_f)B_+^2(N, N_f) + 40B_+^2(N, N_f)N(-4N_f N + 9N^2 + 2) \\
 & \quad - 1600A(N, N_f)N^2(N(16N_f^2 N - 8N_f(9N^2 + 2) + 81N^3 + 1620N) - 1580) \\
 & \quad - 64000N^3 \left[54(8N_f^2 + 273)N^4 + 16N_f(369 - 4N_f^2)N^3 \right. \\
 & \quad \left. + 12(8N_f^2 - 1443)N^2 - 972N_f N^5 - 6384N_f N + 729N^6 + 3176 \right] \\
 & \quad \pm B_-(N, N_f) \left[A^2(N, N_f) + 80A(N, N_f)N(-4N_f N + 9N^2 + 2) - B_+^2(N, N_f) \right. \\
 & \quad \left. \left. + 1600N^2(N(16N_f^2 N - 8N_f(9N^2 + 2) + 81N^3 + 1620N) - 1580) \right] \right\}, \tag{6.38}
 \end{aligned}$$

where we introduced the additional shorthands

$$C(N, N_f) = 57600N^2 \sqrt[3]{\frac{-8N_f^3(N^4+18N^2-18)N^5-3N_f(297N^8+4467N^6-11784N^4+7676N^2+144)N+240N_f^2(3N^2-4)(N^4+6N^2-6)N^2+10(3N^2-4)(2400N^2+891(N^2-1)N^4-1600)}{+3\sqrt{-3N(N^2-1)}} \sqrt{\frac{256N_f^6N^5(N^4+16N^2-16)-5120N_f^5N^6(3N^2-4)+32N_f^4N^3(101N^8+1604N^6-12956N^4+38544N^2-25600)-1280N_f^3N^2(3N^2-4)(51N^6-397N^4+755N^2+36)+N_f^2N[9801N^{12}+319176N^{10}-4186520N^8+19610432N^6-52327856N^4+81169280N^2-40966912]-20N_f(3N^2-4)[9801N^{10}-154836N^8+938980N^6-2536144N^4+2515200N^2+25600]+N^3(99N^2+1)(99N^4-800N^2+1600)^2}{}} \quad (6.39)$$

$$A(N, N_f) = \sqrt{\frac{\frac{1105920000}{C(N, N_f)}N^4 \left[N^2(4N_f^2(N^4+12N^2-12)+80N_fN(4-3N^2)+3(99N^4+301N^2-800))+1600 \right]}{+\frac{C(N, N_f)}{3}+1600N^2(16N_f^2N^2-8N_f(3N^2+2)N+81N^4+36N^2+484)}} \quad (6.40)$$

$$B_{\pm}(N, N_f) = \sqrt{\frac{-\frac{1105920000}{C(N, N_f)}N^4 \left[(4N_f^2+297)N^6+(48N_f^2+903)N^4-48(N_f^2+50)N^2-240N_fN^5+320N_fN^3+1600 \right]}{-\frac{C(N, N_f)}{3}+3200N^2(16N_f^2N^2-8N_f(3N^2+2)N+81N^4+36N^2+484)} \pm \frac{128000N^3}{A(N, N_f)} \left[-64N_f^3N^3+48N_f^2(3N^2+2)N^2-12N_f(27N^4-192N^2+460)N+729N^6-6642N^4+15012N^2+152 \right]} \quad (6.41)$$

Moving on to the sector of chiral symmetry violating 4-fermion operators we find the 1-loop anomalous dimensions

$$\begin{aligned} 4\pi [\gamma_0^{\mathcal{B}}]_{\mathbf{8}}^{(2)} &= \frac{2N}{3} + \frac{3}{N} - \frac{2N_f}{3}, \\ 4\pi [\gamma_0^{\mathcal{B}}]_{\mathbf{9}}^{(2)} &= \frac{11N}{3} + \frac{3}{N} - \frac{2N_f}{3}, \\ 4\pi [\gamma_0^{\mathcal{B}}]_{\mathbf{10-13}}^{(2)} &= \frac{8N}{3} + \frac{1}{N} - \frac{2N_f}{3} \pm \frac{1}{3} \mp \frac{\sqrt{4N^4-11N^2+16}}{N}. \end{aligned} \quad (6.42)$$

The corresponding diagonal basis is again restricted to massless QCD

$$\mathcal{B}_8^{(2)} = \mathcal{O}_{12}^{(2)} - \mathcal{O}_{11}^{(2)} + \frac{1}{N_f} \left(\mathcal{O}_{18}^{(2)} - \mathcal{O}_{19}^{(2)} \right) + \frac{1}{2N_fN} \left(\mathcal{O}_{14}^{(2)} - \mathcal{O}_{13}^{(2)} \right), \quad (6.43)$$

$$\mathcal{B}_9^{(2)} = \mathcal{O}_{17}^{(2)} - \mathcal{O}_{16}^{(2)} + \frac{1}{2N_fN} \left(\mathcal{O}_{18}^{(2)} - \mathcal{O}_{19}^{(2)} \right) + \frac{N^2-1}{4N_fN^2} \left(\mathcal{O}_{13}^{(2)} - \mathcal{O}_{14}^{(2)} \right), \quad (6.44)$$

$$\begin{aligned} \mathcal{B}_{10}^{(2)} &= 36 \left\{ 16N^{17} + 128N^{16} + N^{15}(8S+94) + 2N^{14}(32S-569) + N^{13}(58S-845) \right. \\ &\quad + N^{12}(6200-481S) + N^{11}(1606-336S) + N^{10}(2280S-20038) + N^9(422S+4771) \\ &\quad + N^8(40814-6479S) + N^7(3310S-31178) + 4N^6(2219S-9544) + N^5(58129-10140S) \\ &\quad + N^4(740-3225S) + 92N^3(145S-511) + N^2(40136-10028S) + 4N(886S-3503) \\ &\quad \left. - 484S + 1952 \right\} \left(\mathcal{O}_{11}^{(2)} + \mathcal{O}_{12}^{(2)} \right) \\ &- 18 \left\{ 4N^{16} + 40N^{15} + 2N^{14}(S+36) + N^{13}(20S-109) + N^{12}(59S-688) \right. \\ &\quad - 12N^{11}(9S-58) + N^{10}(2428-246S) + N^9(348S-2327) + N^8(1031S-5214) \\ &\quad + N^7(8312-1306S) + N^6(3542-1186S) + 3N^5(762S-4255) + N^4(849S+2644) \\ &\quad \left. - 4N^3(771S-3157) + 4N^2(743S-2724) + N(4460-1072S) + 164S-640 \right\} \mathcal{O}_{15}^{(2)} \end{aligned}$$

$$\begin{aligned}
 & - \frac{\mathcal{O}_{16}^{(2)} + \mathcal{O}_{17}^{(2)}}{(N^2 - 1)^4 (N^4 - 2N^3 - 8N^2 - 4N + 4)} N \left\{ (2N^7 + 13N^6 + N^5(S - 12) + N^4(2S - 33) \right. \\
 & \quad + N^3(S + 27) + N^2(54 - 7S) + 4N(4S - 11) - 4(S - 5)) \left\{ 2N^7 - 13N^6 + N^5(S - 12) \right. \\
 & \quad + N^4(33 - 2S) + N^3(S + 27) + N^2(7S - 54) + 4N(4S - 11) + 4(S - 5) \left\{ 2N^7 - 13N^6 \right. \\
 & \quad - N^5(S + 12) + N^4(2S + 33) - N^3(S - 27) - N^2(7S + 54) - 4N(4S + 11) - 4(S + 5) \left\{ \right. \\
 & \quad \left. \left\{ 4N^8 + 24N^7 + 2N^6(S + 10) + 12N^5(S - 9) + 6N^4(S - 8) - 3N^3(8S - 75) + N^2(74 - 9S) \right. \right. \\
 & \quad \left. \left. + 6N(11S - 37) - 26S + 112 \right\} \right. \\
 & \quad + 36N(N + 1) \left\{ 8N^{15} + 58N^{14} + N^{13}(4S + 13) + N^{12}(29S - 520) + 6N^{11}(2S + 7) \right. \\
 & \quad - 6N^{10}(35S - 386) - 5N^9(6S + 191) + N^8(957S - 6188) + N^7(6343 - 566S) \\
 & \quad + N^6(6641 - 1579S) + 3N^5(647S - 4235) + 15N^4(71S + 4) - 4N^3(861S - 3254) \\
 & \quad \left. \left. + 4N^2(744S - 2801) + N(4444 - 1076S) + 164S - 640 \right\} \mathcal{O}_{20}^{(2)}, \tag{6.45} \\
 \mathcal{B}_{11}^{(2)} & = 36 \left\{ 16N^{17} - 128N^{16} + N^{15}(8S + 94) + N^{14}(1138 - 64S) + N^{13}(58S - 845) \right. \\
 & \quad + N^{12}(481S - 6200) + N^{11}(1606 - 336S) + N^{10}(20038 - 2280S) + N^9(422S + 4771) \\
 & \quad + N^8(6479S - 40814) + N^7(3310S - 31178) + N^6(38176 - 8876S) + N^5(58129 - 10140S) \\
 & \quad + 5N^4(645S - 148) + 92N^3(145S - 511) + 4N^2(2507S - 10034) + 4N(886S - 3503) \\
 & \quad \left. + 484S - 1952 \right\} \left(\mathcal{O}_{11}^{(2)} + \mathcal{O}_{12}^{(2)} \right) \\
 & + 18 \left\{ 4N^{16} - 40N^{15} + 2N^{14}(S + 36) + N^{13}(109 - 20S) + N^{12}(59S - 688) + 12N^{11}(9S - 58) \right. \\
 & \quad + N^{10}(2428 - 246S) + N^9(2327 - 348S) + N^8(1031S - 5214) + 2N^7(653S - 4156) \\
 & \quad + N^6(3542 - 1186S) - 3N^5(762S - 4255) + N^4(849S + 2644) + 4N^3(771S - 3157) \\
 & \quad \left. + 4N^2(743S - 2724) + 4N(268S - 1115) + 164S - 640 \right\} \mathcal{O}_{15}^{(2)} \\
 & - \frac{\mathcal{O}_{16}^{(2)} + \mathcal{O}_{17}^{(2)}}{(N^2 - 1)^4 (N^4 + 2N^3 - 8N^2 + 4N + 4)} N \left\{ 2N^7 + 13N^6 + N^5(S - 12) + N^4(2S - 33) \right. \\
 & \quad + N^3(S + 27) + N^2(54 - 7S) + 4N(4S - 11) - 4(S - 5) \left\{ 2N^7 - 13N^6 + N^5(S - 12) \right. \\
 & \quad + N^4(33 - 2S) + N^3(S + 27) + N^2(7S - 54) + 4N(4S - 11) + 4(S - 5) \left\{ 2N^7 + 13N^6 \right. \\
 & \quad - N^5(S + 12) - N^4(2S + 33) - N^3(S - 27) + N^2(7S + 54) - 4N(4S + 11) + 4(S + 5) \left\{ \right. \\
 & \quad \left\{ 4N^8 - 24N^7 + 2N^6(S + 10) - 12N^5(S - 9) + 6N^4(S - 8) + 3N^3(8S - 75) + N^2(74 - 9S) \right. \\
 & \quad \left. \left. + N(222 - 66S) - 26S + 112 \right\} \right. \\
 & \quad - 36(N - 1)N \left\{ 8N^{15} - 58N^{14} + N^{13}(4S + 13) + N^{12}(520 - 29S) + 6N^{11}(2S + 7) \right. \\
 & \quad + 6N^{10}(35S - 386) - 5N^9(6S + 191) + N^8(6188 - 957S) + N^7(6343 - 566S) \\
 & \quad + N^6(1579S - 6641) + 3N^5(647S - 4235) - 15N^4(71S + 4) - 4N^3(861S - 3254) \\
 & \quad \left. \left. - 4N^2(744S - 2801) + N(4444 - 1076S) - 164S + 640 \right\} \mathcal{O}_{20}^{(2)}, \tag{6.46} \\
 \mathcal{B}_{12}^{(2)} & = -36 \left\{ 16N^{17} - 128N^{16} + N^{15}(94 - 8S) + 2N^{14}(32S + 569) - N^{13}(58S + 845) \right. \\
 & \quad - N^{12}(481S + 6200) + 2N^{11}(168S + 803) + N^{10}(2280S + 20038) + N^9(4771 - 422S) \\
 & \quad \left. - N^8(6479S + 40814) - 2N^7(1655S + 15589) + 4N^6(2219S + 9544) + N^5(10140S + 58129) \right.
 \end{aligned}$$

$$\begin{aligned}
 & -5N^4(645S + 148) - 92N^3(145S + 511) - 4N^2(2507S + 10034) - 4N(886S + 3503) \\
 & - 4(121S + 488) \Big\} \left(\mathcal{O}_{11}^{(2)} + \mathcal{O}_{12}^{(2)} \right) \\
 & - 9 \Big\{ E_+(N) - E_-(N) \Big\} \mathcal{O}_{15}^{(2)} \\
 & + \frac{\mathcal{O}_{16}^{(2)} + \mathcal{O}_{17}^{(2)}}{(N^2 - 1)^4 (N^4 + 2N^3 - 8N^2 + 4N + 4)} N \Big\{ 2N^7 + 13N^6 + N^5(S - 12) + N^4(2S - 33) \\
 & + N^3(S + 27) + N^2(54 - 7S) + 4N(4S - 11) - 4(S - 5) \Big\} \Big\{ 2N^7 - 13N^6 - N^5(S + 12) \\
 & + N^4(2S + 33) - N^3(S - 27) - N^2(7S + 54) - 4N(4S + 11) - 4(S + 5) \Big\} \Big\{ 2N^7 + 13N^6 \\
 & - N^5(S + 12) - N^4(2S + 33) - N^3(S - 27) + N^2(7S + 54) - 4N(4S + 11) + 4(S + 5) \Big\} \\
 & \Big\{ 4N^8 - 24N^7 - 2N^6(S - 10) + 12N^5(S + 9) - 6N^4(S + 8) - 3N^3(8S + 75) \\
 & + N^2(9S + 74) + 6N(11S + 37) + 26S + 112 \Big\} \\
 & + 36(N - 1)N \Big\{ 8N^{15} - 58N^{14} + N^{13}(13 - 4S) + N^{12}(29S + 520) - 6N^{11}(2S - 7) \\
 & - 6N^{10}(35S + 386) + 5N^9(6S - 191) + N^8(957S + 6188) + N^7(566S + 6343) \\
 & - N^6(1579S + 6641) - 3N^5(647S + 4235) + 15N^4(71S - 4) + 4N^3(861S + 3254) \\
 & + 4N^2(744S + 2801) + 4N(269S + 1111) + 164S + 640 \Big\} \mathcal{O}_{20}^{(2)} \tag{6.47}
 \end{aligned}$$

$$\begin{aligned}
 \mathcal{B}_{13}^{(2)} = & -36 \Big\{ 16N^{17} + 128N^{16} + N^{15}(94 - 8S) - 2N^{14}(32S + 569) - N^{13}(58S + 845) \\
 & + N^{12}(481S + 6200) + 2N^{11}(168S + 803) - 2N^{10}(1140S + 10019) + N^9(4771 - 422S) \\
 & + N^8(6479S + 40814) - 2N^7(1655S + 15589) - 4N^6(2219S + 9544) + N^5(10140S + 58129) \\
 & + 5N^4(645S + 148) - 92N^3(145S + 511) + 4N^2(2507S + 10034) - 4N(886S + 3503) \\
 & + 484S + 1952 \Big\} \left(\mathcal{O}_{11}^{(2)} + \mathcal{O}_{12}^{(2)} \right) \\
 & + 9 \Big\{ E_+(N) + E_-(N) \Big\} \mathcal{O}_{15}^{(2)} \\
 & + \frac{\mathcal{O}_{16}^{(2)} + \mathcal{O}_{17}^{(2)}}{(N^2 - 1)^4 (N^4 - 2N^3 - 8N^2 - 4N + 4)} N \Big\{ 2N^7 - 13N^6 + N^5(S - 12) + N^4(33 - 2S) \\
 & + N^3(S + 27) + N^2(7S - 54) + 4N(4S - 11) + 4(S - 5) \Big\} \Big\{ 2N^7 - 13N^6 - N^5(S + 12) \\
 & + N^4(2S + 33) - N^3(S - 27) - N^2(7S + 54) - 4N(4S + 11) - 4(S + 5) \Big\} \Big\{ 2N^7 + 13N^6 \\
 & - N^5(S + 12) - N^4(2S + 33) - N^3(S - 27) + N^2(7S + 54) - 4N(4S + 11) + 4(S + 5) \Big\} \\
 & \Big\{ 4N^8 + 24N^7 - 2N^6(S - 10) - 12N^5(S + 9) - 6N^4(S + 8) + 3N^3(8S + 75) \\
 & + N^2(9S + 74) - 6N(11S + 37) + 26S + 112 \Big\} \\
 & - 36N(N + 1) \Big\{ 8N^{15} + 58N^{14} + N^{13}(13 - 4S) - N^{12}(29S + 520) - 6N^{11}(2S - 7) \\
 & + 6N^{10}(35S + 386) + 5N^9(6S - 191) - N^8(957S + 6188) + N^7(566S + 6343) \\
 & + N^6(1579S + 6641) - 3N^5(647S + 4235) - 15N^4(71S - 4) + 4N^3(861S + 3254) \\
 & - 4N^2(744S + 2801) + 4N(269S + 1111) - 4(41S + 160) \Big\} \mathcal{O}_{20}^{(2)}. \tag{6.48}
 \end{aligned}$$

Again new shorthands have been introduced

$$S(N) = \sqrt{4N^4 - 11N^2 + 16}, \quad (6.49)$$

$$\begin{aligned} E_{\pm}(N) = & 4N^{16} - 2N^{14}(S - 36) - N^{12}(59S + 688) + N^{10}(246S + 2428) - N^8(1031S + 5214) \\ & + 2N^6(593S + 1771) + N^4(2644 - 849S) - 4N^2(743S + 2724) - 4(41S + 160) \\ & \pm \left\{ 40N^{15} - N^{13}(20S + 109) + 12N^{11}(9S + 58) - N^9(348S + 2327) + 2N^7(653S + 4156) \right. \\ & \left. - 3N^5(762S + 4255) + 4N^3(771S + 3157) + 4N(268S + 1115) \right\}. \end{aligned} \quad (6.50)$$

The massive operators only mix into the mass-dimension 6 operators which simplifies the determination of the diagonal massive basis, remember that all other operators are still lacking massive mixings,

$$\begin{aligned} \mathcal{B}_{14}^{(2)} &= \frac{\text{tr}(M)}{N_f} \mathcal{B}_1^{(1)}, & \mathcal{B}_{15}^{(2)} &= \frac{\text{tr}(M)^2}{N_f^2} \mathcal{B}_1^{(0)}, & \mathcal{B}_{16}^{(2)} &= \bar{\Psi} M^3 \Psi, \\ \mathcal{B}_{17}^{(2)} &= i\bar{\Psi} \Delta M^1 \sigma_{\mu\nu} F_{\mu\nu} \Psi + \frac{4N_f N}{1 - \hat{\beta}_0 N + N^2} \mathcal{B}_{18}^{(2)} + \frac{6(N^2 - 1)}{1 + N^2} \left\{ \mathcal{B}_{22}^{(2)} + \frac{2N_f}{\hat{\beta}_0} \mathcal{B}_{19}^{(2)} \right\}, \\ \mathcal{B}_{18}^{(2)} &= \frac{\text{tr}(M \Delta M^1)}{N_f} \mathcal{B}_1^{(0)}, & \mathcal{B}_{19}^{(2)} &= \frac{\text{tr}(M \Delta M^1)}{N_f} \bar{\Psi} M \Psi, & \mathcal{B}_{20}^{(2)} &= \frac{\text{tr}(M)^2}{N_f^2} \bar{\Psi} \Delta M^1 \Psi, \\ \mathcal{B}_{21}^{(2)} &= \frac{\text{tr}(M)}{N_f} \bar{\Psi} \Delta M^2 \Psi, & \mathcal{B}_{22}^{(2)} &= \bar{\Psi} M^2 \Delta M^1 \Psi, & \mathcal{B}_{23}^{(2)} &= \bar{\Psi} M \Delta M^2 \Psi, \\ \mathcal{B}_{24}^{(2)} &= \bar{\Psi} \Delta M^3 \Psi \end{aligned} \quad (6.51)$$

with corresponding diagonal entries in the anomalous dimension matrix

$$[\hat{\gamma}_0^{\mathcal{B}}]_{14,17}^{(2)} = \frac{2N^2 - 4}{N\hat{\beta}_0}, \quad [\hat{\gamma}_0^{\mathcal{B}}]_{15,18}^{(2)} = 3 \frac{N^2 - 1}{N\hat{\beta}_0} - 1, \quad [\gamma_0^{\mathcal{B}}]_{16,19-24}^{(2)} = 3 \frac{N^2 - 1}{N\hat{\beta}_0}. \quad (6.52)$$

For completeness we also mention here the unusual case of $N_f = 1$. There all $\Delta M^n \equiv 0$ and only the massive operators $\mathcal{B}_{14}^{(2)}$, $\mathcal{B}_{15}^{(2)}$ and $\mathcal{B}_{16}^{(2)}$ of the “mass-degenerate” case remain. Furthermore we can make use of the Fierz identities from eq. (6.24) such that only 5 linearly independent 4-fermion operators remain in our minimal basis, whose (mass-independent) mixing is contained within eq. (6.26). Again reconstructing the EOM vanishing mixing contributions following eq. (6.29), now shrunk to only one flavour, yields for the massless case (the anomalous

dimensions for mass-dependent operators remain unchanged apart from the degeneracy)

$$4\pi [\gamma_0^{\mathcal{O}}]_{N_f=1}^{(2)} = \left(\begin{array}{cccc|cccc} \frac{7N}{3} + \frac{2}{3} & 0 & 0 & \frac{1}{3N^2} + \frac{N}{3} - \frac{5}{3N} + \frac{1}{12} & \frac{3}{2N^2} + \frac{N}{3} - \frac{5}{3N} + \frac{3}{4} & & & \\ -\frac{7N}{15} & \frac{21N}{5} + \frac{2}{3} & \frac{11}{60N} - \frac{11N}{60} & \frac{73N}{960} - \frac{179}{320N} + \frac{19}{160N^2} + \frac{47}{480} & \frac{1}{2N^2} + \frac{73N}{960} - \frac{179}{320N} + \frac{1}{4} & & & \\ \frac{11}{60} & -\frac{11}{15} & \frac{157N}{60} - \frac{157}{60N} & \frac{7N}{320} - \frac{137}{960N} - \frac{13}{160N^2} + \frac{23}{480} & \frac{1}{8N^2} + \frac{7N}{320} - \frac{27}{320N} + \frac{11}{120} & & & \\ 0 & 0 & 0 & \frac{11N}{3} - \frac{2}{3N} + \frac{7}{6} & \frac{11}{6} - \frac{3}{N} & & & \\ 0 & 0 & 0 & \frac{11}{6} - \frac{11}{3N} & \frac{11N}{3} + \frac{7}{6} & & & \\ 0 & 0 & 0 & \frac{1}{3N} - \frac{1}{6} & -\frac{1}{6} & & & \\ 0 & 0 & 0 & \frac{1}{6} - \frac{1}{3N} & \frac{1}{6} & & & \\ 0 & 0 & 0 & 0 & 0 & & & \\ \frac{5N}{6} - \frac{8}{3N} & \frac{8}{3N} - \frac{5N}{6} & 0 & \frac{2}{3N} - \frac{7N}{12} - \frac{3N}{4\lambda_{\overline{\text{MS}}}} & \frac{23N}{6} - \frac{3N}{2\lambda_{\overline{\text{MS}}}} & & & \\ \frac{167N}{480} - \frac{141}{160N} & \frac{141}{160N} - \frac{167N}{480} & 0 & \frac{19}{80N} - \frac{13N}{240} - \frac{N}{4\lambda_{\overline{\text{MS}}}} & \frac{7N}{15} - \frac{N}{2\lambda_{\overline{\text{MS}}}} & & & \\ \frac{13N}{160} - \frac{53}{160N} - \frac{7}{120} & \frac{53}{160N} - \frac{13N}{160} + \frac{7}{120} & 0 & \frac{3N}{80} - \frac{13}{80N} - \frac{7}{60} & \frac{7}{30} & & & \\ \frac{7}{3} & -\frac{7}{3} & 0 & -\frac{4}{3} & 0 & & & \\ -\frac{11}{3} & \frac{11}{3} & 0 & -\frac{4}{3} & 0 & & & \\ \frac{2N}{3} + \frac{3}{N} + \frac{7}{6} & \frac{7}{6} & \frac{1}{2N} - \frac{1}{4} & \frac{2}{3} & 0 & & & \\ \frac{7}{6} & \frac{2N}{3} + \frac{3}{N} + \frac{7}{6} & \frac{1}{2N} - \frac{1}{4} & -\frac{2}{3} & 0 & & & \\ \frac{12}{N} + 6 & \frac{12}{N} + 6 & \frac{14N}{3} - \frac{1}{N} + \frac{7}{3} & 0 & 0 & & & \\ 0 & \frac{N}{2} - \frac{1}{2N} & \frac{3}{2N} - \frac{3N}{2} & 0 & & & & \\ \frac{11Nc}{240} - \frac{11}{240Nc} & \frac{N^2-1}{6N} & -\frac{71(N^2-1)}{120N} & \frac{11(N^2-1)}{60N} & & & & \\ \frac{97}{240Nc} - \frac{97Nc}{240} & \frac{(\lambda_{\overline{\text{MS}}}+3)(1-N^2)}{12\lambda_{\overline{\text{MS}}}N} & \frac{(53\lambda_{\overline{\text{MS}}}-90)(1-N^2)}{120\lambda_{\overline{\text{MS}}}N} & \frac{83(N^2-1)}{60N} & & & & \\ 0 & 0 & 0 & 0 & & & & \\ 0 & 0 & 0 & 0 & & & & \\ 0 & 0 & 0 & 0 & & & & \\ 0 & 0 & 0 & 0 & & & & \\ 0 & 0 & 0 & 0 & & & & \end{array} \right), \quad (6.53)$$

where the operator basis is chosen as

$$\left\{ \mathcal{O}_2^{(2)}, \mathcal{O}_4^{(2)}, \mathcal{O}_{10}^{(2)}, (\bar{u}\gamma_\mu u)^2, (\bar{u}\gamma_\mu \gamma_5 u)^2, (\bar{u}u)^2, (\bar{u}\gamma_5 u)^2, (\bar{u}\sigma_{\mu\nu} u)^2 \right\}$$

and the EOM vanishing part is given by

$$\left\{ \mathcal{E}_4^{(2)}, \mathcal{E}_2^{(2)}, \mathcal{E}_3^{(2)}, \mathcal{E}_1^{(2)}, \bar{u}M(\gamma_\mu D_\mu + M)^2 u, \bar{u}M^2(\gamma_\mu D_\mu + M)u \right\}.$$

In this case we only report the 1-loop anomalous dimensions in the massless case for later use when plotting the spectra

$$[\gamma_0^{\mathcal{B}}]_{N_f=1}^{(2)} = \left\{ [\gamma_0^{\mathcal{B}}]_1^{(2)}, [\gamma_0^{\mathcal{B}}]_2^{(2)}, [\gamma_0^{\mathcal{B}}]_3^{(2)}, [\gamma_0^{\mathcal{B}}]_4^{(2)}, [\gamma_0^{\mathcal{B}}]_6^{(2)}, [\gamma_0^{\mathcal{B}}]_{10}^{(2)}, [\gamma_0^{\mathcal{B}}]_{13}^{(2)} \right\}_{N_f=1}. \quad (6.54)$$

6.4 Renormalisation of the flavoured 4-fermion operator basis at $N_f = 3$

To further check our routines for computing the 1-loop anomalous dimensions we compute the anomalous dimension matrix for set of single flavour and 2-flavour 4-fermion operators at $N_f = 3$ and compare it to the literature [152, 153].

Starting from the intermediate results in eqs. (6.26) and (6.28) we make a change of basis $\mathcal{E}_4^{u(2)} = \tilde{\mathcal{E}}_2^u - \bar{u}\gamma_\mu T^a u \sum_q \bar{q}\gamma_\mu T^a q$ and analogously for all the other building blocks such that these (flavoured) \mathcal{E} are EOM vanishing. In general there are $5N_f$ single flavour and $5N_f(N_f - 1)$ 2-flavour 4-fermion operators which are linearly independent. This amounts to a total of $5N_f^2$ 4-fermion operators. The $N_f = 3$ anomalous dimension matrix of the 4-fermion operators reads

$$4\pi(\gamma_0^{O \cup Q \cup \mathcal{Q}} - 1\beta_0) = \left(\begin{array}{cccccc|cccc} A & 0 & 0 & 0 & 0 & 0 & B & B & 0 \\ 0 & A & 0 & 0 & 0 & 0 & B & 0 & B \\ 0 & 0 & A & 0 & 0 & 0 & 0 & B & B \\ 0 & 0 & 0 & C & 0 & 0 & D & 0 & 0 \\ 0 & 0 & 0 & 0 & C & 0 & 0 & D & 0 \\ 0 & 0 & 0 & 0 & 0 & C & 0 & 0 & D \\ E & E & 0 & F & 0 & 0 & G & H & H \\ E & 0 & E & 0 & F & 0 & H & G & H \\ 0 & E & E & 0 & 0 & F & H & H & G \end{array} \middle| \begin{array}{ccc} R & 0 & 0 \\ 0 & R & 0 \\ 0 & 0 & R \\ 0 & 0 & 0 \\ 0 & 0 & 0 \\ 0 & 0 & 0 \\ S & S & 0 \\ S & 0 & S \\ 0 & S & S \end{array} \right) \quad (6.55)$$

with basis

$$O \cup Q \cup \mathcal{Q} = g_0^2 \{ (\bar{u}\Gamma u)^2, (\bar{d}\Gamma d)^2, (\bar{s}\Gamma s)^2, (\bar{u}\Gamma u)(\bar{d}\Gamma d), (\bar{u}\Gamma u)(\bar{s}\Gamma s), (\bar{d}\Gamma d)(\bar{s}\Gamma s), (\bar{u}\Gamma T^a u)(\bar{d}\Gamma T^a d), (\bar{u}\Gamma T^a u)(\bar{s}\Gamma T^a s), (\bar{d}\Gamma T^a d)(\bar{s}\Gamma T^a s) \}.$$

The part separated by the vertical line indicates contributions of the EOM-vanishing redundant operators $\{\mathcal{E}_4^{u(2)}, \mathcal{E}_4^{d(2)}, \mathcal{E}_4^{s(2)}\}$. We introduced the submatrices

$$A = \begin{pmatrix} \frac{11}{6} - 3N + \frac{3}{N} & \frac{7}{6} & \frac{1}{3N} - \frac{1}{6} & -\frac{1}{6} & \frac{1}{2N} - \frac{1}{4} \\ \frac{7}{6} & \frac{11}{6} - 3N + \frac{3}{N} & \frac{1}{6} - \frac{1}{3N} & \frac{1}{6} & \frac{1}{2N} - \frac{1}{4} \\ \frac{7}{3} & -\frac{7}{3} & \frac{11}{6} - \frac{2}{3N} & \frac{11}{6} - \frac{3}{N} & 0 \\ -\frac{11}{3} & \frac{11}{3} & \frac{11}{6} - \frac{11}{3N} & \frac{11}{6} & 0 \\ \frac{12}{N} + 6 & \frac{12}{N} + 6 & 0 & 0 & N - \frac{1}{N} + 3 \end{pmatrix}, \quad (6.56)$$

$$B = \begin{pmatrix} 0 & 0 & \frac{2}{3} & 0 & 0 \\ 0 & 0 & -\frac{2}{3} & 0 & 0 \\ 0 & 0 & -\frac{4}{3} & 0 & 0 \\ 0 & 0 & -\frac{4}{3} & 0 & 0 \\ 0 & 0 & 0 & 0 & 0 \end{pmatrix}, \quad C = \begin{pmatrix} \frac{3}{N} - 3N & 0 & 0 & 0 & 0 \\ 0 & \frac{3}{N} - 3N & 0 & 0 & 0 \\ 0 & 0 & 0 & 0 & 0 \\ 0 & 0 & 0 & 0 & 0 \\ 0 & 0 & 0 & 0 & N - \frac{1}{N} \end{pmatrix}, \quad (6.57)$$

$$D = \begin{pmatrix} 0 & 0 & 0 & 0 & 1 \\ 0 & 0 & 0 & 0 & 1 \\ 0 & 0 & 0 & -6 & 0 \\ 0 & 0 & -6 & 0 & 0 \\ 24 & 24 & 0 & 0 & 0 \end{pmatrix}, \quad E = \begin{pmatrix} 0 & 0 & 0 & 0 & 0 \\ 0 & 0 & 0 & 0 & 0 \\ \frac{1}{3} & -\frac{1}{3} & \frac{1}{3N} - \frac{1}{6} & -\frac{1}{6} & 0 \\ 0 & 0 & 0 & 0 & 0 \\ 0 & 0 & 0 & 0 & 0 \end{pmatrix}, \quad (6.58)$$

6.4. Renormalisation of the flavoured 4-fermion operator basis at $N_f = 3$

$$F = \begin{pmatrix} 0 & 0 & 0 & 0 & \frac{1}{4} - \frac{1}{4N^2} \\ 0 & 0 & 0 & 0 & \frac{1}{4} - \frac{1}{4N^2} \\ 0 & 0 & 0 & \frac{3}{2N^2} - \frac{3}{2} & 0 \\ 0 & 0 & \frac{3}{2N^2} - \frac{3}{2} & 0 & 0 \\ 6 - \frac{6}{N^2} & 6 - \frac{6}{N^2} & 0 & 0 & 0 \end{pmatrix}, \quad (6.59)$$

$$G = \begin{pmatrix} \frac{3}{N} & 0 & 0 & 0 & \frac{1}{N} - \frac{N}{4} \\ 0 & \frac{3}{N} & 0 & 0 & \frac{1}{N} - \frac{N}{4} \\ 0 & 0 & \frac{4}{3} - \frac{3N}{2} & \frac{3N}{2} - \frac{6}{N} & 0 \\ 0 & 0 & \frac{3N}{2} - \frac{6}{N} & -\frac{3N}{2} & 0 \\ \frac{24}{N} - 6N & \frac{24}{N} - 6N & 0 & 0 & -2N - \frac{1}{N} \end{pmatrix}, \quad (6.60)$$

$$H = \begin{pmatrix} 0 & 0 & 0 & 0 & 0 \\ 0 & 0 & 0 & 0 & 0 \\ 0 & 0 & \frac{2}{3} & 0 & 0 \\ 0 & 0 & 0 & 0 & 0 \\ 0 & 0 & 0 & 0 & 0 \end{pmatrix}, \quad R = \begin{pmatrix} \frac{2}{3} \\ -\frac{2}{3} \\ -\frac{4}{3} \\ -\frac{4}{3} \\ 0 \end{pmatrix}, \quad S = \begin{pmatrix} 0 \\ 0 \\ \frac{2}{3} \\ 0 \\ 0 \end{pmatrix}. \quad (6.61)$$

The submatrices A - E , G and H agree with the results in [153] while F is missing there. Instead in [152] there are values for $N = 3$ that agree as well. In the comparison with [152, 153], one should take into account that we use anti-hermitian rather than hermitian generators T^a and that the normalisation in our conventions differs by an overall factor of 2.

For completeness we also give the full anomalous dimension matrix when using the change of basis from eqs. (6.29)

$$4\pi(\gamma_0^{4\text{-ferm}} - \mathbb{1}\beta_0) = \left(\begin{array}{cc|cccccccc|ccc} \boxed{C} & \boxed{B'} & 0 & 0 & 0 & 0 & 0 & 0 & 0 & 0 & R & 0 & 0 \\ \boxed{F} & \boxed{I} & 0 & 0 & 0 & 0 & 0 & 0 & 0 & 0 & T & 0 & 0 \\ 0 & B & J & 0 & 0 & 0 & 0 & 0 & 0 & 0 & R & 0 & 0 \\ 0 & B/2 & K & A & 0 & 0 & 0 & B & 0 & 0 & R & -R & 0 \\ 0 & B/2 & K & 0 & A & 0 & 0 & 0 & B & 0 & 0 & R & R \\ 0 & 0 & 0 & 0 & 0 & C & 0 & D & 0 & 0 & 0 & 0 & 0 \\ 0 & 0 & 0 & 0 & 0 & 0 & C & 0 & D & 0 & 0 & 0 & 0 \\ 0 & H/2 & -E/2 & E & 0 & F & 0 & G' & 0 & 0 & S & -S & 0 \\ 0 & H/2 & -E/2 & 0 & E & 0 & F & 0 & G' & 0 & 0 & S & S \end{array} \right) \quad (6.62)$$

with basis

$$\begin{aligned} 4\text{-ferm} : & \ g_0^2 \{ (\bar{\Psi}\Gamma\Psi)^2, (\bar{\Psi}\Gamma T^a\Psi)^2, \sum_q (\bar{q}\Gamma q)^2, (\bar{u}\Gamma u)^2 + (\bar{s}\Gamma s)^2, (\bar{d}\Gamma d)^2 + (\bar{s}\Gamma s)^2, \\ & (\bar{u}\Gamma u)(\bar{s}\Gamma s), (\bar{d}\Gamma d)(\bar{s}\Gamma s), (\bar{u}\Gamma T^a u)(\bar{s}\Gamma T^a s), (\bar{d}\Gamma T^a d)(\bar{s}\Gamma T^a s) \} \end{aligned}$$

and additional submatrices

$$B' = B + D, \quad G' = G - H, \quad (6.63)$$

$$I = \begin{pmatrix} \frac{3}{N} & 0 & \frac{1}{3N} & 0 & \frac{1}{N} - \frac{N}{4} \\ 0 & \frac{3}{N} & -\frac{1}{3N} & 0 & \frac{1}{N} - \frac{N}{4} \\ 0 & 0 & 4 - \frac{3N}{2} - \frac{2}{3N} & \frac{3N}{2} - \frac{6}{N} & 0 \\ 0 & 0 & \frac{3N}{2} - \frac{20}{3N} & -\frac{3N}{2} & 0 \\ \frac{24}{N} - 6N & \frac{24}{N} - 6N & 0 & 0 & -2N - \frac{1}{N} \end{pmatrix}, \quad (6.64)$$

$$J = \begin{pmatrix} \frac{3}{2} - 3N + \frac{3}{N} & \frac{3}{2} & 0 & 0 & \frac{1}{2N} - \frac{1}{4} \\ \frac{3}{2} & \frac{3}{2} - 3N + \frac{3}{N} & 0 & 0 & \frac{1}{2N} - \frac{1}{4} \\ 3 & -3 & \frac{3}{2} & \frac{3}{2} - \frac{3}{N} & 0 \\ -3 & 3 & \frac{3}{2} - \frac{3}{N} & \frac{3}{2} & 0 \\ \frac{12}{N} + 6 & \frac{12}{N} + 6 & 0 & 0 & N - \frac{1}{N} + 3 \end{pmatrix}, \quad (6.65)$$

$$K = \begin{pmatrix} -\frac{1}{6} & \frac{1}{6} & \frac{1}{12} - \frac{1}{6N} & \frac{1}{12} & 0 \\ \frac{1}{6} & -\frac{1}{6} & \frac{1}{6N} - \frac{1}{12} & -\frac{1}{12} & 0 \\ \frac{1}{3} & -\frac{1}{3} & \frac{1}{3N} - \frac{1}{6} & -\frac{1}{6} & 0 \\ \frac{1}{3} & -\frac{1}{3} & \frac{1}{3N} - \frac{1}{6} & -\frac{1}{6} & 0 \\ 0 & 0 & 0 & 0 & 0 \end{pmatrix}, \quad T = \begin{pmatrix} \frac{1}{3N} \\ -\frac{1}{3N} \\ 4 - \frac{2}{3N} \\ -\frac{2}{3N} \\ 0 \end{pmatrix}. \quad (6.66)$$

The set of EOM-vanishing operators has been changed to $\{\mathcal{E}_4^{(2)}, \mathcal{E}_4^{\text{d}(2)}, \mathcal{E}_4^{\text{s}(2)}\}$ as well following eq. (6.29c). The blue box in eq. (6.62) marks the part relevant for the SET compatible with $\text{SU}(N_f)_V$ flavour symmetry, which is only a small fraction of the mixing matrix of 4-fermion operators at $N_f = 3$.

Chapter 7

Yang-Mills Gradient flow

The Gradient flow (GF) has become increasingly popular in lattice QCD. Its application ranges from scale setting [155–157] over defining a non-perturbative coupling [155, 158] to composite operator renormalisation [159]. One particularly interesting application, from a theoretical point of view, is the small flow-time expansion, see e.g. [160, 161]. The Yang-Mills Gradient flow is defined through the differential equation

$$\partial_t B_\mu(t, x) = D_\nu G_{\nu\mu}(t, x), \quad B_\mu(0, x) = A_\mu(x), \quad t \geq 0, \quad (7.1)$$

where the initial condition relates the flowed field with the fundamental gauge field, and $G_{\mu\nu}$ is the flowed field strength tensor

$$G_{\mu\nu}(t, x) = \partial_\mu B_\nu(t, x) - \partial_\nu B_\mu(t, x) + [B_\mu(t, x), B_\nu(t, x)]. \quad (7.2)$$

One remarkable property of the Yang-Mills Gradient flow is that operators formed of flowed fields at flow-time $t > 0$ do not require renormalisation after the bare coupling and bare mass have been expressed in terms of their renormalised counterparts [160]. As a consequence any lattice artifacts originating from the flow-time integration at $t > 0$ can be treated classically and only contributions from the QCD boundary at $t = 0$ require additional renormalisation, thus having a non-zero anomalous dimension.

Since the Gradient flow corresponds at leading order in perturbation theory to a Gaussian smearing [155] with radius $\sqrt{8t}$, flowed fields are non-local which negates the applicability of Symanzik effective theory. To circumvent this one can switch to a $4 + 1$ dimensional formulation, where the fifth dimension is the flow-time $t \in [0, \infty[$, resulting in the action [160]

$$S_{\text{GF}} = S_{\text{QCD}} + S_{\text{flow}}, \quad S_{\text{QCD}} = \int d^4x \mathcal{L}_{\text{QCD}}(x), \quad (7.3)$$

$$S_{\text{flow}} = -2 \int_0^\infty dt \int d^4x \operatorname{tr} (L_\mu(t, x) [\partial_t B_\mu(t, x) - D_\nu G_{\nu\mu}(t, x)]), \quad (7.4)$$

where $L_\mu(t, x)$ is an algebra-valued Lagrange multiplier. When $L_\mu(t, x)$ is integrated out it enforces that

$$\partial_t B_\mu(t, x) - D_\nu G_{\nu\mu}(t, x) \equiv 0 \quad \forall t \geq 0, x, \quad (7.5)$$

such that $B_\mu(t, x)$ complies with the flow equation (7.1), which acts as an additional EOM.

Due to the modification of the action the gluonic EOM is modified as well [162]

$$\frac{1}{g_0^2} (D_\nu F_{\nu\mu})^a(x) = \bar{\Psi}(x) \gamma_\mu T^a \Psi(x) - L_\mu^a(0, x). \quad (7.6)$$

Furthermore there is the Lagrange multiplier L_μ with $[L_\mu] = 3$ that can be used to build additional operators. This requires a careful re-examination of the reduction of the operator basis in section 5.2 as well as the inclusion of some completely new operators.

7.1 Operator basis

Since $[L_\mu] = 3$ the number of additionally allowed operators is fairly limited. For purely gluonic operators the list has already been worked out in pure gauge theory [162] and we give here only the new operators with mass dimension 6 missing in eq. (5.29)

$$\begin{aligned}\mathcal{O}_{32}^{(2)} &= g_0^2 \operatorname{tr}(L_\mu L_\mu)|_{t=0}, & \mathcal{O}_{33}^{(2)} &= \operatorname{tr}(L_\mu D_\nu G_{\nu\mu})|_{t=0}, \\ \mathcal{O}_{34}^{(2)} &= \operatorname{tr}(L_\mu \partial_t B_\mu)|_{t=0}, & \mathcal{O}_{35}^{(2)} &= \frac{1}{g_0^2} \partial_t \operatorname{tr}(G_{\mu\nu} G_{\mu\nu})|_{t=0}.\end{aligned}\quad (7.7)$$

Furthermore there are two additional 2-fermion operators

$$\mathcal{O}_{36}^{(2)} = \bar{\Psi} \gamma_\mu \partial_t B_\mu \Psi|_{t=0}, \quad \mathcal{O}_{37}^{(2)} = g_0^2 \bar{\Psi} \gamma_\mu L_\mu \Psi|_{t=0}. \quad (7.8)$$

Making use of the flow equation (7.1) and the initial condition at $t = 0$ we find

$$\mathcal{O}_{34}^{(2)} \stackrel{\text{EOM}}{=} \mathcal{O}_{33}^{(2)}, \quad (7.9)$$

$$\begin{aligned}\mathcal{O}_{35}^{(2)} &\stackrel{\text{EOM}}{=} \frac{2}{g_0^2} \operatorname{tr}(G_{\mu\nu} [D_\mu D_\rho G_{\rho\nu} - D_\nu D_\rho G_{\rho\mu}])|_{t=0} \\ &\stackrel{\text{IBP}}{=} \frac{4}{g_0^2} [\partial_\mu \operatorname{tr}(G_{\mu\nu} D_\rho G_{\rho\nu}) - \operatorname{tr}(D_\mu G_{\mu\rho} D_\nu G_{\nu\rho})]|_{t=0} \\ &= \frac{4}{g_0^2} \partial_\mu \operatorname{tr}(F_{\mu\nu} D_\rho F_{\rho\nu}) - 4\mathcal{O}_3^{(2)},\end{aligned}\quad (7.10)$$

$$\mathcal{O}_{36}^{(2)} \stackrel{\text{EOM}}{=} \mathcal{O}_8^{(2)}. \quad (7.11)$$

The modified gluonic EOM (7.6) yields

$$\mathcal{O}_{32}^{(2)} \stackrel{\text{EOM}}{=} -\mathcal{O}_{33}^{(2)} - \frac{1}{2} \sum_{f=1}^{N_f} \mathcal{O}_{37}^{f(2)}, \quad (7.12)$$

$$\mathcal{O}_{33}^{(2)} \stackrel{\text{EOM}}{=} -\mathcal{O}_3^{(2)} - \frac{1}{2} \sum_f \mathcal{O}_8^{f(2)}, \quad (7.13)$$

$$\mathcal{O}_{37}^{f(2)} \stackrel{\text{EOM}}{=} -\mathcal{O}_8^{f(2)} + \sum_e \mathcal{O}_{18}^{ef(2)}. \quad (7.14)$$

Thus two additional operators (assuming mass-degenerate flavours) are needed for full QCD with unflowed quark fields. For pure gauge theory only one additional operator is needed as has been worked out in [162]. We limit ourselves to the case of pure gauge theory and choose $\mathcal{O}_3^{(2)}$ as the one additional operator for our minimal basis.

7.2 Strategy

To compute the missing anomalous dimension of $\mathcal{O}_3^{(2)}$ and its mixing with the other operators we have to consider a matrix element with insertion of these operators containing a quantity at positive flow-time. Otherwise the matrix elements vanish according to the EOM of pure gauge theory. The occurring flow-time integrals invalidate the previous implementation of collecting only UV-poles as integrating these integrals out prematurely introduces propagators of the form $1/(kp)$ with loop momentum k that invalidates use of eqs. (6.5) and (6.6). We therefore switch towards computing full 1-loop matrix elements. Combined with the contributions from the 1-loop matching coefficients this corresponds to the 1-loop contribution in fixed order perturbation theory to the lattice artifacts of the matrix element. For full 1-loop Renormalisation Group improvement

one would require the 2-loop anomalous dimension. Nonetheless it is useful to compute a matrix element of a commonly used quantity.

One particularly famous quantity in the Gradient flow is the action density

$$E(t, x) = -\frac{1}{2} \text{tr} (G_{\mu\nu}(t, x) G_{\mu\nu}(t, x)), \quad (7.15)$$

which has been used extensively for scale setting [155–157]

$$t^2 \langle E(t) \rangle \Big|_{t=t_c} = c \quad \text{or} \quad t \frac{dt^2 \langle E(t) \rangle}{dt} \Big|_{t=w_c^2} = c, \quad (7.16)$$

with typical choices of $c \in \{0.2, 0.3, 2/3\}$ as well as to define the non-perturbative GF coupling [155]

$$\alpha_{\text{GF}}(\mu) = \frac{32\pi t^2 \langle E(t) \rangle}{3(N^2 - 1)} \quad (7.17)$$

with renormalisation scale $\mu = 1/\sqrt{8t}$ and continuum normalisation factor.

Then, the required matrix elements for the 1-loop lattice artifacts are

$$\int d^4y \langle E(t, x) \mathcal{O}_{i;\overline{\text{MS}}}^{(2)}(y) \rangle = Z_{ij} \int d^4y \langle E(t, x) \mathcal{O}_j^{(2)}(y) \rangle, \quad (7.18)$$

or expressed in terms of momentum space quantities

$$\int_p \langle \tilde{E}(t, p) \tilde{\mathcal{O}}_{i;\overline{\text{MS}}}^{(2)}(0) \rangle e^{ipx} = Z_{ij} \int_p \langle \tilde{E}(t, p) \tilde{\mathcal{O}}_j^{(2)}(0) \rangle e^{ipx}. \quad (7.19)$$

Due to translational invariance the overall momentum integral in eq. (7.19) projects $\tilde{E}(t, p)$ to zero momentum and the overall computation amounts to the computation of vacuum bubbles, where the LO contribution is a trivial 1-loop integral, but the 2-loop integrals needed at NLO are more complicated, see figure 7.1 for some examples. In the following we will explain how to treat the encountered integrals, first for the insertion of an $O(4)$ invariant operator (or unity) and then for the more complicated case of an $O(4)$ symmetry breaking operator. At 1-loop we can reduce the number of flow-time integrals to be evaluated to at most one through integration by parts. Each remaining flow-time integral is kept until the momentum integrals have been computed. We then switch to *Mathematica* to evaluate the flow-time integrals and perform the asymptotic expansion in ϵ making use of the *HypExp* package [163, 164] to handle the occurring hypergeometric functions.

7.2.1 Insertion of an $O(4)$ invariant operator

For $O(4)$ invariant operators we only encounter momentum integrals of the following form

$$\mathcal{F}([a, l], [b, m], [c, n]) = \int_{p, q} [p^2]^l [q^2]^m [(p+q)^2]^n \exp(-ap^2 - bq^2 - c(p+q)^2), \quad l, m, n \in \mathbb{Z}, \quad (7.20)$$

where we use the square brackets on the left hand side to indicate that both values belong together. The function \mathcal{F} is then symmetric since we can always exchange p , q and $(p+q)$ through fitting substitutions, e.g.,

$$\left. \begin{matrix} u = p + q \\ v = -q \end{matrix} \right\} \Leftrightarrow \left\{ \begin{matrix} p = u + v \\ q = -v \end{matrix} \right., \quad d^D u d^D v = (-1)^D d^D p d^D q. \quad (7.21)$$

Before continuing with the reduction of the momentum integrals we consider the additionally occurring flow-time integrals. Firstly, there is the iterated flow-time integral (needed for graphs

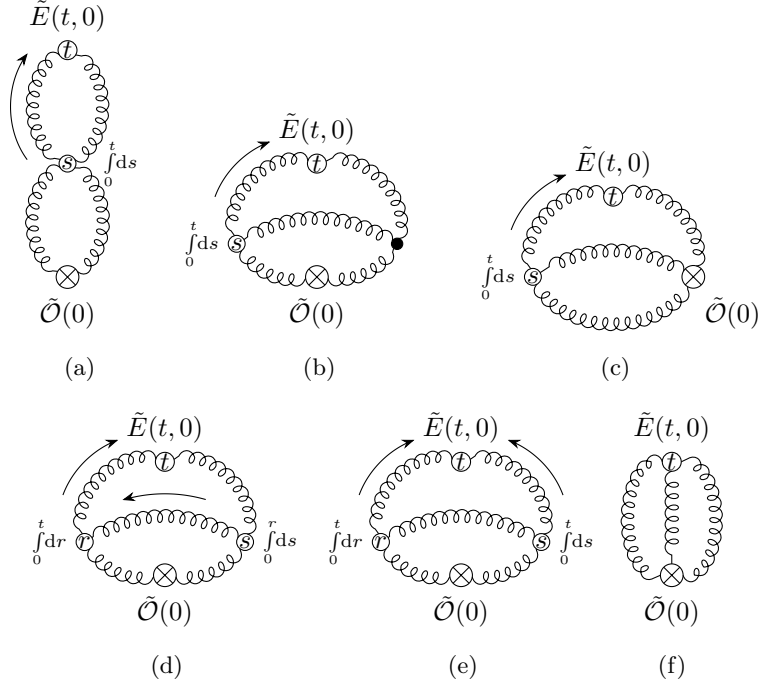


Figure 7.1: Some examples of graphs contributing to $\langle \tilde{E}(t, 0) \tilde{\mathcal{O}}(0) \rangle$ at next-to-leading order. Filled circles are located at flow-time zero as the crossed dots (\otimes), where the latter correspond to vertices of an insertion of the operator $\tilde{\mathcal{O}}(0)$. Gluon lines with an additional arrow are the flow propagators pointing into increasing flow-time.

such as fig. 7.1d)

$$\int_0^t dr \int_0^r ds e^{-(r+s)p^2 - (r-s)B} = \int_0^t dr \int_0^r du e^{-(2r-u)p^2 - uB}, \quad u = r - s, du = -ds \quad (7.22)$$

$$= -\frac{1}{2p^2} \int_0^t dr \partial_r e^{-2rp^2} \int_0^r du e^{-u(B-p^2)} \quad (7.23)$$

$$= -\frac{e^{-2tp^2}}{2p^2} \int_0^t du e^{-u(B-p^2)} + \frac{1}{2p^2} \int_0^t dr e^{-r(p^2+B)}, \quad (7.24)$$

where the chosen flow-time dependence reflects, here and in the following, the only occurring cases and B is a linear combination of p^2 , q^2 and $(p+q)^2$. Thus we can reduce the iterated flow-time integral into an integral of only one flow-time without introducing any new type of denominator like e.g. (pq) . Secondly, there is the case of two independent flow-time integrals (needed for graphs such as fig. 7.1e)

$$\int_0^t dr \int_0^t ds f(r+s) = t \int_0^t ds f(t+s) - \int_0^t dr \int_0^t ds r \partial_r f(r+s) \quad (7.25)$$

$$= t \int_0^t ds f(t+s) - \int_0^t dr r [f(r+t) - f(r)]. \quad (7.26)$$

Having now reduced all flow-time integrals to at most one single integral we come to a more general case, which is most interesting for the momentum integrals, (needed for the simplified integrals from eqs. (7.24) and (7.26) as well as for graphs such as figs. 7.1a, 7.1b and 7.1c)

$$I = \int_0^t ds s^k [p^2]^l [q^2]^{-\tilde{m}} [(p+q)^2]^{-\tilde{n}} e^{-a(s)p^2 - b(s)q^2 - c(s)(p+q)^2}, \quad l, \tilde{m}, \tilde{n} \in \mathbb{N}, \quad \partial_s a(s) = \text{const.} \neq 0. \quad (7.27)$$

The latter integral can be used to reduce the overall powers of momenta via integration by parts

$$I = -\frac{1}{\partial_s a(s)} \int_0^t ds s^k [p^2]^{l-1} [q^2]^{-\tilde{m}} [(p+q)^2]^{-\tilde{n}} \left[\delta(s-t) - \delta(s) - \frac{k}{s} + \partial_s b(s)q^2 + \partial_s c(s)(p+q)^2 \right] \times e^{-a(s)p^2 - b(s)q^2 - c(s)(p+q)^2}, \quad (7.28)$$

which can be iterated until the initial condition $l, \tilde{m}, \tilde{n} \in \mathbb{N}$ no longer applies.

Eventually we can introduce Schwinger parameters

$$[p^2]^l = (-\partial_\alpha)^l e^{-\alpha p^2} \Big|_{\alpha=0}, \quad [p^2]^{-l} = \int_0^\infty d\alpha \frac{\alpha^{l-1}}{\Gamma(l)} e^{-\alpha p^2}, \quad l \in \mathbb{N}, \quad (7.29)$$

to absorb the remaining powers of p^2 , q^2 and $(p+q)^2$. Notice that for dimensional reasons we will only encounter at most two different denominators.

In most cases the resulting Gaussian integral can be simply integrated out

$$\int_{p,q} e^{-ap^2 - bq^2 - c(p+q)^2} = (4\pi)^{-D} [ab + ac + bc]^{-D/2}, \quad (a \neq 0 \wedge b \neq 0) \vee (a \neq 0 \wedge c \neq 0) \vee (b \neq 0 \wedge c \neq 0), \quad (7.30)$$

whereas two of the coefficients a, b, c being zero yields scaleless integrals vanishing in dimensional regularisation except for the combination $(l, m \in \mathbb{N}, n \in \mathbb{N} \cup \{0\})$

$$\begin{aligned} \int_{p,q} \frac{[(p+q)^2]^n}{[p^2]^l [q^2]^m} e^{-c(p+q)^2} &= \frac{\Gamma(l+m)}{\Gamma(l)\Gamma(m)} (-\partial_c)^n \int_0^1 dx \int_{p,q} \frac{(1-x)^{l-1} x^{m-1}}{[(1-x)p^2 + xq^2]^{l+m}} e^{-c(p+q)^2} \\ &= \frac{\Gamma(l+m)}{\Gamma(l)\Gamma(m)} (-\partial_c)^n \int_0^1 dx \int_{p,q} \frac{(1-x)^{l-1} x^{m-1}}{[p^2 + xq^2 - 2xp \cdot q]^{l+m}} e^{-cq^2} \\ &= \frac{\Gamma(l+m)}{\Gamma(l)\Gamma(m)} (-\partial_c)^n \int_0^1 dx \int_{p,q} \frac{(1-x)^{l-1} x^{m-1}}{[p^2 + x(1-x)q^2]^{l+m}} e^{-cq^2} \\ &= \frac{1}{(4\pi)^{D/2}} \frac{\Gamma(l+m-D/2)}{\Gamma(l)\Gamma(m)} (-\partial_c)^n \int_0^1 dx \int_q (1-x)^{l-1} x^{m-1} [x(1-x)q^2]^{D/2-l-m} e^{-cq^2} \\ &= \frac{1}{(4\pi)^{D/2}} \frac{\Gamma(l+m-D/2)\Gamma(D/2-m)\Gamma(D/2-l)}{\Gamma(l)\Gamma(m)\Gamma(D-l-m)} \int_q [q^2]^{D/2+n-l-m} e^{-cq^2} \\ &= \frac{c^{l+m-n-D}}{(4\pi)^D} \frac{\Gamma(l+m-D/2)\Gamma(D/2-m)\Gamma(D/2-l)\Gamma(D-l-m+n)}{\Gamma(l)\Gamma(m)\Gamma(D-l-m)\Gamma(D/2)}. \end{aligned} \quad (7.31)$$

7.2.2 Insertion of an O(4) broken operator

The generalisation to the case of O(4) symmetry violating integrals can now be worked out through use of equation (7.30)

$$\begin{aligned}
 \sum_{\mu} \int_{p,q} p_{\mu}^4 e^{-ap^2 - bq^2 - c(p+q)^2} &= \frac{1}{(4\pi)^D} [ab + ac + bc]^{(1-D)/2} \sum_{\mu} \partial_{a_{\mu}}^2 [a_{\mu}b + a_{\mu}c + bc]^{-1/2} \Big|_{a_{\mu}=a} \\
 &= \frac{D}{(4\pi)^D} \frac{[b+c]^2}{[ab + ac + bc]^{D/2+2}} \\
 &= \frac{3}{D+2} \partial_a^2 \int_{p,q} e^{-ap^2 - bq^2 - c(p+q)^2}, \tag{7.32}
 \end{aligned}$$

$$\begin{aligned}
 \sum_{\mu} \int_{p,q} p_{\mu}^3 q_{\mu} e^{-ap^2 - bq^2 - c(p+q)^2} &= \frac{[ab + ac + bc]^{(1-D)/2}}{2(4\pi)^D} \sum_{\mu} \partial_{a_{\mu}} (\partial_{c_{\mu}} - \partial_{a_{\mu}} - \partial_{b_{\mu}}) [a_{\mu}b_{\mu} + a_{\mu}c + b_{\mu}c_{\mu}]^{-1/2} \Big|_{\substack{a_{\mu}=a \\ b_{\mu}=b \\ c_{\mu}=c}} \\
 &= -\frac{3D}{4(4\pi)^D} \frac{(b+c)c}{[ab + ac + bc]^{D/2+2}} \\
 &= \frac{3}{2(D+2)} \partial_a (\partial_c - \partial_a - \partial_b) \int_{p,q} e^{-ap^2 - bq^2 - c(p+q)^2}, \tag{7.33}
 \end{aligned}$$

$$\begin{aligned}
 \sum_{\mu} \int_{p,q} p_{\mu}^2 q_{\mu}^2 e^{-ap^2 - bq^2 - c(p+q)^2} &= \frac{1}{(4\pi)^D} [ab + ac + bc]^{(1-D)/2} \sum_{\mu} \partial_{a_{\mu}} \partial_{b_{\mu}} [a_{\mu}b_{\mu} + a_{\mu}c + b_{\mu}c]^{-1/2} \Big|_{\substack{a_{\mu}=a \\ b_{\mu}=b}} \\
 &= \frac{D}{(4\pi)^D} \left[\frac{3}{4} \frac{(a+c)(b+c)}{[ab + ac + bc]^{D/2+2}} - \frac{1}{2} \frac{1}{[ab + ac + bc]^{D/2+1}} \right] \\
 &= \frac{D}{4(4\pi)^D} \frac{3c^2 + ab + ac + bc}{[ab + ac + bc]^{D/2+2}} \\
 &= \frac{1}{2(D+2)} [\partial_a^2 + \partial_b^2 + \partial_c^2 + 4\partial_a \partial_b - 2\partial_a \partial_c - 2\partial_b \partial_c] \int_{p,q} e^{-ap^2 - bq^2 - c(p+q)^2}. \tag{7.34}
 \end{aligned}$$

For the third relation we made explicit use of `Mathematica` to derive a suitable combination of derivatives. The cases where eq. (7.30) is not applicable are scaleless integrals that vanish in dimensional regularisation and thus can be dropped right away. The results can be generalised straight forwardly to additional powers of p^2 , q^2 and $(p+q)^2$ as well as to the replacement $p \leftrightarrow q$.

7.3 NLO matrix elements and the 1-loop mixing matrix

To check the validity of our `FORM` scripts we first computed the action density itself again to NLO as has been done before [155, 165]. We find consistently ($N_g = N^2 - 1$)

$$\langle E(t) \rangle = \frac{(D-1)N_g}{2(8\pi t)^{D/2}} g_0^2 \left\{ 1 + \frac{g_0^2 N (32\pi t)^{\epsilon}}{16\pi^2} \left[\frac{11}{3\epsilon} + \frac{52}{9} - 3 \ln(3) + O(\epsilon) \right] + O(g_0^4) \right\}. \tag{7.35}$$

For the bare matrix elements we then find

$$\int_p \left\langle \tilde{E}(t, p) \tilde{\mathcal{O}}_2^{(2)}(0) \right\rangle e^{ipx} = -\frac{(D-1)N_g}{2(8\pi t)^{D/2}} \frac{D}{2t} g_0^2 \times \left\{ 1 + \frac{g_0^2 N(32\pi t)^\epsilon}{16\pi^2} \left[\frac{31}{6\epsilon} + \frac{25}{36} - \frac{9}{2} \ln(3) + \mathcal{O}(\epsilon) \right] + \mathcal{O}(g_0^4) \right\}, \quad (7.36)$$

$$\int_p \left\langle \tilde{E}(t, p) \tilde{\mathcal{O}}_4^{(2)}(0) \right\rangle e^{ipx} = -\frac{(D-1)N_g}{2(8\pi t)^{D/2}} \frac{D+8}{18t} g_0^2 \times \left\{ 1 + \frac{g_0^2 N(32\pi t)^\epsilon}{16\pi^2} \left[\frac{115}{24\epsilon} + \frac{217}{144} - \frac{33}{8} \ln(3) + \mathcal{O}(\epsilon) \right] + \mathcal{O}(g_0^4) \right\}, \quad (7.37)$$

$$\int_p \left\langle \tilde{E}(t, p) \tilde{\mathcal{O}}_3^{(2)}(0) \right\rangle e^{ipx} = -\frac{(D-1)N_g}{2(8\pi t)^{D/2}} \frac{D}{4t} g_0^2 \times \left\{ 1 + \frac{g_0^2 N(32\pi t)^\epsilon}{16\pi^2} \left[\frac{11}{3\epsilon} + \frac{71}{18} - 3 \ln(3) + \mathcal{O}(\epsilon) \right] + \mathcal{O}(g_0^4) \right\}. \quad (7.38)$$

Introducing the renormalised coupling from eq. (3.8) allows to separate the 1-loop divergences for the operators since $E(t, x)$ does not require renormalisation. With use of equation (6.7) this leads to the extended mixing matrix

$$\begin{pmatrix} \mathcal{O}_2^{(2)} \\ \mathcal{O}_4^{(2)} \\ \mathcal{O}_3^{(2)} \end{pmatrix}_{\overline{\text{MS}}} = \begin{pmatrix} 1 + \frac{7}{3\epsilon} C_A \bar{\alpha} & 0 & -\frac{23}{3\epsilon} C_A \bar{\alpha} \\ -\frac{7}{15\epsilon} C_A \bar{\alpha} & 1 + \frac{21}{5\epsilon} C_A \bar{\alpha} & -\frac{157}{60\epsilon} C_A \bar{\alpha} \\ 0 & 0 & 1 \end{pmatrix} \begin{pmatrix} \mathcal{O}_2^{(2)} \\ \mathcal{O}_4^{(2)} \\ \mathcal{O}_3^{(2)} \end{pmatrix} + \mathcal{O}(\alpha_{\overline{\text{MS}}}^2), \quad (7.39)$$

where $4\pi\bar{\alpha} = \alpha_{\overline{\text{MS}}}$ and we used that the renormalised operator $\mathcal{O}_3^{(2)}$ must vanish on the $t = 0$ boundary due to the pure gauge EOMs, i.e., the other operators do not mix into this one.

This results in the diagonalised basis

$$\mathcal{B}_1^{(2)} = \mathcal{O}_2^{(2)} - \frac{23}{7} \mathcal{O}_3^{(2)}, \quad \mathcal{B}_2^{(2)} = \mathcal{O}_4^{(2)} - \frac{1}{4} \mathcal{O}_2^{(2)} - \frac{1}{6} \mathcal{O}_3^{(2)}, \quad \mathcal{B}_3^{(2)} = \mathcal{O}_3^{(2)}, \quad (7.40)$$

with 1-loop anomalous dimensions

$$\hat{\gamma}_1 = \frac{7}{11}, \quad \hat{\gamma}_2 = \frac{63}{55}, \quad \hat{\gamma}_3 = 0. \quad (7.41)$$

Chapter 8

Consequences and outlook for lattice YM theory and lattice QCD

Now that all relevant 1-loop anomalous dimensions have been computed in chapters 6 and 7 we are able to make statements about the asymptotic lattice spacing dependence of spectral quantities using eq. (4.43). The limitation to spectral quantities is due to additional lattice artifacts originating from local fields in the more general case, which then require new operators and thus more anomalous dimensions, see also chapter 4.

To discuss the leading power in the coupling we first take a detour to the matching coefficients $b_i^{\mathcal{B}}$, which for vanishing tree-level coefficient $\bar{b}_i^{\mathcal{B}}$, will introduce an additional power in the coupling. Without further knowledge of matching beyond tree-level we then assume 1-loop as the first non-vanishing order. To account for this we introduce $\hat{\Gamma}_i$ as the (minimal) leading power in the coupling, i.e., here

$$\hat{\Gamma}_i^{(d)} = \begin{cases} [\hat{\gamma}_0^{\mathcal{B}}]_i^{(d)} + n_{\text{I}} & \text{if } n_{\text{I}} > 0, \text{ i.e., perturbatively } (n_{\text{I}} - 1)\text{-loop improved action,} \\ [\hat{\gamma}_0^{\mathcal{B}}]_i^{(d)} + 1 & \text{else if } \bar{b}_i^{\mathcal{B}} = 0, \\ [\hat{\gamma}_0^{\mathcal{B}}]_i^{(d)} & \text{else.} \end{cases} \quad (8.1)$$

We also added the case that the lattice action is perturbatively $(n_{\text{I}} - 1)$ -loop improved, which only shifts the leading powers in the coupling by the overall constant n_{I} , and $n_{\text{I}} = 0$ means no improvement.

8.1 Lattice YM theory and lattice QCD

From 1PI matching conditions, as outlined in section 4.1.1, we can infer that (in the non-diagonal basis \mathcal{O}_i) no four fermion operators contribute at tree-level, because for any of the (fully $\mathcal{O}(a)$ improved) lattice actions we find

$$\underbrace{\text{1PI LPT}}_{\text{lattice theory}} = 0\alpha_{\text{lat}} + \mathcal{O}(\alpha_{\text{lat}}^2) \stackrel{!}{=} \underbrace{\text{1PI}}_{\text{Symanzik effective theory}} - a^2 b_i^{\mathcal{O}} \left[\text{1PI} \right]_i + \mathcal{O}(a^3),$$

where the zero at $O(\alpha)$ is due to the absence of an explicit 4-fermion interaction in the lattice QCD action. This ensures that no 4-fermion interaction can happen at the level of 1PI quark-4-point functions in LPT below 1-loop and thus below $O(\alpha^2)$.

Switching now to the diagonal basis allows the 4-fermion operators to contribute through their mixing into non-4-fermion operators. Since all non-4-fermion operators allowed at mass-dimension 6 for our minimal basis are compatible with chiral symmetry the mixing contributions are restricted to those from 4-fermion operators also compatible with chiral symmetry. This constraint reappears in the complicated diagonal basis at mass-dimension 6 in eq. (6.38) from which we can infer that all 4-fermion operators compatible with chiral symmetry will contribute at tree-level due to mixing. The only scenario in which such contributions do not exist is if all three operators $\mathcal{O}_2^{(2)}$, $\mathcal{O}_4^{(2)}$ and $\mathcal{O}_{10}^{(2)}$ are absent at tree-level in the naive expansion of the lattice action, i.e. the lattice action is additionally $O(a^2)$ improved at tree-level, such that no mixing contributions at this order in the coupling can occur. For general pure gauge actions eq. (5.3) combined with Wilson fermions eq. (4.22) or Overlap fermions eq. (5.9) we find that these three operators are present thus allowing the chirally symmetric 4-fermion operators to contribute at tree-level. All other 4-fermion operators are suppressed by at least one order in the coupling.

With these initial considerations in mind we can give the full spectrum $\hat{\Gamma}_i^{(d)}$ to be expected at mass-dimensions 5 and 6, i.e., $d = 1$ for Wilson fermions and $d = 2$ for non-perturbatively $O(a)$ improved Wilson fermions and Ginsparg-Wilson fermions. We fix $N = 3$ as it is in QCD and use as number of flavours $N_f \in \{0, 1, 2, 3, 4, 8\}$. The choices for N_f include pure gauge theory ($N_f = 0$) and the common cases for full QCD with $N_f = 2$, $N_f = 2 + 1$ as well as $N_f = 2 + 1 + 1$, while $N_f = 8$ is chosen to give an impression on getting closer to the conformal window.

The resulting spectra can be found in figure 8.1 for unimproved Wilson quarks and figure 8.2 for all other cases. We also added the mass-dependent operators, which contribute in the massive case. Note that these additional terms are expected to be suppressed for small quark masses due to $\frac{m_{u,d}}{m_s} \simeq \frac{1}{27} \ll 1$ with typical quark masses $am_{u;RGI} \in [0.001, 0.002]$, see e.g. [166]. For increasing numbers of flavours the additional quark masses are not small when considering physical quark masses and suppression is no longer expected.

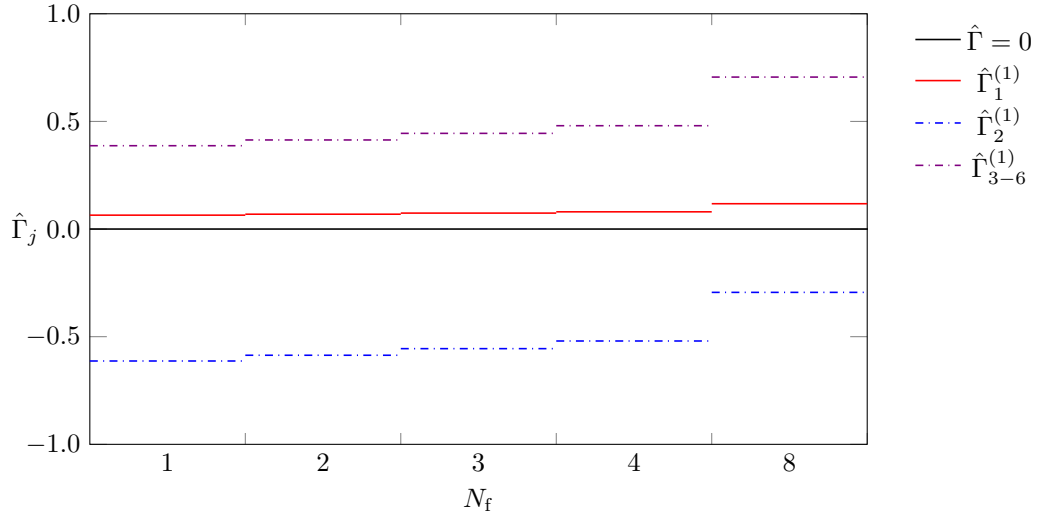
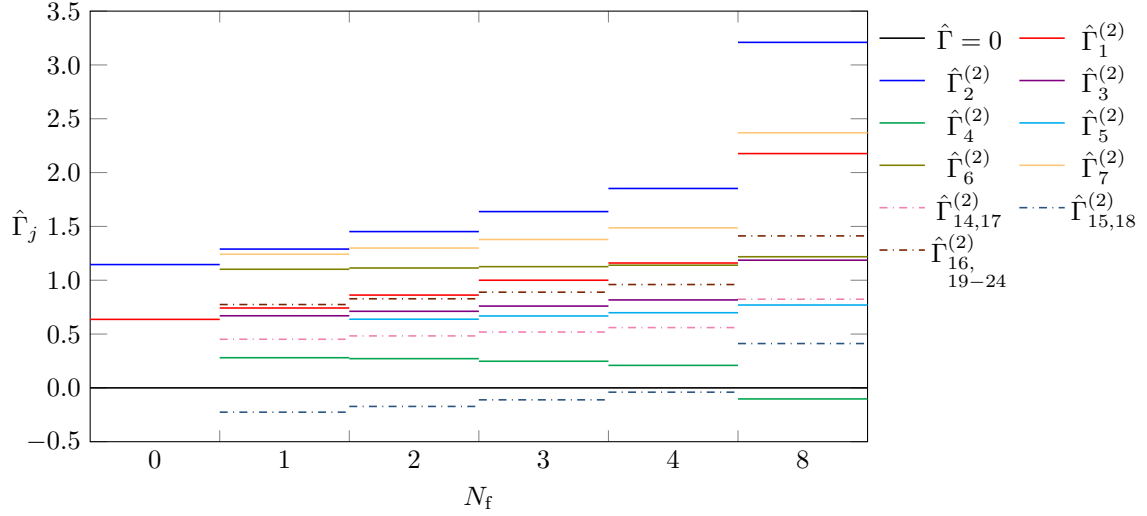


Figure 8.1: Leading powers in the coupling for different number of flavours and $N = 3$ modifying the classical a -corrections of Wilson QCD due to quantum corrections from mass-dimension 5 operators. The dash-dotted lines represent mass-dependent operators and are only relevant in the massive case. Different colours indicate specific anomalous dimensions where black is the naive $O(a)$ term.

Wilson fermions For unimproved Wilson fermions we find the spectrum in figure 8.1 affecting the $O(a)$ contributions, which consists of three distinct 1-loop anomalous dimensions. Only one of these operators, namely $\mathcal{B}_1^{(1)}$, is mass-independent and thus contributes in the massless case. For nonzero quark masses the mass-dependent operator $\mathcal{B}_2^{(1)}$ contributes with a distinctly negative 1-loop anomalous dimension, which worsens the convergence as $a \searrow 0$. Due to a linear quark mass dependence rather than a quadratic dependence the operator $\mathcal{B}_2^{(1)}$ is also less suppressed than $\mathcal{B}_{3-6}^{(1)}$ for decreasing quark masses. Depending on the choice for the mass-degeneracy we find that one (mass-degenerate case) or four (general massive case) of the operators $\mathcal{B}_{3-6}^{(1)}$ contribute, which results in the corresponding multiplicity of this anomalous dimension in the spectrum. Still, for sufficiently small quark masses contributions from $\mathcal{B}_1^{(1)}$ will be dominating and behave almost classically due to a 1-loop anomalous dimension that is very close to zero.



(a) Ginsparg-Wilson fermions.

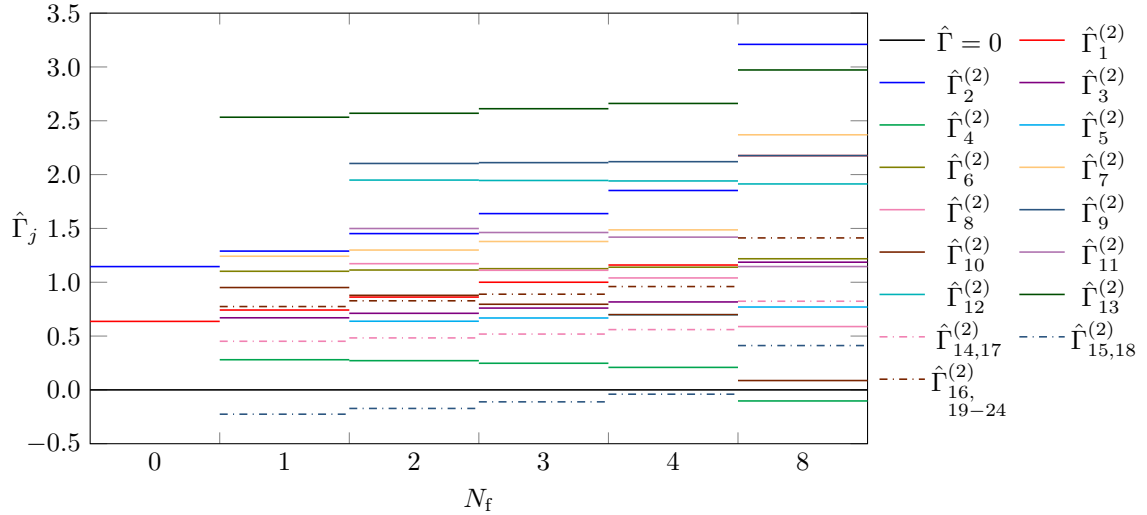

 (b) Non-perturbatively $O(a)$ improved Wilson fermions.

Figure 8.2: Leading powers in the coupling for different numbers of flavours and $N = 3$ modifying the classical a^2 -corrections due to quantum corrections from mass-dimension 6 operators. The dash-dotted lines represent mass-dependent operators and are only relevant in the massive case. Different colours indicate specific anomalous dimensions where black is the naive $O(a^2)$ term.

Improved fermions For both Ginsparg-Wilson fermions (figure 8.2a) and non-perturbatively $O(a)$ improved Wilson fermions (figure 8.2b) we find that the leading powers modifying naive a^2 scaling are $\hat{\Gamma}_i^{(2)} \geq 0$ for $N_f < 8$ and $N = 3$ in the massless case. This means the leading powers improve the convergence as $a \searrow 0$ in comparison to the naive a^2 -extrapolation which assumes $\hat{\Gamma}^{(2)} = 0$. Only with non-zero quark masses the minimal power of the coupling to be expected is reduced to $\hat{\Gamma}_i^{(2)} \gtrsim -0.28$ for $N_f < 8$, which is still close to the naive power law. Due to the presence of a multitude of operators the spectrum is dense, such that deciding which contributions actually dominate is difficult and pile-ups or cancellations can potentially occur. Due to non-perturbative improvement of the Wilson quarks there exist no $O(a)$ terms in the effective to any power in the coupling and thus contact terms arising from double operator insertions integrated over spacetime can play no role here.

For increasing numbers of flavours of massless Ginsparg-Wilson fermions the gap between the two lowest lying powers in the coupling increases, which may allow to treat the smallest power as the truly dominating contribution. Also the overall density of the spectrum is reduced.

To give a general idea of the deviation from the naive a^2 power law we also show the leading logarithms in figure 8.3 for fixed number of flavours $N_f = 3$ again with $N = 3$, where we assumed identical prefactors for all operators of the minimal basis. Depending on the prefactors of the different contributions the overall picture will of course look vastly different. We still learn that the largest anomalous dimensions suppress contributions such that they get close to the naive a^4 power-law. Especially for Wilson fermions these are almost indistinguishable from classical a^4 corrections in the range of lattice spacings covered in the plot. However, for Wilson fermions the next-to-leading order in the lattice spacing is $O(a^3)$ in contrast to Ginsparg-Wilson fermions where it is $O(a^4)$. All contributions for Wilson fermions getting close (or below) the black dashed line in figure 8.3 will thus be indistinguishable from $O(a^3)$ corrections in the range of lattice spacings covered here.

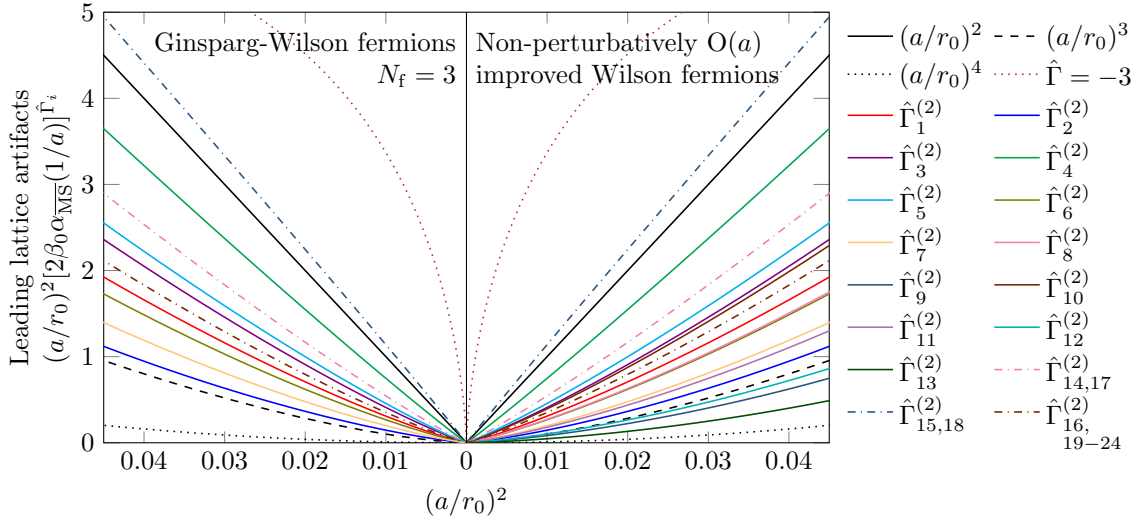


Figure 8.3: Different leading logarithms modifying the classical a^2 power-law due to quantum corrections from mass-dimension 6 operators at $N_f = 3$ and $N = 3$. The dash-dotted lines represent mass-dependent operators and are only relevant in the massive case. Different colours indicate specific anomalous dimensions. The solid black line is the naive a^2 term, the dashed black line is the naive a^3 term and the dotted black line is the classical a^4 correction. The brownish dotted line is plotted to give a comparison to the $O(3)$ model, where the smallest value encountered is $\hat{\Gamma} = -3$, and has been **scaled by a relative factor of 1/10 due to steepness**. All other contributions have been given the same prefactor 100. We use $r_0 \Lambda_{\overline{MS}}^{N_f=3} = 0.806$ from FLAG [49] to derive $\alpha_{\overline{MS}}(1/a)$ from 5-loop running [167].

Pure gauge theory and the lattice YM Gradient flow In case of pure gauge theory the situation is much simpler compared to full QCD since no $O(a)$ corrections occur and only two operators need to be considered at $O(a^2)$. Assuming the $O(a^4)$ and higher order contributions are negligible one can use both powers in the coupling in a fit ansatz or choose the dominating one since contributions from $\mathcal{B}_2^{(2)}$ are suppressed by the power $\Delta\hat{\Gamma} \approx 0.509$ in the coupling compared to $\mathcal{B}_1^{(2)}$, which may allow to distinguish them. Both anomalous dimensions are larger zero improving the convergence as $a \searrow 0$ compared to the naive a^2 -extrapolation.

When extending the Symanzik effective theory to include the Yang-Mills Gradient flow only one additional mass-dimension 6 operator $\mathcal{O}_3^{(2)}$ must be taken into account. This operator is located at the zero flow-time boundary of the 5-dimensional theory as are the other two operators. Due to pure gauge EOMs all contributions of $\mathcal{O}_3^{(2)}$ to on-shell matrix elements vanish at zero flow-time. At positive flow-time this is no longer the case due to changed EOMs eq. (7.6) in the 5-dimensional theory. A consequence from this is that pure gauge actions, which have been on-shell improved on the zero flow-time boundary, still contribute $O(a^2)$ terms at tree-level for matrix elements at positive flow-time unless the additional operator is eliminated as well. As found in chapter 7 this additional operator has a vanishing 1-loop anomalous dimension and thus does not affect the classical a^2 power-law at tree-level of the matching. Whether this holds true to all orders in perturbation theory is unknown. The two other operators with non-vanishing 1-loop anomalous dimensions are suppressed by powers in the coupling $\hat{\Gamma}_1^{(2)} \approx 0.636$ and $\hat{\Gamma}_2^{(2)} \approx 1.145$. For matrix-elements entirely located at positive flow-time, contributions from the three mass-dimension 6 operators are the only lattice artifacts to $O(a^2)$, which cannot be described classically. All contributions of lattice artifacts from local fields at positive flow-time or the flow action can be treated classically as only quantities at zero flow-time require renormalisation [160].

8.2 Twisted mass QCD with Wilson fermions

As pointed out in sections 5.1.3 and 5.4 we can infer the anomalous dimensions needed for twisted mass QCD from non-twisted QCD. For simplicity we restrict considerations to the case of maximal twist, which is also the most interesting case due to “automatic” $O(a)$ improvement. The absence of T_1 -even operators below mass-dimension 6 in our minimal basis for tmQCD ensures that T_1 -even n -point functions computed on the lattice have no $O(a)$ corrections originating from the action. However this does not set any matching coefficients of the mass-dimension 5 operators to zero and they become relevant at $O(a^2)$ due to the insertion of two rather than one mass-dimension 5 operator, which results again in an overall T_1 -even insertion. Additional powers in the coupling are thus to be expected of the form ($i \leq j$)

$$\hat{\Gamma}_{i,j}^{(2)} = \begin{cases} [\hat{\gamma}_0^{\mathcal{B}}]_i^{(1)} + [\hat{\gamma}_0^{\mathcal{B}}]_j^{(1)} + 2n_I & \text{if } n_I > 0, \text{ perturbatively } (n_I - 1)\text{-loop } O(a) \text{ improved action,} \\ [\hat{\gamma}_0^{\mathcal{B}}]_i^{(1)} + [\hat{\gamma}_0^{\mathcal{B}}]_j^{(1)} & \text{else.} \end{cases} \quad (8.2)$$

All relevant mass-dimension 5 operators have in general nonzero tree-level matching coefficients, which one can infer again from the naive expansion of eq. (5.10) which amounts to the naive expansion of the Wilson Dirac operator we did before just in the twisted basis. In comparison to non-twisted $O(a)$ improved Wilson QCD the spectrum remains almost the same. The only new contribution due to double operator insertion not vanishing in the massless case yields $\hat{\Gamma}_{1,1}^{(2)} \approx 0.138$ and is slightly closer to the classically expected zero than the value found in massless non-twisted $O(a)$ improved Wilson QCD.

Since double operator insertions of the mass-dimension 5 operators are integrated over space-time there will in general be contact-terms, once both operators are located at the same spacetime points. In our renormalisation strategy this effect can be checked by inserting two operators rather than one, each at zero momentum, in eq. (6.4). Such an operator at zero momentum is equivalent

to its Fourier transform integrated over spacetime

$$\tilde{\mathcal{O}}(0) = \int d^D x \mathcal{O}(x) e^{-ipx}|_{p=0} = \int d^D x \mathcal{O}(x) \quad (8.3)$$

such that contact terms will certainly occur when two operators are inserted at zero momentum. Due to symmetry constraints all contact terms can be parametrised by operators \mathcal{O}_n of our minimal basis in the operator product expansion, see e.g. [149, p. 612ff.],

$$\mathcal{O}(x)\mathcal{O}(y) \stackrel{x \rightarrow y}{=} \sum_n C_n(x-y) \mathcal{O}_n(y), \quad (8.4)$$

with Wilson coefficients C_n . We are only concerned about additional UV divergences arising from these contact terms, which must be subtracted additionally during renormalisation by choosing proper counterterms from our minimal basis. While this will keep the diagonal entries of the anomalous dimensions unaffected to all orders, the matching coefficients of the diagonalised mass-dimension 6 operator basis will be changed in comparison to the case where no mass-dimension 5 operators were present. So the argument, that there are no 4-fermion operators present at tree-level that violate chiral symmetry must be revisited. Without further knowledge we cannot make that assumption because a double insertion of the Sheikholeslami-Wohlert term may lead to a contact terms parametrised by such 4-fermion operators in the operator product expansion and thus lead to non-vanishing tree-level matching coefficients. This shifts the spectrum of chiral symmetry violating operators back down by one order in the coupling such that the smallest anomalous dimension and thus power in the coupling is $\hat{\Gamma}_{10}^{(2)} \approx -0.122$, again ignoring operators with overall mass-dependence. The modified spectrum for tmQCD at maximal twist can be found in figure 8.4. The same issue occurs for perturbatively $\mathcal{O}(a)$ improved Wilson fermions where not only $\mathcal{O}(a)$ corrections persist at higher loop order but also contact terms will affect $\mathcal{O}(a^2)$ due to double insertions of the remaining mass-dimension 5 operators.

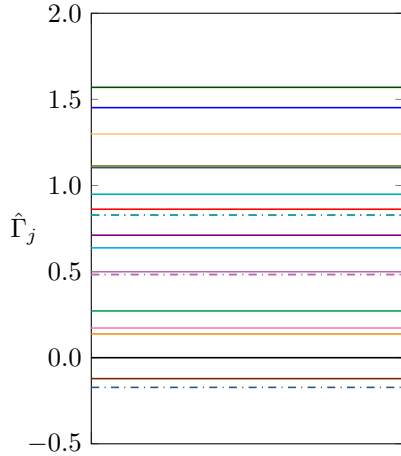


Figure 8.4: Leading powers in the coupling for 2-flavour Wilson twisted mass QCD with $N = 3$ and maximal twist modifying the classical a^2 -corrections due to quantum corrections from mass-dimension 6 operators as well as double insertions of mass-dimension 5 operators. The dash-dotted lines represent mass-dependent operators and are only relevant in the massive case. Different colours indicate specific anomalous dimensions where black is the naive $\mathcal{O}(a^2)$ term.

8.3 Impact of non-zero anomalous dimensions on the continuum extrapolation

With all the information on the leading logarithmic corrections at hand we will now try to sketch some possible use cases when doing the continuum extrapolation. This involves both different strategies for improvement of the convergence and error estimates using the spectra from the previous part as input. In order to perform perturbative improvement we will stick to pure gauge

theory, where less operators are present and the matching coefficients are known at $O(a^2)$ at tree-level [60–62] and to 1-loop order in the Symanzik tree-level improved case [62]. For completeness we also list here the tree-level matching coefficients for common choices of lattice gauge actions in table 8.1 for our minimal diagonal basis according to

$$\bar{b}_1^{\mathcal{B}} = \frac{1}{48} + \frac{3e_1(0) + 4e_2(0) - 3e_3(0)}{12}, \quad (8.5)$$

$$\bar{b}_2^{\mathcal{B}} = \frac{1}{12} + e_1(0) - e_3(0), \quad (8.6)$$

$$\bar{b}_3^{\mathcal{B}} = \frac{83}{1008} + \frac{83e_1(0) + 120e_2(0) + e_3(0)}{84}, \quad (8.7)$$

where we use the coefficients $e_i(g_0)$ as introduced in eq. (5.3). Notice that for pure gauge theory without the Gradient flow $\bar{b}_3^{\mathcal{B}}$ can be arbitrary as it does not affect on-shell quantities. In this case, without the twisted chair, i.e. $e_2(0) = 0$, one also finds the useful relation

$$\bar{b}_2^{\mathcal{B}} = 4\bar{b}_1^{\mathcal{B}}, \quad (8.8)$$

which amounts to a single prefactor $\bar{b}_1^{\mathcal{B}}$ of the leading order lattice artifacts for various lattice pure gauge actions and thus allows to compare the relative sizes of the leading order lattice artifacts. For the ones given in table 8.1 one finds the ratio

$$\text{Wilson} : \text{Iwasaki} : \text{DBW2} \approx 1 : -3 : -16. \quad (8.9)$$

Table 8.1: Tree-level matching coefficients $\bar{b}_i^{\mathcal{B}}$ for lattice pure gauge theory and lattice YM Gradient flow in the diagonal basis and the tree-level coefficients $e_i(0)$ for the plaquette ($i = 0$), rectangle ($i = 1$), twisted chair ($i = 2$) and chair ($i = 3$) as used in eq. (5.3) with normalisation $1 = e_0(0) + 8e_1(0) + 8e_2(0) + 16e_3(0)$.

Action	$\bar{b}_1^{\mathcal{B}}$	$\bar{b}_2^{\mathcal{B}}$	$\bar{b}_3^{\mathcal{B}}$	$e_1(0)$	$e_2(0)$	$e_3(0)$
Wilson plaquette [69]	$\frac{1}{48}$	$\frac{1}{12}$	$\frac{83}{1008}$	0	0	0
Iwasaki [168]	-0.0619	-0.2477	-0.2447	-0.331	0	0
DBW2 [169, 170]	-0.3309	-1.3236	-1.3078	-1.4069	0	0
Symanzik improved [60–62]	0	0	0	$-\frac{1}{12}$	0	0

8.3.1 Symanzik improvement versus improvement of an expectation value

The discussion on perturbative (tree-level) improvement follows along the lines of [3]. However we use here the action density $E(t)$ at small flow-time $t > 0$ as an example since the YM Gradient flow offers a more diverse set of lattice artifacts. Secondly we already computed the boundary contributions to 1-loop in fixed order perturbation theory

$$\begin{aligned} \frac{\langle E(t; a) \rangle}{\langle E(t; 0) \rangle} &= 1 - \frac{a^2}{t} \left(b_1^{\mathcal{B}} \frac{9}{7} \left[1 + \left\{ \frac{29}{9} + \frac{7}{3} (\ln(3) - \gamma_E - \ln(8t/a^2)) \right\} N^{\frac{\alpha_{\overline{\text{MS}}}(1/a)}{4\pi}} \right] \right. \\ &\quad \left. - b_2^{\mathcal{B}} \frac{71}{60} N^{\frac{\alpha_{\overline{\text{MS}}}(1/a)}{4\pi}} - b_3^{\mathcal{B}} \left[1 - \frac{11}{6} N^{\frac{\alpha_{\overline{\text{MS}}}(1/a)}{4\pi}} \right] \right) \\ &\quad + \left[O(a^2) \text{ discretisation errors of the} \right. \\ &\quad \left. \text{flow action and the action density} \right] + O(a^2 \alpha_{\overline{\text{MS}}}^2(1/a), a^4) \end{aligned} \quad (8.10)$$

as a byproduct of the operator renormalisation in chapter 7. This result is only valid if the flow-time t is sufficiently small with $a^2 \ll 8t \ll 1/\Lambda_{\overline{\text{MS}}}^2$ as otherwise evaluating $\langle E(t) \rangle$ at renormalisation

8.3. Impact of non-zero anomalous dimensions on the continuum extrapolation

scale $\mu = 1/a$ introduces severely large logarithms and the perturbative expansion in the coupling breaks down. Notably the contribution of $\mathcal{B}_2^{(2)}$ vanishes at leading order. As mentioned earlier the additional lattice artifacts from local fields and the flow action can all be treated classically [160] and can be computed via

$$\left[\begin{array}{l} \text{O}(a^2) \text{ discretisation errors of the} \\ \text{flow action and the action density} \end{array} \right] = a^2 \frac{\langle \delta E^{(2)}(t) \rangle - 2 \int_0^t ds \int d^4y \langle E(t, x; 0) \text{tr} (L_\mu(s, y) \delta \mathcal{F}_\mu^{(2)}(s, y)) \rangle}{\langle E(t; 0) \rangle}, \quad (8.11)$$

where $\delta \mathcal{F}_\mu^{(2)}$ are the $\text{O}(a^2)$ corrections to the flow equation, i.e.,

$$\partial_t B_\mu(t, x) = D_\nu G_{\nu\mu}(t, x) + a^2 \delta \mathcal{F}_\mu^{(2)}(t, x) + \text{O}(a^4), \quad (8.12)$$

and $\delta E^{(2)}$ are the $\text{O}(a^2)$ corrections of the action density, which of course depend on the chosen discretisations. Being able to treat both contributions classically implies that matching of the coefficients in $\delta \mathcal{F}_\mu^{(2)}$ and $\delta E^{(2)}$ in our SET reduces to the naive expansion in the lattice spacing. Thus using Symanzik tree-level $\text{O}(a^2)$ improved flow action and local fields at positive flow-time leads to $\text{O}(a^2)$ improvement to all orders [162] up to the contributions on the zero flow-time boundary, which in our SET are parametrised by the three operators $\mathcal{B}_1^{(2)}$, $\mathcal{B}_2^{(2)}$ and $\mathcal{B}_3^{(2)}$. The latter contributions are given to 1-loop order in eq. (8.10). In case of the flow action Symanzik $\text{O}(a^2)$ improvement can e.g. be achieved by choosing the Zeuthen flow [162, 171], and the action density only needs to be classically improved¹.

A common technique for dimensionless short-distance observables, i.e. here small flow-time, is to perform improvement at the level of the expectation value using perturbative results such as eq. (8.10) as input, see e.g. [63, 64] for tree-level improvement or [65–68] for examples with higher orders in perturbation theory and with a combination of improvement of action and observable. For simplicity we assume for now that both the flow action and the action density are Symanzik improved to keep the formulae compact. Tree-level improvement of $\langle E(t) \rangle$ can then be achieved through

$$t^2 \langle E(t; a) \rangle^{\text{TL}} = \frac{t^2 \langle E(t; a) \rangle}{1 - \frac{a^2}{t} \left(\frac{9}{7} \bar{b}_1^{\mathcal{B}} - \bar{b}_3^{\mathcal{B}} \right)} \quad (8.13)$$

$$= t^2 \langle E(t; 0) \rangle \left[1 - \frac{a^2 \alpha_{\overline{\text{MS}}}(1/a)}{4\pi t} \left(\bar{b}_1^{\mathcal{B}} \left\{ \frac{29}{7} - 3\gamma_E + 3 \ln(3) - 3 \ln(8t/a^2) \right\} N - \frac{71N}{60} \bar{b}_2^{\mathcal{B}} + \frac{11N}{6} \bar{b}_3^{\mathcal{B}} + \frac{36\pi}{7} \bar{b}_1^{\mathcal{B}} - 4\pi \bar{b}_3^{\mathcal{B}} \right) + \text{O}(a^2 \alpha_{\overline{\text{MS}}}^2(1/a), a^4) \right], \quad (8.14)$$

but also a subtraction or similar prescriptions as well as proper combinations of different discretisations of the same local field are valid. Here $\bar{b}_i^{\mathcal{B}}$ denote the 1-loop matching coefficients. After removing (here: dividing out) the tree-level lattice artifacts the remainder in eq. (8.14) contains a term with $\ln(8t/a^2) \alpha_{\overline{\text{MS}}}(1/a)$ at 1-loop order. Keeping the flow-time t fixed as $a \searrow 0$ this term shrinks slower than all the other terms and will eventually dominate the behaviour at smallest a . This contradicts the name “tree-level improvement” which suggests that the leading term is a constant times $\alpha_{\overline{\text{MS}}}(1/a)$. Such terms are known as *leading logarithms* (LL) and can be absorbed into Renormalisation Group Improvement [110]. In our example this means that we rewrite the LL as

$$\left[\frac{\alpha_{\overline{\text{MS}}}(1/a)}{\alpha_{\overline{\text{MS}}}(1/\sqrt{8t})} \right]^{\hat{\gamma}_1^{\mathcal{B}}} = 1 - \beta_0 \hat{\gamma}_1^{\mathcal{B}} \ln(8t/a^2) \alpha_{\overline{\text{MS}}}(1/a) + \text{O}(\alpha_{\overline{\text{MS}}}^2(1/a)), \quad (8.15)$$

¹Classical improvement means that no $\text{O}(a^2)$ terms are present in the naive lattice spacing expansion.

remember $\hat{\gamma}_i^{\mathcal{B}} = (\gamma_0)_i^{\mathcal{B}}/\beta_0$, and instead divide out

$$t^2 \langle E(t; a) \rangle^{\text{TL,RG}} = \frac{t^2 \langle E(t; a) \rangle}{1 - \frac{a^2}{t} \left(\frac{9}{7} \bar{b}_1^{\mathcal{B}} \left[\frac{\alpha_{\overline{\text{MS}}}(1/a)}{\alpha_{\overline{\text{MS}}}(1/\sqrt{8t})} \right]^{\hat{\gamma}_1^{\mathcal{B}}} - \bar{b}_3^{\mathcal{B}} \right)} \quad (8.16)$$

$$= t^2 \langle E(t; 0) \rangle \left[1 - \frac{a^2 \alpha_{\overline{\text{MS}}}(1/a)}{4\pi t} \left(\bar{b}_1^{\mathcal{B}} \left\{ \frac{29}{7} - 3\gamma_E + 3 \ln(3) \right\} N - \frac{71N}{60} \bar{b}_2^{\mathcal{B}} + \frac{11N}{6} \bar{b}_3^{\mathcal{B}} + \frac{36\pi}{7} \bar{b}_1^{\mathcal{B}} - 4\pi \bar{b}_3^{\mathcal{B}} \right) + \mathcal{O}(a^2 \alpha_{\overline{\text{MS}}}^2(1/a), a^4) \right]. \quad (8.17)$$

The result has no logarithmic dependence on the lattice spacing at 1-loop order and is thus not only tree-level but also Renormalisation Group improved. In case the contribution from $\mathcal{B}_2^{(2)}$ does not vanish at tree-level one would only need to add a third term analogously to the one for $\mathcal{B}_1^{(2)}$. For 1-loop improvement we could have just as well divided out the entire 1-loop boundary contribution from eq. (8.10), assuming that the 1-loop matching coefficients $\bar{b}_i^{\mathcal{B}}$ are known. In this case the lack of Renormalisation Group Improvement only gets shifted by one loop order, i.e. we expect *next-to-leading logarithm* (NLL) contributions of the form $\ln^n(8t/a^2) \alpha_{\overline{\text{MS}}}^2(1/a)$ with $n = 1, 2$ which are again troublesome for $a \searrow 0$ at fixed t . All these issues stem from dividing out lattice artifacts a posteriori and can be avoided by using a (perturbatively) Symanzik on-shell improved action, which automatically ensures Renormalisation Group Improvement. On the other hand performing both tree-level and Renormalisation Group improvement a posteriori should yield a comparable reduction of lattice artifacts compared to Symanzik improvement with slightly differing 1-loop and higher order coefficients for the $\mathcal{O}(a^2)$ lattice artifacts. These corrections then depend on the chosen improvement strategy, i.e. dividing out, subtraction etc. of $\mathcal{O}(a^2)$ lattice artifacts to LL order.

For lattice artifacts from the flow action or local fields at positive flow-time Symanzik improvement is even more advantageous compared to tree-level improvement at the level of the flowed quantity. The latter only removes all tree-level corrections at $\mathcal{O}(a^2)$ for the flowed quantity as discussed earlier but keeps all lattice artifacts at higher loop order in $\mathcal{O}(a^2)$ and thus also contributions from the flow action and local fields. At first this may seem counter-intuitive as vertices parametrising lattice artifacts from the flow action or the local fields can only occur in so called “tree-graphs” [155, 160], but this refers only to contributions at positive flow time and makes no statement on the zero flow-time boundary where all loop corrections are located. Then performing tree-level improvement at the level of a flowed quantity only ensures that the linear combination of all tree-level corrections vanishes while Symanzik improvement systematically removes all vertices parametrising the $\mathcal{O}(a^2)$ corrections of both flow action and local fields at positive flow-time. Of course this is only true because the matching coefficients of the flow action and local fields are identical to the tree-level coefficients. For all lattice artifacts originating from the zero flow-time boundary Symanzik $(n_I - 1)$ -loop improvement only sets the first n_I matching coefficients to zero.

Practical example $t^2 \langle E(t; a) \rangle$ To highlight some details of tree-level improvement at the level of the expectation value we consider here results for the action density in the pure gauge ensembles *sftn* with $n \in \{2, 3, 4, 5, 6\}$.² These configurations are at very small lattice spacings and the corresponding $\overline{\text{MS}}$ couplings reached are $\alpha_{\overline{\text{MS}}}(1/a) \in \{0.176(1), 0.1530(8), 0.1405(6), 0.1261(5), 0.1175(5)\}$ according to 5-loop running [167] in continuum pure gauge theory using $\sqrt{8t_0} \Lambda_{\overline{\text{MS}}} = 0.6227(94)$ [158] as input. So we are well within the perturbative region for $\alpha_{\overline{\text{MS}}}(1/a)$. Unfortunately these ensembles did not use the Lüscher-Weisz action nor the Zeuthen flow but the Wilson action and Wilson flow, i.e. no Symanzik improved action or flow. For the discretisation of the action density a linear

²These ensembles use spatially periodic boundary conditions and open boundary conditions in time direction with large volumina, such that translational invariance is approximately restored sufficiently off the time boundary with $x_0 \gtrsim \sqrt{20t_0}$ [82]. The bare couplings $\beta = \frac{6}{g_0^2} \in \{6.2556, 6.5619, 6.7859, 7.1146, 7.36\}$ translate roughly into the lattice spacings $100a \in \{6.2, 4.2, 3.1, 2.1, 1.6\} \text{fm}$ for the ensembles used here.

8.3. Impact of non-zero anomalous dimensions on the continuum extrapolation

combination of the plaquette and clover discretisation with weights ξ and $(1 - \xi)$ respectively is available. The required naive expansion in the lattice spacing can be found in [162]

$$\delta E^{(2)} \Big|_{\xi}(t, x) = \left\{ \frac{\xi}{12} + \frac{1 - \xi}{3} \right\} \sum_{\mu} \text{tr} (D_{\mu} G_{\mu\nu}(t, x) D_{\mu} G_{\mu\nu}(t, x)) + \partial_{\mu} K_{\mu}, \quad (8.18)$$

$$\delta \mathcal{F}_{\mu}^{(2)} \Big|_{\text{Wilson}}(t, x) = \frac{1}{12} \sum_{\nu} D_{\nu}^3 G_{\nu\mu}(t, x) - \frac{1}{6} [D_{\nu}^2, D_{\rho}] G_{\rho\sigma}(t, x) \delta_{\mu\nu\sigma}. \quad (8.19)$$

The additional total divergences, here called $\partial_{\mu} K_{\mu}$, in $\delta E^{(2)}$ can be dropped in anticipation of translational invariance of the vacuum expectation value $\langle E(t, x) \rangle$ in infinite volume. The leading order contributions from the flow action and action density are then known

$$\frac{t \langle \delta E^{(2)} \Big|_{\xi}(t, x) \rangle}{\langle E(t; 0) \rangle} = - \left\{ \frac{\xi}{12} + \frac{1 - \xi}{3} \right\} \frac{2}{3} + \mathcal{O}(\alpha_{\overline{\text{MS}}}(1/a)), \quad (8.20)$$

$$-2 \frac{t \int_0^t ds \int d^4 y \langle E(t, x; 0) \text{tr} (L_{\mu}(s, y) \delta \mathcal{F}_{\mu}^{(2)}(s, y)) \rangle}{\langle E(t; 0) \rangle} = \frac{1}{8} + \mathcal{O}(\alpha_{\overline{\text{MS}}}(1/a)). \quad (8.21)$$

With this input we already know that tree-level $\mathcal{O}(a^2)$ improvement of the vacuum expectation value $\langle E(t) \rangle$ can be achieved by the choice $\xi = 1/4$, which ensures that all $\mathcal{O}(a^2)$ effects from the zero flow-time boundary, flow action and observable cancel out at tree-level. As already discussed, this does not ensure absence of the LL corrections occurring in eq. (8.10), which can be eliminated additionally. In case of the Wilson action these LL are

$$\frac{\langle E(t; a) \rangle^{\text{TL}} - \langle E(t; 0) \rangle^{\text{TL}}}{\langle E(t; 0) \rangle^{\text{TL}}} = \frac{a^2}{t} \frac{3}{16} \ln(8t/a^2) \frac{\alpha_{\overline{\text{MS}}}(1/a)}{4\pi} + \mathcal{O}(a^2 \alpha_{\overline{\text{MS}}}(1/a), a^2 \alpha_{\overline{\text{MS}}}^{1.636}(1/a), a^2 \alpha_{\overline{\text{MS}}}^{2.145}(1/a), a^4) \quad (8.22)$$

$$= - \frac{a^2}{t} \frac{3}{112} \left\{ \left[\frac{\alpha_{\overline{\text{MS}}}(1/a)}{\alpha_{\overline{\text{MS}}}(1/\sqrt{8t})} \right]^{7/11} - 1 \right\} + \mathcal{O}(a^2 \alpha_{\overline{\text{MS}}}(1/a), a^2 \alpha_{\overline{\text{MS}}}^{1.636}(1/a), a^2 \alpha_{\overline{\text{MS}}}^{2.145}(1/a), a^4), \quad (8.23)$$

where the subleading a^2 -terms are indicated in the $\mathcal{O}(\dots)$ with their respective leading powers in the coupling.

Before we can attempt a continuum extrapolation we first need to discuss another contribution of lattice artifacts due to scale setting. This is needed to fix the flow-time t in units of a scale, here the flow-time t_c defined through

$$t^2 \langle E(t) \rangle \Big|_{t=t_c} = c. \quad (8.24)$$

We discuss the two cases $c \in \{0.085, 0.3\}$, which we identify with the scales $\tau_0 \equiv t_{0.085}$ and $t_0 \equiv t_{0.3}$, where t_0 and t_0/τ_0 are needed for continuum running of the coupling to obtain $\alpha_{\overline{\text{MS}}}(1/a)$ and $\alpha_{\overline{\text{MS}}}(1/\sqrt{8t})$ while τ_0 is used to actually fix the flow-time at finite lattice spacing. We know from the SET that these scales t_c will also introduce lattice artifacts according to

$$\frac{t_c^2(a)}{t_c^2(0)} = \frac{\langle E(t_c; 0) \rangle}{\langle E(t_c; a) \rangle}. \quad (8.25)$$

The value of c or equivalently t_c determines whether the LL of the additional lattice artifacts can be described perturbatively, i.e. $\alpha_{\overline{\text{MS}}}(1/\sqrt{8t_c})$ is sufficiently small or not. For τ_0/t_0 this is not the case because t_0 is too large and we cannot perform Renormalisation Group Improvement by dividing out the LL. So we have to extrapolate in plain a^2 , which is then the leading order due to zero 1-loop anomalous dimension, see figure 8.5.

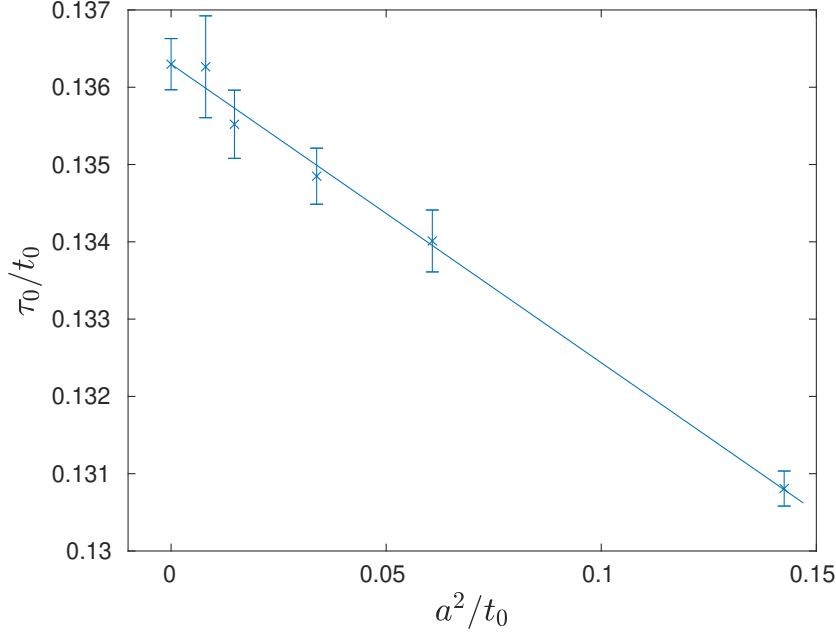


Figure 8.5: Continuum extrapolation of τ_0/t_0 . A plain a^2 -extrapolation was used due to t_0 being in the non-perturbative region and leading anomalous dimension being zero.

Table 8.2: Continuum extrapolated values of tree-level improved $t^2 \langle E(t; a) \rangle$ at small flow-times with and without the leading logarithmic corrections divided out.

t/t_0	$[10^{-2}]$	5.02(1)	6.03(1)	10.02(3)	11.02(3)
$t^2 \langle E(t) \rangle^{\text{TL}}$	$[10^{-2}]$	6.1833(19)	6.5001(19)	7.6079(11)	7.8624(9)
$t^2 \langle E(t) \rangle^{\text{TL,RG}}$	$[10^{-2}]$	6.1843(18)	6.5008(17)	7.6083(10)	7.8627(8)

For the continuum extrapolation of the action density we then consider the dimensionless quantity $(t(a) = (t/\tau_0)_{\text{fixed}} \tau_0(a))$

$$\begin{aligned}
 \frac{t^2(a) \langle E(t; a) \rangle^{\text{TL}}}{t^2(0) \langle E(t; 0) \rangle^{\text{TL}}} &= 1 + \frac{3a^2}{112\tau_0} \left\{ \left[\frac{\alpha_{\overline{\text{MS}}}(1/a)}{\alpha_{\overline{\text{MS}}}(1/\sqrt{8}\tau_0)} \right]^{7/11} - 1 \right\} - \frac{3a^2}{112t} \left\{ \left[\frac{\alpha_{\overline{\text{MS}}}(1/a)}{\alpha_{\overline{\text{MS}}}(1/\sqrt{8}t)} \right]^{7/11} - 1 \right\} \\
 &+ \mathcal{O}(a^2 \alpha_{\overline{\text{MS}}}(1/a), a^2 \alpha_{\overline{\text{MS}}}^{1.636}(1/a), a^2 \alpha_{\overline{\text{MS}}}^{2.145}(1/a), a^4). \quad (8.26)
 \end{aligned}$$

Dividing out this leading term ensures Renormalisation Group improvement such that the leading order corrections are $\mathcal{O}(a^2 \alpha_{\overline{\text{MS}}}(1/a))$ without additional logarithms. Although the overall prefactor of the LL correction in case of the Wilson plaquette action is fairly small, we still find a non-negligible effect in figure 8.6 when dividing out the LL corrections. Both cases without and with LL corrections divided out have been continuum extrapolated with an a^2 ansatz and an $a^2 \alpha_{\overline{\text{MS}}}(1/a)$ ansatz respectively, where the three or four of the smallest lattice spacings were included, which corresponds roughly to $a^2/t \lesssim 2/3$. The results at the four different flow-times are listed in table 8.2. Both extrapolations yield the same result well within the uncertainties but the Renormalisation Group improved expectation value of the action density has a less steep dependence on the lattice spacing amounting to a reduction of $\mathcal{O}(20 \sim 30\%)$ of the lattice artifacts at the flow-times and largest lattice spacing included in the extrapolations.

8.3. Impact of non-zero anomalous dimensions on the continuum extrapolation

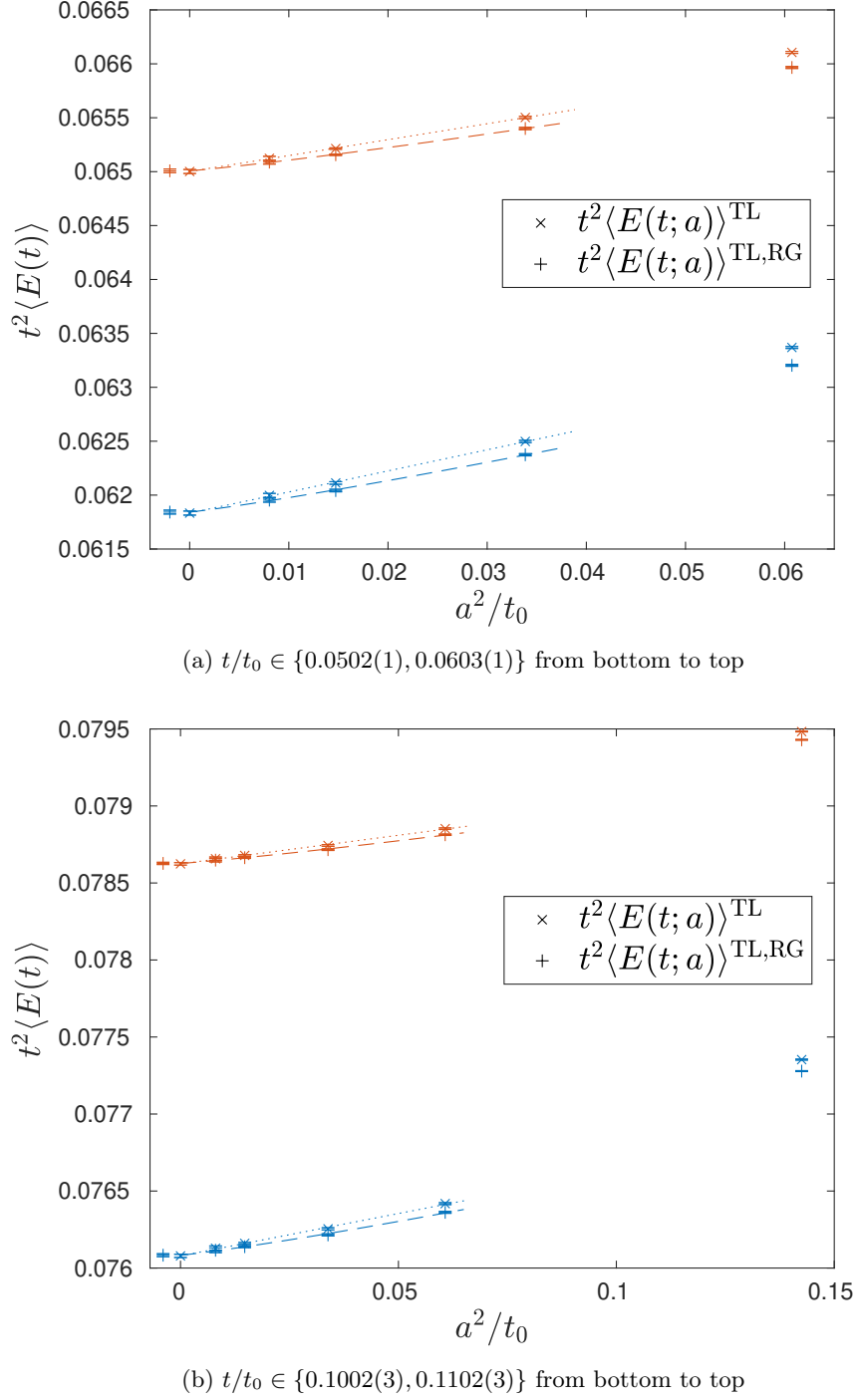


Figure 8.6: Continuum extrapolation of the action density $\langle E(t) \rangle$ using the linear combination (plaquette, clover) = (1/4, 3/4) to achieve tree-level $\mathcal{O}(a^2)$ improvement in combination with the Wilson action and Wilson flow (\times). As a second step, the leading logarithm from the operator at zero flow-time is divided out ($+$). The dotted line is a naive a^2 extrapolation while the dashed line makes use of the known leading power in the coupling $a^2\alpha_{\overline{\text{MS}}}(1/a)$, where the coupling has been obtained from 5-loop running [167] using $\sqrt{8t_0}\Lambda_{\overline{\text{MS}}} = 0.6227(94)$ [158] as input. The continuum extrapolated value of the Renormalisation Group improved case has been shifted to the left for readability.

8.3. Impact of non-zero anomalous dimensions on the continuum extrapolation

where we normalised the chosen \mathbf{r} to ensure comparability while on the lattice one must of course choose integer valued multiple of the lattice spacing. In this example the smallest lattice artifacts are found for the face diagonal. To continue the discussion we choose the on-axis direction as it offers the minimum distance available on the lattice. Assuming the lattice derivative ∂_r^{latt} in eq. (8.27) is chosen as

$$\partial_r^{\text{latt}} f(r + a/2) = \frac{9}{8} \frac{f(r + a) - f(r)}{a} - \frac{f(r + 2a) - f(r - a)}{24a} = \partial_r f(r + a/2) + \mathcal{O}(a^4) \quad (8.34)$$

ensures that no additional $\mathcal{O}(a^2)$ effects arise from the discretised lattice derivative. Then the only $\mathcal{O}(a^2)$ effects relevant at tree-level are those from the operator $\mathcal{O}_4^{(2)}$ or its counterpart in the diagonal basis $\mathcal{B}_2^{(2)}$

$$\frac{\alpha_{\text{qq}}(r; a)}{\alpha_{\text{qq}}(r; 0)} = 1 + 9 \frac{a^2}{r^2} \bar{b}_2^{\mathcal{B}} + \mathcal{O}(a^4, a^2 \alpha_{\overline{\text{MS}}}(1/a)), \quad (8.35)$$

where we switched to the diagonal basis which does not change anything here since the contribution of the second operator vanishes to the given order. From Symanzik Effective theory we thus know that the tree-level and Renormalisation Group improved coupling is

$$\alpha_{\text{qq}}^{\text{TL, RG}}(r; a) = \frac{\alpha_{\text{qq}}(r; a)}{1 + 9 \frac{a^2}{r^2} \bar{b}_2^{\mathcal{B}} \left[\frac{\alpha_{\overline{\text{MS}}}(1/a)}{\alpha_{\overline{\text{MS}}}(1/r)} \right]^{\hat{\gamma}_2}} \quad (8.36)$$

and the leading lattice artifacts are then expected to be of the form

$$\begin{aligned} \alpha_{\text{qq}}^{\text{TL, RG}}(r; a) - \alpha_{\text{qq}}(r; 0) &\sim a^2 [\alpha_{\overline{\text{MS}}}(1/a)]^{1+\hat{\gamma}_1} + \mathcal{O}(a^4, a^2 [\alpha_{\overline{\text{MS}}}(1/a)]^{1+\hat{\gamma}_2}) \\ &\sim a^2 [\alpha_{\overline{\text{MS}}}(1/a)]^{1.636} + \mathcal{O}(a^4, a^2 [\alpha_{\overline{\text{MS}}}(1/a)]^{2.145}). \end{aligned} \quad (8.37)$$

In case the tree-level improvement is performed to all orders in the lattice spacing, see e.g. [64] where an improved distance r_I is defined such that all tree-level lattice artifacts of the force are eliminated, the Renormalisation Group improvement at $\mathcal{O}(a^2)$ can still be established by additionally dividing out

$$\alpha_{\text{qq}}^{\text{TL(all), RG}}(r_I; a) = \frac{\alpha_{\text{qq}}(r_I; a)}{1 + 9 \frac{a^2}{r_I^2} \bar{b}_2^{\mathcal{B}} \left(\left[\frac{\alpha_{\overline{\text{MS}}}(1/a)}{\alpha_{\overline{\text{MS}}}(1/r_I)} \right]^{\hat{\gamma}_2} - 1 \right)}. \quad (8.38)$$

For the improved force a modified version of the improved distance r_I must be used to ensure absence of TL lattice artifacts to all orders in the lattice spacing. The benefit of using an improved derivative is that the different couplings $\alpha_{\overline{\text{MS}}}(1/r_I)$ and $\alpha_{\overline{\text{MS}}}(1/a)$ do not get mixed in the $\mathcal{O}(a^2)$ lattice artifacts. On the other hand the use of an improved derivative limits the available short distance region further and it may be beneficial to use an unimproved derivative instead, for which the prescription of Renormalisation Group Improvement in eq. (8.38) remains unchanged.

The generalisation to arbitrary short-distance observables as well as different tree-level improvement strategies is straight forward. It requires only the tree-level $\mathcal{O}(a^{n_{\text{min}}})$ contributions of the minimal basis computable in Symanzik Effective theory.

8.3.2 Using $\hat{\Gamma}_i$ for an error estimate

We can only speculate on how the leading anomalous dimensions will be used in the future. Especially for full lattice QCD the large number of anomalous dimensions and dense spectrum thereof will make an explicit use difficult due to various contributions competing as the leading ones. Instead the uncertainty stated for the continuum extrapolation should incorporate the various possibilities for leading powers in the coupling and of course take into account that the next-to-leading order lattice artifacts, i.e. $a^{n_{\text{min}}+1}$, are not necessarily subleading depending on the considered range of lattice spacings. The latter should be done anyway by now. It is also important to keep

in mind that the spectra in figure 8.2 have a broad range of values such that the subleading powers in the coupling for the smallest $\hat{\Gamma}_i$ will be as important as the larger $\hat{\Gamma}_i$ or even dominant over the larger $\hat{\Gamma}_i$ when considering non-perturbatively $O(a)$ improved Wilson quarks.

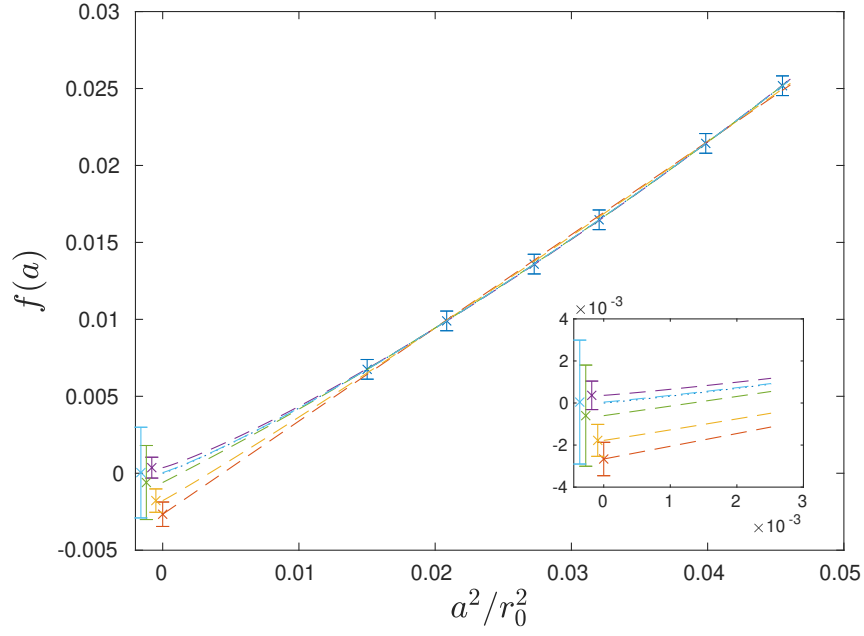
To get an idea what might happen due to the various powers in the coupling we consider massless Ginsparg-Wilson fermions with several choices for the $O(a^2)$ coefficients corresponding to each leading power in the coupling, i.e. we neglect subleading powers both in the coupling and in the lattice spacing. Firstly we consider the case with identical leading order contributions for each power in the coupling. Since this will not reflect the typical lattice data – in general we expect accidental cancellations and pile-ups of lattice artifacts – we also give three examples of coefficients chosen with a Gaussian distribution³ around zero which may cover some more realistic scenarios. According to any of these coefficients we may now generate dummy data lying on our theoretical curve with equally sized dummy uncertainties. Keep in mind that we neglect here the statistical fluctuations of the central values which one would of course encounter for statistical estimates extracted from lattice data. We also use a larger number of data points than what is usually available.

Using the dummy data we may then use fit ansätze guided by our results but also some typical choices in the literature and compare the deviation from the true continuum value as has been done in figure 8.8. Depending on the chosen coefficients (and of course also on the somewhat arbitrary uncertainties, here chosen to be 2.5 % of the difference between the minimum and maximum value of the predicted curve in the considered range of lattice spacings), we find that the naive a^2 -extrapolation can deviate up to 3 standard deviations from the correct continuum value for data points that seem indistinguishable from a straight line in the considered range of lattice spacings and also the ansatz $a^2[\alpha_{\overline{\text{MS}}}(1/a)]^{\min(\hat{\Gamma}_i)}$ does not improve the situation by much, while the ansatz $a^2[\alpha_{\overline{\text{MS}}}(1/a)]^{\tilde{\Gamma}}$ with $\tilde{\Gamma} = \frac{1}{7} \sum_i \hat{\Gamma}_i$ sometimes overcompensates. A special case is figure 8.8d, which at least hints at the fact that a straight line of the last three points may be a bad choice for an extrapolation due to its curvature. It also shows how problematic pile-ups and cancellations can be already for the limited dense spectrum of Ginsparg-Wilson fermions. In all four cases the three parameter extrapolations both with naive a^2 plus naive a^4 term and with guided choice of the leading powers in the coupling, here $a^2[\alpha_{\overline{\text{MS}}}(1/a)]^{\min(\hat{\Gamma}_i)}$ plus $a^2[\alpha_{\overline{\text{MS}}}(1/a)]^{\tilde{\Gamma}}$, yield results which are at least closer to the correct continuum value. Again, keep in mind that we neglected a^4 or higher order corrections entirely. Instead the three parameter extrapolations may serve as an important check whether a seemingly straight line behaves more like $a^2[\alpha_{\overline{\text{MS}}}(1/a)]^{\min(\hat{\Gamma}_i)}$ or $a^2[\alpha_{\overline{\text{MS}}}(1/a)]^{\tilde{\Gamma}}$ by comparing the central values and more generally whether a two parameter ansatz of a^2 accompanied by some power in the coupling is reasonable. The three parameter ansätze also give a more reasonable error estimate considering the difference between both ansätzen $a^2[\alpha_{\overline{\text{MS}}}(1/a)]^{\min(\hat{\Gamma}_i)}$ and $a^2[\alpha_{\overline{\text{MS}}}(1/a)]^{\tilde{\Gamma}}$, which should be taken into account somehow.

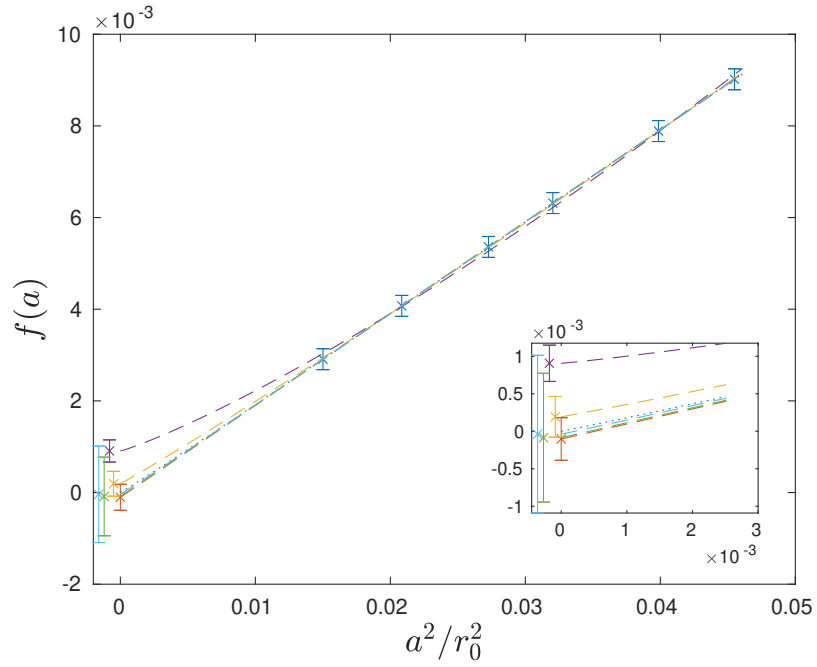
The samples are used here only to highlight the main issues arising from the various contributions to $O(a^2)$. There are certainly much more thoughts required on how to make proper error estimates as well as on how to treat data that is curved as in figure 8.8d. At least now we know the leading powers in the coupling for each contribution. For pure gauge theory all of this will be less difficult due to having to deal with only two (or three for Gradient flow) anomalous dimensions instead of 7 for massless Ginsparg-Wilson fermions or even more for non-perturbatively $O(a)$ improved Wilson fermions.

³The coefficients were chosen from $O(25)$ different samples, where cases like figure 8.8d occurred roughly three times. We make no claim on representativeness of the chosen number of cases.

8.3. Impact of non-zero anomalous dimensions on the continuum extrapolation



(a) $d = (1, 1, 1, 1, 1, 1)/7$



(b) $d \approx (0.18, -0.16, 0.14, 0.26, -0.20, 0.01, -0.06)$

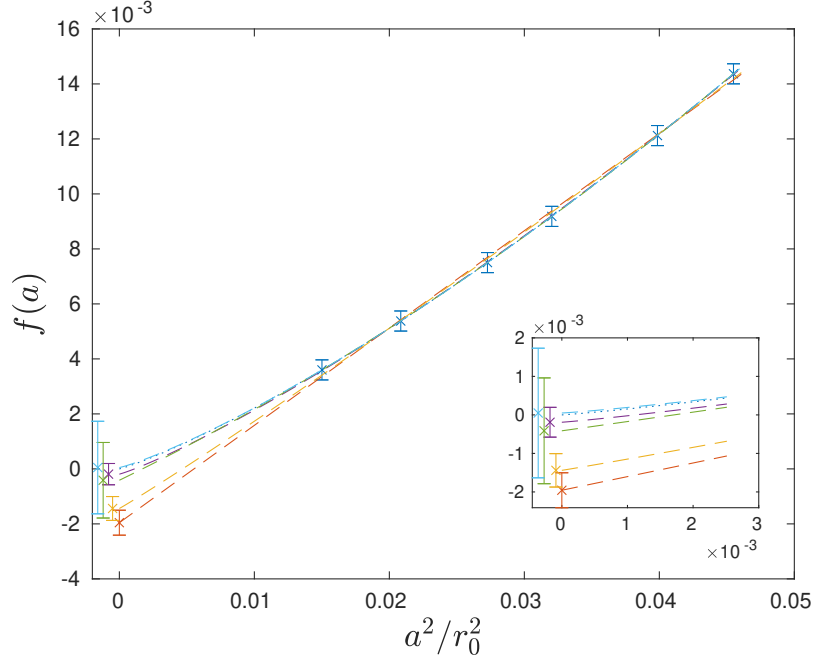
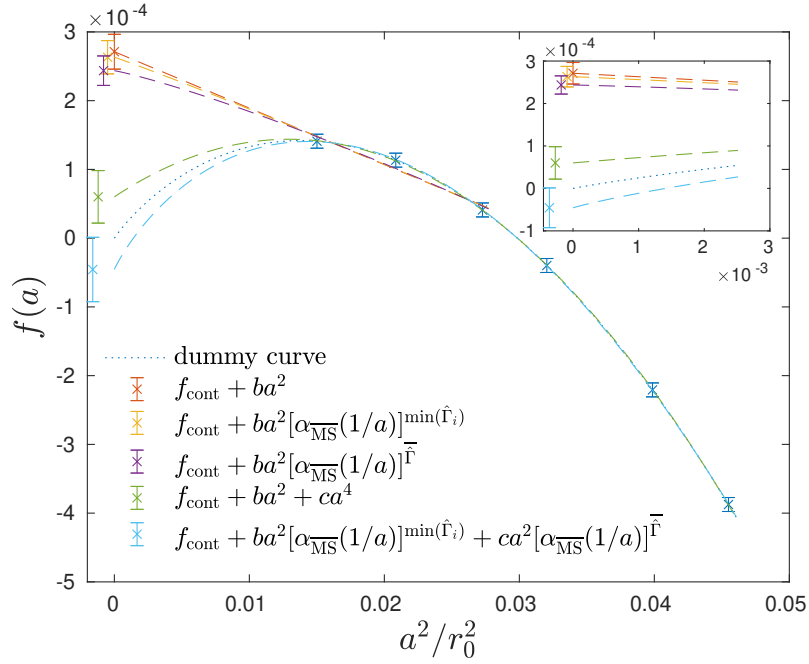

 (c) $d \approx (-0.01, 0.10, -0.03, -0.02, 0.21, 0.20, 0.20)$

 (d) $d \approx (-0.20, -0.28, 0.06, 0.06, 0.01, 0.07, 0.15)$

Figure 8.8: Examples for continuum extrapolations with dummy data using our results for massless Ginsparg-Wilson quarks with $N_f = 3$. The various $O(a^2)$ terms are summed $a^2 \sum_i d_i [2\beta_0 \alpha_{\overline{\text{MS}}}(1/a)]^{\hat{\Gamma}_i}$ with coefficients d_i , chosen to be identical (top left) or Gaussian distributed (others), and $\hat{\Gamma} \approx (1, 1.64, 0.76, 0.25, 0.67, 1.14, 1.49)$. For better readability the different extrapolation attempts have been shifted to the left. All ansätze used can be found in the legend of the plot at the bottom, where $\bar{\Gamma} = \frac{1}{7} \sum_i \hat{\Gamma}_i$ is the average power in the coupling.

8.4 Using multiple lattice fermion actions

As mentioned earlier the use of more than one lattice discretisation for different flavours inevitably breaks flavour permutation symmetry. Nonetheless the symmetry constraints for the subsets of flavours simulated with either discretisation do not change.

To understand the implications let us assume for now only two different lattice discretisations e.g. Ginsparg-Wilson fermions for the set of flavours q and Wilson fermions for the set Q with $N_f = N_f^q + N_f^Q$ and $N_f^q, N_f^Q > 1$. The choices for N_f^q, N_f^Q exclude $N_f^q = 1$ or $N_f^Q = 1$ as in this case less operators would contribute due to Fierz identities. While the overall flavour symmetries such as $SU(N_f)_V$ and even flavour permutation symmetry are broken, the symmetry constraints for the subsets q and Q remain intact, i.e. here $SU(N_f^q)_L \times SU(N_f^q)_R \times U(1)_V$ for the set q and $SU(N_f^Q)_V$ for the set Q . Other symmetries like H_4 symmetry, gauge symmetry or \mathcal{C} , \mathcal{P} , \mathcal{T} invariance remain intact as well. Consequently our considerations for the minimal basis remain the same and we expect only more combinations in flavour space.

For our specific example the minimal basis at mass-dimension 6 (we assume here $O(a)$ improved Wilson fermions) then reads

$$\begin{aligned}
& \frac{1}{g_0^2} \text{tr} (D_\mu F_{\nu\rho} D_\mu F_{\nu\rho}), & \frac{1}{g_0^2} \sum_\mu \text{tr} (D_\mu F_{\mu\rho} D_\mu F_{\mu\rho}), & \sum_\mu \bar{q} \gamma_\mu D_\mu^3 q, & \sum_\mu \bar{Q} \gamma_\mu D_\mu^3 Q, \\
& (\bar{q} \Gamma_{\text{chiral}} q)^2, & (\bar{q} \Gamma_{\text{chiral}} T^a q)^2, & (\bar{Q} \Gamma Q)^2, & (\bar{Q} \Gamma T^a Q)^2, \\
& (\bar{q} \Gamma_{\text{chiral}} q) (\bar{Q} \Gamma_{\text{chiral}} Q), & (\bar{q} \Gamma_{\text{chiral}} T^a q) (\bar{Q} \Gamma_{\text{chiral}} T^a Q), & & \\
& \Gamma = \{\mathbb{1}, \gamma_5, \gamma_\mu, \gamma_\mu \gamma_5, \sigma_{\mu\nu}\}, & \Gamma_{\text{chiral}} = \{\gamma_\mu, \gamma_\mu \gamma_5\}. & &
\end{aligned} \tag{8.39}$$

The only truly new operators are $(\bar{q} \Gamma_{\text{chiral}} q) (\bar{Q} \Gamma_{\text{chiral}} Q)$ and $(\bar{q} \Gamma_{\text{chiral}} T^a q) (\bar{Q} \Gamma_{\text{chiral}} T^a Q)$ while the others were to be expected due to the symmetry constraints on the flavour subsets. Notice that operators from both sets of flavours are allowed to mix as they transform trivially under one another's flavour symmetry transformations. Operators with explicit mass-dependence have been discarded again but we expect an increased number of such operators as well.

While the absence of 4-fermion operators that break chiral symmetry and mix the flavour subsets is due to symmetry constraints it reveals something about the mixing between differently flavoured 4-fermion operators in eq. (6.55), in particular the subblocks B and H in eqs. (6.57) and (6.61). There one finds that only operators invariant under chiral rotations are allowed to mix into differently flavoured 4-fermion operators. If this was not the case our minimal basis in eq. (8.39) would be incomplete.

All information on the mixing of the operators in eq. (8.39) is actually contained in the mixing of the single flavour bilinears as well as single flavour and 2-flavour 4-fermion operators (plus some redundant part, see e.g. section 6.4). For the 4-fermion operators the relevant information can be found in eqs. (6.26) and (6.28), while their contributions to the pure gauge operators and fermion bilinears have been given only for flavour singlets so far. To give the reader all results necessary to cover the cases discussed here we also give the fully flavoured mixing matrix that we obtained during our computations for the flavour singlet basis at mass-dimension $[\mathcal{O}] < 6$

$$\begin{aligned}
\mathcal{O}_{1;\overline{\text{MS}}}^{f(-1)} &= \left\{ 1 - \frac{3}{2\epsilon} \frac{N^2 - 1}{N} \bar{\alpha} \right\} \mathcal{O}_1^{f(-1)} + O(\bar{\alpha}^2), \\
\mathcal{O}_{1;\overline{\text{MS}}}^{(0)} &= \left\{ 1 - \left(\frac{11}{3\epsilon} N - \frac{2}{3\epsilon} N_f \right) \bar{\alpha} \right\} \mathcal{O}_1^{(0)} + 3 \frac{N^2 - 1}{N} \frac{\bar{\alpha}}{\epsilon} \sum_f m_{\overline{\text{MS}}}^f \mathcal{O}_1^{f(-1)} + O(\bar{\alpha}^2), \\
\mathcal{O}_{4;\overline{\text{MS}}}^{f(1)} &= \left\{ 1 + \frac{N^2 - 5}{2N\epsilon} \bar{\alpha} \right\} \mathcal{O}_4^{f(1)} - 4 \frac{\bar{\alpha}}{\epsilon} m_{\overline{\text{MS}}}^f \mathcal{O}_1^{(0)} - 6 \frac{N^2 - 1}{N} \frac{\bar{\alpha}}{\epsilon} \left(m_{\overline{\text{MS}}}^f \right)^2 \mathcal{O}_1^{f(-1)}. \tag{8.40}
\end{aligned}$$

and at mass-dimension 6

$$\begin{aligned}
 \begin{pmatrix} \mathcal{O}_2^{(2)} \\ \mathcal{O}_4^{(2)} \\ \mathcal{O}_{10}^{f(2)} \end{pmatrix}_{\overline{\text{MS}}} &= \begin{pmatrix} 1 + \left(\frac{7}{3}N + \frac{2}{3}N_f\right) \frac{\bar{\alpha}}{\epsilon} & 0 & 0 \\ -\frac{7}{15}N \frac{\bar{\alpha}}{\epsilon} & 1 + \left(\frac{21}{5}N + \frac{2}{3}N_f\right) \frac{\bar{\alpha}}{\epsilon} & -\frac{11}{60} \frac{N^2-1}{N} \frac{\bar{\alpha}}{\epsilon} \sum_{f'} \\ \frac{11}{60} \frac{\bar{\alpha}}{\epsilon} & -\frac{11}{15} \frac{\bar{\alpha}}{\epsilon} & 1 + \frac{157}{60} \frac{N^2-1}{N} \frac{\bar{\alpha}}{\epsilon} \delta^{ff'} \end{pmatrix} \begin{pmatrix} \mathcal{O}_2^{(2)} \\ \mathcal{O}_4^{(2)} \\ \mathcal{O}_{10}^{f'(2)} \end{pmatrix} \\
 &+ \sum_{e'=f'} \begin{pmatrix} \frac{5N^2-16}{6N} \delta_{j,11} + \frac{16-5N^2}{6N} \delta_{j,12} \\ \frac{167N^2-423}{480N} \delta_{j,11} + \frac{423-167N^2}{480N} \delta_{j,12} \\ \frac{7}{240} \{-2\delta_{j,11} + 2\delta_{j,12} + \frac{N-2}{N} \delta_{j,13} + \delta_{j,14}\} \end{pmatrix} \frac{\bar{\alpha}}{\epsilon} \mathcal{O}_j^{e'f'(2)} \\
 &+ \sum_{e'=f'} \begin{pmatrix} \frac{4N^3+N^2-20N+4}{12N^2} \delta_{j,13} + \frac{4N^3+9N^2-20N+18}{12N^2} \delta_{j,14} \\ \frac{73N^3+94N^2-537N+114}{960N^2} \delta_{j,13} + \frac{73N^3+240N^2-537N+480}{960N^2} \delta_{j,14} \\ \frac{13N^2-53}{160N} (\delta_{j,11} - \delta_{j,12}) \delta^{fe'f'} \end{pmatrix} \frac{\bar{\alpha}}{\epsilon} \mathcal{O}_j^{e'f'(2)} \\
 &+ \begin{pmatrix} 0 \\ 0 \\ \left\{ \frac{7N^3+6N^2-27N-26}{320N^2} \delta_{j,13} + \frac{7N^3+20N^2-27N+40}{320N^2} \delta_{j,14} \right\} \delta^{fe'f'} \end{pmatrix} \frac{\bar{\alpha}}{\epsilon} \mathcal{O}_j^{e'f'(2)} \\
 &+ \sum_{e'<f'} \begin{pmatrix} (3 - \frac{3}{N^2}) \delta_{j,14} + (\frac{N}{3} + \frac{4}{3N}) \delta_{j,18} + (\frac{12}{N} - 3N) \delta_{j,19} \\ (1 - \frac{1}{N^2}) \delta_{j,14} + (\frac{47N}{120} + \frac{19}{40N}) \delta_{j,18} + (\frac{4}{N} - N) \delta_{j,19} \\ \left(\frac{N^2-1}{8N^2} \delta_{j,14} + \frac{3N^2-13}{80N} \delta_{j,18} - \frac{N^2-4}{8N} \delta_{j,19} \right) (\delta^{fe'} + \delta^{ff'}) - \frac{7}{30} \delta_{j,18} \end{pmatrix} \frac{\bar{\alpha}}{\epsilon} \mathcal{O}_j^{e'f'(2)} \\
 &+ \begin{pmatrix} \frac{3}{2} N \frac{\bar{\alpha}}{\epsilon} \delta^{e'f'} \\ \left(\frac{79}{240}N + \frac{11}{240N} \right) \frac{\bar{\alpha}}{\epsilon} \delta^{ef'} \\ \left(\frac{37}{240}N + \frac{83}{240N} \right) \frac{\bar{\alpha}}{\epsilon} \delta^{fe'f'} \end{pmatrix} m_{\overline{\text{MS}}}^{e'} \mathcal{O}_4^{f'(1)} + \begin{pmatrix} 0 \\ 0 \\ \frac{\bar{\alpha}}{\epsilon} \delta^{fe'} \end{pmatrix} \left(m_{\overline{\text{MS}}}^{e'} \right)^2 \mathcal{O}_1^{(0)} \\
 &+ \begin{pmatrix} \frac{4}{N} \frac{N^2-1}{N} \frac{\bar{\alpha}}{\epsilon} \delta^{e'f'} \\ \frac{149}{120} \frac{N^2-1}{N} \frac{\bar{\alpha}}{\epsilon} \delta^{ef'} \\ \frac{197}{120} \frac{N^2-1}{N} \frac{\bar{\alpha}}{\epsilon} \delta^{fe'f'} \end{pmatrix} \left(m_{\overline{\text{MS}}}^{e'} \right)^3 \mathcal{O}_1^{f'(-1)}, \tag{8.41}
 \end{aligned}$$

where again $4\pi\bar{\alpha} = \alpha_{\overline{\text{MS}}}$, $\sum_{f'}$ denotes the summation over all flavours f' and for multiple indices in a Kronecker delta applies the rule from eq. (A.18). The generalisation to more/different actions with flavour subsets compatible to our symmetry constraints is thus straight forward but requires a specific choice of the $N_f^{q,Q,\dots}$. In particular the extension to $N_f^q = 1$ or $N_f^Q = 1$ is of course possible. For each choice the renormalisation of the proper minimal basis can be reconstructed from the fully flavoured mixing but depends on the $N_f^{q,Q,\dots}$, which makes a general statement complicated, except that even more operators will contribute.

Chapter 9

Discussion

We started the analysis of the leading logarithmic corrections to lattice artifacts from the action of lattice pure gauge theory and lattice QCD at $O(a)$ and $O(a^2)$ under the impression of the $O(3)$ model, where such corrections $a^2[\alpha_{\overline{\text{MS}}}(1/a)]^{\hat{\Gamma}^{(2)}}$ can be as problematic as $\hat{\Gamma}^{(2)} = -3$ [1, 2]. Contributions from the action are the only relevant ones for spectral quantities and we will limit the discussion here to such quantities unless mentioned otherwise. For both, lattice pure gauge theory and lattice QCD with Wilson, twisted Wilson or Ginsparg-Wilson quarks we do not find such problematic behaviour. Lattice pure gauge theory has only two operators at mass-dimension 6 with leading powers in the coupling $\hat{\Gamma}^{(2)} \in \{0.636, 1.145\}$ parametrising all lattice artifacts relevant for spectral quantities, thus improving the convergence as $a \searrow 0$ compared to classical a^2 behaviour. Generalisation of pure gauge theory to static quarks does not introduce any new operators to the minimal basis at $O(a^2)$ nor does the use of smeared gauge links in the static quark action change the tree-level matching coefficients and we expect precisely the same behaviour of the leading lattice artifacts. The situation for lattice QCD is more difficult.

Firstly, there are $O(a)$ corrections for unimproved Wilson quarks, which introduce one mass-independent mass-dimension 5 operator, the so called Sheikholeslami-Wohlert term, and several mass-dependent operators. While the Sheikholeslami-Wohlert term again improves convergence due to $\hat{\Gamma}_1^{(1)} = \frac{2}{33-6N_f}$ at $N = 3$, the mass-dependent operators have only $\hat{\Gamma}^{(1)} \gtrsim -0.6$ for $N_f \leq 8$ and thus worsen the convergence as $a \searrow 0$. This may not be an issue for sufficiently small quark masses, e.g. $N_f < 4$ for physical quark masses, since the additional mass-dependence is expected to suppress the contributions. However, the fact that such contributions are present should be kept in mind and the impact thereof should be checked if possible. Assuming $\hat{\Gamma}_1^{(1)}$ is in fact the leading contribution, the continuum extrapolation should be performed with leading correction $a[\alpha_{\overline{\text{MS}}}(1/a)]^{\hat{\Gamma}_1^{(1)}}$ rather than the classical a , but this is not expected to have a large impact as e.g. for $N_f = 3$ we find $\hat{\Gamma}_1^{(1)} \approx 0.133$ rather close to zero. For incompletely $O(a)$ improved Wilson quarks, i.e. perturbatively $(n_I - 1)$ -loop improved Wilson quarks, not only some (depending on n_I) severely suppressed $O(a)$ effects remain as the overall spectrum is shifted by $\hat{\Gamma}(1) \rightarrow \hat{\Gamma}^{(1)} + n_I$ but also additional contact terms contribute to $O(a^2)$ due to the double insertions of the remaining mass-dimension 5 operators and have to be taken into account in the perturbative matching of SET and the underlying lattice theory.

In the case of non-perturbatively $O(a)$ improved Wilson quarks or Ginsparg-Wilson quarks the impact of massive operators is less severe and one finds $\hat{\Gamma}^{(2)} \gtrsim -0.28$ for $N_f \leq 8$. For $N_f < 8$ all leading powers in the coupling from operators persistent in the zero mass limit improve convergence, but the smallest power is $\hat{\Gamma}_4^{(2)} \gtrsim 0.005$, which is much closer to zero than in the case of pure gauge theory. A more troubling feature of the spectra for both Wilson and Ginsparg-Wilson fermions is the presence of 4-fermion operators which leads to a very dense spectrum of several $\hat{\Gamma}^{(2)}$ such that no contribution clearly dominates. This will in general lead to cancellations and pile-ups amounting to complicated lattice artifacts. While Ginsparg-Wilson fermions have only seven

operators contributing in the massless case, improved Wilson fermions have already 13 different ones. The range of leading powers in the coupling goes (at $N_f = 3$) up to $\hat{\Gamma}_2^{(2)} \approx 1.6$ for Ginsparg-Wilson fermions and up to $\hat{\Gamma}_{13}^{(2)} \approx 2.7$ for improved Wilson fermions, which will yield contributions indistinguishable from a^3 or maybe even a^4 -corrections for the latter at small lattice spacings. Due to the wide spread of the leading powers in the coupling the subleading corrections of the mass-dimension 6 operators with smallest leading powers may still be larger than the leading corrections of mass-dimension 6 operators with largest leading powers.

When considering two maximally twisted Wilson quarks the overall spectrum to be expected is almost the same as for non-perturbatively $O(a)$ improved Wilson quarks but with three additional leading powers in the coupling due to double insertions of mass-dimension 5 operators. These double insertions also lead to contact terms that affects the matching coefficients at $O(a^2)$ and thus may invalidate the vanishing of the tree-level matching coefficients for chiral symmetry violating 4-fermion operators. This reduces the corresponding leading powers in the coupling by one compared to non-perturbatively $O(a)$ improved Wilson quarks. The minimal power for operators present in the massless limit is then $\hat{\Gamma}^{(2)} \approx -0.122$ or if the tree-level matching coefficients still vanishes despite of contact terms $\hat{\Gamma}_{1,1}^{(2)} \approx 0.138$. In both cases the leading powers are very close to zero and thus do not impact the classical a^2 behaviour particularly. For $(n_1 - 1)$ -loop perturbative $O(a)$ improved twisted Wilson quarks the leading power is at least shifted up by one, while $\hat{\Gamma}_{1,1}^{(2)}$ is even shifted by $2n_1$. In the case of non-perturbative $O(a)$ improvement $\hat{\Gamma}_{1,1}^{(2)}$ and any other leading powers due to double insertions of mass-dimension 5 operators are absent, which yields exactly the same spectrum as for untwisted non-perturbatively $O(a)$ improved Wilson quarks.

The generalisation of our results to two or more different lattice discretisations for separate flavours does not yield anything new except a few more operators in the minimal basis due to broken flavour permutation symmetry. The overall spectrum then depends on the specific discretisation choices for different flavours and can be obtained from the flavour dependent mixing given in section 8.4.

A special case is the Yang-Mills Gradient flow as local fields at positive flow-time do not introduce additional non-zero anomalous dimensions and can be treated fully classically. At zero flow-time this would not be the case, which is the reason we limited ourselves to spectral quantities so far as anomalous dimensions would depend on the local fields involved. Hence for the Yang-Mills Gradient flow corrections from local fields at positive flow time can be easily worked into the SET by doing the naive expansion in the lattice spacing to obtain tree-level matching coefficients. Alternatively one can immediately choose classically improved local fields, which then limits contributions of leading order lattice artifacts to the action at zero flow-time or the flow action unless the latter is classically improved as well. This fact also allows to severely limit all contributions relevant to $O(a^2)$ by classically improving all flow quantities as well as the flow action, which then only leaves the anomalous dimensions (and contributions) from the mass-dimension 6 operators of the pure gauge action at zero flow-time and any local fields also present at zero flow-time. Due to modified EOMs in the 4+1-dimensional theory of the Yang-Mills Gradient flow one additional operator is needed to parametrise all lattice artifacts from the action to $O(a^2)$. As it turns out this operator has a vanishing 1-loop anomalous dimension and thus behaves classically to that order (and tree-level contributions can be easily divided out without leaving large leading logarithms at $O[a^2 \alpha_{\overline{\text{MS}}}(1/a)]$). Whether this is by accident or holds true to all orders by some symmetry argument is unknown and needs additional insight. If contributions of this third operator are not removed it dominates the leading lattice artifacts together with any lattice artifacts from any unimproved flow quantities, which all give naive a^2 corrections while the other two operators at zero flow time again introduce leading powers in the coupling $\hat{\Gamma}^{(2)} \in \{0.636, 1.145\}$ as in the case of pure gauge theory without the flow.

What we can learn from this is fourfold. Firstly, as mentioned before, the approach of the continuum limit as $a \searrow 0$ is in all considered lattice theories expected to be well-behaving, i.e., no significantly negative powers in the coupling such that the leading logarithms either worsen the

naive a^n ($n = 1, 2$) power-law only slightly or even improve convergence.

Secondly, we have now the leading logarithmic corrections $a^n[\alpha_{\overline{\text{MS}}}(1/a)]^{\hat{\Gamma}^{(n)}}$ to the a^n power-law, which should be used in continuum extrapolations as a proper ansatz rather than the naive a^n . However, for full QCD and $O(a^2)$ corrections this will likely not be very effective due to the dense spectrum such that one should refrain from using one (or multiple) explicit $\hat{\Gamma}$ and instead modify the $\hat{\Gamma}$ in the range of powers predicted by the SET to get a better handle on the overall systematic uncertainty of the continuum extrapolation. How this can be done in practice remains to be seen. Thirdly, aside the observation that SET can give helpful insight into the small lattice spacing dependence, we find that perturbative Symanzik improvement will significantly improve the convergence when tree-level improvement is carried out. Especially for non-perturbatively $O(a)$ improved Wilson and Ginsparg-Wilson fermions we find that removing only the three operators $\mathcal{O}_2^{(2)}$, $\mathcal{O}_4^{(2)}$ and $\mathcal{O}_{10}^{(2)}$ of the non-diagonal basis (apart from massive operators) at tree-level will roughly increase the minimum of the spectrum by 1 and thus do the same for the leading powers in the coupling. Since all three operators preserve chiral symmetry, the shift in the spectrum applies only to all chirally symmetric elements of our minimal basis, while the spectrum of operators violating chiral symmetry remains unaffected, which is only relevant for the Wilson case, while for Ginsparg-Wilson fermions the entire spectrum gets shifted. For twisted mass QCD at maximal twist also the mass-dimension 5 operators would need perturbative $(n_I - 1)$ -loop improvement to shift their contributions through double operator insertions, which also introduce contact terms modifying the tree-level matching coefficients. Perturbative $O(a)$ improvement of maximally twisted QCD then immediately shifts all these contributions to the spectrum at $O(a^2)$ by $2n_I$. The benefit of Symanzik improvement becomes even more apparent for the Yang-Mills Gradient flow, where one can remove all contributions at $O(a^2)$ to all orders in perturbation theory that do not originate from the zero flow-time boundary [162].

Fourthly, short-distance observables with distance r , which have been tree-level improved at the level of expectation values, suffer from leading logarithmic corrections $O(a^n \ln(a/r) \alpha_{\overline{\text{MS}}}(1/a))$ that remain. These $\ln(a/r)$ can be taken care of by Renormalisation Group improvement, which requires exactly the anomalous dimensions computed here (plus additional anomalous dimensions for each local field for non-spectral quantities). Upon removal of the leading logarithms the remainder is finally of $O(a^n \alpha_{\overline{\text{MS}}}(1/a))$ without any logarithms of the lattice spacing at 1-loop. For higher order perturbative improvement with Renormalisation Group Improvement the anomalous dimensions are also needed to higher loop orders.

So far we focused on parts which are contained within the results of this thesis – probably requiring some effort to extract the desired information. There are, however, topics we did not consider or explicitly excluded from the beginning. We give here only an overview of some aspects that should be done making no claim to be exhaustive.

Staggered quarks Due to reduced symmetry constraints for staggered quarks the minimal basis of operators at mass-dimension 6 has to be derived. We only know that the entire minimal basis of Ginsparg-Wilson fermions will be present as a subset due to less restrictive symmetry constraints. Thus the minimal spread of the anomalous dimensions as well as both lower and upper bounds for the maximum and minimum values of $\hat{\Gamma}$ are known. Whether the additional operators introduce additional anomalous dimensions within these bounds is unknown and should be checked. This is particularly important because of the prominent position staggered fermions have in lattice QCD simulations due to low computational cost. Two things should also be established alongside these leading logarithms. Firstly a proof of renormalisability of staggered quarks to all orders in perturbation theory as has been done for Wilson [88] and Ginsparg-Wilson fermions [89], using the power counting theorem for staggered quarks [172]. Secondly a proof that rooted staggered quarks give in fact the correct continuum physics as $a \searrow 0$, see e.g. [173]. Both are needed to ensure that SET with QCD as the continuum action is applicable.

Gradient flow for full QCD In this thesis we only computed the anomalous dimensions needed for the Yang-Mills Gradient flow, i.e. pure gauge theory. In the presence of quarks there is also an additional fermion bilinear needed for the minimal basis at the zero flow-time boundary as derived in section 7.1. To distinguish the mixing of these operators one then needs a second renormalisation condition because we would have now two different mixing contributions mixing among each other and into the full QCD on-shell basis that are not available from QCD at zero flow-time. Since the additional fermion bilinear vanishes at tree-level when inserted into the vacuum expectation value of the action density $E(t)$ or any other operator at positive flow-time without fermions one likely must go to higher loop orders to obtain the 1-loop mixing of this operator. In case also the quark fields are flowed, see e.g. [174, 175], multiple new operators will become relevant including new $O(a)$ terms for Wilson quarks and local fields at positive flow-time involving quark fields or the associated Lagrange multipliers require renormalisation [174]. This complicates the situation as composite operators at positive flow-time now carry anomalous dimensions, which are known, if quark fields are present.

Corrections from local fields Except for the Yang-Mills Gradient flow all considerations have been limited to spectral quantities like masses of hadrons. In case one is interested in non-spectral quantities like e.g. matrix elements also the contributions from local fields used to extract the desired matrix element from the lattice need to be taken into account. For spectral quantities these additional contributions cancel out. Each local field then has its own minimal basis of higher dimensional operators constrained by the transformation properties of the local field, where each element of the basis contributes an additional anomalous dimension. Apart from total divergence operators, which now need to be kept in the basis for the local fields, the entire analysis can proceed as for the minimal basis of the action and then be used in eq. (4.42) generalised to n -point functions. One example of such anomalous dimensions has been briefly discussed in [3] for the $O(a)$ corrections of the non-singlet vector and axial vector current for Wilson quarks following [176]

$$V_\mu^{r,s}(x) = \bar{\psi}_r(x) \gamma_\mu \psi_s(x) + a c^V \partial_\nu T_{\mu\nu}^{r,s}(x), \quad (9.1)$$

$$A_\mu^{r,s}(x) = \bar{\psi}_r(x) \gamma_\mu \gamma_5 \psi_s(x) + a c^A \partial_\mu P^{r,s}(x). \quad (9.2)$$

The additional anomalous dimensions for the non-singlet tensor current $T_{\mu\nu}^{r,s}(x)$ and the pseudo scalar density $P^{r,s}(x)$ can be found in the literature [177, 178]

$$\hat{\gamma}^T = \frac{3(N^2 - 1)}{2N(11N - 2N_f)} \stackrel{N=3}{=} \frac{4}{33 - 2N_f}, \quad \hat{\gamma}^P = -3\hat{\gamma}^T. \quad (9.3)$$

The tree-level matching coefficients $c^{V,A}$ are zero due to vanishing of the $O(a)$ terms in the naive expansion in the lattice spacing of both vector and axial vector currents, i.e. $\hat{\Gamma} \in \{1 + \hat{\gamma}^V, 1 + \hat{\gamma}^P\}$. Again both leading powers in the coupling modifying the classical a power-law are larger zero (for $N_f < 11$) and thus improve convergence. However there is no guarantee that this will always be the case for other local fields and their additional anomalous dimensions. The only way to be certain is to compute all the relevant 1-loop anomalous dimensions. For fermion bilinear operators with Wilson fermions the necessary $O(a)$ improvement coefficients (and thus the corresponding minimal operator basis) have been worked out in [176, 179, 180].

Acknowledgements

First of all, I would like to thank my supervisor Rainer Sommer for offering me this project that suited my interests very well. Although this project is a bit off the daily projects of the group he encouraged me to work on this topic and develop my own solutions and strategies to emerging problems. I learned a lot from our discussions and the literature he suggested to me if I needed more insights.

I would also like to thank my second supervisor Peter Marquard for helping me with questions on perturbative renormalisation but also on the analytical solutions to complicated flow-time and Schwinger parameter integrals. For the latter I have to thank Johannes Blümlein, too, for his consult on how to typically treat such integrals.

Many thanks go to Kay Schönwald sharing an office with me for some time, who had valuable insight into renormalisation of QCD and shared his thoughts on current and future projects in particle physics, as well as to Hubert Simma for the many discussions on the general concepts and ideas of Symanzik Effective theory, renormalisation etc. but also on topics beyond the project of this thesis. This helped to challenge but also improve my own understanding of the project and lead me to new ideas what to check or try, while broadening my view on particle physics. In particular Hubert Simma helped me to keep my sanity during the measures against the Corona virus through virtual coffee breaks on a regular basis.

Appendix A

Conventions

A.1 Abbreviations

1PI	one-particle irreducible	$\overline{\text{MS}}$	modified minimal subtraction
1LPI	one-light-particle-irreducible	MS lat	lattice minimal subtraction
BGF	background field	QCD	Quantum Chromodynamics
EOM	equation of motion	QFT	Quantum Field Theory
GW	Ginsparg-Wilson	RGE	Renormalisation Group Equation
HQET	Heavy Quark Effective Theory	RGI	Renormalisation Group Invariant
IBP	integration by parts	RI	regulator independent
IR	infrared	SET	Symanzik effective theory
LL	leading logarithm	SM	Standard Model
NLL	next-to-leading logarithm	tmQCD	twisted mass QCD
LPT	lattice perturbation theory	UV	ultraviolet
LRT	lattice regularised theory	YM	Yang-Mills

A.2 Index conventions

Unless mentioned otherwise indices occurring exactly twice imply summation based on the Einstein summation convention. The occurring indices are distinguished in the following way:

- **Space-time components:**
Lower-case Greek indices as subscripts run over all dimensions, e.g. p_μ with $\mu \in \{0, 1, \dots, (D-1)\}$ denotes any component of a vector.
- **Purely space components:**
Lower-case Latin indices as subscripts run over all dimensions except time, e.g. p_j with $j \in \{1, 2, \dots, (D-1)\}$ denotes any component of a vector excluding time. There are exceptions from this rule:
 - Indices numbering our operators of mass dimension 5 and 6 and the corresponding renormalisation factors as well as coefficients,
 - Indices numbering external fields in a Green's function.
- **Colour components in the adjoint representation:**
Lower-case Latin indices as superscripts run over all generators of the $\mathfrak{su}(N)$ algebra, e.g. ϕ^a with $a \in \{1, 2, \dots, (N^2 - 1)\}$ is the component of the field $\phi = \phi^a T^a$ corresponding to the generator T^a labelled by the index a .

- **Colour components in the fundamental representation:**

Upper-case Latin indices as subscripts run over all colours, e.g. ψ_A with $A \in \{1, 2, \dots, N\}$ is the fermionic field with colour A .

A.3 $\mathfrak{su}(N)$ algebra

The generators T^a of the $\mathfrak{su}(N)$ algebra are chosen to be anti-hermitian and are normalised to

$$\text{tr} (T^a T^b) = -T_F \delta^{ab}. \quad (\text{A.1})$$

They obey the commutation relations

$$[T^a, T^b] = f^{abc} T^c, \quad (\text{A.2})$$

with the totally antisymmetric structure constants f^{abc} , which fulfil

$$f^{abc} f^{abd} = C_A \delta^{cd}, \quad f^{ade} f^{abc} = f^{aeb} f^{acd} + f^{ace} f^{abd}, \quad (\text{A.3})$$

where C_A is a constant. These generators can be used to define gauge fields

$$A_\mu(x) = A_\mu^a(x) T^a \in \mathfrak{su}(N), \quad A_\mu^a(x) \in \mathbb{R}. \quad (\text{A.4})$$

From these gauge fields one can construct the field strength tensor

$$F_{\mu\nu} = \partial_\mu A_\nu - \partial_\nu A_\mu + [A_\mu, A_\nu] \equiv [D_\mu, D_\nu], \quad (\text{A.5})$$

and the dual field strength tensor

$$\tilde{F}_{\mu\nu} = \frac{1}{2} \epsilon_{\mu\nu\rho\sigma} F_{\rho\sigma}, \quad (\text{A.6})$$

where D_μ is the covariant derivative. In the fundamental representation the covariant derivative takes the following form

$$D_\mu = \partial_\mu + A_\mu, \quad \overleftarrow{D}_\mu = \overleftarrow{\partial}_\mu - A_\mu, \quad (\text{A.7})$$

while one finds in the adjoint representation

$$D_\mu^{ab} = \delta^{ab} \partial_\mu + f^{acb} A_\mu^c. \quad (\text{A.8})$$

The generators fulfil the identity [181, p. 141ff.]

$$T_{AB}^a T_{CD}^a = \alpha (\delta_{AD} \delta_{BC} - \beta \delta_{AB} \delta_{CD}),$$

with free coefficients α, β . Contracting the above relation on both sides with δ_{AB} or T_{BA}^b yields

$$\begin{aligned} 0 &= \alpha(1 - \beta N) \delta_{CD} \Rightarrow \beta = \frac{1}{N}, \\ -T_F T_{CD}^b &= \alpha T_{CD}^b \Rightarrow \alpha = -T_F. \end{aligned}$$

With these ingredients we can now write down the following useful relations

$$\begin{aligned} T_{AB}^a T_{CD}^a &= -T_F \left(\delta_{AD} \delta_{BC} - \frac{1}{N} \delta_{AB} \delta_{CD} \right), \\ T_{AB}^a T_{BC}^a &= -C_F \delta_{AC}, \quad \text{with } C_F = T_F \frac{N^2 - 1}{N}, \\ T_{AB}^a T_{BC}^b T_{CD}^a &= -\frac{T_F}{N} T_{AD}^b = -(C_F - N T_F) T_{AD}^b, \\ f^{abc} f^{abd} &= \frac{1}{T_F^2} \text{tr} ([T^a, T^b] T^c) \text{tr} ([T^a, T^b] T^d) = 2N T_F \delta^{cd}. \end{aligned} \quad (\text{A.9})$$

Thus we find for our conventions

$$T_F = \frac{1}{2}, \quad C_A = N, \quad C_F = \frac{N^2 - 1}{2N}. \quad (\text{A.10})$$

A.4 Miscellaneous

For the gamma matrices we use the hermitian Euclidean set fulfilling the Clifford algebra, see e.g. [71, p. 330f.],

$$\{\gamma_\mu, \gamma_\nu\} = 2\delta_{\mu\nu} \mathbb{1}_{4 \times 4}. \quad (\text{A.11})$$

These matrices are connected to the ones in Minkowski space as $\gamma_0 = \gamma_0^{\text{M}}$ and $\gamma_j = -i\gamma_j^{\text{M}}$ for $j = 1, 2, 3$. Additionally we define

$$\gamma_5 = \gamma_0 \gamma_1 \gamma_2 \gamma_3 = \frac{1}{4!} \varepsilon_{\alpha\beta\gamma\delta} \gamma_\alpha \gamma_\beta \gamma_\gamma \gamma_\delta = \gamma_5^\dagger, \quad (\text{A.12})$$

for which we find the useful relations

$$\gamma_\mu \gamma_5 = \frac{1}{3!} \varepsilon_{\mu\alpha\beta\gamma} \gamma_\alpha \gamma_\beta \gamma_\gamma, \quad (\text{A.13})$$

$$\sigma_{\mu\nu} \gamma_5 = -\frac{i}{2} \varepsilon_{\mu\nu\alpha\beta} \gamma_\alpha \gamma_\beta, \quad (\text{A.14})$$

where $\sigma_{\mu\nu} = \frac{i}{2} [\gamma_\mu, \gamma_\nu]$. The γ -matrices form a complete orthonormal basis $\Gamma_{\{\mu\}}$ of the hermitian 4×4 matrices with scalar product

$$\langle \Gamma_{\{\mu\}}, \circ \rangle \stackrel{\text{def}}{=} \frac{1}{4} \text{tr}_4 (\Gamma_{\{\mu\}} \circ), \quad \Gamma_{\{\mu\}} \in \{\mathbb{1}, \gamma_\mu, \gamma_5, i\gamma_\mu \gamma_5, \sigma_{\mu\nu}/\sqrt{2}\}, \quad (\text{A.15})$$

where tr_4 denotes the trace on 4×4 matrices.

The following shorthand notations are used for the momentum integrals

$$\int_p \stackrel{\text{def}}{=} \int \frac{d^D p}{(2\pi)^D}, \quad \int_{\{p\}} \stackrel{\text{def}}{=} \prod_{j=1}^n \int \frac{d^D p_j}{(2\pi)^D}, \quad \text{where } \{p\} = \{p_1, \dots, p_n\}. \quad (\text{A.16})$$

Another shorthand notation used for 4-vectors is

$$p^n \stackrel{\text{def}}{=} \sum_\mu p_\mu^n, \quad n \in \mathbb{N} \setminus \{1\}, \quad p \in \mathbb{R}^4, \quad (\text{A.17})$$

where all cases $n > 2$ imply broken $O(4)$ symmetry. For broken $O(4)$ symmetry we use a generalisation of the Kronecker delta

$$\delta_{\mu_1 \dots \mu_n} = \begin{cases} 1 & \text{if } \mu_i = \mu_j \forall i, j = 1, \dots, n \\ 0 & \text{else.} \end{cases} \quad (\text{A.18})$$

Our conventions for Fourier transforms in the continuum are

$$f(x) = \int \frac{d^D p}{(2\pi)^D} \tilde{f}(p) e^{ipx} \quad (\text{A.19})$$

and on the lattice in infinite volume we use for vector fields the convention

$$V_\mu(x) = \int_{-\pi/a}^{\pi/a} \frac{d^4 p}{(2\pi)^4} \tilde{V}_\mu(p) e^{ip(x+a\hat{\mu}/2)}, \quad (\text{A.20})$$

$$\tilde{V}_\mu(p) = a^4 \sum_x V_\mu(x) e^{-ip(x+a\hat{\mu}/2)}, \quad (\text{A.21})$$

while the Fourier transform of scalar fields on the lattice with infinite volume is defined as

$$f(x) = \int_{-\pi/a}^{\pi/a} \frac{d^4 p}{(2\pi)^4} \tilde{f}(p) e^{ix}, \quad (\text{A.22})$$

$$\tilde{f}(p) = a^4 \sum_x f(x) e^{-ipx}. \quad (\text{A.23})$$

Appendix B

Dimensional regularisation: rules and tools

In case we can substitute the momentum to be integrated over in such a way that the denominator only depends on its squared value, all momenta with free indices to be integrated over can be replaced by, see e.g. [149, p. 806f.],

$$\int_p f(p^2) p_{\alpha_1} \cdots p_{\alpha_{2n}} = \frac{\Gamma(D/2)}{2^n \Gamma(D/2 + n)} \delta_{(\alpha_1 \alpha_2 \cdots \alpha_{2n-1} \alpha_{2n})} \int_p f(p^2) (p^2)^n, \quad (\text{B.1})$$

where $\delta_{(\alpha_1 \alpha_2 \cdots \alpha_{2n-1} \alpha_{2n})}$ denotes the sum of products of Kronecker deltas $\delta_{\mu\nu}$ symmetric under index permutation. Eventually the following formula can be applied

$$\int_p \frac{(p^2)^m}{(p^2 + \Omega)^n} = \frac{\Omega^{D/2+m-n}}{(4\pi)^{D/2}} \frac{\Gamma(n-m-D/2) \Gamma(m+D/2)}{\Gamma(n) \Gamma(D/2)}, \quad m, n \in \mathbb{N}. \quad (\text{B.2})$$

Integrals of this form where $\Omega = 0$ are called *scaleless* and vanish in dimensional regularisation due to a cancellation of the UV- and IR-poles. When collecting all UV-poles this rule cannot be used.

B.1 Useful integrals

The Fourier transform of $(p^2)^{-n}$ for $n > 0$ can be rewritten as

$$\begin{aligned} \int \frac{d^D p}{(2\pi)^D} \frac{e^{ipx}}{(p^2)^n} &= \int_0^\infty d\lambda \frac{\lambda^{n-1}}{\Gamma(n)} \int \frac{d^D p}{(2\pi)^D} e^{-\lambda p^2 + ipx} \\ &= \frac{1}{(4\pi)^{D/2}} \int_0^\infty d\lambda \frac{\lambda^{n-1-D/2}}{\Gamma(n)} e^{-x^2/(4\lambda)}, \end{aligned} \quad (\text{B.3})$$

where we introduced the Schwinger parameter λ in the first line. The resulting integral can be evaluated using

$$\begin{aligned} \int_0^\infty d\lambda \lambda^m \exp\left(-\frac{x^2}{4\lambda}\right) &= \left(\frac{x^2}{4}\right)^{m+1} \int_0^\infty du u^{-2-m} e^{-u} \\ &= \left(\frac{x^2}{4}\right)^{m+1} \Gamma(-1-m). \end{aligned} \quad (\text{B.4})$$

Appendix B. Dimensional regularisation: rules and tools

For the NLO contributions of the Gradient flow we also need the D -dimensional Gaussian

$$\begin{aligned}\int_p (p^2)^n e^{-tp^2} &= \frac{2}{(4\pi)^{D/2} \Gamma(D/2)} \int_0^\infty dp p^{2n+D-1} e^{-tp^2} \\ &= \frac{t^{-n-D/2}}{(4\pi)^{D/2}} \frac{\Gamma(n+D/2)}{\Gamma(D/2)}.\end{aligned}\tag{B.5}$$

Appendix C

Reduction of the operator basis

The discrete transformations used in section 5.2 are, see e.g. [71],

- Charge conjugation (\mathcal{C}):

$$\bar{\psi} \xrightarrow{\mathcal{C}} -\psi^T C, \psi \xrightarrow{\mathcal{C}} C^{-1} \bar{\psi}^T, A_\mu \xrightarrow{\mathcal{C}} -A_\mu^T, C\gamma_\mu C^{-1} = -\gamma_\mu^T, \quad (\text{C.1})$$

- Parity transformation (\mathcal{P}):

$$\begin{aligned} \bar{\psi}(x_0, \mathbf{x}) &\xrightarrow{\mathcal{P}} \bar{\psi}(x_0, -\mathbf{x})\gamma_0, \psi(x_0, \mathbf{x}) \xrightarrow{\mathcal{P}} \gamma_0\psi(x_0, -\mathbf{x}), \\ A_0(x_0, \mathbf{x}) &\xrightarrow{\mathcal{P}} A_0(x_0, -\mathbf{x}), A_i(x_0, \mathbf{x}) \xrightarrow{\mathcal{P}} -A_i(x_0, -\mathbf{x}), i = 1, 2, 3, \end{aligned} \quad (\text{C.2})$$

- (Euclidean) Time reflection (\mathcal{T}):

$$\begin{aligned} \bar{\psi}(x_0, \mathbf{x}) &\xrightarrow{\mathcal{T}} \bar{\psi}(-x_0, \mathbf{x})\gamma_5\gamma_0, \psi(x_0, \mathbf{x}) \xrightarrow{\mathcal{T}} \gamma_0\gamma_5\psi(-x_0, \mathbf{x}) \\ A_0(x_0, \mathbf{x}) &\xrightarrow{\mathcal{T}} -A_0(-x_0, \mathbf{x}), A_i(x_0, \mathbf{x}) \xrightarrow{\mathcal{T}} A_i(-x_0, \mathbf{x}), i = 1, 2, 3. \end{aligned} \quad (\text{C.3})$$

For multiple occurrences of the dual field strength tensor one finds

$$\tilde{F}_{\mu\nu} \dots \tilde{F}_{\nu\rho} = \frac{\delta_{\mu\rho}}{2} F_{\nu\sigma} \dots F_{\sigma\nu} - F_{\rho\nu} \dots F_{\nu\mu}. \quad (\text{C.4})$$

As pre-considerations we also look at the parity transformation of the field strength tensor

$$F_{\mu\nu} \xrightarrow{\mathcal{P}} [\delta_{\mu i} \delta_{\nu j} F_{ij} - \delta_{\mu 0} \delta_{\nu j} F_{0j} - \delta_{\mu i} \delta_{\nu 0} F_{i0}](x_0, -\mathbf{x}), \quad (\text{C.5})$$

$$F_{\mu\alpha} F_{\alpha\nu} \xrightarrow{\mathcal{P}} [\delta_{\mu 0} \delta_{\nu 0} F_{0\alpha} F_{\alpha 0} + \delta_{\mu i} \delta_{\nu j} F_{i\alpha} F_{\alpha j} - \delta_{\mu 0} \delta_{\nu j} F_{0\alpha} F_{\alpha j} - \delta_{\mu i} \delta_{\nu 0} F_{i\alpha} F_{\alpha 0}](x_0, -\mathbf{x}). \quad (\text{C.6})$$

Hence we find

$$\begin{aligned} \tilde{F}_{\nu\mu} F_{\mu\alpha} F_{\alpha\nu} &\xrightarrow{\mathcal{P}} \frac{1}{2} \epsilon_{\nu\mu\rho\sigma} [(\delta_{\rho m} \delta_{\sigma n} F_{mn} - \delta_{\rho 0} \delta_{\sigma n} F_{0n} - \delta_{\rho m} \delta_{\sigma 0} F_{m0}) \\ &\quad (\delta_{\mu i} \delta_{\nu j} F_{i\alpha} F_{\alpha j} - \delta_{\mu 0} \delta_{\nu j} F_{0\alpha} F_{\alpha j} - \delta_{\mu i} \delta_{\nu 0} F_{i\alpha} F_{\alpha 0})](x_0, -\mathbf{x}) \\ &= -[\tilde{F}_{j0} F_{0\alpha} F_{\alpha j} + \tilde{F}_{0j} F_{j\alpha} F_{\alpha 0} + \tilde{F}_{ji} F_{i\alpha} F_{\alpha j}](x_0, -\mathbf{x}) \\ &= -[\tilde{F}_{\nu\mu} F_{\mu\alpha} F_{\alpha\nu}](x_0, -\mathbf{x}), \end{aligned} \quad (\text{C.7})$$

$$F_{\nu\mu} F_{\mu\alpha} F_{\alpha\nu} \xrightarrow{\mathcal{P}} [F_{\nu\mu} F_{\mu\alpha} F_{\alpha\nu}](x_0, -\mathbf{x}). \quad (\text{C.8})$$

C.1 Total divergence operators

As mentioned in [151], there is a useful relation for fields X and Y in the adjoint representation for covariant derivatives and total divergences

$$\partial_\mu \text{tr}(XY) = \text{tr}(XD_\mu Y) + \text{tr}(YD_\mu X), \quad (\text{C.9})$$

which of course can be easily extended to derivatives of higher order, e.g. the only other for us relevant case

$$\partial_\mu \partial_\nu \text{tr}(XY) = \text{tr}(YD_\mu D_\nu X) + \text{tr}(XD_\mu D_\nu Y) + \text{tr}(D_\mu XD_\nu Y) + \text{tr}(D_\nu XD_\mu Y). \quad (\text{C.10})$$

The generalisation to colour vectors $\psi, \bar{\psi}$ yields

$$\partial_\mu (\bar{\psi} X \psi) = \bar{\psi} \overleftarrow{D}_\mu X \psi + \bar{\psi} D_\mu X \psi + \bar{\psi} X D_\mu \psi. \quad (\text{C.11})$$

With this input it is possible to reduce the basis into a minimal basis of linearly independent operators and some total divergence operators. The latter are irrelevant for the minimal basis used in the effective action (unless the theory has boundaries). Nonetheless they can be used to renormalise the minimal on-shell basis at nonzero momentum which serves as a test of the FORM scripts and is discussed briefly in appendix E.2.

Of course the same symmetries as for the on-shell basis have to apply to this set of total divergence operators. Thus we can use the $\Gamma_{\{\mu\}}$ from (5.33) derived for the on-shell basis and find for the different mass-dimensions

- $[\phi] = 4$:

$$\partial_\mu (\bar{\Psi} \gamma_\mu \Psi) \stackrel{\text{EOM}}{=} 0. \quad (\text{C.12})$$

- $[\phi] = 5$:

$$\begin{aligned} \partial^2 (\bar{\Psi} \Psi) &\equiv \partial_\mu \partial_\nu (\bar{\Psi} \gamma_\mu \gamma_\nu \Psi) \\ \partial^2 (\bar{\Psi} \Psi) &= \partial_\mu \left(\bar{\Psi} D_\mu \Psi + \bar{\Psi} \overleftarrow{D}_\mu \Psi \right) \end{aligned} \quad (\text{C.13})$$

$$\begin{aligned} \partial_\mu \partial_\nu (\bar{\Psi} \gamma_\mu \gamma_\nu \Psi) &\stackrel{\text{EOM}}{=} 2\partial_\mu (\bar{\Psi} M \gamma_\mu \Psi) + 2\partial_\mu (\bar{\Psi} D_\mu \Psi) \\ &\stackrel{\text{EOM}}{=} 2\partial_\mu (\bar{\Psi} D_\mu \Psi) \end{aligned} \quad (\text{C.14})$$

$$\begin{aligned} &\stackrel{\text{EOM}}{=} 2\partial_\mu \left(\bar{\Psi} \overleftarrow{D}_\mu \Psi \right) \\ \partial_\mu (\bar{\Psi} D_\mu \Psi) &= \mathcal{O}_3^{(1)} + \bar{\Psi} \overleftarrow{D}_\mu D_\mu \Psi, \end{aligned} \quad (\text{C.15})$$

$$\begin{aligned} i\partial_\mu \partial_\nu (\bar{\Psi} \sigma_{\mu\nu} \Psi) &= 0 \\ &= i\partial_\mu \left(\bar{\Psi} \sigma_{\mu\nu} D_\nu \Psi + \bar{\Psi} \overleftarrow{D}_\nu \sigma_{\mu\nu} \Psi \right) \end{aligned} \quad (\text{C.16})$$

$$\begin{aligned} i\partial_\mu (\bar{\Psi} \sigma_{\mu\nu} D_\nu \Psi) &\stackrel{\text{EOM}}{=} \partial_\mu (\bar{\Psi} D_\mu \Psi) + \partial_\mu (\bar{\Psi} M \gamma_\mu \Psi) \\ &\stackrel{\text{EOM}}{=} \partial_\mu (\bar{\Psi} D_\mu \Psi) \\ &= \frac{1}{2} \mathcal{O}_4^{(1)} + \frac{i}{2} \bar{\Psi} \overleftarrow{D}_\mu \sigma_{\mu\nu} D_\nu \Psi. \end{aligned} \quad (\text{C.17})$$

- $[\Phi] = 6$:

$$\partial^2 \partial_\mu (\bar{\Psi} \gamma_\mu \Psi) \stackrel{\text{EOM}}{=} 0 \quad (\text{C.18})$$

$$\begin{aligned} &= \partial_\mu \partial_\nu \left(\bar{\Psi} \overleftarrow{D}_\nu \gamma_\mu \Psi + \bar{\Psi} \gamma_\mu D_\nu \Psi \right) \\ \partial_\mu \partial_\nu (\bar{\Psi} \gamma_\mu D_\nu \Psi) &= \partial_\mu \left(\bar{\Psi} \overleftarrow{D}_\nu \gamma_\mu D_\nu \Psi + \bar{\Psi} \gamma_\mu D^2 \Psi \right) \\ &\stackrel{\text{EOM}}{=} \partial_\nu (\bar{\Psi} \gamma_\mu D_\mu D_\nu \Psi) + \partial_\nu (\bar{\Psi} M D_\nu \Psi) \\ &\stackrel{\text{EOM}}{=} \partial_\nu (\bar{\Psi} \gamma_\mu F_{\mu\nu} \Psi) \\ \partial_\nu (\bar{\Psi} \gamma_\mu D_\mu D_\nu \Psi) &= \mathcal{O}_7^{(2)} + \bar{\Psi} \overleftarrow{D}_\nu \gamma_\mu D_\mu D_\nu \Psi \quad (\text{C.19}) \end{aligned}$$

$$\partial_\nu (\bar{\Psi} \gamma_\mu F_{\mu\nu} \Psi) = \mathcal{O}_9^{(2)} - \mathcal{O}_8^{(2)} + \bar{\Psi} \overleftarrow{D}_\nu \gamma_\mu F_{\mu\nu} \Psi \quad (\text{C.20})$$

$$\partial_\mu (\bar{\Psi} \gamma_\mu D^2 \Psi) \stackrel{\text{EOM}}{=} \mathcal{O}_6^{(2)} + \bar{\Psi} M D^2 \Psi, \quad (\text{C.21})$$

and O(4) symmetry broken operators for which equation (C.11) suffices.

The minimal basis of total divergence operators complying with the symmetry constraints of the (untwisted) on-shell basis then reads

$$\begin{aligned} \phi_1^{(1)} &= \partial^2 (\bar{\Psi} \Psi) \\ \phi_1^{(2)} &= \partial_\mu \partial_\nu (\bar{\Psi} \gamma_\mu D_\nu \Psi), \quad \phi_2^{(2)} = \sum_\mu \partial_\mu (\bar{\Psi} \gamma_\mu D_\mu^2 \Psi), \quad \phi_3^{(2)} = \sum_\mu \partial_\mu^2 (\bar{\Psi} \gamma_\mu D_\mu \Psi), \\ \phi_4^{(2)} &= \sum_\mu \partial_\mu^3 (\bar{\Psi} \gamma_\mu \Psi), \quad \phi_5^{(2)} = \frac{1}{g_0^2} \partial_\mu \text{tr} (F_{\rho\nu} D_\mu F_{\rho\nu}), \quad \phi_6^{(2)} = \frac{1}{g_0^2} \sum_\mu \partial_\mu \text{tr} (F_{\mu\nu} D_\mu F_{\mu\nu}). \end{aligned} \quad (\text{C.22})$$

C.2 Equation of motion vanishing operators

During the reduction of the desired on-shell bases in the sections 5.2.1–5.2.3 we dropped several operators due to the EOMs, denoted by $\stackrel{\text{EOM}}{=}$. Here we collect the corresponding minimal set of EOM vanishing operators (\mathcal{E}) but omit total divergence operators

$$\begin{aligned} \mathcal{E}_1^{(0)} &= \bar{\Psi} [\gamma_\mu D_\mu + M] \Psi, \\ \mathcal{E}_2^{(1)} &= \bar{\Psi} [\gamma_\mu D_\mu + M]^2 \Psi, \\ \mathcal{E}_1^{(2)} &= \bar{\Psi} [\gamma_\mu D_\mu + M]^3 \Psi, \quad \mathcal{E}_2^{(2)} = \frac{1}{g_0^2} \text{tr} (D_\mu F_{\mu\nu} D_\rho F_{\rho\nu}) + \frac{1}{2} \bar{\Psi} \gamma_\mu D_\nu F_{\nu\mu} \Psi, \\ \mathcal{E}_3^{(2)} &= \bar{\Psi} \gamma_\mu [D_\mu, D^2] \Psi, \quad \mathcal{E}_4^{(2)} = \bar{\Psi} \gamma_\mu T^a \Psi \left(D_\nu F_{\nu\mu}^a - g_0^2 \bar{\Psi} \gamma_\mu T^a \Psi \right). \end{aligned} \quad (\text{C.23})$$

These operators are required for off-shell renormalisation of the minimal basis for the effective action with the background field method. Again we drop operators with overall powers of masses. Up to mass-dimension 6 there are no O(4) symmetry breaking EOM vanishing operators.

Appendix D

Implementation of the FORM scripts

In the following the general steps are explained according to their order in which they are performed in the script(s).

D.1 Obtain Feynman rules from the operator basis

For the operators considered here, each order in the coupling corresponds to a different number of fields $\{\bar{\psi}, \psi, A_\mu, \dots\}$ contributing to “legs” in a Feynman rule. At fixed order of the coupling one now has to perform the following steps for each of these field types:

1. Collect all fields of the current field type.
2. Label all collected fields with distinct identifiers.
3. Generate all possible permutations of the current field type with regard to its statistics, i.e. fermions require additional relative minuses, see e.g. [182].
4. Apply the values (indices, momenta etc.) reserved for each leg to the corresponding field determined by the identifier and let FORM handle the indices, i.e. combining all occurrences that are identical due to (anti-)symmetric tensors in the expressions left over.

Eventually one is able to remove all fields, which leaves over free indices for all legs of the Feynman rule. These reserved indices and momenta can now be used in a typical `id` statement in the main program applying the Feynman rules obtained here, see also the section D.3. The full FORM script is given in listing D.1 with operator prototypes in D.2.

Listing D.1: FORM script “feynmanRulesFull.frm” to generate Feynman rules from a prototype from listing D.2. The current prototype must be chosen by the command line argument `-D op=...` according to the names found in listing D.2.

```
***** Usage: form -D op=... -D POW=n feynmanRulesFull
** where n is the power of the coupling g^n.
#define sign "(+1)";
#define cfcnt "10";
#define ccnt "30";
#define icnt "1";
#define fcnt "1";
**#define bgField "1";
```

```
Symbol CF,M,CA,TF,xi,Nc;
Autodeclare Index spt,co,cf,ind,fl;
CTensor FC(antisymmetric),DC(symmetric),TC,Trtemp,Tr(cyclesymmetric);
```

D.1. Obtain Feynman rules from the operator basis

```

CFunction DO4v(symmetric),MOMENTA,COLs,CFs,SPTs,FLs,ordering(antisymmetric),
    DUMMY,vert,L;
CFunction Bbuffer,Abuffer,Psibarbuffer,Psibuffer,Psib,Psibarb,Bb,Ab;
CFunction OPF,FL;
** F = [D,D]/g
NFunction Psibar,Psi,A,F,Cbar,C,B;

*****
** Derivatives:
**   D(spt)  :: \partial_spt
**   Dcovf   :: Dcovf = D + g A
**   Dcova   :: Dcova = D* + g[A,*]
**   BLOB    :: D BLOB = 0, BLOB = 1, can be used to stop product rule from
               including following elements
*****
Nfunction D,Dcova,Dcovf,BLOB;
NFunction GAMMA,GAMMA5,sigma,FIELDS;
Symbol g;
** external particles
Index alpha,beta,gamma,delta,mu,nu;
Autodeclare Vector imp;
Vector p,q,r,s,t,u;
Index b,c,d,e,f,h;

Local rules =
#include rawOps # 'op'
;

** replace field strength tensor
#do dummy=1,1
  id,once F(imp1?,imp2?,spt1?,spt2?,col?) = 'sign'*i_?imp1(spt1)*A(spt2,
    imp1,col) - 'sign'*i_?imp1(spt2)*A(spt1,imp1,col) + FC(col,col{'ccnt',col{'
    ccnt'+1}})*A(spt1,imp1,col{'ccnt'})*A(spt2,imp2,col{'ccnt'+1});
  redefine ccnt "{ 'ccnt'+2 }";
  if(count(F,1)>0) redefine dummy "0";
  .sort;
#enddo

** switch to perturbative description A -> g*A
id A(?args) = g*A(?args);

** Handle covariant derivatives
#do dummy=1,1
  id,once Dcovf(imp?,spt?,cf1?,cf2?) = DO4v(cf1,cf2)*D(spt)+g*TC(col{'ccnt',
    cf1,cf2})*A(spt,imp,col{'ccnt'});
  redefine ccnt "{ 'ccnt'+1 }";
  if(count(Dcovf,1)>0) redefine dummy "0";
  .sort;
#enddo
#do dummy=1,1
  id,once Dcova(imp?,spt?,col1?,col2?) = DO4v(col1,col2)*D(spt)+g*FC(col1,
    col{'ccnt',col2})*A(spt,imp,col{'ccnt'});
  redefine ccnt "{ 'ccnt'+1 }";
  if(count(Dcova,1)>0) redefine dummy "0";
  .sort;
#enddo

```

Appendix D. Implementation of the FORM scripts

```

#ifdef 'bgField'
  id A(?args) = A(?args)+B(?args);
  ** make sure to add BGF gauge-fixing term to the QCD action - is postponed
    after the substitution A -> A+B
  #if ('op'==QCD)
    .sort;
    Local rules2 = rules -1/xi*(D(spt0)*A(spt1,imp1,col1)+g*FC(col1,col2,col3)
      )*B(spt0,imp2,col2)*A(spt1,imp3,col3))*BLOB*(D(spt2)*A(spt3,imp1,col4)
      +g*FC(col4,col5,col6)*B(spt2,imp2,col5)*A(spt3,imp3,col6))*TC(col1,cf0
      ,cf1)*TC(col4,cf1,cf0)*DO4v(spt2,spt3))/g^2*DO4v(spt0,spt1)*DO4v(spt2,
      spt3);
  #endif
#endif

** Handle derivatives
repeat;
  id ,once D(spt1?)*A(spt2?,imp?,col?) = 'sign'*i_*imp(spt1)*A(spt2,imp,col)
    +A(spt2,imp,col)*D(spt1);
  id ,once D(spt1?)*Psi(fl?,imp?,cf?) = 'sign'*i_*imp(spt1)*Psi(fl,imp,cf);
  id ,once D(spt1?)*Psibar(fl?,imp?,cf?) = 'sign'*i_*imp(spt1)*Psibar(fl,imp
    ,cf)+Psibar(fl,imp,cf)*D(spt1);
  id ,once D(spt?)*Cbar(imp?,col?) = 'sign'*i_*imp(spt)*Cbar(imp,col)+Cbar(
    imp,col)*D(spt);
  id ,once D(spt?)*C(imp?,col?) = 'sign'*i_*imp(spt)*C(imp,col)+C(imp,col)*D
    (spt);
  id D(spt1?)*GAMMA(fl?,spt2?) = GAMMA(fl,spt2)*D(spt1);
  id D(spt1?)*sigma(fl?,spt2?,spt3?) = sigma(fl,spt2,spt3)*D(spt1);
  id D(spt?)*BLOB = 0;
endrepeat;
id BLOB = 1;
id D(spt?) = 0;

** collect only desired power in the coupling
if(count(g,1)!='POW') discard;

** translate into usual index and momenta notation
#do dummy=1,1
  id ,once Psibar(fl?,imp?,cf?) = Psibarbuffer(ind'icnt',fl,imp,cf)*Psibar(
    ind'icnt');
  redefine icnt "{'icnt'+1}";
  if(match(Psibar(fl?,imp?,cf?))>0) redefine dummy "0";
  .sort;
#enddo
#do dummy=1,1
  id ,once Psi(fl?,imp?,cf?) = Psibuffer(ind'icnt',fl,imp,cf)*Psi(ind'icnt')
    ;
  redefine icnt "{'icnt'+1}";
  if(match(Psi(fl?,imp?,cf?))>0) redefine dummy "0";
  .sort;
#enddo
#do dummy=1,1
  id ,once A(spt?,imp?,col?) = Abuffer(ind'icnt',spt,imp,col)*A(ind'icnt');
  redefine icnt "{'icnt'+1}";
  if(match(A(spt?,imp?,col?))>0) redefine dummy "0";
  .sort;

```

```

#enddo
#do dummy=1,1
  id ,once B(spt?,imp?,col?) = Bbuffer(ind'icnt',spt,imp,col)*B(ind'icnt');
  redefine icnt "{ 'icnt'+1}";
  if(match(B(spt?,imp?,col?))>0) redefine dummy "0";
  .sort;
#enddo

** construct all possible permutations of external fields (currently
    fermions and gauge bosons)
repeat;
id A?{Psi,A,B,GAMMA,GAMMA5,sigma}(?args)*Psibar(?args2) = Psibar(?args2)*A(?
  args);
id A?{A,B,GAMMA,GAMMA5,sigma}(?args)*Psi(?args2) = Psi(?args2)*A(?args);
id Psi?{B,GAMMA,GAMMA5,sigma}(?args)*A(?args2) = A(?args2)*Psi(?args);
id Psi?{GAMMA,GAMMA5,sigma}(?args)*B(?args2) = B(?args2)*Psi(?args);
endrepeat;
chainin Psibar;
id Psibar(?args) = perm_(1,Psibar,?args);
chainin Psi;
id Psi(?args) = perm_(1,Psi,?args);
chainin A;
id A(?args) = perm_(A,?args);
chainin B;
id B(?args) = perm_(B,?args);
id Psi(?args) = Psib(?args);
id Psibar(?args) = Psibarb(?args);
id A(?args) = Ab(?args);
id B(?args) = Bb(?args);
if(count(Psibarb,1)==0) multiply Psibarb;
if(count(Psib,1)==0) multiply Psib;
if(count(Ab,1)==0) multiply Ab;
if(count(Bb,1)==0) multiply Bb;

id Psibarb(?args1)*Ab(?args2)*Bb(?args4)*Psib(?args3) = FIELDS(?args1,?args3
  ,?args2,?args4);
multiply MOMENTA(p,q,r,s,t,u)*COLs(b,c,d,e,f,h)*CFs(cfp1,...,cfp6)*SPTs(
  sptp1,...,sptp6)*FLs(flp1,...,flp6);
#do dummy=1,1
  id FIELDS(ind?,?args)*Psibarbuffer(ind?,fl?,imp?,cf?)*MOMENTA(imp2?,?
    args2)*SPTs(spt?,?args6)*CFs(cf2?,?args3)*FLs(fl2?,?args4) = FIELDS(?
    args)*MOMENTA(?args2)*SPTs(?args6)*CFs(?args3)*FLs(?args4)*replace_(
    imp,imp2,cf,cf2,fl,fl2)*vert(Psibar(imp2,cf2,fl2));
  id FIELDS(ind?,?args)*Psibuffer(ind?,fl?,imp?,cf?)*MOMENTA(imp2?,?args2)*
    SPTs(spt?,?args6)*CFs(cf2?,?args3)*FLs(fl2?,?args4) = FIELDS(?args)*
    MOMENTA(?args2)*SPTs(?args6)*CFs(?args3)*FLs(?args4)*replace_(imp,imp2
    ,cf,cf2,fl,fl2)*vert(Psi(imp2,cf2,fl2));
  id FIELDS(ind?,?args)*Abuffer(ind?,spt?,imp?,col?)*MOMENTA(imp2?,?args2)*
    COLs(col2?,?args3)*SPTs(spt2?,?args4) = FIELDS(?args)*MOMENTA(?args2)*
    COLs(?args3)*SPTs(?args4)*replace_(imp,imp2,col,col2,spt,spt2)*vert(A(
    imp2,spt2,col2));
  if(count(Psibuffer,1,Abuffer,1,Psibarbuffer,1)>0) redefine dummy "0";
  id FIELDS(ind?,?args)*Bbuffer(ind?,spt?,imp?,col?)*MOMENTA(imp2?,?args2)*
    COLs(col2?,?args3)*SPTs(spt2?,?args4) = FIELDS(?args)*MOMENTA(?args2)*
    COLs(?args3)*SPTs(?args4)*replace_(imp,imp2,col,col2,spt,spt2)*vert(B(
    imp2,spt2,col2));

```

Appendix D. Implementation of the FORM scripts

```

    if (count (Psibuffer ,1 ,Abuffer ,1 ,Bbuffer ,1 ,Psibarbuffer ,1)>0) redefine
        dummy "0";
    . sort ;
#enddo
id FIELDS?{FIELDS,MOMENTA,COLs,CFs,SPTs,FLs}(? args) = 1;
chainin vert;

id sigma (fl ?,spt1?,spt2?) = i_ /2*(GAMMA (fl ,spt1)*GAMMA (fl ,spt2)-GAMMA (fl ,
    spt2)*GAMMA (fl ,spt1));
id DO4v (spt1?,spt2?) = d_ (spt1 ,spt2);
#do dummy=0, 'ccnt'
sum cf 'dummy';
#enddo
id TC (col1?,cf1?,cf2?)*TC (col2?,cf2?,cf1?) = TF*d_ (col1 ,col2);
id TF = -1/2;
multiply replace_ (cfp1 ,cf1 ,cfp2 ,cf2 ,cfp3 ,cf3 ,cfp4 ,cf4 ,sptp1 ,spt1 ,sptp2 ,spt2 ,
    sptp3 ,spt3 ,sptp4 ,spt4 ,flp1 ,fl1 ,flp2 ,fl2 ,flp3 ,fl3 ,flp4 ,fl4);
. sort ;
id vert (? args) = 1;
Print "%t ";
. end;

```

Listing D.2: FORM script “rawOps” containing the operator prototypes.

```

***** pure gauge *****
*—#| DFDF_O4:
- Dcova (imp0,spt0,col0,col1)*F (imp1,imp2,spt1,spt2,col2)*BLOB*Dcova (imp3,
    spt3,col3,col4)*F (imp4,imp5,spt4,spt5,col5)*DO4v (col1,col2)*DO4v (col0,
    col3)/2*DO4v (spt0,spt3)*DO4v (spt1,spt4)*DO4v (spt5,spt2)*DO4v (col4,col5)/g
    ^2
*—#| DFDF_O4:
*—#| F3:
F (imp0,imp1,spt0,spt1,col0)*F (imp2,imp3,spt2,spt3,col1)*F (imp4,imp5,spt4,
    spt5,col2)*TC (col0,cf0,cf1)*TC (col1,cf1,cf2)*TC (col2,cf2,cf0)/g^2*DO4v (
    spt1,spt2)*DO4v (spt3,spt4)*DO4v (spt5,spt0)
*—#| F3:
*—#| F2:
F (imp0,imp1,spt0,spt1,col0)*F (imp2,imp3,spt2,spt3,col1)*TC (col0,cf0,cf2)*TC (
    col1,cf2,cf0)/g^2*DO4v (spt1,spt2)*DO4v (spt3,spt0)
*—#| F2:
*—#| DFDF:
- Dcova (imp0,spt0,col0,col1)*F (imp1,imp2,spt1,spt2,col2)*BLOB*Dcova (imp3,
    spt3,col3,col4)*F (imp4,imp5,spt4,spt5,col5)*DO4v (col1,col2)*DO4v (col0,
    col3)/2*DO4v (spt0,spt3,spt1,spt4)*DO4v (spt5,spt2)*DO4v (col4,col5)/g^2
*—#| DFDF:

***** fermionic *****
*—#| PsiSigmaFPsi:
i_ *Psibar (fl0,imp0,col0)*sigma (flc0,spt3,spt4)*F (imp1,imp2,spt1,spt2,col1)*
    Psi (fl1,imp3,col3)*TC (col1,col0,col3)*DO4v (spt1,spt3)*DO4v (spt2,spt4)*FL (
    fl0,flc0,fl1)*OPF (flc0)
*—#| PsiSigmaFPsi:
*—#| PsiGammaFDPsi:
Psibar (fl0,imp0,cf0)*GAMMA (flc0,spt0)*TC (col0,cf0,cf1)*F (imp1,imp2,spt1,spt2,
    col1)*Dcovf (imp3,spt3,cf1,cf2)*Psi (fl1,imp4,cf2)*DO4v (spt0,spt1)*DO4v (
    spt2,spt3)*DO4v (col0,col1)*FL (fl0,flc0,fl1)*OPF (flc0)
*—#| PsiGammaFDPsi:

```



```

*—#| PsiGammaD3Psi:
Psibar (fl0 ,imp0 ,cf0 )*GAMMA( flc0 ,spt0 )*DO4v(spt0 ,spt1 ,spt2 ,spt3 )*Dcovf(imp1 ,
    spt1 ,cf1 ,cf2 )*Dcovf(imp2 ,spt2 ,cf3 ,cf4 )*Dcovf(imp3 ,spt3 ,cf5 ,cf6 )*Psi( fl1 ,
    imp4 ,cf7 )*DO4v( cf0 ,cf1 )*DO4v( cf2 ,cf3 )*DO4v( cf4 ,cf5 )*DO4v( cf6 ,cf7 )*FL( fl0 ,
    flc0 ,fl1 )*OPF( flc0 )
*—#| PsiGammaD3Psi:

***** building blocks for EOM vanishing operators *****
*—#| DF2_O4:
— Dcova(imp0 ,spt0 ,col0 ,col1 )*F(imp1 ,imp2 ,spt1 ,spt2 ,col2 )*BLOB*Dcova(imp3 ,
    spt3 ,col3 ,col4 )*F(imp4 ,imp5 ,spt4 ,spt5 ,col5 )*DO4v( col1 ,col2 )*DO4v( col0 ,
    col3 )/2*DO4v(spt0 ,spt1 )*DO4v(spt3 ,spt4 )*DO4v(spt5 ,spt2 )*DO4v( col4 ,col5 )/g
    ^2
*—#| DF2_O4:
*—#| Psi[DslashD2]Psi:
Psibar (fl0 ,imp0 ,cf0 )*GAMMA( flc0 ,spt0 )*(Dcovf(imp1 ,spt1 ,cf0 ,cf1 )*Dcovf(imp2 ,
    spt2 ,cf1 ,cf2 )*Dcovf(imp3 ,spt3 ,cf2 ,cf3 )—Dcovf(imp2 ,spt2 ,cf0 ,cf1 )*Dcovf(
    imp3 ,spt3 ,cf1 ,cf2 )*Dcovf(imp1 ,spt1 ,cf2 ,cf3 ))*Psi( fl1 ,imp4 ,cf3 )*DO4v(spt0 ,
    spt1 )*DO4v(spt2 ,spt3 )*FL( fl0 ,flc0 ,fl1 )*OPF( flc0 )
*—#| Psi[DslashD2]Psi:
*—#| PsiD0Psi:
Psibar (fl0 ,imp0 ,cf0 )*(GAMMA( flc0 ,spt0 )*DO4v(spt0 ,spt1 )*Dcovf(imp1 ,spt1 ,cf0 ,
    cf1 )+M*DO4v(cf0 ,cf1 ))*Psi( fl1 ,imp4 ,cf1 )*FL( fl0 ,flc0 ,fl1 )*OPF( flc0 )
*—#| PsiD0Psi:
*—#| PsiD02Psi:
Psibar (fl0 ,imp0 ,cf0 )*(GAMMA( flc0 ,spt0 )*Dcovf(imp1 ,spt1 ,cf0 ,cf1 )*DO4v(spt0 ,
    spt1 )+M*DO4v(cf0 ,cf1 ))*(GAMMA( flc0 ,spt2 )*Dcovf(imp2 ,spt3 ,cf1 ,cf2 )*DO4v(
    spt2 ,spt3 )+M*DO4v(cf1 ,cf2 ))*
Psi( fl1 ,imp4 ,cf2 )*FL( fl0 ,flc0 ,fl1 )*OPF( flc0 )
*—#| PsiD02Psi:
*—#| PsiD03Psi:
Psibar (fl0 ,imp0 ,cf0 )*(GAMMA( flc0 ,spt0 )*Dcovf(imp1 ,spt1 ,cf0 ,cf1 )*DO4v(spt0 ,
    spt1 )+M*DO4v(cf0 ,cf1 ))*(GAMMA( flc0 ,spt2 )*Dcovf(imp2 ,spt3 ,cf1 ,cf2 )*DO4v(
    spt2 ,spt3 )+M*DO4v(cf1 ,cf2 ))*
(GAMMA( flc0 ,spt4 )*Dcovf(imp3 ,spt5 ,cf2 ,cf3 )*DO4v(spt4 ,spt5 )+M*DO4v(cf2 ,cf3 ))*
Psi( fl1 ,imp4 ,cf3 )*FL( fl0 ,flc0 ,fl1 )*OPF( flc0 )
*—#| PsiD03Psi:
*—#| PsiD2D0Psi:
Psibar (fl0 ,imp0 ,cf0 )*Dcovf(imp2 ,spt2 ,cf0 ,cf1 )*Dcovf(imp3 ,spt3 ,cf1 ,cf2 )*(
    GAMMA( flc0 ,spt0 )*DO4v(spt0 ,spt1 )*Dcovf(imp1 ,spt1 ,cf2 ,cf3 )+M*DO4v(cf2 ,cf3 )
    )*Psi( fl1 ,imp4 ,cf3 )*FL( fl0 ,flc0 ,fl1 )*OPF( flc0 )*DO4v(spt2 ,spt3 )
*—#| PsiD2D0Psi:
*—#| PsiGammaDFPsi:
Psibar (fl0 ,imp0 ,cf0 )*GAMMA( flc0 ,spt0 )*TC(col0 ,cf0 ,cf1 )*Dcova(imp1 ,spt1 ,col2 ,
    col1 )*F(imp2 ,imp3 ,spt2 ,spt3 ,col3 )*BLOB*Psi( fl1 ,imp4 ,cf1 )*DO4v(spt0 ,spt3 )*
    DO4v(spt2 ,spt1 )*FL( fl0 ,flc0 ,fl1 )*OPF( flc0 )*DO4v( col0 ,col2 )*DO4v( col1 ,col3
    )
*—#| PsiGammaDFPsi:

***** 4-fermion operators *****
*—#| PsiPsi2:
Psibar (fl0 ,imp0 ,cf0 )*Psi( fl1 ,imp1 ,cf1 )*Psibar( fl2 ,imp2 ,cf2 )*Psi( fl3 ,imp3 ,cf3
    )*DO4v(cf0 ,cf1 )*DO4v(cf2 ,cf3 )*FL( fl0 ,flc0 ,fl1 )*FL( fl2 ,flc1 ,fl3 )*OPF( flc0 ,
    flc1 )
*—#| PsiPsi2:
*—#| PsiTPsi2:

```

```

Psibar(f10,imp0,cf0)*TC(col0,cf0,cf1)*Psi(f11,imp1,cf1)*Psibar(f12,imp2,cf2)
*TC(col0,cf2,cf3)*Psi(f13,imp3,cf3)*FL(f10,flc0,f11)*FL(f12,flc1,f13)*OPF
(flc0,flc1)
*—#] PsiTPsi2:
*—#] PsiGammaPsi2:
Psibar(f10,imp0,cf0)*GAMMA(flc0,spt0)*Psi(f11,imp1,cf1)*Psibar(f12,imp2,cf2)
*GAMMA(flc1,spt0)*Psi(f13,imp3,cf3)*DO4v(cf0,cf1)*DO4v(cf2,cf3)*FL(f10,
flc0,f11)*FL(f12,flc1,f13)*OPF(flc0,flc1)
*—#] PsiGammaPsi2:
*—#] PsiGammaTPsi2:
Psibar(f10,imp0,cf0)*TC(col0,cf0,cf1)*GAMMA(flc0,spt0)*Psi(f11,imp1,cf1)*
Psibar(f12,imp2,cf2)*TC(col0,cf2,cf3)*GAMMA(flc1,spt0)*Psi(f13,imp3,cf3)*
FL(f10,flc0,f11)*FL(f12,flc1,f13)*OPF(flc0,flc1)
*—#] PsiGammaTPsi2:
*—#] PsiGammaGamma5Psi2:
Psibar(f10,imp0,cf0)*GAMMA(flc0,spt0)*GAMMA5(flc0)*Psi(f11,imp1,cf1)*Psibar(
f12,imp2,cf2)*GAMMA(flc1,spt0)*GAMMA5(flc1)*Psi(f13,imp3,cf3)*DO4v(cf0,
cf1)*DO4v(cf2,cf3)*FL(f10,flc0,f11)*FL(f12,flc1,f13)*OPF(flc0,flc1)
*—#] PsiGammaGamma5Psi2:
*—#] PsiGammaGamma5TPsi2:
Psibar(f10,imp0,cf0)*TC(col0,cf0,cf1)*GAMMA(flc0,spt0)*GAMMA5(flc0)*Psi(f11,
imp1,cf1)*Psibar(f12,imp2,cf2)*TC(col0,cf2,cf3)*GAMMA(flc1,spt0)*GAMMA5(
flc1)*Psi(f13,imp3,cf3)*FL(f10,flc0,f11)*FL(f12,flc1,f13)*OPF(flc0,flc1)
*—#] PsiGammaGamma5TPsi2:
*—#] PsiSigmaPsi2:
Psibar(f10,imp0,cf0)*sigma(flc0,spt0,spt1)*Psi(f11,imp1,cf1)*Psibar(f12,imp2
,cf2)*sigma(flc1,spt0,spt1)*Psi(f13,imp3,cf3)*DO4v(cf0,cf1)*DO4v(cf2,cf3)
*FL(f10,flc0,f11)*FL(f12,flc1,f13)*OPF(flc0,flc1)
*—#] PsiSigmaPsi2:
*—#] PsiSigmaTPsi2:
Psibar(f10,imp0,cf0)*TC(col0,cf0,cf1)*sigma(flc0,spt0,spt1)*Psi(f11,imp1,cf1
)*Psibar(f12,imp2,cf2)*TC(col0,cf2,cf3)*sigma(flc1,spt0,spt1)*Psi(f13,
imp3,cf3)*FL(f10,flc0,f11)*FL(f12,flc1,f13)*OPF(flc0,flc1)
*—#] PsiSigmaTPsi2:

***** others *****
*—#] GradFlow:
-g*L(spt0,col0)*(
+ Dcova(imp1,spt1,col1,col2)*F(imp2,imp3,spt2,spt3,col3)*DO4v(col0,col1)*
DO4v(col2,col3)*DO4v(spt0,spt3)*DO4v(spt1,spt2)
+ xi*Dcova(imp1,spt1,col1,col2)*D(spt2)*A(spt3,imp2,col3)*DO4v(col0,col1)*
DO4v(col2,col3)*DO4v(spt2,spt3)*DO4v(spt1,spt0))/g^2
*—#] GradFlow:

```

D.2 Determine contributing Feynman graphs (QGRAF)

To obtain all Feynman graphs contributing to the desired n -point function at 1-loop order we use QGRAF [145, 146] in version 3.4. We start by listing all propagators and vertices to be considered and specify whether we have fermions or bosons at hand. For the vertices one only has to specify the particles at in-/out-going legs. The used model files are given in listings D.3, D.4 and D.5.

As suggested in [183] we also introduce additional (scalar) fields, called “anchor”, to be able to insert operators into our n -point functions by defining new vertices with one additional external scalar field, whose momentum is set to the overall momentum of the operator.

After specifying the desired n -point function and some options, QGRAF produces the desired

set of graphs already combined with symmetry factors and minuses for closed fermion loops. The options chosen here are either **onepi** for all operator insertions but the 1-flavour 4-fermion operators. The latter are implemented through another scalar **mediator** field as highlighted in eq. (6.22) to obtain all possible combinations of the quarks lines, which leads to discarding the **onepi** option in favour of

```
true = iprop[mediator,2,2];
true = bridge[gluon,0,0];
true = bridge[quark,0,0];
```

which avoids graphs which can be split into two graphs by cutting either a gluon or quark propagator. The output can be modified such that one directly obtains **FORM** compatible code snippets.

Listing D.3: QGRAF model file containing all propagators and vertices for $N_f \geq 2$ Symanzik Effective theory and considered 1-loop n -point functions from figure 6.1. Only 1-flavoured 4-fermion operators are missing. **anchor** denotes the insertion of an operator, **bgf** are background fields, while the other field names should be self-explanatory.

```
% propagators (QCD)
[ gluon, gluon, +, notadpole ]
[ ghost, aghost, -, notadpole ]
[ quark, aquark, - ]
[ quark2, aquark2, - ]
[ anchor, anchor, +, external ]
[ bgf, bgf, +, external ]

% pure gauge vertices (QCD)
[ gluon, gluon, gluon ]
[ gluon, gluon, bgf ]
[ gluon, bgf, bgf ]
[ bgf, bgf, bgf ]
[ gluon, gluon, gluon, gluon ]
[ gluon, gluon, gluon, bgf ]
[ gluon, gluon, bgf, bgf ]
[ gluon, bgf, bgf, bgf ]
[ bgf, bgf, bgf, bgf ]

[ aghost, ghost, gluon ]
[ aghost, ghost, bgf ]

[ aghost, ghost, gluon, bgf ]
[ aghost, ghost, bgf, bgf ]

% fermionic vertices (QCD)
[ aquark, quark, gluon ]
[ aquark, quark, bgf ]
[ aquark2, quark2, gluon ]
[ aquark2, quark2, bgf ]

% gauge vertices (eff. th., mass dim. 6)
[ gluon, gluon, anchor ]
[ gluon, bgf, anchor ]
[ bgf, bgf, anchor ]

[ gluon, gluon, gluon, anchor ]
[ gluon, gluon, bgf, anchor ]
[ gluon, bgf, bgf, anchor ]
[ bgf, bgf, bgf, anchor ]
```

Appendix D. Implementation of the FORM scripts

```

[ gluon , gluon , gluon , gluon , anchor]
[ gluon , gluon , gluon , bgf , anchor]
[ gluon , gluon , bgf , bgf , anchor]
[ gluon , bgf , bgf , bgf , anchor]

[ gluon , gluon , gluon , gluon , gluon , anchor]
[ gluon , gluon , gluon , gluon , bgf , anchor]
[ gluon , gluon , gluon , bgf , bgf , anchor]
[ gluon , gluon , bgf , bgf , bgf , anchor]

[ gluon , gluon , gluon , gluon , gluon , gluon , anchor]
[ gluon , gluon , gluon , gluon , gluon , bgf , anchor]
[ gluon , gluon , gluon , gluon , bgf , bgf , anchor]
[ gluon , gluon , gluon , bgf , bgf , bgf , anchor]
% and so on...

% ferm. vertices (eff. th.)
[ aquark , quark , anchor]

[ aquark , quark , gluon , anchor]
[ aquark , quark , bgf , anchor]

[ aquark , quark , gluon , gluon , anchor]
[ aquark , quark , gluon , bgf , anchor]
[ aquark , quark , bgf , bgf , anchor]

[ aquark , quark , gluon , gluon , gluon , anchor]
[ aquark , quark , gluon , gluon , bgf , anchor]
[ aquark , quark , gluon , bgf , bgf , anchor]
[ aquark , quark , bgf , bgf , bgf , anchor]

[ aquark2 , quark2 , anchor]

[ aquark2 , quark2 , gluon , anchor]
[ aquark2 , quark2 , bgf , anchor]

[ aquark2 , quark2 , gluon , gluon , anchor]
[ aquark2 , quark2 , gluon , bgf , anchor]
[ aquark2 , quark2 , bgf , bgf , anchor]

[ aquark2 , quark2 , gluon , gluon , gluon , anchor]
[ aquark2 , quark2 , gluon , gluon , bgf , anchor]
[ aquark2 , quark2 , gluon , bgf , bgf , anchor]
[ aquark2 , quark2 , bgf , bgf , bgf , anchor]

% 4-fermion vertex of 2 different flavours
[ aquark , quark , aquark2 , quark2 , anchor]

```

Listing D.4: QGRAF model file containing all propagators and vertices for $N_f \geq 2$ Symanzik Effective theory and considered 1-loop n -point functions from figure 6.1. **anchor** denotes **here** the insertion of a 1-flavour 4-fermion operator, **mediator** is scalar field to properly implement two quark lines of the same flavour, **bgf** are background fields, while the other field names should be self-explanatory.

```

% propagators (QCD)
[ gluon , gluon , + , notadpole ]

```

D.2. Determine contributing Feynman graphs (QGRAF)

```

[ ghost , aghost , -, notadpole ]
[ quark , aquark , - ]
[ quark2 , aquark2 , - ]
[ anchor , anchor , + , external ]
[ mediator , mediator , + ]
% [ src , src , + , external ]
[ bgf , bgf , + , external ]

% pure gauge vertices (QCD)
[ gluon , gluon , gluon ]
[ gluon , gluon , bgf ]
[ gluon , bgf , bgf ]
[ bgf , bgf , bgf ]
[ gluon , gluon , gluon , gluon ]
[ gluon , gluon , gluon , bgf ]
[ gluon , gluon , bgf , bgf ]
[ gluon , bgf , bgf , bgf ]
[ bgf , bgf , bgf , bgf ]

[ aghost , ghost , gluon ]
[ aghost , ghost , bgf ]

[ aghost , ghost , gluon , bgf ]
[ aghost , ghost , bgf , bgf ]

% fermionic vertices (QCD)
[ aquark , quark , gluon ]
[ aquark , quark , bgf ]
[ aquark2 , quark2 , gluon ]
[ aquark2 , quark2 , bgf ]

% 4-fermion vertex
[ aquark , quark , mediator ]
[ mediator , mediator , anchor ]

```

Listing D.5: QGRAF model file containing all propagators and vertices relevant for Yang-Mills Gradient flow. **anchor** denotes the insertion of an operator of the minimal on-shell basis, **src** corresponds to $\tilde{E}(t, p)$, **src2** is used when $\tilde{E}(t, p)$ or equivalently $\delta\tilde{E}^{(2)}(t, p)$ are to be computed without additional operator insertions, **frc** amounts to the insertion of a correction to the flow equation due to lattice artifacts, while the other field names should be self-explanatory.

```

% propagators (QCD)
[ gluon , gluon , + ]
[ L , B , + , notadpole ]
[ ghost , aghost , - ]
[ quark , aquark , - ]
[ anchor , anchor , + , external ]
[ src , src , + , external ]
[ src2 , src2 , + , external ]
[ frc , frc , + , external ]

% pure gauge vertices (QCD)
[ gluon , gluon , gluon ]
[ gluon , gluon , gluon , gluon ]
[ aghost , ghost , gluon ]

```

Appendix D. Implementation of the FORM scripts

```

% flow vertices (Harlander et al.)
[ B, L, L ]
[ B, L, gluon ]
[ B, gluon, gluon ]
[ B, L, L, L ]
[ B, L, L, gluon ]
[ B, L, gluon, gluon ]
[ B, gluon, gluon, gluon ]

% gauge vertices (eff. th., mass dim. 6)
[ gluon, gluon, anchor]
[ gluon, gluon, gluon, anchor]
[ gluon, gluon, gluon, gluon, anchor]
[ gluon, gluon, gluon, gluon, gluon, anchor]
[ gluon, gluon, gluon, gluon, gluon, gluon, anchor]

% sources contributing to the action density
[ gluon, gluon, src]
[ gluon, gluon, gluon, src]
[ gluon, gluon, gluon, gluon, src]
[ L, gluon, src]
[ L, gluon, gluon, src]
[ L, gluon, gluon, gluon, src]
[ L, L, src]
[ L, L, gluon, src]
[ L, L, gluon, gluon, src]
[ L, L, L, src]
[ L, L, L, gluon, src]
[ L, L, L, L, src]

% sources contributing to the action density (w/o additional operator insertion)
[ gluon, gluon, src2, src2]
[ gluon, gluon, gluon, src2, src2]
[ gluon, gluon, gluon, gluon, src2, src2]
[ L, gluon, src2, src2]
[ L, gluon, gluon, src2, src2]
[ L, gluon, gluon, gluon, src2, src2]
[ L, L, src2, src2]
[ L, L, gluon, src2, src2]
[ L, L, gluon, gluon, src2, src2]
[ L, L, L, src2, src2]
[ L, L, L, gluon, src2, src2]
[ L, L, L, L, src2, src2]

% sources contributing to corrections of the flow equation
[ B, gluon, frc]
[ B, L, frc]
[ B, gluon, gluon, frc]
[ B, L, gluon, frc]
[ B, L, L, frc]
[ B, gluon, gluon, gluon, frc]
[ B, L, gluon, gluon, frc]
[ B, L, L, gluon, frc]
[ B, L, L, L, frc]

```

D.3 Apply Feynman rules

The output of **QGRAF** contains a set of **propagator** and **vertex** expressions, which carry the information what particles they belong to accompanied by momenta, distinct indices for space-time, colour etc. Hence we only need to replace **propagator** with the appropriate mathematical expression and do the same for **vertex**, where we additionally have to read out what particles are present as legs to determine which vertex it is. One difficulty is to ensure that expressions containing γ -matrices are inserted in the correct ordering.

D.4 Use of dimensional regularisation

The general rules of dimensional regularisation are listed in appendix B. Since we are only interested in the 1-loop UV divergences we can evaluate the traces of γ matrices in four dimensions

$$\text{tr}_D(\gamma_{\mu_1} \dots \gamma_{\mu_N}) = \text{tr}_4(\gamma_{\mu_1} \dots \gamma_{\mu_N}) + \mathcal{O}(\epsilon), \quad (\text{D.1})$$

which is expected to yield an error of $\mathcal{O}(\epsilon)$ and thus affects only 1-loop finite terms.

How to extract only the 1-loop UV-poles has been explained in section 6.1.

Once the loop momenta have been integrated out, we are left with a set of Γ functions of the form $\Gamma(n + \epsilon)$, where $n \in \mathbb{Z}$ and ϵ is a small real number. There are multiple relevant cases

$$\Gamma(\epsilon) = \frac{1}{\epsilon} - \gamma_E + \left(\frac{\gamma_E^2}{2} + \frac{\pi^2}{12} \right) \epsilon + \mathcal{O}(\epsilon^2) \quad (\text{D.2})$$

$$\frac{1}{\Gamma(\epsilon)} = \epsilon + \gamma_E \epsilon^2 + \mathcal{O}(\epsilon^3) \quad (\text{D.3})$$

$$\Gamma(n + \epsilon) = \Gamma(n) \left(1 + \sum_{l=1}^n \frac{\epsilon}{l} - \gamma_E \epsilon \right) + \mathcal{O}(\epsilon^2), \quad \forall n \in \mathbb{N} \quad (\text{D.4})$$

$$\frac{(-1)^n}{\Gamma(n + \epsilon)} = \frac{1 - \sum_{l=1}^n \frac{\epsilon}{l} + \gamma_E \epsilon}{\Gamma(n)} + \mathcal{O}(\epsilon^2), \quad \forall n \in \mathbb{N} \quad (\text{D.5})$$

$$\Gamma(\epsilon - n) = \left(\frac{1}{\epsilon} - \gamma_E + \sum_{l=1}^n \frac{1}{l} \right) \frac{(-1)^n}{\Gamma(n)} + \mathcal{O}(\epsilon), \quad \forall n \in \mathbb{N}. \quad (\text{D.6})$$

Appendix E

Listing of checks and reference values

To ensure validity of the obtained anomalous dimension matrix we performed the following consistency checks:

1. Gauge-invariance of physical on-shell quantities, i.e. independence of the final result from the gauge-fixing parameter. In off-shell renormalisation this ensures independence of the mixing matrix from the gauge-fixing parameter for all entries except those of EOM vanishing operators. Also the contraction of matrix elements with the momenta of external gluons must vanish, see e.g. [72, p. 118ff.].
2. Cross-check of already known results:
 - Euclidean Feynman rules from the continuum Lagrangian density, cf. [184],
 - Wave-function and coupling renormalisation, see e.g. [72, p. 521ff.],
 - Operator renormalisation, which will be done in section E.1.
3. Green's functions with inserted total divergence operators vanish at zero momentum of the operator.
4. Validity of full QCD $\xrightarrow{N_f \rightarrow 0}$ pure gauge for purely gluonic operators.
5. Consistency between both on-shell and BGF approach as will be explained in section E.2.

E.1 Reference values

Since operators of higher mass-dimension are often used for effective field theories, e.g. for BSM physics [133], multiple results already exist. We will give here a listing of existing (on-shell) results. We provide the replacement rule required on our results to arrive at the reference paper's conventions. In case identical symbols as ours are used we introduce a hat for the translated symbols.

1. Jamin et al. (1985, 2015) [152, 153]:
 - Available operators: One and two flavour 4-fermion operators as discussed in section 6.4.
2. Alonso et al. (2013) [133]:
 - Available operators: $\mathcal{O}_1^{(2)} = \frac{1}{g_0^2} \text{tr} (F_{\mu\nu} F_{\nu\rho} F_{\rho\mu})$ and in principle some 4-fermion operators (not checked because choice of 4-fermion operator basis is very different from ours).

- Conversion: $\dot{C}_G/C_G/g_3^2 = 2(\gamma_0)_1 - 4\pi\beta_0$
Notice that there is a single additional coupling g present in our conventions due to a different normalisation of the operator.
- 3. Lüscher and Weisz (2011) [160]:
 - Available results: poles of 1-loop Gradient flow vertex functions Γ_{AA} , Γ_{LA} , Γ_{LB} and Γ_{LL} .
- 4. Lüscher (2010) [155] and Harlander (2016) [165]
 - Available results: action density $E(t)$ to NLO order and beyond, some Feynman rules for flowed fields.
- 5. Gracey (2002, Erratum: 2004) [151]
 - Available operators: $\mathcal{O}_1^{(2)} = \frac{1}{g_0^2} \text{tr}(F_{\mu\nu}F_{\nu\rho}F_{\rho\mu})$, and pure gauge total divergence operators.
 - Conversion: $\alpha_{\overline{\text{MS}}} \rightarrow 4\pi a$, $N_f \rightarrow 0$ and

$$-(\gamma_0)_1 \alpha_{\overline{\text{MS}}} \stackrel{\Delta}{=} \gamma_{61}(a) - \frac{11}{6}Na. \quad (\text{E.1})$$

Caveat: The stated definition of the anomalous dimension there lacks a factor 2 as can be seen when looking at $\gamma_{62}(a) = -\frac{11}{3}Na$, which they claim to be the 1-loop coefficient of the beta-function.

- 6. Narrison and Tarrach (1983) [150]:
 - Available operators: $\mathcal{O}_4^{(1)} = i\bar{u}\sigma_{\mu\nu}F_{\mu\nu}u$, $\mathcal{O}_1^{(2)} = \frac{1}{g_0^2} \text{tr}(F_{\mu\nu}F_{\nu\rho}F_{\rho\mu})$ ($\mathcal{O}_{11}^{(2)}$ but not in agreement).
 - Conversion: $(D-4)/2 = -\epsilon \rightarrow \hat{\epsilon}$, $N_f \rightarrow 1$ and drop EOM-vanishing parts.

Something is wrong with their renormalisation of the 4-fermion operator $(\bar{u}u)^2$. It seems that they lost a combinatorial factor 2 for the 4-fermion operators in the EOM vanishing operator, which then correctly reproduces the off-diagonal entries but does not fix the diagonal entry. Their result not only disagrees with ours but also with the one found in [152, 153].

E.2 On-shell renormalisation of the minimal basis at non-zero momentum

Apart from the literature values we also checked the results from the off-shell renormalisation with the BGF method as explained in section 6.1 against an on-shell renormalisation strategy that uses connected graphs rather than 1PI ones.

For the on-shell renormalisation we choose the simpler Faddeev-Popov gauge-fixing without the background field and enforce the on-shell condition $(p_i)_0^2 = -(\mathbf{p}_i)^2$ on external legs corresponding to gluons or massless quarks. For each gluon we also multiply with the polarisation η_i and enforce $p_i \cdot \eta_i = \sum_\mu (p_i)_\mu (\eta_i)_\mu = 0$. Due to momentum conservation, this would exclude connected 3-point functions of fundamental fields with an operator insertion at zero momentum as a renormalisation condition. To avoid the cumbersome gluonic 4-point function we therefore insert the operators of the minimal basis at nonzero momentum following [151], which then requires the inclusion of total divergence operators irrelevant for our on-shell basis for the effective action as argued in chapter 6. The complete basis of total divergence operators is listed in appendix C.1. Instead the insertion of

Appendix E. Listing of checks and reference values

EOM vanishing operators (or any other only BRST-invariant operators) yields vanishing on-shell n -point functions and thus can be ignored. The modified renormalisation condition then reads

$$\begin{aligned} & \left(\begin{array}{c} \tilde{\mathcal{G}}_{\mathcal{O}}^{(l,m,n)} \\ \tilde{\mathcal{G}}_{\phi}^{(l,m,n)} \end{array} \right)_{\overline{\text{MS}}} (p_1, \dots, p_{l+m+n}; q; \alpha_{\overline{\text{MS}}}; \epsilon) = \\ & Z_{\Psi}^{m+n}(\alpha_{\overline{\text{MS}}}; \epsilon) Z_A^l(\alpha_{\overline{\text{MS}}}; \epsilon) \begin{pmatrix} Z^{\mathcal{O}} & Z^{\mathcal{O}\phi} \\ 0 & Z^{\phi} \end{pmatrix} \left(\begin{array}{c} \tilde{\mathcal{G}}_{\mathcal{O}}^{(l,m,n)} \\ \tilde{\mathcal{G}}_{\phi}^{(l,m,n)} \end{array} \right) (p_1, \dots, p_{l+m+n}; q; \alpha; \epsilon). \end{aligned} \quad (\text{E.2})$$

Again the triangular mixing matrix allows to extract $Z^{\mathcal{O}}$ easily. In the massless case we find the same operator mixing from the on-shell renormalisation condition as from the off-shell renormalisation condition with background fields using the 2-, 3- and 4-point functions with insertion of an operator as depicted in figure 6.1 but with non-zero momentum q for the operator insertion.

Appendix F

Miscellaneous

F.1 Expansion of connected graphs yields connected graphs

From a graph theoretical point of view it should be obvious that an expansion of connected graphs stays connected. Nonetheless, let us consider two partition functions with fundamental fields ϕ

$$\mathcal{Z}_{\text{eff}}[\hat{j}] = \int \mathcal{D}\phi \exp(-S[\phi] - \Delta S[\epsilon, \phi] + \hat{j} \cdot \mathcal{O}[\phi]) , \quad \mathcal{Z}[\hat{j}] = \int \mathcal{D}\phi \exp(-S[\phi] + \hat{j} \cdot \mathcal{O}[\phi]) , \quad (\text{F.1})$$

where \hat{j}_i is a source of the local field \mathcal{O}_i , S is the action and, if ϵ is small, ΔS is a small deviation from this action parametrised as

$$\Delta S[\epsilon, \phi] = \sum_{k=1}^N \epsilon^k \Delta S_k[\phi] \stackrel{\text{def}}{=} \sum_{k=1}^N z_k \Delta S_k[\phi] . \quad (\text{F.2})$$

Here ΔS_k is a deviation of order $\epsilon^k \stackrel{\text{def}}{=} z_k$. As usual we can obtain the connected graphs in the “effective” theory via the generating functional, see e.g. [105, p. 26ff.],

$$\langle \mathcal{O}_1(x_1) \dots \mathcal{O}_n(x_n) \rangle_{\text{con}}^{\text{eff}} = \left[\prod_{i=1}^n \frac{\delta}{\delta \hat{j}_i(x_i)} \ln(\mathcal{Z}_{\text{eff}}[\hat{j}]) \right]_{\hat{j}=0} , \quad x_i \neq x_k \forall i \neq k . \quad (\text{F.3})$$

Splitting now the exponential of the effective partition function into two parts yields

$$\begin{aligned} \ln(\mathcal{Z}_{\text{eff}}[\hat{j}]) &= \ln \left(\left\langle e^{-\Delta S[\epsilon, \phi]} \right\rangle [\hat{j}] \mathcal{Z}[\hat{j}] \right) \\ &= \ln(\mathcal{Z}[\hat{j}]) + \ln \left(\left\langle e^{-\Delta S[\epsilon, \phi]} \right\rangle [\hat{j}] \right) , \end{aligned} \quad (\text{F.4})$$

where $\langle \dots \rangle [\hat{j}]$ denotes the expectation value in the unperturbed theory but without setting the sources to zero. While $\ln(\mathcal{Z})$ is just the generating functional of connected graphs in the unperturbed theory the other logarithm is the one in question. Expanding now this logarithm in the different z_k leads to

$$\ln \left\langle e^{-\Delta S[\epsilon, \phi]} \right\rangle [\hat{j}] = \sum_{n_1, \dots, n_N} \left(\prod_{k=1}^N \frac{\epsilon^{kn_k}}{n_k!} \frac{\partial^{n_k}}{\partial z_k^{n_k}} \right) \ln \left\langle e^{-z_l \Delta S_l[\phi]} \right\rangle [\hat{j}] \Big|_{\vec{z}=0} , \quad (\text{F.5})$$

where $n_k \in \mathbb{N} \cup \{0\}$. Since the zero order contribution vanishes and \mathcal{Z} is a constant w.r.t. z_k we can reintroduce \mathcal{Z}_{eff} . Additionally we reorder the summation by fixing the number of occurring derivatives

$$\ln \left\langle e^{-\Delta S[\epsilon, \phi]} \right\rangle [\hat{j}] = \sum_{s=1}^{\infty} \sum_{\sum_i n_i = s} \left(\prod_{k=1}^N \frac{\epsilon^{kn_k}}{n_k!} \frac{\partial^{n_k}}{\partial z_k^{n_k}} \right) \ln \mathcal{Z}_{\text{eff}}[\hat{j}] \Big|_{\vec{z}=0} . \quad (\text{F.6})$$

Noting that the latter expression is analogous to a generating functional of connected graphs with “sources” z_k allows us to rewrite this expression as

$$\ln \left\langle e^{-\Delta S[\epsilon, \phi]} \right\rangle [j] = \sum_{s=1}^{\infty} \sum_{\sum_i n_i = s} \left\langle \prod_{k=1}^N \frac{1}{n_k!} (-\epsilon^k \Delta S_k[\phi])^{n_k} \right\rangle_{\text{con}}. \quad (\text{F.7})$$

Applying now the constraint $\sum_i n_i = s$ to eliminate n_N yields

$$\begin{aligned} \ln \left\langle e^{-\Delta S[\epsilon, \phi]} \right\rangle [j] &= \sum_{s=1}^{\infty} \frac{1}{s!} \sum_{n_1, \dots, n_{N-1}} \frac{s!}{n_1! \dots n_{N-1}! (s - n_1 - \dots - n_{N-1})!} \\ &\quad \left\langle \left(\prod_{k=1}^{N-1} (-\epsilon^k \Delta S_k[\phi])^{n_k} \right) (-\epsilon^N \Delta S_N[\phi])^{s - n_1 - \dots - n_{N-1}} \right\rangle_{\text{con}} [j] \\ &= \sum_{s=1}^{\infty} \frac{1}{s!} \langle (-\Delta S[\epsilon, \phi])^s \rangle_{\text{con}} [j] \\ &\equiv \left\langle e^{-\Delta S[\epsilon, \phi]} - 1 \right\rangle_{\text{con}} [j], \end{aligned} \quad (\text{F.8})$$

where we used that the inner sum in the first line is just the multinomial formula. At this point we only need to remember that a derivative of a connected graph with respect to a source yields again a connected graph and so on, which is the basis of the generating functional in equation (F.3). Thus we find

$$\langle \mathcal{O}_1(x_1) \dots \mathcal{O}_n(x_n) \rangle_{\text{con}}^{\text{eff}} = \left\langle \mathcal{O}_1(x_1) \dots \mathcal{O}_n(x_n) e^{-\Delta S[\epsilon, \phi]} \right\rangle_{\text{con}}, \quad x_i \neq x_k \forall i \neq k. \quad (\text{F.10})$$

F.2 Conversion between α , g^2 etc.

To ease comparison between different conventions in the literature we give here some rudimentary relations of the coupling and β -function. We start with the case of the conversion of the coupling between two renormalisation schemes

$$\begin{aligned} \alpha' &= \alpha \left(1 + \sum_{n>0} k_n \alpha^n \right) = \frac{g^2}{4\pi} \left(1 + \sum_{n>0} \frac{k_n}{(4\pi)^n} (g^2)^n \right) \stackrel{\text{def}}{=} \frac{g^2}{4\pi} \left(1 + \sum_{n>0} c_n (g^2)^n \right) \\ &\Rightarrow c_n = \frac{k_n}{(4\pi)^n}. \end{aligned} \quad (\text{F.11})$$

For the β -function multiple conventions can be found in the literature. We will list here the necessary conversion between the two choices preferred by us, which can be easily generalised to different choices:

$$\beta(\alpha) = \mu^2 \frac{d\alpha}{d\mu^2} = -\alpha^2 \sum_{n \geq 0} \beta_n \alpha^n = \frac{1}{2} \mu \frac{d\alpha}{d\mu} \quad (\text{F.12})$$

$$\begin{aligned} &= - \left(\frac{g^2}{4\pi} \right)^2 \sum_{n \geq 0} \frac{\beta_n}{(4\pi)^n} g^{2n} = \frac{g}{2\pi} \mu^2 \frac{dg}{d\mu^2} \\ &= \frac{g}{4\pi} \mu \frac{dg}{d\mu} \stackrel{\text{def}}{=} \frac{g}{4\pi} \beta'(g) \end{aligned} \quad (\text{F.13})$$

$$\beta'(g) = \mu \frac{dg}{d\mu} = -g^3 \sum_{n \geq 0} b_n g^{2n} \Rightarrow b_n = \frac{\beta_n}{(4\pi)^{n+1}}. \quad (\text{F.14})$$

Consequently we find $\mu^k \rightarrow \mu$ yields a global factor $1/k$ and $\alpha \rightarrow c\alpha$ yields a factor c^{n+1} for the n -th coefficient of the β -function.

Bibliography

- [1] J. Balog, F. Niedermayer, P. Weisz, *The Puzzle of apparent linear lattice artifacts in the 2d non-linear sigma-model and Symanzik's solution*, Nucl. Phys. **B824**, 563 (2010), 0905.1730
- [2] J. Balog, F. Niedermayer, P. Weisz, *Logarithmic corrections to $O(a^2)$ lattice artifacts*, Phys. Lett. **B676**, 188 (2009), 0901.4033
- [3] N. Husung, P. Marquard, R. Sommer, *Asymptotic behavior of cutoff effects in Yang-Mills theory and in Wilson's lattice QCD*, Eur. Phys. J. C **80**, 200 (2020), 1912.08498
- [4] N. Husung, P. Marquard, R. Sommer, *Logarithmic corrections to \mathbf{a}^2 scaling in lattice Yang Mills theory*, in *37th International Symposium on Lattice Field Theory (LATTICE2019)* (2019), 1912.02058
- [5] N. Husung, A. Nada, R. Sommer, *Yang Mills short distance potential and perturbation theory*, in *37th International Symposium on Lattice Field Theory (LATTICE2019)* (2020)
- [6] C.N. Yang, R.L. Mills, *Conservation of Isotopic Spin and Isotopic Gauge Invariance*, Phys. Rev. **96**, 191 (1954)
- [7] S.L. Glashow, *Partial Symmetries of Weak Interactions*, Nucl. Phys. **22**, 579 (1961)
- [8] A. Salam, J.C. Ward, *Electromagnetic and weak interactions*, Phys. Lett. **13**, 168 (1964)
- [9] S. Weinberg, *A Model of Leptons*, Phys. Rev. Lett. **19**, 1264 (1967)
- [10] F. Englert, R. Brout, *Broken Symmetry and the Mass of Gauge Vector Mesons*, Phys. Rev. Lett. **13**, 321 (1964), [157(1964)]
- [11] P.W. Higgs, *Broken Symmetries and the Masses of Gauge Bosons*, Phys. Rev. Lett. **13**, 508 (1964), [160(1964)]
- [12] G. Arnison et al. (UA1), *Experimental Observation of Lepton Pairs of Invariant Mass Around 95-GeV/c**2 at the CERN SPS Collider*, Phys. Lett. B **126**, 398 (1983)
- [13] P. Bagnaia et al. (UA2), *Evidence for $Z^0 \rightarrow e^+ e^-$ at the CERN anti-p p Collider*, Phys. Lett. B **129**, 130 (1983)
- [14] J. Alitti et al. (UA2), *An Improved determination of the ratio of W and Z masses at the CERN $\bar{p}p$ collider*, Phys. Lett. B **276**, 354 (1992)
- [15] G. Arnison et al. (UA1), *Experimental Observation of Isolated Large Transverse Energy Electrons with Associated Missing Energy at $s^{*}(1/2) = 540$ -GeV*, Phys. Lett. B **122**, 103 (1983)
- [16] M. Banner et al. (UA2), *Observation of Single Isolated Electrons of High Transverse Momentum in Events with Missing Transverse Energy at the CERN anti-p p Collider*, Phys. Lett. B **122**, 476 (1983)

BIBLIOGRAPHY

- [17] F. Abe et al. (CDF), *A Measurement of the W boson mass*, Phys. Rev. Lett. **65**, 2243 (1990)
- [18] G. Aad et al. (ATLAS), *Observation of a new particle in the search for the Standard Model Higgs boson with the ATLAS detector at the LHC*, Phys. Lett. B **716**, 1 (2012), 1207.7214
- [19] S. Chatrchyan et al. (CMS), *Observation of a New Boson at a Mass of 125 GeV with the CMS Experiment at the LHC*, Phys. Lett. B **716**, 30 (2012), 1207.7235
- [20] Y. Ne'eman, *Derivation of strong interactions from a gauge invariance*, Nucl. Phys. **26**, 222 (1961)
- [21] M. Gell-Mann, *The Eightfold Way: A Theory of strong interaction symmetry* (1961)
- [22] H. Fritzsch, M. Gell-Mann, H. Leutwyler, *Advantages of the Color Octet Gluon Picture*, Phys. Lett. B **47**, 365 (1973)
- [23] M. Gell-Mann, *A Schematic Model of Baryons and Mesons*, Phys. Lett. **8**, 214 (1964)
- [24] G. Zweig, *An $SU(3)$ model for strong interaction symmetry and its breaking. Version 2* (1964), pp. 22–101
- [25] D.J. Gross, F. Wilczek, *Ultraviolet Behavior of Non-Abelian Gauge Theories*, Phys. Rev. Lett. **30**, 1343 (1973)
- [26] D.J. Gross, F. Wilczek, *Asymptotically Free Gauge Theories. I*, Phys. Rev. D **8**, 3633 (1973)
- [27] H.D. Politzer, *Reliable perturbative results for strong interactions?*, Phys. Rev. Lett. **30**, 1346 (1973)
- [28] D.J. Gross, F. Wilczek, *Asymptotically free gauge theories. II*, Phys. Rev. D **9**, 980 (1974)
- [29] M. Breidenbach, J.I. Friedman, H.W. Kendall, E.D. Bloom, D. Coward, H. DeStaebler, J. Drees, L.W. Mo, R.E. Taylor, *Observed Behavior of Highly Inelastic electron-Proton Scattering*, Phys. Rev. Lett. **23**, 935 (1969)
- [30] J. Bjorken, *Asymptotic Sum Rules at Infinite Momentum*, Phys. Rev. **179**, 1547 (1969)
- [31] R. Brandelik et al. (TASSO), *Evidence for Planar Events in e^+e^- Annihilation at High-Energies*, Phys. Lett. B **86**, 243 (1979)
- [32] P. Zyla et al. (Particle Data Group), *Review of Particle Physics*, PTEP **2020**, 083C01 (2020)
- [33] G. Brandt, *Review of Current Standard Model Results from ATLAS*, Few Body Syst. **59**, 128 (2018)
- [34] G. Pásztor (ATLAS, CMS), *Precision tests of the Standard Model at the LHC with the ATLAS and CMS detectors*, PoS **FFK2019**, 005 (2020)
- [35] F. Zwicky, *Die Rotverschiebung von extragalaktischen Nebeln*, Helv. Phys. Acta **6**, 110 (1933)
- [36] D. Clowe, M. Bradac, A.H. Gonzalez, M. Markevitch, S.W. Randall, C. Jones, D. Zaritsky, *A direct empirical proof of the existence of dark matter*, Astrophys. J. **648**, L109 (2006), astro-ph/0608407
- [37] Y. Fukuda et al. (Super-Kamiokande), *Evidence for oscillation of atmospheric neutrinos*, Phys. Rev. Lett. **81**, 1562 (1998), hep-ex/9807003
- [38] Q. Ahmad et al. (SNO), *Direct evidence for neutrino flavor transformation from neutral current interactions in the Sudbury Neutrino Observatory*, Phys. Rev. Lett. **89**, 011301 (2002), nucl-ex/0204008

- [39] M. Aker et al. (KATRIN), *Improved Upper Limit on the Neutrino Mass from a Direct Kinematic Method by KATRIN*, Phys. Rev. Lett. **123**, 221802 (2019), 1909.06048
- [40] S. Bifani, S. Descotes-Genon, A. Romero Vidal, M.H. Schune, *Review of Lepton Universality tests in B decays*, J. Phys. G **46**, 023001 (2019), 1809.06229
- [41] R. Aaij et al. (LHCb), *Test of lepton universality with $\Lambda_b^0 \rightarrow pK^-\ell^+\ell^-$ decays*, JHEP **05**, 040 (2020), 1912.08139
- [42] T. Aoyama et al., *The anomalous magnetic moment of the muon in the Standard Model*, Phys. Rept. **887**, 1 (2020), 2006.04822
- [43] F. Jegerlehner, *Muon $g - 2$ theory: The hadronic part*, EPJ Web Conf. **166**, 00022 (2018), 1705.00263
- [44] M. Davier, A. Hoecker, B. Malaescu, Z. Zhang, *Reevaluation of the hadronic vacuum polarisation contributions to the Standard Model predictions of the muon $g - 2$ and $\alpha(m_Z^2)$ using newest hadronic cross-section data*, Eur. Phys. J. C **77**, 827 (2017), 1706.09436
- [45] A. Keshavarzi, D. Nomura, T. Teubner, *Muon $g - 2$ and $\alpha(M_Z^2)$: a new data-based analysis*, Phys. Rev. D **97**, 114025 (2018), 1802.02995
- [46] A. Gérardin, M. Cè, G. von Hippel, B. Hörz, H.B. Meyer, D. Mohler, K. Ottnad, J. Wilhelm, H. Wittig, *The leading hadronic contribution to $(g - 2)_\mu$ from lattice QCD with $N_f = 2 + 1$ flavours of $O(a)$ improved Wilson quarks*, Phys. Rev. D **100**, 014510 (2019), 1904.03120
- [47] B. Chakraborty, C. Davies, P. de Oliveira, J. Koponen, G. Lepage, R. Van de Water, *The hadronic vacuum polarization contribution to a_μ from full lattice QCD*, Phys. Rev. D **96**, 034516 (2017), 1601.03071
- [48] T. Blum, P. Boyle, V. Gülpers, T. Izubuchi, L. Jin, C. Jung, A. Jüttner, C. Lehner, A. Portelli, J. Tsang (RBC, UKQCD), *Calculation of the hadronic vacuum polarization contribution to the muon anomalous magnetic moment*, Phys. Rev. Lett. **121**, 022003 (2018), 1801.07224
- [49] S. Aoki et al. (Flavour Lattice Averaging Group), *FLAG Review 2019*, Eur. Phys. J. **C80**, 113 (2020), 1902.08191
- [50] K. Symanzik, *Cutoff dependence in lattice ϕ_4^4 theory*, NATO Sci. Ser. B **59**, 313 (1980)
- [51] K. Symanzik, *Some Topics in Quantum Field Theory*, in *Mathematical Problems in Theoretical Physics. Proceedings, 6th International Conference on Mathematical Physics, West Berlin, Germany, August 11-20, 1981* (1981), pp. 47–58
- [52] K. Symanzik, *Continuum Limit and Improved Action in Lattice Theories. 1. Principles and ϕ^4 Theory*, Nucl. Phys. **B226**, 187 (1983)
- [53] K. Symanzik, *Continuum Limit and Improved Action in Lattice Theories. 2. $O(N)$ Nonlinear Sigma Model in Perturbation Theory*, Nucl. Phys. **B226**, 205 (1983)
- [54] P. Weisz, *Renormalization and lattice artifacts*, in *Modern perspectives in lattice QCD: Quantum field theory and high performance computing. Proceedings, International School, 93rd Session, Les Houches, France, August 3-28, 2009* (2010), pp. 93–160, 1004.3462
- [55] J.B. Kogut, L. Susskind, *Hamiltonian Formulation of Wilson's Lattice Gauge Theories*, Phys. Rev. D **11**, 395 (1975)
- [56] H. Sharatchandra, H. Thun, P. Weisz, *Susskind Fermions on a Euclidean Lattice*, Nucl. Phys. B **192**, 205 (1981)

BIBLIOGRAPHY

- [57] M. Lüscher, P. Weisz, *On-Shell Improved Lattice Gauge Theories*, Commun. Math. Phys. **97**, 59 (1985), [Erratum: Commun.Math.Phys. 98, 433 (1985)]
- [58] M. Lüscher, S. Sint, R. Sommer, P. Weisz, U. Wolff, *Nonperturbative $O(a)$ improvement of lattice QCD*, Nucl. Phys. **B491**, 323 (1997), hep-lat/9609035
- [59] P. Weisz, *Continuum Limit Improved Lattice Action for Pure Yang-Mills Theory (I)*, Nucl. Phys. **B212**, 1 (1983)
- [60] P. Weisz, R. Wohlert, *Continuum Limit Improved Lattice Action for Pure Yang-Mills Theory (II)*, Nucl. Phys. **B236**, 397 (1984), [Erratum: Nucl. Phys.B247,544(1984)]
- [61] G. Curci, P. Menotti, G. Paffuti, *Symanzik's Improved Lagrangian for Lattice Gauge Theory*, Phys. Lett. **130B**, 205 (1983), [Erratum: Phys. Lett.135B,516(1984)]
- [62] M. Lüscher, P. Weisz, *Computation of the Action for On-Shell Improved Lattice Gauge Theories at Weak Coupling*, Phys. Lett. B **158**, 250 (1985)
- [63] R. Sommer, *A New way to set the energy scale in lattice gauge theories and its applications to the static force and alpha-s in $SU(2)$ Yang-Mills theory*, Nucl. Phys. B **411**, 839 (1994), hep-lat/9310022
- [64] S. Necco, R. Sommer, *The $N(f) = 0$ heavy quark potential from short to intermediate distances*, Nucl. Phys. B **622**, 328 (2002), hep-lat/0108008
- [65] G. de Divitiis, R. Frezzotti, M. Guagnelli, M. Lüscher, R. Petronzio, R. Sommer, P. Weisz, U. Wolff (Alpha), *Universality and the approach to the continuum limit in lattice gauge theory*, Nucl. Phys. **B437**, 447 (1995), hep-lat/9411017
- [66] A. Bode, P. Weisz, U. Wolff (ALPHA), *Two loop computation of the Schrodinger functional in lattice QCD*, Nucl. Phys. **B576**, 517 (2000), [Erratum: Nucl. Phys.B600,453(2001)], hep-lat/9911018
- [67] C. Alexandrou, M. Constantinou, H. Panagopoulos (ETM), *Renormalization functions for $N_f=2$ and $N_f=4$ twisted mass fermions*, Phys. Rev. **D95**, 034505 (2017), 1509.00213
- [68] M. Dalla Brida, P. Fritzsch, T. Korzec, A. Ramos, S. Sint, R. Sommer (ALPHA), *A non-perturbative exploration of the high energy regime in $N_f = 3$ QCD*, Eur. Phys. J. **C78**, 372 (2018), 1803.10230
- [69] K.G. Wilson, *Confinement of quarks*, Phys. Rev. D **10**, 2445 (1974)
- [70] K.G. Wilson, *Quarks and Strings on a Lattice*, in *New Phenomena in Subnuclear Physics: Proceedings, International School of Subnuclear Physics, Erice, Sicily, Jul 11-Aug 1 1975. Part A* (1975), p. 99
- [71] C. Gattringer, C.B. Lang, *Quantum Chromodynamics on the lattice*, Number 788 in Lecture Notes in Physics (Springer-Verlag, 2010)
- [72] M.D. Schwartz, *Quantum Field Theory and the Standard Model* (Cambridge University Press, 2014), ISBN 1107034736, 9781107034730
- [73] M. Lüscher, *Construction of a Selfadjoint, Strictly Positive Transfer Matrix for Euclidean Lattice Gauge Theories*, Commun. Math. Phys. **54**, 283 (1977)
- [74] M. Lüscher, R. Narayanan, P. Weisz, U. Wolff, *The Schrödinger Functional: A Renormalizable Probe for Non-Abelian Gauge Theories*, Nucl. Phys. **B384**, 168 (1992), hep-lat/9207009

- [75] S. Sint, *On the Schrödinger functional in QCD*, Nucl. Phys. **B421**, 135 (1994), [hep-lat/9312079](#)
- [76] M. Lüscher, S. Schaefer, *Lattice QCD without topology barriers*, JHEP **07**, 036 (2011), [1105.4749](#)
- [77] M. Lüscher, *Volume Dependence of the Energy Spectrum in Massive Quantum Field Theories. 1. Stable Particle States*, Commun. Math. Phys. **104**, 177 (1986)
- [78] M. Lüscher, *Volume Dependence of the Energy Spectrum in Massive Quantum Field Theories. 2. Scattering States*, Commun. Math. Phys. **105**, 153 (1986)
- [79] K. Symanzik, *Schrödinger representation and Casimir effect in renormalizable quantum field theory*, Nuclear Physics B **190**, 1 (1981), volume B190 [FS3] No.2 To Follow in Approximately Two Months
- [80] M. Della Morte, R. Sommer, S. Takeda, *On cutoff effects in lattice QCD from short to long distances*, Phys. Lett. **B672**, 407 (2009), [0807.1120](#)
- [81] S. Sint, *The Chirally rotated Schrödinger functional with Wilson fermions and automatic $O(a)$ improvement*, Nucl. Phys. **B847**, 491 (2011), [1008.4857](#)
- [82] N. Husung, M. Koren, P. Krah, R. Sommer, *$SU(3)$ Yang Mills theory at small distances and fine lattices*, EPJ Web Conf. **175**, 14024 (2018), [1711.01860](#)
- [83] S. Capitani, *Lattice perturbation theory*, Phys. Rept. **382**, 113 (2003), [hep-lat/0211036](#)
- [84] K. Osterwalder, R. Schrader, *Axioms for euclidean green's functions*, Communications in Mathematical Physics **31**, 83 (1973)
- [85] K. Osterwalder, R. Schrader, *Axioms for euclidean green's functions. ii*, Comm. Math. Phys. **42**, 281 (1975)
- [86] J.C. Collins, *Renormalization: An Introduction to Renormalization, the Renormalization Group and the Operator-Product Expansion*, Cambridge Monographs on Mathematical Physics (Cambridge University Press, 1984), ISBN 0-521-3117-2
- [87] G. 't Hooft, M. Veltman, *Combinatorics of gauge fields*, Nucl. Phys. B **50**, 318 (1972)
- [88] T. Reisz, *Lattice Gauge Theory: Renormalization to All Orders in the Loop Expansion*, Nucl. Phys. **B318**, 417 (1989)
- [89] T. Reisz, H.J. Rothe, *Renormalization of lattice gauge theories with massless Ginsparg Wilson fermions*, Nucl. Phys. **B575**, 255 (2000), [hep-lat/9908013](#)
- [90] V. Gimenez, L. Giusti, S. Guerriero, V. Lubicz, G. Martinelli, S. Petrarca, J. Reyes, B. Taglienti, E. Trevigne, *Non-perturbative renormalization of lattice operators in coordinate space*, Phys. Lett. **B598**, 227 (2004), [hep-lat/0406019](#)
- [91] J. Callan, Curtis G., *Broken scale invariance in scalar field theory*, Phys. Rev. D **2**, 1541 (1970)
- [92] K. Symanzik, *Small distance behavior in field theory and power counting*, Commun. Math. Phys. **18**, 227 (1970)
- [93] G. 't Hooft, M.J.G. Veltman, *Regularization and Renormalization of Gauge Fields*, Nucl. Phys. **B44**, 189 (1972)
- [94] G. 't Hooft, *Dimensional regularization and the renormalization group*, Nucl. Phys. **B61**, 455 (1973)

BIBLIOGRAPHY

- [95] W.A. Bardeen, A.J. Buras, D.W. Duke, T. Muta, *Deep Inelastic Scattering Beyond the Leading Order in Asymptotically Free Gauge Theories*, Phys. Rev. **D18**, 3998 (1978)
- [96] M. Lüscher, P. Weisz, *Computation of the relation between the bare lattice coupling and the \overline{MS} coupling in $SU(N)$ gauge theories to two loops*, Nucl. Phys. **B452**, 234 (1995), hep-lat/9505011
- [97] M. Lüscher, *SELECTED TOPICS IN LATTICE FIELD THEORY*, Conf. Proc. C **880628**, 451 (1988)
- [98] L. Faddeev, V. Popov, *Feynman diagrams for the Yang-Mills field*, Physics Letters B **25**, 29 (1967)
- [99] M. Lüscher, P. Weisz, *Background field technique and renormalization in lattice gauge theory*, Nucl. Phys. **B452**, 213 (1995), hep-lat/9504006
- [100] L.F. Abbott, *Introduction to the Background Field Method*, Acta Phys. Polon. **B13**, 33 (1982)
- [101] G. 't Hooft, *The Background Field Method in Gauge Field Theories*, in *Functional and Probabilistic Methods in Quantum Field Theory. 1. Proceedings, 12th Winter School of Theoretical Physics, Karpacz, Feb 17-March 2, 1975* (1975), pp. 345–369
- [102] L.F. Abbott, *The Background Field Method Beyond One Loop*, Nucl. Phys. **B185**, 189 (1981)
- [103] C. Becchi, A. Rouet, R. Stora, *Renormalization of Gauge Theories*, Annals Phys. **98**, 287 (1976)
- [104] M. Iofa, I. Tyutin, *Gauge Invariance of Spontaneously Broken Nonabelian Theories in the Bogolyubov-Parasiuk-HEPP-Zimmerman Method*, Teor. Mat. Fiz. **27**, 38 (1976)
- [105] R.J. Rivers, *PATH INTEGRAL METHODS IN QUANTUM FIELD THEORY*, Cambridge Monographs on Mathematical Physics (Cambridge University Press, 1988), ISBN 9780521368704, 9781139241861
- [106] S.D. Joglekar, B.W. Lee, *General Theory of Renormalization of Gauge Invariant Operators*, Annals Phys. **97**, 160 (1976)
- [107] H. Simma, *Equations of motion for effective Lagrangians and penguins in rare B decays*, Z. Phys. **C61**, 67 (1994), hep-ph/9307274
- [108] J.C. Collins, R.J. Scalise, *The Renormalization of composite operators in Yang-Mills theories using general covariant gauge*, Phys. Rev. **D50**, 4117 (1994), hep-ph/9403231
- [109] H. Georgi, *On-shell effective field theory*, Nucl. Phys. **B361**, 339 (1991)
- [110] G. Grunberg, *Renormalization Group Improved Perturbative QCD*, Phys. Lett. **95B**, 70 (1980), [Erratum: Phys. Lett.110B,501(1982)]
- [111] M. Papinutto, C. Pena, D. Preti, *On the perturbative renormalization of four-quark operators for new physics*, Eur. Phys. J. **C77**, 376 (2017), [Erratum: Eur. Phys. J.C78,no.1,21(2018)], 1612.06461
- [112] B. Sheikholeslami, R. Wohlert, *Improved Continuum Limit Lattice Action for QCD with Wilson Fermions*, Nucl. Phys. **B259**, 572 (1985)
- [113] L. Lellouch, R. Sommer, B. Svetitsky, A. Vladikas, L.F. Cugliandolo, eds., *Modern perspectives in lattice QCD: Quantum field theory and high performance computing. Proceedings, International School, 93rd Session, Les Houches, France, August 3-28, 2009* (Oxford, UK: Univ. Pr., 2011)

- [114] G. Parisi, *Symanzik's improvement program*, Nucl. Phys. **B254**, 58 (1985)
- [115] H. Georgi, *Effective field theory*, Ann. Rev. Nucl. Part. Sci. **43**, 209 (1993)
- [116] P.H. Ginsparg, K.G. Wilson, *A Remnant of Chiral Symmetry on the Lattice*, Phys. Rev. **D25**, 2649 (1982)
- [117] M. Lüscher, *Exact chiral symmetry on the lattice and the Ginsparg-Wilson relation*, Phys. Lett. B **428**, 342 (1998), [hep-lat/9802011](#)
- [118] S. Chandrasekharan, *Lattice QCD with Ginsparg-Wilson fermions*, Phys. Rev. D **60**, 074503 (1999), [hep-lat/9805015](#)
- [119] H. Neuberger, *Exactly massless quarks on the lattice*, Phys. Lett. B **417**, 141 (1998), [hep-lat/9707022](#)
- [120] H. Neuberger, *More about exactly massless quarks on the lattice*, Phys. Lett. B **427**, 353 (1998), [hep-lat/9801031](#)
- [121] P. Hernandez, K. Jansen, M. Lüscher, *Locality properties of Neuberger's lattice Dirac operator*, Nucl. Phys. B **552**, 363 (1999), [hep-lat/9808010](#)
- [122] D.B. Kaplan, *A Method for simulating chiral fermions on the lattice*, Phys. Lett. B **288**, 342 (1992), [hep-lat/9206013](#)
- [123] V. Furman, Y. Shamir, *Axial symmetries in lattice QCD with Kaplan fermions*, Nucl. Phys. B **439**, 54 (1995), [hep-lat/9405004](#)
- [124] H. Neuberger, *Vector - like gauge theories with almost massless fermions on the lattice*, Phys. Rev. D **57**, 5417 (1998), [hep-lat/9710089](#)
- [125] R. Frezzotti, P.A. Grassi, S. Sint, P. Weisz, *A Local formulation of lattice QCD without unphysical fermion zero modes*, Nucl. Phys. Proc. Suppl. **83**, 941 (2000), [hep-lat/9909003](#)
- [126] R. Frezzotti, P.A. Grassi, S. Sint, P. Weisz (Alpha), *Lattice QCD with a chirally twisted mass term*, JHEP **08**, 058 (2001), [hep-lat/0101001](#)
- [127] R. Frezzotti, G.C. Rossi, *Twisted mass lattice QCD with mass nondegenerate quarks*, Nucl. Phys. Proc. Suppl. **128**, 193 (2004), [[193\(2003\)](#)], [hep-lat/0311008](#)
- [128] C. Pena, S. Sint, A. Vladikas, *Twisted mass QCD and lattice approaches to the Delta I = 1/2 rule*, JHEP **09**, 069 (2004), [hep-lat/0405028](#)
- [129] S. Sint, *Lattice QCD with a chiral twist*, in *Workshop on Perspectives in Lattice QCD Nara, Japan, October 31-November 11, 2005* (2007), [hep-lat/0702008](#)
- [130] A. Vladikas, *Three Topics in Renormalization and Improvement*, in *Les Houches Summer School: Session 93: Modern perspectives in lattice QCD: Quantum field theory and high performance computing* (2011), pp. 161–222, [1103.1323](#)
- [131] S. Aoki, O. Bär, *Automatic $O(a)$ improvement for twisted-mass QCD*, PoS **LAT2006**, 165 (2006), [hep-lat/0610098](#)
- [132] G. Kilcup, S.R. Sharpe, *A Tool Kit for Staggered Fermions*, Nucl. Phys. B **283**, 493 (1987)
- [133] R. Alonso, E.E. Jenkins, A.V. Manohar, M. Trott, *Renormalization Group Evolution of the Standard Model Dimension Six Operators III: Gauge Coupling Dependence and Phenomenology*, JHEP **04**, 159 (2014), [1312.2014](#)

BIBLIOGRAPHY

- [134] O. Bär, G. Rupak, N. Shoresh, *Chiral perturbation theory at $O(a^{**2})$ for lattice QCD*, Phys. Rev. D **70**, 034508 (2004), [hep-lat/0306021](#)
- [135] N. Isgur, M.B. Wise, *Weak Decays of Heavy Mesons in the Static Quark Approximation*, Phys. Lett. B **232**, 113 (1989)
- [136] E. Eichten, B. Hill, *An effective field theory for the calculation of matrix elements involving heavy quarks*, Physics Letters B **234**, 511 (1990)
- [137] E. Eichten, B.R. Hill, *STATIC EFFECTIVE FIELD THEORY: $1/m$ CORRECTIONS*, Phys. Lett. B **243**, 427 (1990)
- [138] H. Georgi, *An Effective Field Theory for Heavy Quarks at Low-energies*, Phys. Lett. B **240**, 447 (1990)
- [139] B. Grinstein, *The Static Quark Effective Theory*, Nucl. Phys. B **339**, 253 (1990)
- [140] A. Hasenfratz, F. Knechtli, *Flavor symmetry and the static potential with hypercubic blocking*, Phys. Rev. D **64**, 034504 (2001), [hep-lat/0103029](#)
- [141] M. Della Morte, A. Shindler, R. Sommer, *On lattice actions for static quarks*, JHEP **08**, 051 (2005), [hep-lat/0506008](#)
- [142] M. Albanese et al. (APE), *Glueball Masses and String Tension in Lattice QCD*, Phys. Lett. B **192**, 163 (1987)
- [143] C. Morningstar, M.J. Peardon, *Analytic smearing of $SU(3)$ link variables in lattice QCD*, Phys. Rev. D **69**, 054501 (2004), [hep-lat/0311018](#)
- [144] M. Kurth, R. Sommer (ALPHA), *Renormalization and $O(a)$ improvement of the static axial current*, Nucl. Phys. B **597**, 488 (2001), [hep-lat/0007002](#)
- [145] P. Nogueira, *Automatic feynman graph generation*, Journal of Computational Physics **105**, 279 (1993)
- [146] P. Nogueira, *Abusing qgraf*, Nucl. Instrum. Meth. **A559**, 220 (2006)
- [147] K.G. Chetyrkin, M. Misiak, M. Münz, *Beta functions and anomalous dimensions up to three loops*, Nucl. Phys. **B518**, 473 (1998), [hep-ph/9711266](#)
- [148] M. Misiak, M. Münz, *Two loop mixing of dimension five flavor changing operators*, Phys. Lett. **B344**, 308 (1995), [hep-ph/9409454](#)
- [149] M.E. Peskin, D.V. Schroeder, *An Introduction to Quantum Field Theory*, Advanced book program (Westview Press Reading, Boulder (Colo.), 1995), ISBN 0-201-50397-2
- [150] S. Narison, R. Tarrach, *Higher dimensional renormalization group invariant vacuum condensates in quantum chromodynamics*, Physics Letters B **125**, 217 (1983)
- [151] J.A. Gracey, *Classification and one loop renormalization of dimension-six and dimension-eight operators in quantum gluodynamics*, Nucl. Phys. **B634**, 192 (2002), [Erratum: Nucl. Phys. **B696**, 295 (2004)], [hep-ph/0204266](#)
- [152] M. Jamin, M. Kremer, *Anomalous Dimensions of Spin 0 Four Quark Operators Without Derivatives*, Nucl. Phys. B **277**, 349 (1986)
- [153] D. Boito, D. Hornung, M. Jamin, *Anomalous dimensions of four-quark operators and renormalon structure of mesonic two-point correlators*, JHEP **12**, 090 (2015), [1510.03812](#)

- [154] A.J. Buras, P.H. Weisz, *QCD Nonleading Corrections to Weak Decays in Dimensional Regularization and 't Hooft-Veltman Schemes*, Nucl. Phys. B **333**, 66 (1990)
- [155] M. Lüscher, *Properties and uses of the Wilson flow in lattice QCD*, JHEP **08**, 071 (2010), [Erratum: JHEP03,092(2014)], 1006.4518
- [156] S. Borsanyi et al., *High-precision scale setting in lattice QCD*, JHEP **09**, 010 (2012), 1203.4469
- [157] R. Sommer, *Scale setting in lattice QCD*, PoS **LATTICE2013**, 015 (2014), 1401.3270
- [158] M. Dalla Brida, A. Ramos, *The gradient flow coupling at high-energy and the scale of $SU(3)$ Yang-Mills theory*, Eur. Phys. J. C **79**, 720 (2019), 1905.05147
- [159] R.V. Harlander, Y. Kluth, F. Lange, *The two-loop energy-momentum tensor within the gradient-flow formalism*, Eur. Phys. J. C **78**, 944 (2018), [Erratum: Eur.Phys.J.C 79, 858 (2019)], 1808.09837
- [160] M. Lüscher, P. Weisz, *Perturbative analysis of the gradient flow in non-abelian gauge theories*, JHEP **02**, 051 (2011), 1101.0963
- [161] H. Suzuki, *Energy-momentum tensor from the Yang-Mills gradient flow*, PTEP **2013**, 083B03 (2013), [Erratum: PTEP2015,079201(2015)], 1304.0533
- [162] A. Ramos, S. Sint, *Symanzik improvement of the gradient flow in lattice gauge theories*, Eur. Phys. J. C **76**, 15 (2016), 1508.05552
- [163] T. Huber, D. Maitre, *HypExp: A Mathematica package for expanding hypergeometric functions around integer-valued parameters*, Comput. Phys. Commun. **175**, 122 (2006), hep-ph/0507094
- [164] T. Huber, D. Maitre, *HypExp 2, Expanding Hypergeometric Functions about Half-Integer Parameters*, Comput. Phys. Commun. **178**, 755 (2008), 0708.2443
- [165] R.V. Harlander, T. Neumann, *The perturbative QCD gradient flow to three loops*, JHEP **06**, 161 (2016), 1606.03756
- [166] M. Bruno, I. Campos, P. Fritzsch, J. Koponen, C. Pena, D. Preti, A. Ramos, A. Vladikas (ALPHA), *Light quark masses in $N_f = 2 + 1$ lattice QCD with Wilson fermions*, Eur. Phys. J. C **80**, 169 (2020), 1911.08025
- [167] T. Luthe, A. Maier, P. Marquard, Y. Schröder, *Complete renormalization of QCD at five loops*, JHEP **03**, 020 (2017), 1701.07068
- [168] Y. Iwasaki, *Renormalization Group Analysis of Lattice Theories and Improved Lattice Action. II. Four-dimensional non-Abelian $SU(N)$ gauge model* (1983), 1111.7054
- [169] T. Takaishi, *Heavy quark potential and effective actions on blocked configurations*, Phys. Rev. **D54**, 1050 (1996)
- [170] P. de Forcrand et al. (QCD-TARO), *Search for effective lattice action of pure QCD*, Nucl. Phys. Proc. Suppl. **53**, 938 (1997), hep-lat/9608094
- [171] S. Sint, A. Ramos, *On $O(a^2)$ effects in gradient flow observables*, PoS **LATTICE2014**, 329 (2015), 1411.6706
- [172] J. Giedt, *Power-counting theorem for staggered fermions*, Nucl. Phys. B **782**, 134 (2007), hep-lat/0606003

BIBLIOGRAPHY

- [173] S.R. Sharpe, *Rooted staggered fermions: Good, bad or ugly?*, PoS **LAT2006**, 022 (2006), [hep-lat/0610094](#)
- [174] M. Lüscher, *Chiral symmetry and the Yang–Mills gradient flow*, JHEP **04**, 123 (2013), [1302.5246](#)
- [175] K. Hieda, H. Suzuki, *Small flow-time representation of fermion bilinear operators*, Mod. Phys. Lett. A **31**, 1650214 (2016), [1606.04193](#)
- [176] M. Lüscher, S. Sint, R. Sommer, P. Weisz, *Chiral symmetry and $O(a)$ improvement in lattice QCD*, Nucl. Phys. **B478**, 365 (1996), [hep-lat/9605038](#)
- [177] S.A. Larin, *The Renormalization of the axial anomaly in dimensional regularization*, Phys. Lett. **B303**, 113 (1993), [hep-ph/9302240](#)
- [178] D.J. Broadhurst, A.G. Grozin, *Matching QCD and HQET heavy - light currents at two loops and beyond*, Phys. Rev. **D52**, 4082 (1995), [hep-ph/9410240](#)
- [179] T. Bhattacharya, R. Gupta, W.j. Lee, S.R. Sharpe, J.M. Wu, *Improved bilinears in unquenched lattice QCD*, Nucl. Phys. B Proc. Suppl. **129**, 441 (2004), [hep-lat/0309087](#)
- [180] T. Bhattacharya, R. Gupta, W. Lee, S.R. Sharpe, J.M. Wu, *Improved bilinears in lattice QCD with non-degenerate quarks*, Phys. Rev. D **73**, 034504 (2006), [hep-lat/0511014](#)
- [181] A. Grozin, *Lectures on QED and QCD: Practical calculation and renormalization of one- and multi-loop Feynman diagrams* (World Scientific (2007), Hackensack, USA, 2007)
- [182] M. Paraskevas, *Dirac and Majorana Feynman Rules with four-fermions* (2018), [1802.02657](#)
- [183] I. Bierenbaum, J. Blümlein, S. Klein, *Mellin Moments of the $O(\alpha^3(s))$ Heavy Flavor Contributions to unpolarized Deep-Inelastic Scattering at $Q^2 \gg m^2$ and Anomalous Dimensions*, Nucl. Phys. **B820**, 417 (2009), [0904.3563](#)
- [184] J. Artz, R.V. Harlander, F. Lange, T. Neumann, M. Prausa, *Results and techniques for higher order calculations within the gradient flow formalism*, JHEP **06**, 121 (2019), [1905.00882](#)

Selbstständigkeitserklärung

Ich erkläre, dass ich die Dissertation selbständig und nur unter Verwendung der von mir gemäß § 7 Abs. 3 der Promotionsordnung der Mathematisch-Naturwissenschaftlichen Fakultät, veröffentlicht im Amtlichen Mitteilungsblatt der Humboldt-Universität zu Berlin Nr. 42/2018 am 11.07.2018, angegebenen Hilfsmittel angefertigt habe.

Berlin, den 21.12.2020

Nikolai Husung